Université Paris-Sud 11
Ecole Doctorale "Gènes, Génomes, Cellules"
91405 Orsay, France

Institute of Biochemistry and Biophysics
Polish Academy of Sciences
Department of Genetics
Pawinskiego 5A
02-106 Warsaw, Poland

CEA/Saclay
Institut de Biologie et de Technologies de Saclay
Service de Biologie Intégrative et Génétique Moléculaire
91191 Gif-sur-Yvette, France

PhD Thesis

Regulation of a gene transcription by RNA Polymerase III in *Saccharomyces cerevisiae*. The role of evolutionarily conserved domains of the Maf1 protein, RNA Polymerase III repressor.

Etude de la régulation de la transcription par l'ARN polymérase III chez *Saccharomyces cerevisiae*. Rôle des domaines conservées au cours de l'évolution de la protéine Maf1, un répresseur de l'ARN polymérase III.

Anna Ewa GAJDA

Defended on 9 December 2010, composition of the jury:

Prof. Magdalena BOGUTA	: Thesis Director
Dr hab. Olivier LEFEBVRE	: Thesis Director
Prof. Iwona FIJALKOWSKA	: Reviewer
Prof. Zofia SZWEYKOWSKA – KULINSKA	: Reviewer
Prof. Michel JACQUET	: Reviewer

I am very grateful to Prof. Magdalena Boguta for supervising my work and encouraging me to follow the “cotutelle” PhD studies. I thank her for the patience, forbearance, kindness and cordial atmosphere.

I also thank all my polish team, especially: Asia Towpik, Iwona Karkusiewicz and Tomek Turowski for their helpfulness, support, for amusing talks and a great time we spent together.

Je souhaiterais présenter mes remerciements à Monsieur Olivier Lefebvre qui m'a beaucoup aidée dans mes recherches et qui a facilité mon intégration à la vie en France. Monsieur Lefebvre m'a guidée précieusement dans mon travail, il m'a montré la beauté des recherches scientifiques et a toujours eu confiance en mes capacités intellectuelles. Je le remercie aussi pour le "Résumé substantiel" qu'il a eu la bonté de rédiger pour moi.

Je remercie Arounie Tavenet pour l'amitié qu'elle m'a offerte, pour nos entretiens et pour le temps que nous avons passé ensemble. Je tiens à exprimer ma gratitude envers Arlette qui a préparé un matériel immense pour mes expériences, se montrant toujours patiente et souriante. Je remercie également Nicolas Caudy pour les disques de musique de cinéma qui m'ont remonté le moral ainsi que Christine Conesa et Joël Acker pour leurs précieux conseils.

From the bottom of my heart, I thank my best friends: Marta Miller, Justyna Rudzka, Eliza Orzechowska, Paula Belino-Studzińska and Marta Marciniak for being with me in the most difficult moments.

Dziękuję również mojemu Tacie za wszelką pomoc w rzeczach małych i dużych, bez której nie mogłabym ukończyć tej pracy, jak i Urszuli za zrozumienie, wsparcie, „kobiecą solidarność” :) i prawdziwą Przyjaźń...

Summary**:**

Regulation of a gene transcription by RNA Polymerase III in *Saccharomyces cerevisiae*. The role of evolutionary conserved domains of the Maf1 protein, RNA Polymerase III repressor.

Yeast cell encounters numerous environmental situations that require a rapid and efficient adaptation of the cellular metabolism to changing life conditions. One of the first responses, is the inhibition of RNA polymerase III (Pol III) transcription. The Maf1 protein, the unique negative regulator of the Pol III apparatus in *Saccharomyces cerevisiae* (Sc), is conserved through evolution. The family of eukaryotic Maf1 share highly conserved amino acid sequence with two easily recognizable regions called A and BC domains. The work performed during this PhD thesis concerns the role of these evolutionary conserved domains in the activity of ScMaf1. I have constructed a library of Maf1, identified and localized the mutations of corresponding Maf1 proteins and studied the phenotype. Using yeast two-hybrid system, I have found the A and BC domains interact physically and defined the minimal 34 aa fragment of the A domain involved in this interaction. Using genetic screen for internal suppressor mutations, I have identified that mutations localized in the BC domain (D250E, V260D-N344I) recovered the activity of Maf1 mutated in the A domain (K35E), as deduced from no defected growth, efficient Pol III repression, phosphorylation and cellular localization of identified suppressors. The identified K35E mutation disrupted physical interaction between Maf1 domains, unless the presence of additional D250E or V260D-N344I suppressor mutations occurred. The Take Home message from the results obtained during my PhD thesis is that: “Full repression of Pol III requires the physical interaction between Maf1 domains”.

Résumé :

Etude de la régulation de la transcription par l’ARN polymérase III chez *Saccharomyces cerevisiae*. Rôle des domaines conservés au cours de l’évolution de la protéine Maf1, un répresseur de l’ARN polymérase III.

Dans l’environnement, la levure doit faire face à des conditions variées qui nécessitent une adaptation rapide du métabolisme cellulaire. Une des premières réponses est l’inhibition de la transcription par l’ARN polymérase III (Pol III). La protéine Maf1, le seul régulateur de la machinerie de la Pol III chez Saccharomyces cerevisiae (Sc), est conservée au cours de l’évolution. Les protéines Maf1 des Eucaryotes contiennent deux domaines A et BC phylogénétiquement conservés. Ce travail de thèse a cherché à identifier le rôle de ces domaines dans la fonction de la protéine ScMaf1. J’ai construit une banque de mutants de Maf1, identifié les changements dans leurs séquences ainsi que leurs phénotypes. En utilisant la technique du double-hybride, j’ai montré que les domaines A et BC interagissent physiquement et que l’extrémité N-terminale de 34 acides aminés du domaine A est le fragment minimal nécessaire à cette interaction. Grâce à un crible génétique, j’ai mis en évidence que les mutations du domaine BC (D250E et V260D-N344I) permettent de restaurer l’activité de Maf1 mutée dans le domaine A (K35E). Cette restauration est observable pour le phénotype, la répression efficace de la transcription par la Pol III, le niveau de phosphorylation et la localisation cellulaire de Maf1. La technique du double-hybride m’a permis aussi de montrer que la mutation K35E inactive partiellement l’interaction entre les domaines de Maf1 qui est restaurée par les mutations suppresseurs D250E et V260D-N344I. Les résultats permettent de conclure que : « la répression de la transcription par la Pol III requiert l’interaction physique des domaines de Maf1

CONTENTS :

ABBREVIATIONS:

A600 :	absorbance 600 nm
aa:	amino acid
α:	antibody
BLAST:	Basic Local Alignment Search Tool
bp:	base pair
BSA:	bovine serum albumin
β-gal:	β-galactosidase
ca.:	circa
ChIP on Chip:	Chromatin Immunoprecipitation analyzed on DNA microarray
CPZ:	chlorpromazine
DAPI:	4',6-diamidino-2-phenylindole
DISOPRED:	Prediction of Protein Disorder
DNA:	deoxyrybonucleic acid
DomPred:	Protein Domain Prediction
EDTA:	ethylenediaminetetraacetic acid
EtBr:	ethidium bromide
Exp.:	exponential growth phase
e.g:	for example
Gal4AD:	Gal4 Activating domain
Gal4BD:	Gal4 Binding domain
GST:	Glutathione S-transferase
HA:	hemagglutinin
HCA:	Hydrophobic Cluster Analysis
HIS:	Histidine
HRP:	Horse radish Peroxidase
HU :	hydroxyurea
IP:	immunopurification / immunoprecipitation
kb:	kilo base
kDA:	kilo Dalton
LEU / Leu:	Leucine
MMS :	methyl methane sulfonate
NLS :	nuclear localization sequence
nt:	nucleotide
OD:	optical density
ORF:	open reading frame
PCR:	polymerase chain reaction
Phe:	Phenyloalanine

Pol I:	RNA polymerase I
Pol III:	RNA polymerase III
pre-tRNA:	premature transfer RNA
PSI-BLAST:	Position specific iterative BLAST
PSIPRED:	Protein Structure Prediction
PSORT:	Prediction of protein sorting signals and localization sites
Rap.:	Rapamycin
Rb:	Retinoblastoma protein
RNA	deoxyribonucleic acid
SC:	synthetic complete medium
SDS:	sodium dodecyl sulfate
SDS-PAGE:	sodium dodecyl sulfate polyacrylamide gel electrophoresis
TCA:	trichloroacetic acid
tDNA:	transfer DNA
TOR:	Target of Rapamycin
TORC1:	TOR complex 1
TORC2:	TOR complex 2
tRNA:	transfer RNA
U6 snRNA:	U6 small nuclear RNA
WT:	wild-type
X-gal:	bromo-chloro-indolyl-galactopyranoside
Y2H:	yeast-two-hybrid system
YPD:	yeast extract peptone dextrose
YPGly:	yeast extract peptone glycerol
2D / 3D:	2/3 - dimension
5S rDNA:	5S ribosomal DNA
5S rRNA:	5S ribosomal RNA

I. INTRODUCTION

In eukaryotic cells, RNA polymerases (Pol) I and III are responsible for the synthesis of RNA species involved in ribosome biogenesis and the translation process. RNA synthesis by Pol I and Pol III represents more than 80% of all *S. cerevisiae* nuclear transcription activity and is controlled in a coordinated way in response to various cellular and environmental conditions (Willis *et al.,* 2004; Warner *et al.,* 2001; Warner, 1999).

Pol III is responsible for the transcription of ~400 genes in *S. cerevisiae* (class III genes), mostly tRNA genes and 5S rRNA genes (Harismendy *et al.,* 2003; Roberts *et al.,* 2003; Moqtaderi *et al.,* 2004). Analyses of the Pol III transcription system in *S. cerevisiae* have revealed a series of protein-DNA and protein-protein interactions leading to the recruitment of Pol III to its target tRNA genes: binding of the six-subunit TFIIIC factor to the intragenic promoter, TFIIIC-directed recruitment and assembly of the three components of TFIIIB (TBP, Brf1 and Bdp1), and subsequent recruitment of the seventeen-subunit Pol III enzyme (Geiduschek and Kassavetis, 2001) (Fig. 1).

The Pol III machinery is remarkably conserved between yeast and human cells. The most conserved components are those involved in assembly of the transcription complex: the τ131 subunit of TFIIIC and two components of TFIIIB (TBP, Brf1). The five Pol III-specific subunits in *S. cerevisiae* (C31, C34, C37, C53 and C82, Fig. 2) all have structural and functional homologs in human cells (Schramm and

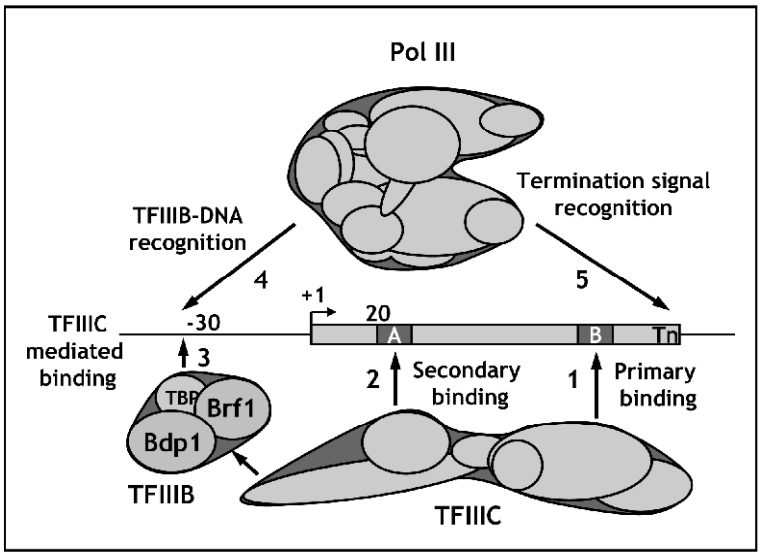

Figure 1. Assembly of the transcription complex on *S. cerevisiae* tRNA gene. The scheme depicts the multistep pathway of transcription complex formation: (1, 2) promoter recognition by TFIIIC, (3) TFIIIC-directed assembly of the initiation factor TFIIIB, (4) recruitment of Pol III and (5) termination of transcription. Adapted from Harismendy *et al.,* 2003.

Hernandez, 2002; Canella *et al.,* 2010). These Pol III-specific subunits form two subcomplexes (Fig. 2). The C53/37 subcomplex is involved in promoter opening, elongation, termination and reinitiation (Cramer *et al.,* 2008; Carter and Drouin, 2009; Kassaventis *et al.,* 2010; Landrieux *et al.,* 2006), whereas the C82/34/31 subcomplex is involved in promoter recognition and initiation. C34 interacts with TFIIIB, which recruits Pol III to promoters (Thuillier *et al.,* 1995; Werner *et al.,* 1993) and is involved in open complex formation (Brun *et al.,* 1997).

Also Maf1, the general Pol III repressor, is conserved across eukaryotic organisms from yeast to man (Pluta *et al.,* 2001). This conservation is of particular interest considering that misregulation of Pol III in human cells has been linked to malignant transformation. Excessive activation of Pol III-directed transcription can lead to tumorgenesis (Marshall *et al.,* 2008; Marshall *et al.,* 2008; Johnson *et al.,* 2008). In line with this observation, two mammalian tumor suppressors, Rb and p53, have been shown to act as global repressors of Pol III transcription (White, 2008). Recent results of several groups report Maf1-mediated repression of Pol III transcription in human cells implicating *H. sapiens* Maf1 ortholog as a new class of mammalian Pol III regulators (Goodfellow *et al.,* 2008; Reina *et al.,* 2006; Johnson *et al.,* 2007; Rollins *et al.,* 2007). The involvement of *H. sapiens* Maf1 in the aberrant control of Pol III transcription in cancer cells remains to be elucidated. In the light of the high evolutionarily conservation of the Pol III machinery including Maf1, insights into Pol III (mis)regulation by Maf1 attained by studying model organisms, such as yeast, should provide some insight into the role of *H. sapiens* Maf1 in cancer development.

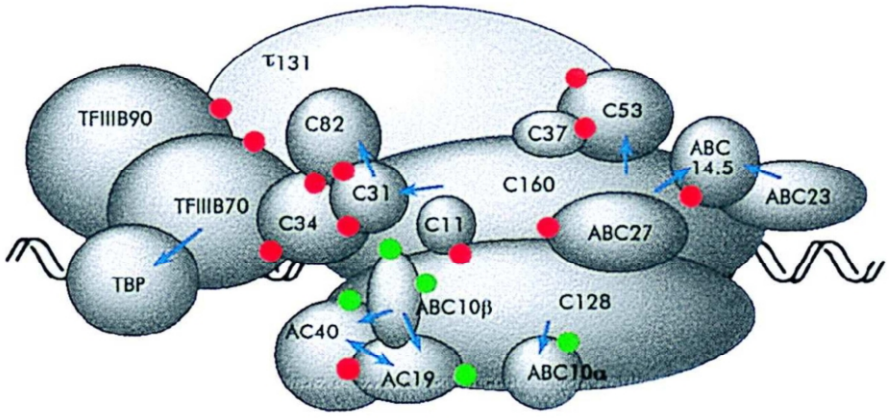

Figure 2. A model of the Pol III transcription initiation complex. A model of the Pol III transcription initiation complex. Protein–protein contacts observed by the two-hybrid system are indicated by red dots. Green dots indicate the interaction between AC40, AC19, ABC10α and ABC10β with A190 and A135 Pol I subunits homologous to C160 and C128. Genetic interactions observed by using multicopy suppression experiments of full-length mutations are indicated by arrows. The arrowhead points toward the subunit harboring the suppressed mutation. For the sake of simplicity, only the τ131 subunit of TFIIIC is represented. Adapted from Flores *et al.,* 1999.

1. Maf1-mediated repression of RNA polymerase III-dependent transcription.

The Maf1 protein was identified originally in *Saccharomyces cerevisiae* in a genome-wide screen for mutations that decrease the nonsense suppressor efficiency of *SUP11* (tRNA-Tyr(UAA)) (Fig. 3). The isolated mutation (*maf1-1*) conferred temperature-sensitivity in medium containing glycerol (a nonfermentable carbon source) (Murawski *et al.,* 1994). The identified *maf1-1* mutation besides inactivating the *MAF1* gene (*maf1*Δ) lead also to the increase of tRNA level, suggesting a deregulation of Pol III transcription (Pluta *et al.,* 2001; Kwapisz *et al.,* 2002; Upadhya *et al.,* 2002). The disturbance of *S. cerevisiae* cell growth in respiratory conditions at high temperatures was explained by the toxic effect of tRNA accumulation (Ciesla *et al.,* 2007). Performed investigations placed Maf1 as a main repressor of Pol III, involved in transduction of signals from diverse signaling pathways to the Pol III apparatus (Upadhya *et al.,* 2002).

Maf1 represses Pol III transcription in response to unfavorable growth conditions (various drug treatment, oxidative stress), secretory pathway defects and during stationary phase and respiratory growth. Inactivation of *MAF1* gene (*maf1*Δ) blocks repression of Pol III transcription under all these conditions (Upadhya *et al.,* 2002). Moreover, it was shown that under conditions of carbon source starvation, endoplasmic

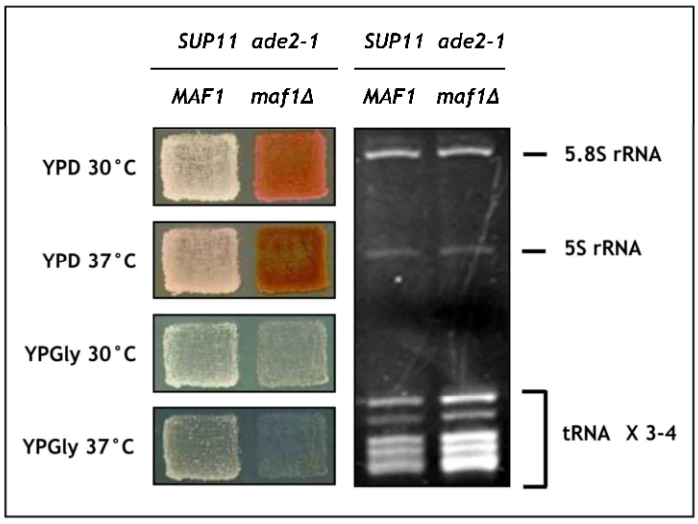

Figure 3. The *maf1*Δ mutation results in increased tRNA level and antisuppressor phenotype. The presence of *ade2-1* nonsense mutation leads to an accumulation of red pigment and can be overcome by a functional tRNA-Tyr (UAA) suppressor, *SUP11*. *S. cerevisiae* strain *SUP11 ade2-1* (MB159-4D) is white, while *SUP11 ade2-1 maf1*Δ (MB159-4DΔ) is red, indicating that the deletion of the chromosomal *MAF1* counteracts the effect of *SUP11* and acts as an antisuppressor. Moreover, the *maf1*Δ mutation results in temperature-sensitive growth on glycerol-containing medium (YPGly), and an increase of tRNA to a level 3-4-fold higher than the level in parental isogenic *SUP11 ade2-1* cells. Adapted from Kwapisz *et al.,* 2002.

reticulum stress (induced by DTT, 1,4-dithiothretiol) and during oxidative stress (induced by hydrogen peroxide) *S. cerevisiae* cells also lack Pol III repression in the absence of *MAF1* (Desai *et al.*, 2005, Boisnard *et al.*, 2009). Maf1 was also shown to be essential for the regulation of Pol III transcription during the transition of *S. cerevisiae* cells from medium with fermentable to a nonfermentable carbon source inducing respiratory growth conditions (Fig. 4, Ciesla *et al.*, 2007).

Recent data on Maf1 suggested possible connection between replication and transcription processes (Nguyen *et al.,* 2010). In *S. cerevisiae*, active tRNA genes act as "replication fork barriers" during cell proliferation as Pol III with concomitant TFIIIB/TFIIIC transcription factors interfere with the elongation process carried out by processive DNA polymerases (Deshpande *et al.,* 1996) in a way that might promote chromosome breakage. Checkpoint repression occurs in co-directional tRNA genes, which are replicated in the same direction as they are transcribed. The sensor kinase (Mec1), the signaling adaptor (Mrc1) and the transducer kinase (Rad53), involved in replication checkpoint, relay signals, which globally repress tRNA gene transcription in noneffected growth conditions and under replication stress (HU, hydroxyurea). Maf1 was shown to mediate replication stress signaling and pre-tRNA synthesis as shown by Rad53-dependent dephosphorylation of Maf1 in HU-treated

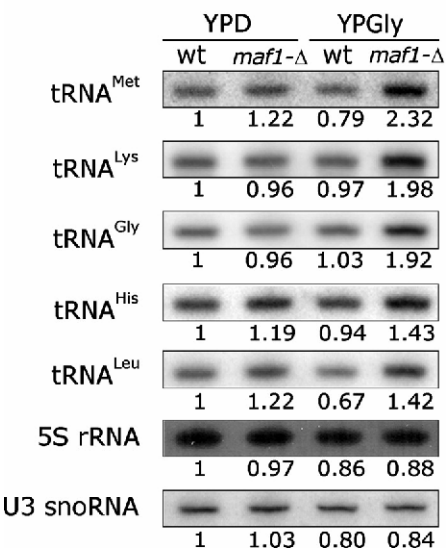

Figure 4. Inactivation of *MAF1* leads to tRNA accumulation that is increased during cell growth on nonfermentable carbon sources. Cells with inactivated Maf1 grown in glycerol medium (YPGly) at 37°C have markedly higher levels of each type of tRNA tested, compared to WT cells, although this increase is different for the individual tRNA species. Northern blotting analysis. RNA from WT and *maf1*Δ cells (YPH500 *S. cerevisiae* strain) were separated on polyacrylamide gels, followed by hybridization using labeled oligonucleotide probes complementary to various tRNAs, 5S rRNA and U3 snoRNA. Numbers below represent quantification of the relative levels of each RNA present in WT and *maf1*Δ cells grown in glucose (YPD) and glycerol-containing medium (YPGly). Adapted from Ciesla *et al.,* 2007.

cells (Nguyen *et al.,* 2010). Cells lacking Maf1 exhibit elevated tRNA synthesis and are more sensitive to HU-directed replication stress.

These results have shown that *S. cerevisiae* cells require Maf1 to achieve Pol III repression and that Maf1 mediates multiple signals for Pol III regulation.

In human cells, Maf1 seems to play a similar role as in *S. cerevisiae*, mediating Pol III repression. At least Reina *et al.* (2006) show that in response to MMS and rapamycin, knock-down of Maf1 diminishes repression of Pol III.

Moreover, novel unpublished data on *D. melanogaster* Maf1 ortholog show an important global Maf1 effect on cellular growth and cell maintainance. Similarly to mammalian and *S. cerevisiae* cells, in *D. melanogaster* cells inhibition of tRNA synthesis occurs in response to nutrient deprivation in correlation with TOR (Target of rapamycin) signaling pathway inhibition. Moreover, in *D. melanogaster,* Maf1 was shown to regulate the development of larvae in response to nutrient availability. Diminished expression of Maf1 by RNA silencing (siRNA) caused increased tRNA levels, in spite of TOR inhibition induced by starvation. This correlated not only with faster larvae development, but also with their increased sensitivity and lower survival in response to starvation (Rideout and Grewal, 2010 – data unpublished).

The mechanism of Pol III regulation by Maf1 affects several components of Pol III transcription apparatus. One of the phenomena occurring during regulation of Pol III activity is a physical interaction of Maf1 with Pol III largest subunit, C160. This was initially demonstrated by overexpression of the C160 N-terminal fragment, which led to suppression of *maf1-1* temperature-sensitivity on a nonfermentable carbon source (Boguta *et al.,* 1997). Further investigations provided some more evidences for the observed genetic interaction. Mutations in *RPC160* (gene encoding C160) were obtained and described as spontaneous suppressors of *maf1-1* and *maf1*Δ (Pluta *et al.*, 2001). Also, co-immunopurification experiments revealed that *S. cerevisiae* Maf1 in cell extracts associates, directly or indirectly, with C160. Pull-down experiments have revealed that *S. cerevisiae* Maf1 interacts, most probably directly, with the N-terminal domain of C160 (235 residues) (Oficjalska-Pham *et al.*, 2006) and weakly but specifically with Brf1 (TFIIIB – related factor), a subunit of Pol III transcription initiation factor TFIIIB (Desai *et al.,* 2005) involved in recruitment of Pol III to promoters. Desai *et al.* (2005) postulated that repression of Pol III by Maf1 occurs as a two step process: by blocking the assembly of the TFIIIB–DNA complex and subsequently by recruitment of Pol III to pre-existing TFIIIB–DNA complexes.

Similar results supporting the hypothesis of interaction with components of Pol III, were obtained for human Maf1. Co-immunoprecipitation experiments indicated that human Maf1 interacts with Rpc1 (the largest subunit of Pol III – reported as C160 in *S. cerevisiae* cells), Brf1 (*S. cerevisiae* Brf1 homologue) and Brf2 (a subunit of the TFIIIB complex required for transcription of U6 snRNA, 7SK and H1 genes) (Reina *et al.*, 2006; Rollins *et al.*, 2007; Goodfellow *et al.*, 2008).

In yeast *S. cerevisiae,* inhibition of Pol III activity by Maf1 was studied also in conditions involving the nutrient-sensing signal transduction pathway and during stationary growth phase.

Inhibition of Pol III occurs during stationary growth phase or under rapamycin treatment, which mimics nutrient deprivation. It was estimated that the level of Pol III-dependent transcription decreases up to 10-20% after a 25-min. induction by rapamycin (Harismendy *et al.*, 2003; Roberts *et al.*, 2003). In the stationary growth phase, down-regulation of Pol III transcription occurs by decrease in Pol III, Brf1 and Bdp1 (subunits of Pol III transcription factor - TFIIIB) recruitment to class III genes as shown by ChIP on chip analysis (Harismendy *et al.,* 2003; Oficjalska-Pham *et al.,* 2006). In the absence of Maf1, Pol III occupancy on class III genes strongly increases compared with the exponential phase of growth, Brf1 is present at similar levels while the presence of Bdp1 is slightly affected with very vivid Pol III-dependent transcription to (Oficjalska-Pham *et al.,* 2006). Under rapamycin treatment, Pol III and TFIIIB (Brf1 and Bdp1) occupancy on class III genes decreases in control cells, while in cells lacking Maf1 the occupancy decreases slightly or does not change. Moreover, Maf1 occupancy on class III genes is increased during cell starvation (rapamycin treatment, nutrient deprivation) as shown by Oficjalska-Pham *et al.* (2006) and Roberts *et al.* (2006). In addition, interaction of Pol III with Maf1 is increased after treatment with rapamycin or in the stationary phase of growth (Oficjalska-Pham *et al.*, 2006).

All these results show that independently from the pathway inducing the down-regulation of Pol III transcription, Maf1 acts in a similar way by affecting directly the assembly of TFIIIB onto class III genes promoters and recruitment of Pol III to the transcription initiation complex.

The activity of Maf1 is regulated at posttranslational level by phosphorylation that occurs in favorable conditions (Oficjalska-Pham *et al.,* 2006; Moir *et al.,* 2006; Willis and Moir, 2007). Furthermore *S. cerevisiae* Maf1 was shown to serve as a target for either PKA or Sch9 kinases (Lee *et al.,* 2009; Huber *et al.,* 2009). Huber *et*

al. (2010) have demonstrated predominant role of the Sch9 kinase in Maf1 phosphorylation in normally growing *S. cerevisiae* cells and Maf1-dependent Pol III down-regulation *via* Sch9 inhibition. Maf1 contains six motifs fitting the R(R/K)xS consensus, which is often attributed to AGC family kinases (S90, S101, S177, S178, S209 and S210) Huber *et al.* (2010) in an *in vitro* assay indicated these sites, and additionally S179, as a targets for the Sch9 kinase.

In exponentially growing *S. cerevisiae* cells, Maf1 is phosphorylated and migrates as several bands corresponding to different phosphorylation states on modified SDS/PAGE polyacrylamide gels (Oficjalska-Pham *et al.*, 2006). Different stress conditions, like rapamycin, stationary phase, chlorpromazine (CPZ), methyl methane sulfonate (MMS) or nutrient depletion that induce down-regulation of Pol III transcription, causes dephosphorylation of Maf1 and its migration as a single band, which is interpreted as a fast-migrating dephosphorylated form (Oficjalska-Pham *et al.*, 2006; Roberts *et al.*, 2006; Moir *et al.*, 2006). Maf1 interacts with Pol III in its dephosphorylated form (Fig. 5, Oficjalska-Pham *et al.*, 2006; Roberts *et al.*, 2006, Huber *et al.,* 2009), which indicates phosphorylation as a form of regulating Maf1 activity.

Similarly to *S. cerevisiae* Maf1, human Maf1 also exhibits phosphorylation-dependent activity. It was shown that, the inactive form of human Maf1 remains phosphorylated (Reina *et al.*, 2006; Rollins *et al.*, 2007; Goodfellow *et al.*, 2008; Michels *et al.,* 2010). The human Maf1 is phosphorylated on serines: S60, S68 and S75 (*nota bene*: amino acids positions in human Maf1 are not the same for *S. cerevisiae* Maf1), by mTORC1 kinase (Michels *et al.,* 2010; Shor *et al.,* 2010; Kantidakis *et al.,* 2010). After treatment of human cells with rapamycin, Torin1 or MMS, Maf1 is dephosphorylated and migrates as a single fast-migrating form, in contrast, to unaffected cells presenting additional slow-migrating bands.

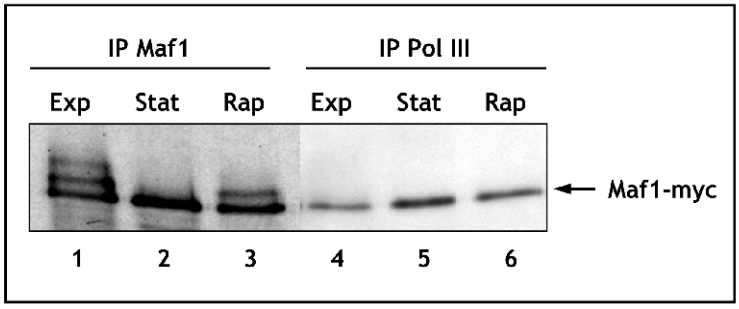

Figure 5. Pol III-Maf1 interaction increases in stress conditions. Maf1 is phosphorylated, but only the dephosphorylated form of Maf1 interacts with Pol III. Western blot analysis using a modified acrylamide:bisacrylamide ratio SDS-PAGE of Maf1-myc immunopurified from exponential phase (Exp.), stationary phase (Stat.), or rapamycin-treated (Rap.) cells (IP Maf1, lanes 1–3) and of Maf1-myc co-immunopurified with C160 from the same cells (IP Pol III, lanes 4–6). Adapted from Oficjalska-Pham *et al.,* 2006.

The dephosphorylated form of human Maf1 like *S. cerevisiae* Maf1 interacts with Pol III (Reina *et al.*, 2006).

S. cerevisiae Maf1 is also dephosphorylated under respiratory growth conditions, which are induced by the change from fermentable (glucose) to nonfermentable (glycerol) carbon source. Transfer from glucose to glycerol medium results in Maf1 dephosphorylation (Ciesla *et al.,* 2007). Re-transition of *S. cerevisiae* cells to glucose medium, is followed by Maf1 re-phosphorylation (Fig. 6, Towpik *et al.,* 2008).

The phosphorylation state of Maf1 is correlated with its cellular localization. In exponentially growing *S. cerevisiae* cells, Maf1 is phosphorylated and is present at the same concentration in the cytoplasm and the nucleus, as observed by immunofluorescent microscopy. Different stress conditions, treatment of cells with rapamycin, nutrient deprivation, stationary phase or respiratory growth conditions lead to dephosphorylation and nuclear concentration of Maf1, which is associated with repression of Pol III-dependent transcription (Oficjalska-Pham *et al.*, 2006; Roberts *et al.*, 2006; Moir *et al.*, 2006; Towpik *et al.,* 2008). Dephosphorylation of PKA/Sch9 sites that occurs under rapamycin treatment, correlates with Maf1 relocation into the nucleus (Moir *et al.,* 2006; Huber *et al.,* 2009). However, it is not known whether dephosphorylation precedes, follows or is simultaneous with import of Maf1 into the nucleus (Moir *et al.,* 2006).

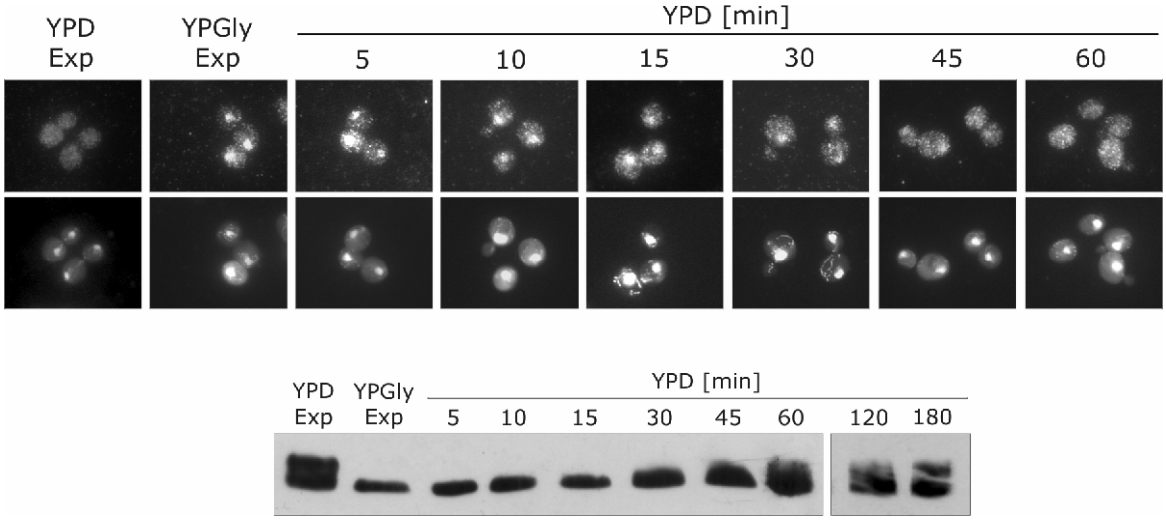

Figure 6. Maf1 is re-phosphorylated and exported out of the nucleus after transferring cells from respiratory conditions (glycerol medium, YPGly) to glucose medium (YPD). Maf1 becomes dephosphorylated upon transition from glucose to glycerol medium (compare YPD and YPGly lanes), the opposite transition results in gradual Maf1 phosphorylation (compare YPGly and YPD lanes; 5 min to 1 h). Relocation of Maf1 to the cytoplasm in response to glucose appeared to be concomitant with Maf1 hyperphosphorylation. Localization of Maf1 was analyzed by immunofluorescence microscopy using polyclonal anti-Maf1 antibodies. Nuclei were stained with 4,6-diamidino-2-phenylindole (DAPI) (top panel). Crude extracts prepared from the same cells by trichloroacetic acid precipitation were analyzed using SDS-PAGE with a modified acrylamide:bisacrylamide ratio, followed by immunoblotting with polyclonal anti-Maf1 antibodies (bottom panel). The slower-migrating diffuse band corresponds to phosphorylated forms of Maf1. Adapted from Towpik *et al.,* 2008.

Nuclear import of *S. cerevisiae* Maf1 is directed by two nuclear localization sequences (NLS1 and NLS2). Activity of the N-terminal NLS (NLS1) was proposed to be regulated *via* phosphorylation, while the C-terminal NLS is regulated independently of the phosphorylation state (Moir *et al.,* 2006). The accumulation of Maf1 in nucleus due to the lack of the Msn5 exportin protein is not sufficient to cause Pol III repression in the absence of additional factors that are triggered by cellular signaling pathways. Moreover, Maf1 was dephosphorylated and phosphorylated normally in the *msn5*Δ mutant and Pol III was under proper regulation (Fig. 7, Towpik *et al.,* 2008).

Recent investigations point that Maf1 localization does not depend only on shuffling between the nucleus and the cytoplasm, but also its presence in the nucleolus is detectable and has a crucial role for Maf1 activity in pathway involving TOR (Target of rapamycin) (Wei *et al.,* 2009). TOR is an evolutionarily conserved P13K-related kinase and a central regulator of cell growth found originally in *S. cerevisiae* (Heitman *et al.,* 1991). TOR proteins form two functional complexes: TOR complex 1 (TORC1) and TOR complex 2 (TORC2) (Loewith *et al.,* 2002). The anticancer drug - rapamycin inhibits specifically TORC1. TORC1 regulates a broad spectrum of growth-related processes, including ribosome biogenesis and protein translation (Wullschleger *et al.,* 2006). TORC1 is a major regulator of transcription in *S. cerevisiae*, counting all ribosomal genes transcribed by the three major RNA polymerases (Warner, 1999; Moss and Stefanovsky, 2002). Rapamycin (by

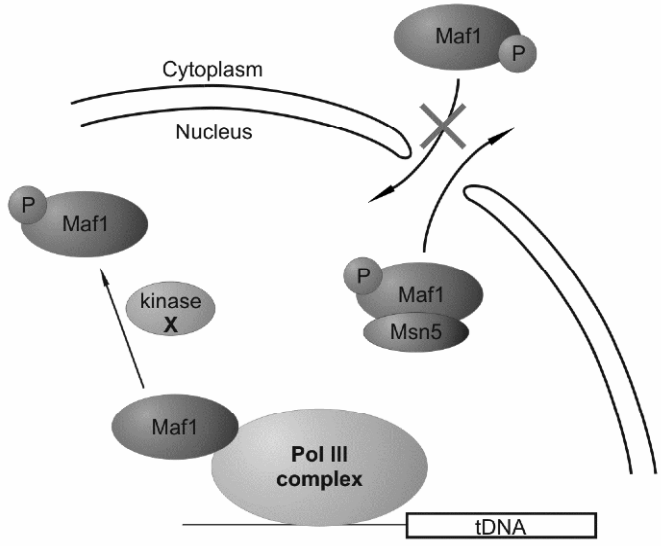

Figure 7. Model of Maf1 regulation during transfer of *S. cerevisiae* cells from respiratory conditions to glucose. In response to the shift of respiratory growing culture to medium with glucose, nuclear Maf1 is phosphorylated (P) by an unknown kinase (X). Phosphorylation of Maf1 prevents its interaction with Pol III and enables binding to the Msn5 carrier and export out of the nucleus. In parallel, protein kinase A-directed phosphorylation at different sites prevents nuclear import of the cytosolic Maf1. Adapted from Towpik *et al.,* 2008.

approaching TORC1) and nutrient starvation cause rapid repression of the TOR signaling pathway in correlation with ribosomal genes repression.

Wei *et al.* (2009) showed that TORC1 (TOR complex 1) indirectly regulates synthesis of tRNA by Pol III through Maf1 phosphorylation. Moreover, TORC1 regulates Maf1 translocation from the nucleoplasm to the nucleolus, a subnuclear compartment, in which, 5S rDNA is transcribed by Pol III. Maf1 is normally excluded from nucleolus. Inhibition of TORC1 by rapamycin promotes Maf1 nucleolar localization and association with 5S rDNA, a Pol III transcribed chromatin.

The scheme of Maf1-dependent Pol III transcription regulation in response to nutrient availability is presented on Figure 8. The graphic presentation shows also the simultaneous regulation of Pol I, which is coordinated at the same time by TORC1 effector, common for all eukaryotic RNA polymerases,.

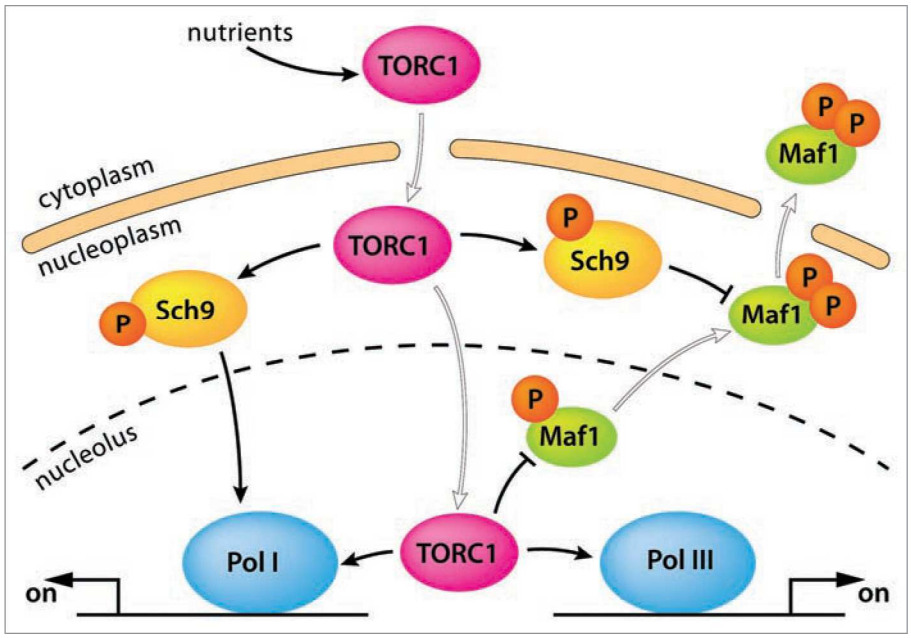

Figure 8. Model of Pol III transcription regulation mediated by Maf1 in response to nutrient depletion. TORC1 regulates simultaneously Pol I and Pol III according to nutrient availability. Sch9 partially mediates TORC1 signaling to activate Pol I and Pol III transcription by the nutrients. In the presence of nutrients TORC1 promotes Pol I and Pol III transcription in the nucleolus and phosphorylates Maf1 preventing its negative effect on Pol III . Additionally, TORC1 activates Sch9 and uses Sch9 to phosphorylate Maf1 in the nucleus and promote its export to the cytoplasm. Bold lines, activation/repression; empty lines, changes in localization (from Boguta, 2009).

2. Search of evolutionarily conserved domains within the Maf1 sequence.

The *Saccharomyces cerevisiae MAF1* gene (Boguta *et al.,* 1997) encodes a hydrophilic protein of 395 amino acids (aa) rich in serine and asparagine residues with a predicted molecular mass of 44.7 kDa. Comparison of the *S. cerevisiae* Maf1 sequence with multiple databases using the BLAST server revealed more than a hundred orthologs in humans, animals (50), plants (28) and lower eukaryotes (27). No potential prokaryotic orthologs were identified. Although eukaryotic Maf1 differ in molecular mass, ranging from 26 kDa (*S. pombe*, *H. sapiens*) up to 45 kDa (*S. cerevisiae*) (Willis *et al.*, 2004), they all share a common organization pattern.

The family of Maf1 proteins contains three phylogenetically conserved sequence regions, labeled A, B and C (Pluta *et al.,* 2001). The C-terminal acidic tail is present in most Maf1 orthologs. Similarity of Maf1 sequences is presented in Figure 9 (Gajda *et al.,* 2010). A short distance of approximately aa 10 between B and C segments is constant in evolution, with the exception of *A. nidulans* (showing insertion of aa 15), therefore this region could be considered as a single domain and is referred hereafter as the BC domain. In contrast, the space between A and B regions is different between species. A and BC domains are fused in *E. cuniculi*, whereas yeast *S. cerevisiae* and *C. glabrata* Maf1 orthologs have long linkers of aa 182 and aa 174, respectively. Within the BC domain, signature sequences indicative of the Maf1 protein family can be identified (PDYDFS and LWSFnYFFYNKklKR, Fig. 9) (Pluta *et al.,* 2001). Interestingly, in the majority of Maf1 orthologs, the second motif includes a nuclear targeting signal, proven to be functional in *S. cerevisiae* Maf1 (Moir *et al.,* 2006). The PSORT program found in *S. cerevisiae* Maf1 two possible nuclear targeting signals: KRRK (position 204, NLS1) and a double signal RKRK-KRKR (positions 327 and 328, NLS2) (Pluta *et al.,* 2001).

Despite numerous data on Maf1, no functional information has been obtained from its amino acid sequence due to lack of significant homology with protein domains of known function.

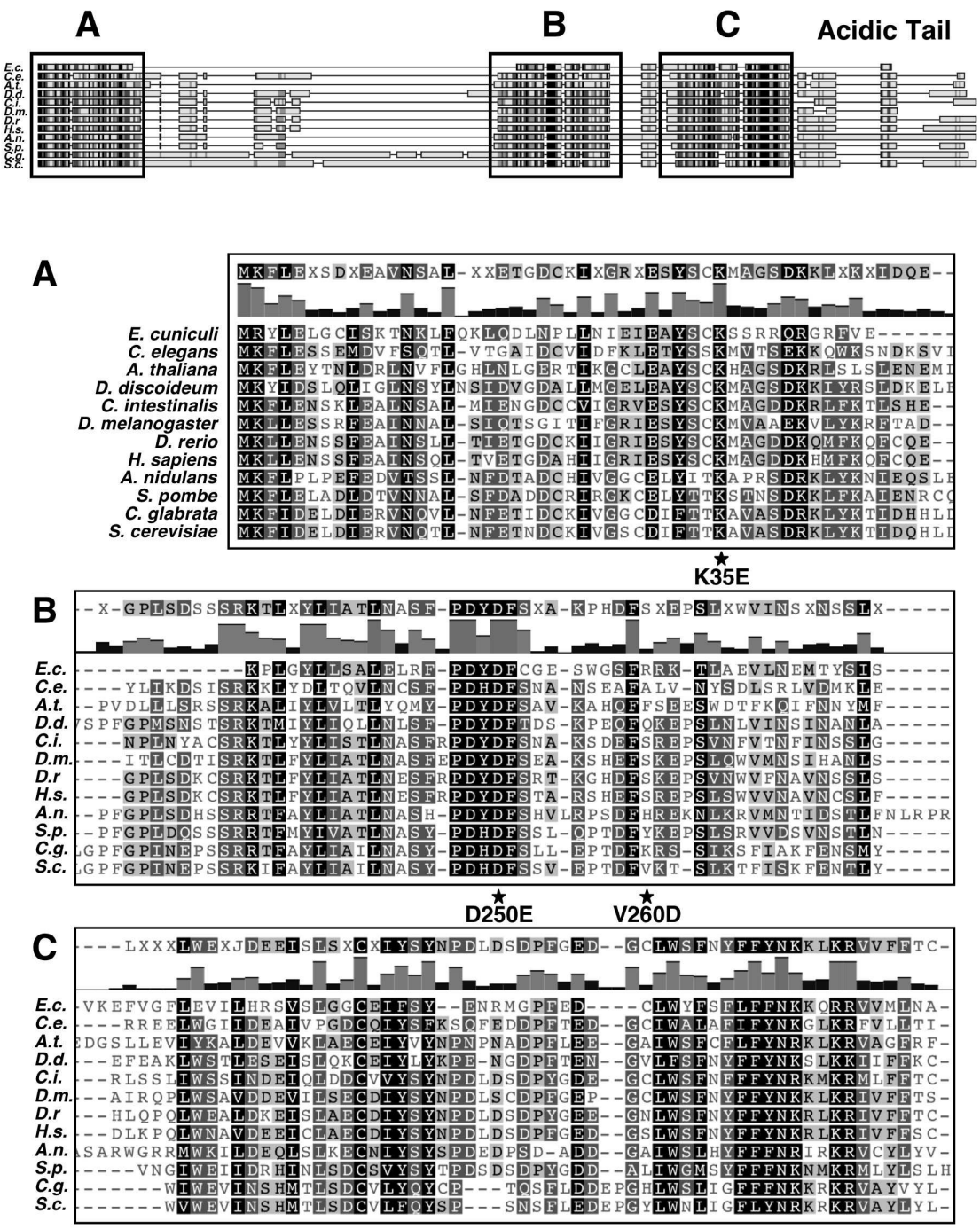

Figure 9. Alignment of Maf1 sequences. Schematic representation of Maf1 protein sequences from different species: *Encephalitozoon cuniculi* (gi|19069247|, size: 161 aa), *Caenorhabditis elegans* (gi|17506011|, size: 245 aa), *Arabidopsis thaliana* (gi|22326767|, size: 224 aa), *Dictyostelium discoideum* (gi|66816633|, size: 278 aa), *Ciona intestinalis* gi|198415188|, size: 233 aa), *Drosophila melanogaster* (gi|46409204|, size: 226 aa), *Danio rerio* (gi|47087413|, size: 247 aa), *Homo sapiens* (gi|49065352|, size: 256 aa), *Aspergillus nidulans* (gi|67901388|, size: 314 aa), *Schizosaccharomyces pombe* (gi|254745531|, size: 238 aa), *Candida glabrata* (gi|49529111|, size: 391 aa) and *Saccharomyces cerevisiae* (gi|1170854|, size: 395 aa). Protein sequences have been aligned with MUSCLE multiple alignment software (41) and the figure created with Geneious Pro 4.5.4 software. Conserved domains are boxed and labeled by letters: A, B and C on the upper panel. Sequence alignments of each conserved domain (A, B and C) are shown in the lower panel. Histograms above the alignments indicate the percentage of identity among the sequences. Consensus sequences are shown above the alignments. Positions of K35E, D250E and V260D mutations are indicated by a star below the alignments (N344I mutation is located 6 aa after the end of the BC domain and therefore is not represented).

Classical methods of analyzing protein sequences focus on the detection of the highest amino acids identity.

If the sequence of a protein with unknown structure is similar to one with known architecture, it is assumed, that the fold of the main polypeptide chain will share the same conformation. If the similarity between two sequences is statistically high this method may be very efficient. Yet in case of sequences with low similarity this method is not valuable, although differences between the investigated sequences may not imply any important differences in the three-dimensional (3D) folding of the proteins. This can be explained by the fact that sequence alignments compare whole amino acid sequences but do not take into account neither the formation of regular secondary structures by some sets of sequences and the concomitant spacial architecture of the protein imposed by the solvent, nor the biochemical properties of amino acids composing the polypeptide chain (Gaboriaud *et al.,* 1987).

The HCA (Hydrophobic cluster analysis) is an unconventional, highly efficient and sensitive method of analyzing protein sequences. HCA serves as a powerful tool to investigate the three-dimensional (3D) structure of a protein. Furthermore, it provides data to understand features of protein stability and folding (Callebaut *et al.,* 1997). The idea of HCA was firstly reported by Gaboriaud *et al.* (1987) and Lemesle-Varloot *et al.* (1990). It originates from a two-dimensional (2D) helical representation of protein sequence and focuses on the presence of possible hydrophobic clusters formed by internal hydrophobic residues in amino acid sequence.

The principles of HCA analysis are based on simple biological phenomena of hydrophobic and hydrophilic molecular entities that behave in a regular manner. Mostly hydrophobic amino acids dominate the internal core, while mostly hydrophilic amino acids lie on the protein surface to protect the core from solvent (water, ions). This dichotomic behaviour of hydrophobic and hydrophilic residues is due to the fast escape of hydrophobic amino acids from water under the pressure of entropic and enthalpic forces. In consequence, the hydrophobic amino acids create stable and compact structures that are typical for a particular fold. These structures are called clusters (Callebaut *et al.,* 1997). Clusters of hydrophobic amino acids are statistically found in close correspondence with the internal features of regular secondary structures (Woodcock *et al.,* 1992). Hydrophobic amino acids are known to be favored within the internal faces of regular secondary structures (α-helices and β-strands) and disfavored within the main irregular

secondary structures (loops) (Eudes *et al.,* 2007). The HCA analysis divides amino acids into two main classes: the hydrophobic ones and the others, which are hydrophilic and/or indifferent to their environment.

The hydrophobic amino acids are devided into two groups: strong hydrophobic amino acids (valine (V), isoleucine (I), leucine (L), phenylalanine (F)), which have the major impact on creating hydrophobic internal features of secondary structures and moderately hydrophobic amino acids (methionine (M), tryptophan (W), tyrosine (Y)) that may be exposed or semi-exposed to the outer surface. Tryptophan and tyrosine are thought to mediate often intermolecular interactions and tyrosine often favors loop formation. In HCA strong and moderately hydrophobic amino acids are grouped together and are highlighted as a hydrophobic clusters. Proline (P) due to distinctive cyclic structure of its side chain, acts as a structural disruptor in the middle of regular secondary structure elements, such as α-helices and β-strands. However, proline is commonly found as the first residue of an α-helices as well as on the boundaries of β-strands. Proline is also commonly localized in turns, which may account for the curious fact that proline is usually solvent-exposed, despite having a completely aliphatic side chain. In HCA, proline is currently considered to be a cluster breaker. All the other amino acids are considered as a single class of residues that have a minor impact on the development of hydrophobic clusters. Although these amino acids are regarded as a neutral for the formation of hydrophobic cores, they share some specific properties. For example arginine (R) and lysine (K), both, are polar amino acids with a long aliphatic stems. Sometimes these amino acids substitute hydrophobic amino acids, in situation when, their heads reach a polar environment (solvent or ionic pairs). Asparagine (N) can adopt a left helical main chain conformation otherwise mainly occupied by glycine (G). Alanine (A) occupies both hydrophobic and hydrophilic areas although it favours forming α-helices. Cysteine (C) is regarded as a nonpolar, hydrophobic residue, which suggests its participation in group of hydrophobic cluster formers. However, its ability to form disulphide bonds is a factor that excludes cysteine from mentioned group and its presence in polypeptide chain is always worth detailed consideration when analyzing the possible 3D structure of a protein. Threonine (T), a branched amino acid, frequently replaces valine (V) or isoleucine (I) in β-strands and, like serine (S), may mask its polarity inside α-helices. Serine is thought to mimic proline rings. Glutamic acid (E) and aspartic acid (D) are polar amino acids occupying hydrophilic areas (Callebaut *et al.,* 1997).

In summary, the main driving forces of regular secondary structures are strong hydrophobic amino acids (V, I, L, F) as well as moderately hydrophobic amino acids (M, Y, W), while the main driving forces of loops are P, G, D, N and S.

To make the representation of protein structures more clear and understandable by avoiding too many one-letter code symbols, HCA uses four symbols for particular amino acids: a star for proline (P), which has the greatest influence on the polypeptide chain, a diamond for glycine (G), which, in contrast, does not have a great impact on the conformation of the chain, squares with or without a dot - for serine (S) and threonine (T) respectively, which despite sharing polar properties, may mask their polarity by creating H-bonds with the carbonyl groups of the main chain, particularly within helices.

The main principles of HCA presentation are explained on the example of human α1-antitrypsin (Callebaut *et al.,* 1997, Fig. 10). The G246-S283 fragment of human α1-antitrypsin is displayed as a α-helix (3,6 aa per turn) formed on a cylinder (Fig. 10a). Residues from G246 to E264 have similar positions, which are parallel to the axis of the cylinder. Subsequently the cylinder has been cut to its axis and unrolled (Fig. 10b). Unfolding of the cylinder separates some adjacent amino acids. In order to preserve the natural environment of all residues and give a better impression of the sequence, the representation has been duplicated (Fig. 10c). Hydrophobic residues have been contoured (Fig.10d).

Hydrophobic amino acids commonly form the previously mentioned clusters. These clusters correspond to regular secondary structures (Woodcock *et al.,* 1992). The vertical clusters, as shown experimentally, are associated with β-strands whereas the horizontal ones are mostly α-helices. This points the connection between the general shape of the cluster that indicates particular secondary structure. Between recognizable group of clusters there may occur visible stretches of sequences that are revealing a presence of loops or unstructured regions between the protein's domains. The 2D α-helical presentation of hydrophobic clusters matches best match the observed regular α or β secondary structures of globular proteins.

The HCA analysis of *S. cerevisiae* Maf1 reveals the presence of two highly structured regions, corresponding to the A and BC domains, which are separated by unstructured region, matching to the linker region between Maf1 domains. This linker region is poor in hydrophobic residues suggesting that *in vivo* it might be exposed on the outer surface, during protein folding. Moreover, comparison of the HCA analysis for the *S. cerevisiae* and *H. sapiens* Maf1 proteins, reveals their

similar organization indicative of the high conservation of these folds through evolution (Fig. 11).

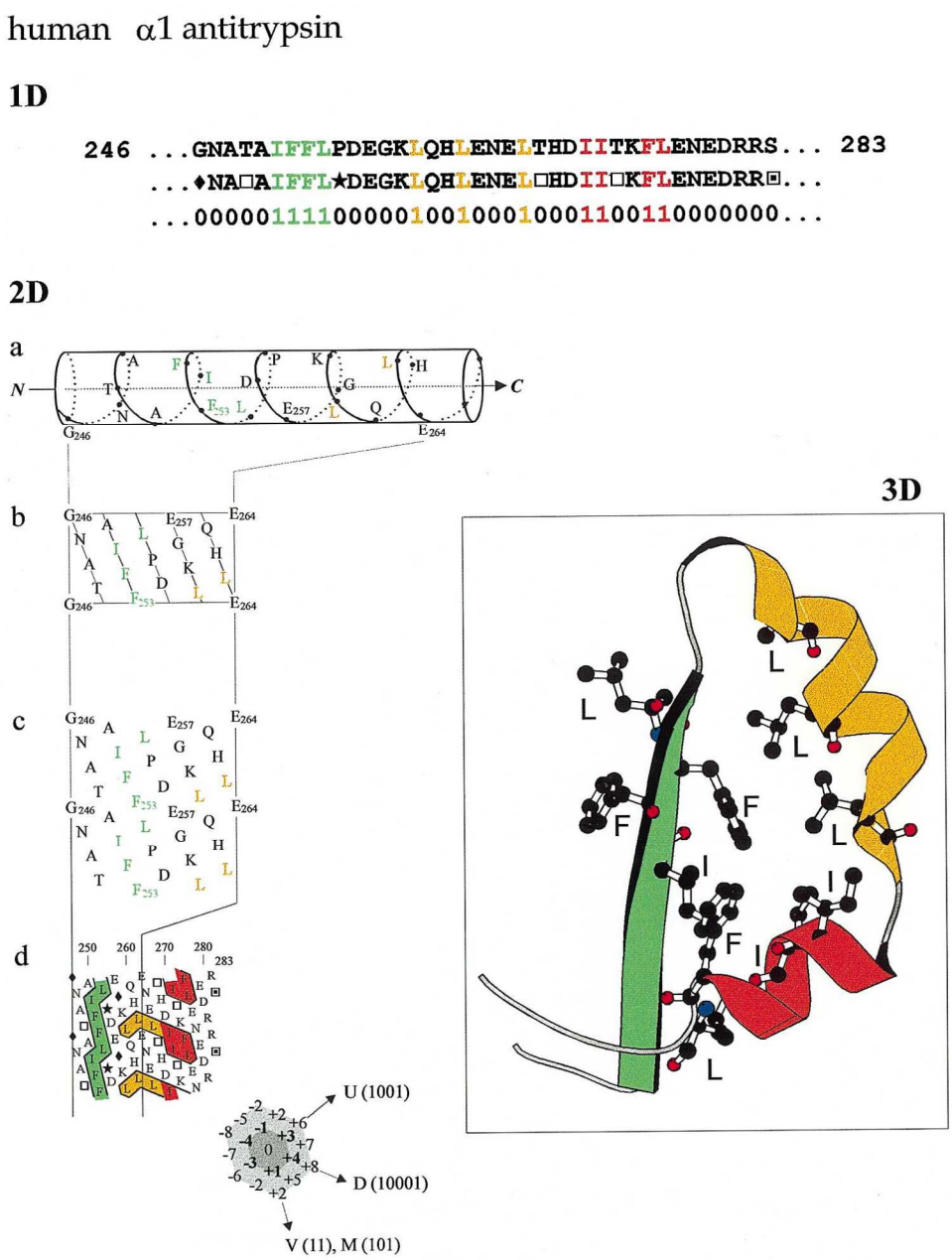

Figure 10. The main principles of HCA 2D presentation. (Adapted from Callebaut *et al.*, 1997).

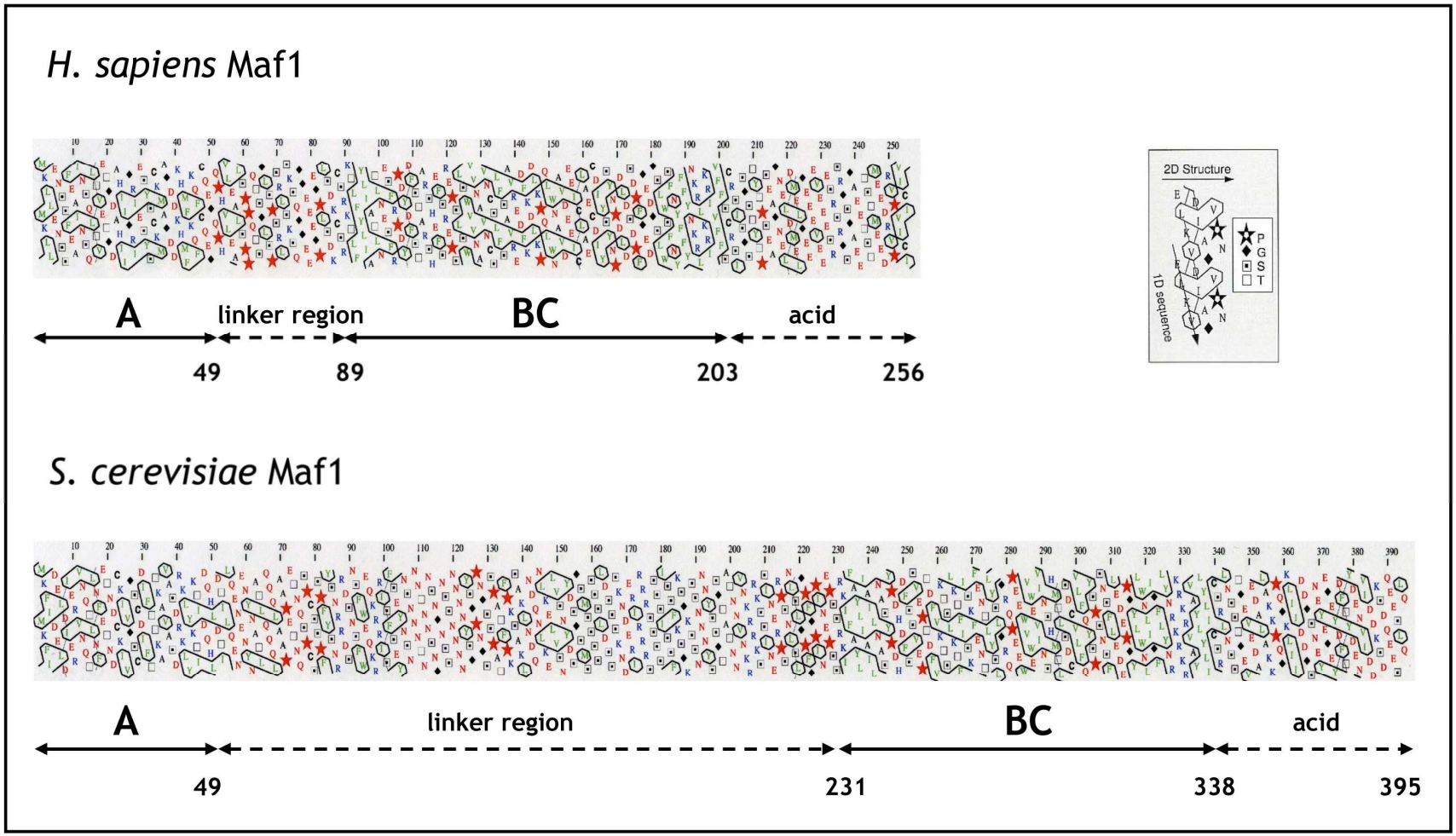

Figure 11. Hydrophobic Cluster Analysis (HCA) of Maf1 sequences. Schematic representation of predicted 3D structure of the *S. cerevisiae vs H. sapiens* Maf1 proteins. Red star indicates proline, diamond – glycine, squares with or without a dot – serine and threonine, respectively. Acidic residues (E, Q, N) are in red, basic residues (K, R) are in blue. Hydrophobic amino acids form clusters shown as green contoured areas). Vertical clusters correspond to β-strands whereas horizontal clusters are associated with α-helical structures. For further information see Callebaut *et al.,* 1997. Localization of the A and BC domains of Maf1 is indicated with black arrows.

If the crystal structure of a protein is unavailable as in the case of Maf1 there is still a possibility to presume its structural organization. The bioinformatic field provides a wide range of different software tools for predicting a variety of protein structural features, such as secondary structures (e.g. PSIPRED), a presence of natively disordered regions (e.g. DISOPRED2) as well as boundaries of protein domains (e.g. DomPred). One of the most popular servers, the PSIPRED server, has been developed in the Bioinformatics Unit at the University College London. It consists of several independent servers dedicated to characterizing the protein features mentioned above as well as predicting of protein folds (e.g. mGenTHREADER), transmembrane helix topology (e.g. MEMSAT2) and 3D models of tertiary structures (e.g. BioSerf) (Bryson *et al.,* 2005).

PSIPRED is a highly accurate secondary structure prediction method based on the PSI-BLAST (Position Specific Iterated BLAST) (Altschul *et al.,* 1997) output. PSIPRED has been estimated to achieve an average accuracy of 76,5%, which places this method among the most accurate softwares for predicting the secondary structure of the proteins. The PSIPRED server, apart from, the pure data analysis provides also a graphical representation of the secondary structure prediction, which makes the output visible and clearl to understand by the user (McGuffin *et al.,* 2000). Comparison of *S. cerevisiae* and *H. sapiens* Maf1 sequences, according to PSIPRED analysis, revealed highly similar organization of secondary structures. In the A domain, PSIPRED prediction indicated the presence of two α-helices separated by two adjacent β-strands, while for the BC domain - five α-helices and concomitant four β-strands are predicted (Fig. 12). No secondary structure elements were predicted for the linker region.

The DISOPRED2 server is commonly used for prediction of unstructured regions called regions of native disorders (http://bioinf.cs.ucl.ac.uk/disopred/). In contrast to PSIPRED, it is devoted to analyzing protein regions, that do not posses any static structures, but are in a constant change between different structures (Bryson *et al.,* 2005). The DISOPRED method was estimated to be one of the best methods of false positive rates. The method has an accuracy of ~93% per residue when using the 5% false positive rate threshold (Ward *et al.,* 2004). Analysis of *S. cerevisiae* Maf1 amino acid sequence showed the presence of two structured regions of approximate localization: aa 1-50 and aa 225-325 (Fig. 13B, lower panel). These regions correspond to the A and BC domains of *S. cerevisiae* Maf1 (aa 1- 49 and aa 231-338 respectively), separated by an unstructured region (aa 50-225) corresponding to the linker region separating Maf1 A and BC domains (aa 49-231).

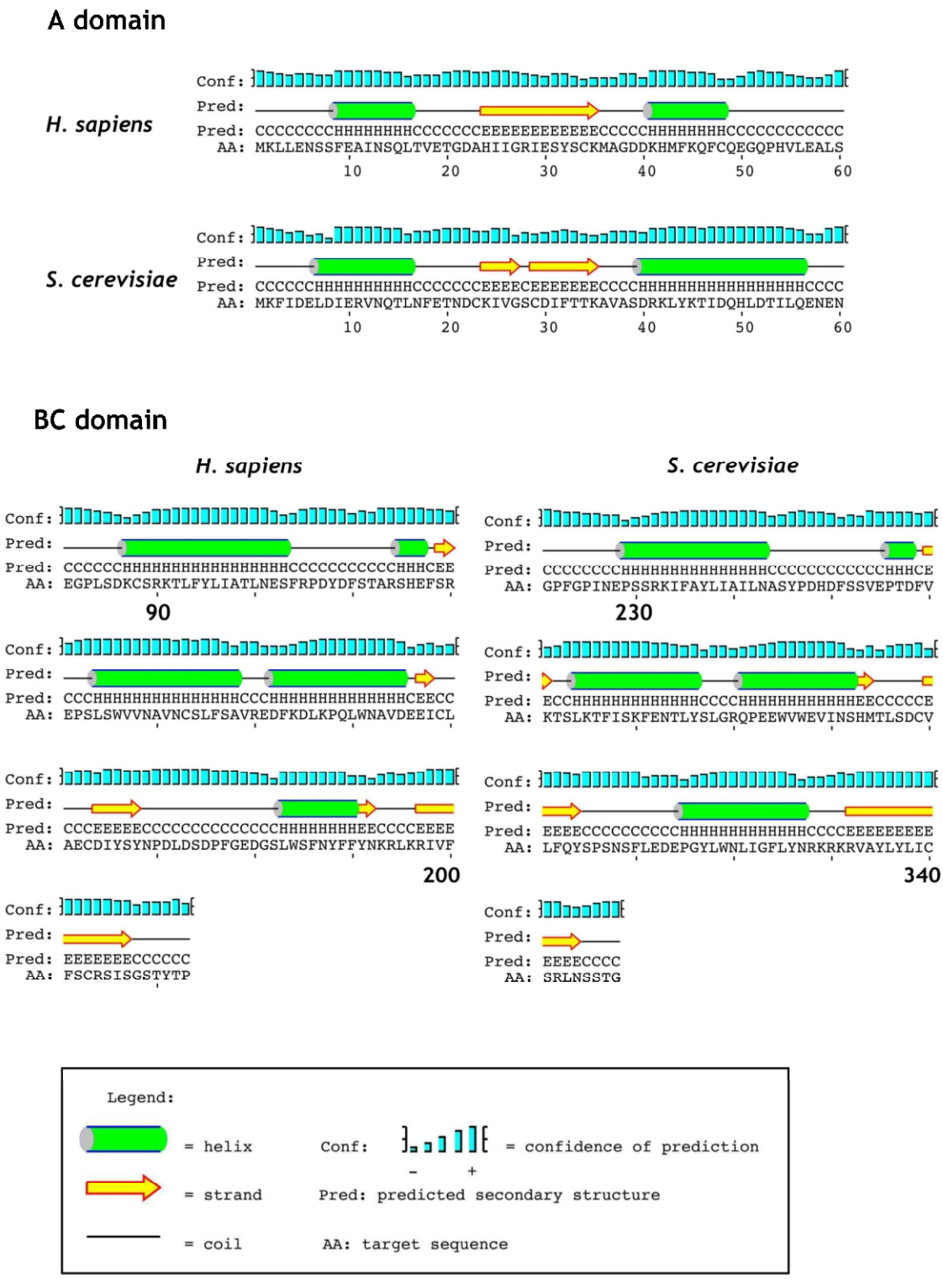

Figure 12. Secondary structure prediction of Maf1 protein. PSIPRED v 2.6 protein structure prediction server was used to identify the secondary structures of *S. cerevisiae* and *H. sapiens* Maf1 proteins. Only A and BC domains are presented. Green tube (or H letter), yellow arrow (or E letter) and black line (or C letter) represent alpha helix, beta strand and coil, respectively.

There is also a visible second unstructured region (aa 340- 395) that is related to the acidic tail of Maf1. Similar analysis of the *H. sapiens* Maf1 sequence revealed its analogous organization to the *S. cerevisiae* Maf1 protein. According to DISOPRED2, *H. sapiens* Maf1 present two structured regions of approximate localization: aa 1-50 and aa 85-210 (Fig. 13A, upper panel). These regions correlate with the position of the A and BC domains of human Maf1 (aa 1-49 and aa 83-203 respectively). The identified structured regions are separated by an unstructured region (aa 50-85), which corresponds to the linker in *H. sapiens* Maf1 localized between aa 49-83. The graphical representation of the protein, reveals also a second unstructured region between aa 210-240, which is related to the acidic tail of *H. sapiens* Maf1 (aa 203-256).

The DomPred (Protein Domain Prediction Server) serves as a tool to predict domain boundaries while predicting the overall fold of the protein (http://bioinf.cs.ucl.ac.uk/dompred)(Marsden *et al.,* 2002). Analysis of the *S. cerevisiae* Maf1 amino acid sequence showed, similarly to the DISOPRED prediction, the presence of 2 domains (Fig. 14B, lower panel). According to the computational analysis, the boundary between the identified domains ranges between aa 100-240. This fragment could in approximate relate to the linker region between the A and BC domains of *S. cerevisiae* Maf1, as indicated by the sequence alignment (Fig. 9). Similar analysis performed for the *H. sapiens* Maf1 revealed different organization of the protein. Indeed, the DomPred software detected the presence of only one obvious domain (Fig. 14A, upper panel), corresponding to the A domain of *H. sapiens* Maf1 (aa 1-49). The fragment ranging from ca. aa 60-100 might be related to the linker region of *H. sapiens* Maf1 (aa 49-83), while the structured region located ca. between aa 100-160 that could correspond to the conserved B domain of *H. sapiens* Maf1. The DomPred software failed to detect the anticipated, conserved remaining C domain, indicating, a “boundary” region (aa 160-190) in its place, instead.

Discrepancies between the DISOPRED and DomPred analyses does not exclude each other, as bioinformatic tools serve mostly as a guide for further genetic or biochemical protein analysis. However, all together, the results of HCA, DISOPRED and DomPred analyses with PSI-BLAST alignments show that Maf1 is organized in two structured regions separated by an unstructured linker.

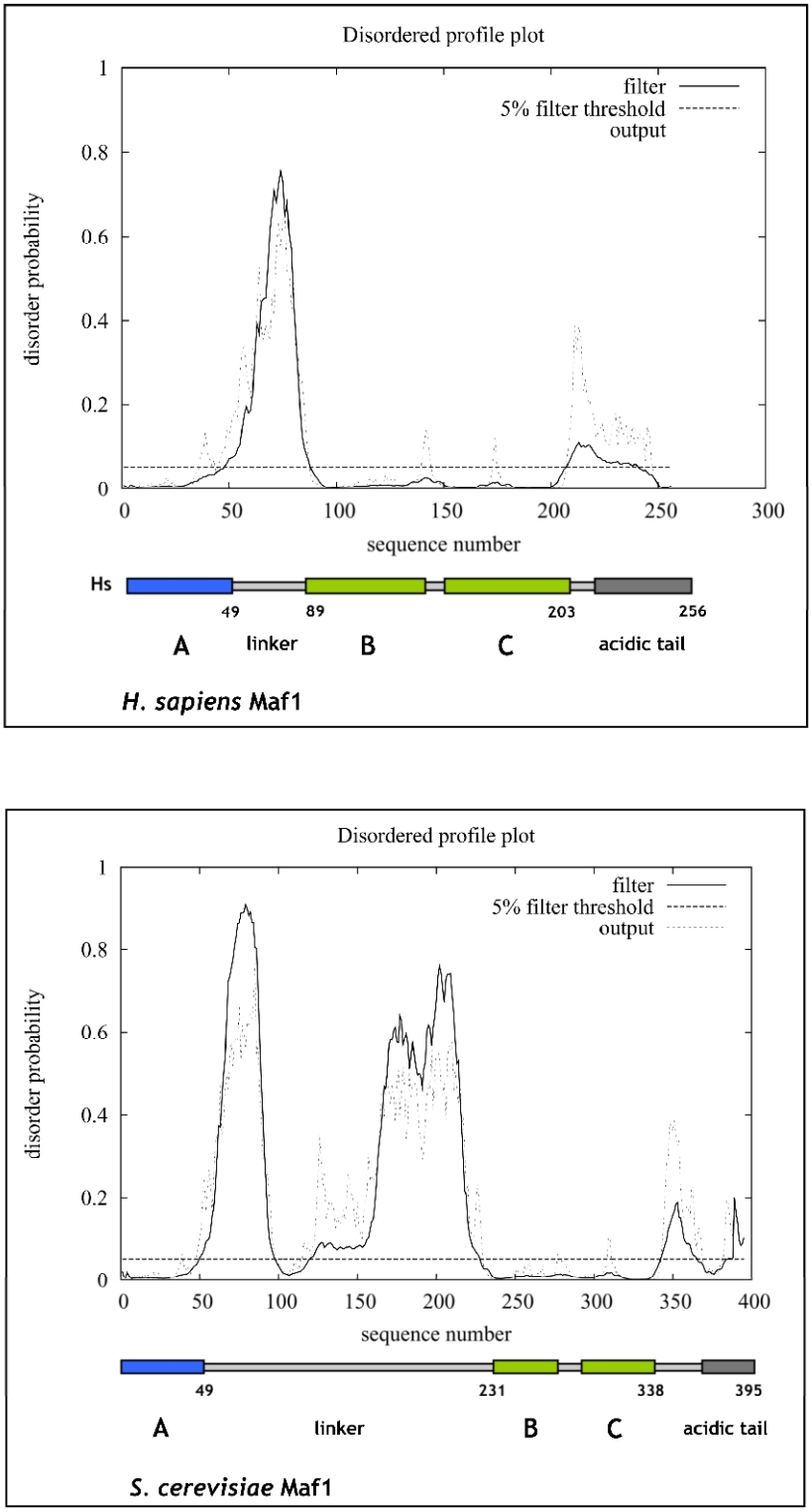

Figure 13. Prediction of unstructured regions in Maf1 sequences. Graphical representation of native disorders existing in the Maf1 protein predicted by DISOPRED2, Prediction of protein disorder server (http://bioinf.cs.ucl.ac.uk/disopred/). False positive threshold is 5%. Visible peacks correspond to the unstructured regions of Maf1. Underneath a schematic representation of Maf1 organization. Upper panel. *H. sapiens* Maf1; the A domain (aa 1-49) is indicated in blue, the BC domain (aa 89-203) is indicated in green color. Lower panel. *S. cerevisiae* Maf1; the A domain (aa 1-49), the BC domain (aa 231-338), indicated as described.

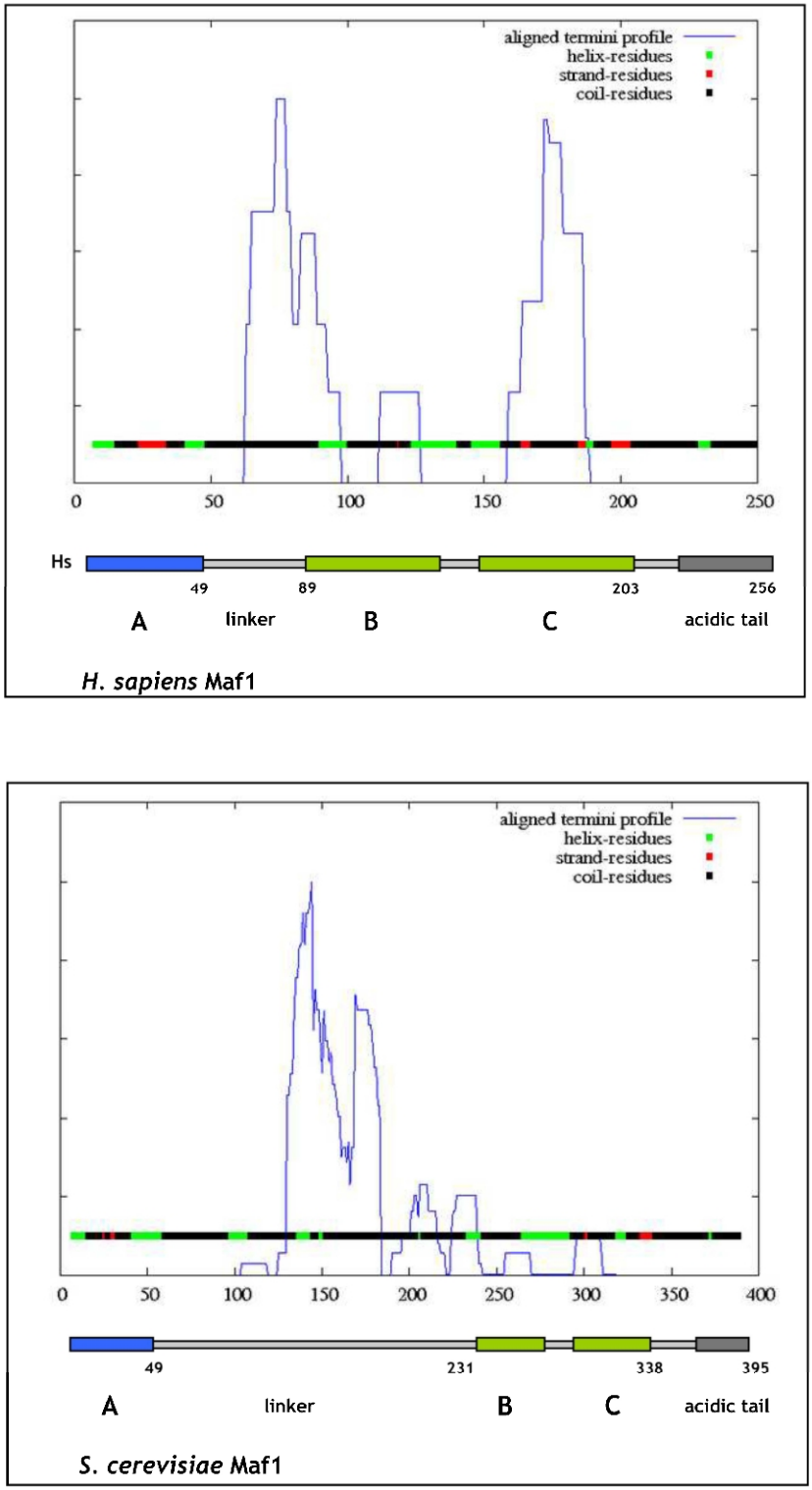

Figure 14. Prediction of domain boundaries in Maf1 sequence. Graphical representation of the domain boundaries existing in Maf1 protein as predicted by DomPred, Protein Domain Prediction Server (http://bioinf.cs.ucl.ac.uk/dompred). Visible peacks correspond to unstructured boundary regions of Maf1 domains. Underneath a schematic representation of Maf1 organization as described in the legend to Fig. 13. Upper panel; *H. sapiens* Maf1. Lower panel; *S. cerevisiae* Maf1.

Apart from bioinformatic analyses, some experimental prerequisites also allow to consider Maf1 as a structured protein, which activity depends on organization of its folds.

First approaches to distinguish the impact of particular parts of Maf1 on its potential to inhibit Pol III activity were made by Desai *et al.* (2005). The group investigated recombinant forms of different orthologs of Maf1: SpMaf1 (full-length protein from *S. pombe* in bacteria) and ScMaf1(B+C) (truncated form of Maf1 from *S. cerevisiae* containing only B and C sequence blocks). Both recombinant forms of Maf1 were able to inhibit tRNA-Leu and U6 snRNA synthesis *in vitro*. In addition, binding of these Maf1 recombinant forms to Brf1 blocked the assembly of TFIIIB onto DNA (Desai *et al.*, 2005). These results suggested that the roles of A, B and C blocks in the activity of Maf1 are not equal. A domain seemed to be unnecessary for inhibition of Pol III-dependent transcription (at least for the *S. cerevisiae* Pol III transcription machinery). Further studies on the functions of Maf1 parts in its activity were investigated in the human ortholog.

Considering the remarkable conservation of the yeast and human Pol III machineries, it could be also imagined, that the regulatory mechanisms involving Maf1 may be similar in yeast and man. Indeed, recent results presented by several research groups show Maf1-mediated repression of Pol III transcription in human cells indicating Maf1 orthologs as a new class of mammalian Pol III regulators (Goodfellow *et al.,* 2008; Reina *et al.,* 2006; Johnson *et al.,* 2007; Rollins *et al.,* 2007).

For the human Maf1, Pol III subunits and Brf1 were shown to associate with different regions of Maf1 (Reina *et al.,* 2006). Two truncated versions of human Maf1, containing only the conserved A domain sequence (Maf1 aa 1-81) or both, the A and B domains, sequences (Maf1 aa 1-142) were investigated for potential interaction with Pol III subunits. The GST pull-down experiment showed that Rpc1 (corresponding to C160 in *S. cerevisiae*) and Rpac2 (corresponding to AC19 in *S. cerevisiae*) were associated with the Maf1 aa 1-81 truncated version. In conclusion, Reina *et al.* (2006) postulated that the first 81 amino acids of human Maf1 are sufficient for its association with Pol III subunits and that the B domain of Maf1 is required for association with Brf1. These results clearly show that there is a link between the structure and activity of the Maf1 protein and that particular Maf1 folds might be involved in different aspects of Maf1 activity as a repressor.

Furthermore, a detailed study over the *H. sapiens* Maf1 (HsMaf1) has been subjected in laboratory of Christoph Műller (Grenoble at that time) with

collaboration with the laboratory directed by Olivier Lefebvre (CEA/Saclay). To experimentally characterize the structural organization of human Maf1 (HsMaf1), they have carried out limited proteolysis experiments in combination with size-exclusion chromatography (Detailed description in supplementary material – Appendix 1, Gajda *et al.,* 2010).

Proteolytically stable fragments are considered to be structurally well defined, whereas protease-sensitive sites often correlate with disordered protein regions. Using limited proteolysis with trypsin, HsMaf1 protein (aa 256) was digested into two major stable fragments that were identified as HsMaf1 aa 1-45 and Maf1 aa 75-234 using a combination of N-terminal sequencing and mass spectrometry (Q-Tof). These fragments corresponded to the A and BC domains of HsMaf1. The HsMaf1 linker region between those fragments (aa 46-74) and the C-terminal acidic tail (aa 235-256) were degraded and thus presumably unstructured. Both fragments were further analyzed by size-exclusion chromatography. Surprisingly, the two HsMaf1 fragments, although of substantially different molecular masses, co-eluted at an apparent 1:1 stoichiometry, suggesting an intramolecular interaction between them. Moreover, co-expression of these N-terminal and C-terminal fragments of HsMaf1 in bacterial cells and their subsequent purification revealed that the His-Tag A fragment of HsMaf1 co-precipitates with the un-tagged BC protein fragment at an apparent 1:1 stoichiometry, suggesting a direct interaction between these fragments. These results were also confirmed by co-elution using size-exclusion chromatography supporting a direct interaction between the A and BC domains of HsMaf1 (Fig. 15, Gajda *et al.,* 2010).

The results obtained by Christoph Műller's group on the *H. sapiens* Maf1 as well as the good sequence conservation of the A and BC domains along evolution were an indication to study the relation of the A and BC domains in *S. cerevisiae*, an organism more amenable to study structure-function relationships.

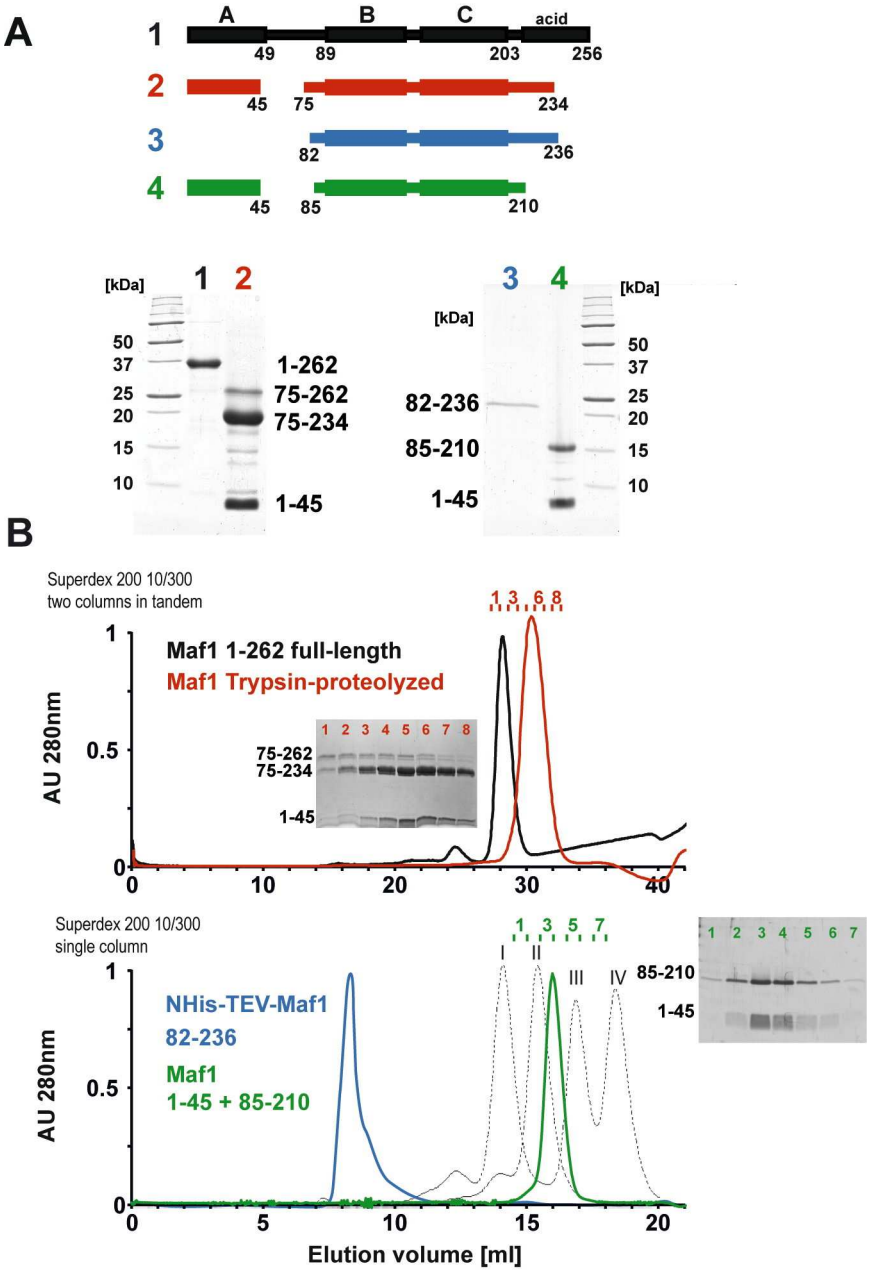

Figure 15. Domain structure of human Maf1. A. Limited proteolysis and resulting proteolytic fragments of HsMaf1. SDS-PAGE of full-length human HsMaf1 protein (1, black) that is digested into two stable fragments aa 1-45 and aa 75-234 using trypsin (2, red). Bacterially co-expressed and co-purified HsMaf1 domains aa 1-45 and aa 85-210 (4, green). HsMaf1 aa 82-236 (3, blue) lacking the N-terminal 45 residues was expressed as a control. B. Size-exclusion chromatography profiles. Samples presented in (A) were separated on single or tandem Superdex 200 10/300 size-exclusion columns (GE Healthcare). Only the HsMaf1 construct 82-236 eluates in the void volume of the Superdex 200 size-exclusion column, while all other samples are monodispersed and elute approximately at volumes corresponding to monomers. The elution profile of different molecular weight standards is shown as a dashed line. Peaks I, II, III and IV correspond to ovalbumin (Mr=44000), carbonic-anhydrase (Mr=29000), ribonuclease A (Mr=13700) and aprotinin (Mr=6500), respectively. Fractions corresponding to the red and green elution profiles were analyzed by denaturing gel electrophoresis and shown as insets. Fragment 1-45 co-elutes with proteolytic fragments - 75-234 and 75-262 (red profile) and with the recombinant fragment 85-210 (green profile). Adapted from Gajda *et al.*, 2010.

II. AIM OF THE WORK

The Maf1 protein was identified in the early '90 in the laboratory directed by Prof. Boguta. Since then numerous studies concerning Maf1 function as a Pol III repressor have been directed. Currently, Maf1 is considered as the one and only Pol III repressor in *S. cerevisiae* cells that conveys signals from the diverse signaling pathways on Pol III apparatus.

Maf1 is highly conserved through evolution. The common organization for *S. cerevisiae* Maf1, described as two structured regions of high similarity separated by an unstructured linker region, is typical for all eukaryotic Maf1 orthologs. These regions of high similarity, called the A and BC domains have no functional homology with the identified protein domains.

Since Maf1 organization is conserved through evolution it must be of high importance for Maf1 activity as a Pol III repressor.

This work addressed two main questions:

Is there a structure-function relation between the A and BC domains of Maf1 and the regulation of Pol III transcription?

Are the A and BC Maf1 domains involved in phosphorylation or the cellular localization of the protein?

To explore these matters and evaluate the significance of the A and BC domains of Maf1, libraries of *maf1* mutants harboring mutations localized in sequence encoding each particular domain were constructed and the cellular behavior of chosenMaf1 mutant proteins was investigated.

Supported by the biochemical analysis done by Christoph Műller's group indicating direct interaction between the domains of human Maf1, also in this work the genetic suppressor approach and yeast-two-hybrid system were applied to explore the potential interaction between the A and BC domains of *S. cerevisiae* Maf1.

Finally, to investigate how Maf1 affects the Pol III apparatus, a search for partner proteins of Maf1 using parts of Maf1 A and BC domains as a bait was performed.

Altogether, the aim of this study was devoted to a deeper understanding of the structure-function relationship between Maf1 domains and its capacity to repress Pol III.

III. RESULTS

1. Construction of *S. cerevisiae* Maf1 mutated in evolutionarily conserved regions - A and BC domains.

The common approach in analyzing the relationship between the primary sequence of a protein and its activity is to construct several mutants in the gene encoding this protein and investigate their changed cellular behavior depending on the carried mutations. To gain a better understanding of Maf1 functions in *S. cerevisiae* yeast cell, the *MAF1* gene was mutagenized in order to generate defined mutations localized in each particular domain. The obtained *maf1* mutants have been initially characterized due to amino acid substitutions and the growth phenotype.

1.1. Maf1 mutations in the A domain.

To obtain library of Maf1 protein mutated in the evolutionarily conserved A domain, the rapid method of "Gap repair" for localized mutagenesis has been applied (Muhlrad *et al.,* 1992). The strategy of constructing *MAF1* mutants was based on low-fidelity PCR. Sequence encoding A domain and the linker (aa 1-180) has been amplified under conditions that predicted obtaining 1-2 mutations in this region. Co-transformation of the *maf1Δ* strain with the low fidelity PCR product and gapped plasmid containing regions of *MAF1* flanking the A domain enabled *in vivo* recombination to repair the gap with mutagenized DNA encoding A domain (Fig. 16). The phenotype of 10 000 transformants was screened. Preliminary analysis revealed that among screened transformants nearly 1 000 exhibited temperature-sensitive growth on medium containing glycerol, a nonfermentable carbon source (characteristic phenotype for mutated *maf1* strain, Boguta *et al.,* 1997). Potential *maf1* mutants were used to isolate plasmid DNA that was subsequently examined by PCR to confirm the presence of the mutagenized region of Maf1 A domain. Approximately 500 plasmids harboured the A domain encoding sequence. After PCR verification, selected plasmids were amplified in *E. coli* and analyzed with endonuclease *Eco*RI. Plasmids giving an appropriate restriction pattern (61) were retransformed to the *maf1Δ S. cerevisiae* strain (YPH500 *maf1Δ*) to confirm that the observed phenotype results from mutations in *maf1* allele. Sequencing revealed the type of mutation of the *maf1* gene in each of the analyzed plasmids. Selected mutants were additionally examined by Western blotting to confirm the expression of the Maf1 protein.

Transformants were once more replica plated on medium containing glycerol and incubated for 3 days at 37°C. The growth phenotype observed for the analyzed *S. cerevisiae* cells expressing mutated Maf1s ranged from: lack of growth (-) similar to the *maf1Δ* strain, moderate growth defect (+/-) up to no growth defect (WT). No correlation between the observed growth phenotype and the mutagenized region of Maf1 was noted. Moreover, the K→E mutations of the second amino acid obtained in this screen seemed not to change the predicted *in vivo* half-life of Maf1 protein as reported by the "N-end rule" (Varshavsky, 1997).

Sixty-one isolated *maf1* mutants were classified based on the type of identified mutations: missense, frameshift or STOP codon. Missense *maf1* mutants (32) represented mutations in sequence encoding: the A domain alone (22), the A domain and the linker region between the A and BC domains (5) or only the linker region (5).

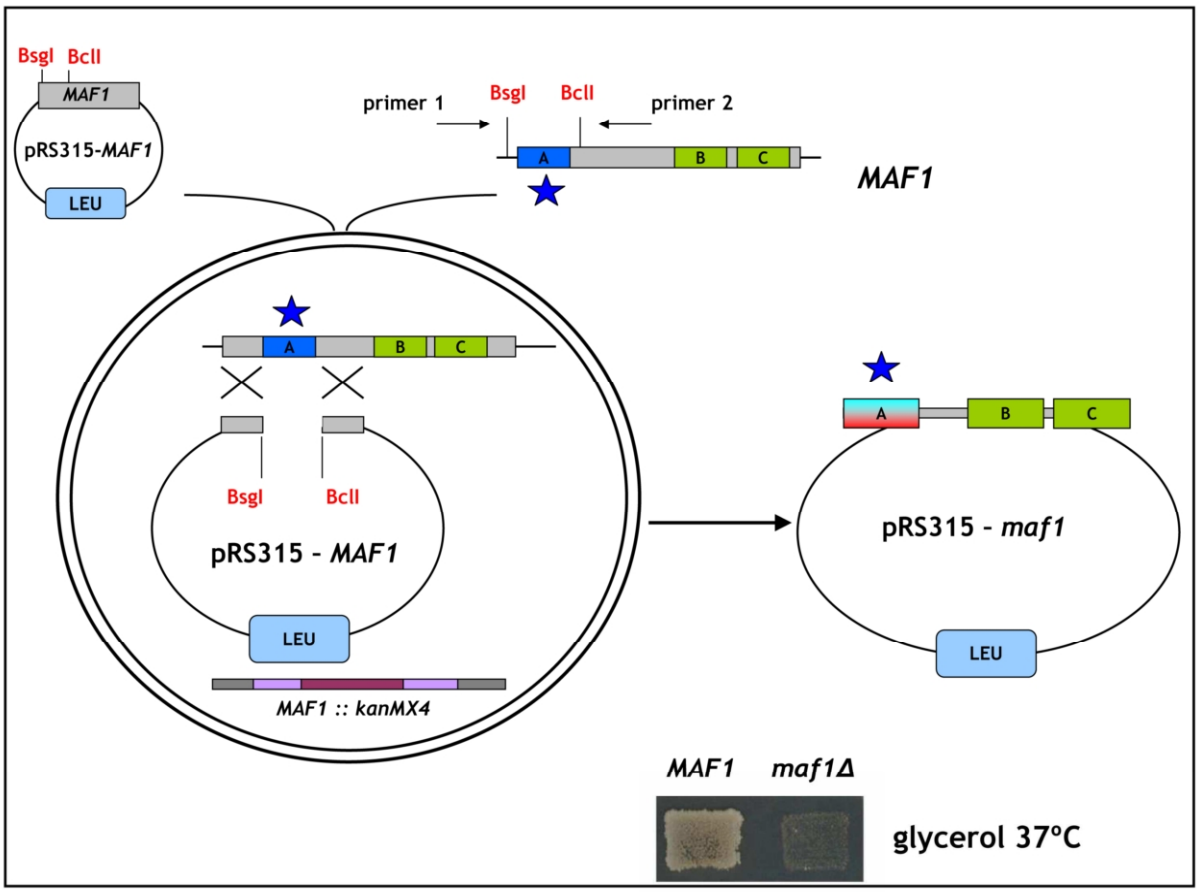

Figure 16. Schematic representation of the experimental strategy applied to construct Maf1 mutated in the A domain. The Maf1 A domain is indicated with blue color. The "gap-repair" system based on homologous recombination *in vivo* has been presented. Sequence, mutated by low-fidelity PCR encoding the A domain is designated with a blue star. Resulting plasmid harboring *maf*1 mutated in the sequence encoding A domain is presented on the right.

Among the identified missense *maf1* mutants: 16 represented single amino acid substitution, 10 - double amino acid substitutions and 6 - triple amino acid substitutions. The description of plasmids harboring the identified mutations conveying temperature-sensitive growth phenotype is included in Table 1A.

The remaining *maf1* mutants (29) represented: mutations in the intron sequence (3), defective start codon (5) (included in Table 1A), premature stop codons (9) (Supplementary material - Table S1) and frameshift mutations (12) (Table S2).

Plasmids harboring *maf1* but that transmitted WT growth phenotype (15) are included in Table 1B.

Noteworthy are *maf1* mutants with mutations localized in the intron sequence (80 nt sequence localized in *MAF1* between 7-86 nt). Mutation A → T (54 nt) in the "pAG64" *maf1* mutant confers lack of growth on glycerol-containing medium indicating a nonfunctional Maf1 (Table 1A). Moreover, R11S (pAG34), S28G-K35E (pAG48) and S131P (pAG72) *maf1* mutants, which, apart from missense mutations localized in the sequence encoding A domain, retain an additional mutations localized in the intron sequence (Table 1A), also exhibit lack of growth on glycerol-containing medium. In addition, preliminary Western blotting analysis with polyclonal anti-Maf1 antibodies did not reveal the presence of Maf1 in these mutants (Marlena Maciak 2008, data unpublished). Collectively, these data suggest impairement of the *MAF1* mRNA maturing process and point to these *maf1* mutants as a valuable objects for studying *MAF1* mRNA splicing.

Introns are composed of 3 sequences required for splicing. These consensus sequences are: 5'-GTATGT, bridge-TACTAAC and TGA-3'. In *MAF1* they are located at 7-12 nt, 49-55 nt and 64-66 nt). Interestingly S28G-K35E (pAG48), "pAG64" and S131P (pAG72) *maf1* mutants are mutated in these sequences responsible for appropriate splicing but not the R11S (pAG34) *maf1* mutant (Table 1A).

Worth noting is the growth phenotype observed of the Y84H (pAG16) *maf1* mutant, which exhibits superior growth on glycerol-containing medium comparing to the wild-type (WT) yeast cells (Table 1B). The Y84H (pAG16) *maf1* mutant retain single amino acid substitution Y84→H, which is localized in the linker between the A and BC Maf1 domains. The linker region is not conserved through evolution and appears to be unstructured, which makes the observed growth phenomena surprising. Amino acid substitution at this residue (Y84), but of a different kind, was also observed in Y84C (pAG59) *maf1* mutant, which exhibited lack of growth in the studied conditions. This may be explained by the fact that the Y84C (pAG59)

Table 1A. Plasmids carrying *maf1* allele mutated in sequence encoding A domain and the linker. Table represents plasmids encoding Maf1 mutated in either A domain or linker between the A and BC domains or both regions, start codon or intron. Growth phenotype on glycerol-containing medium at 37ºC (YPGly) signed as a: lack of growth (-) or moderate growth defect (+/-). Protein expression in several cases confirmed by Western blotting analysis with polyclonal anti-Maf1 antibodies – marked (+) for expressed (-) for expression not detected or (NT) not tested. Plasmids organized according to the region mutagenized, growth phenotype resulting from mutated *maf1* allele and number of missense mutations that occur (relative to translation start site).

Plasmid	Mutated region	No. missense mutations	Amino acid substitution	Change in codon	Silent mutations	Mutations in promoter region	Mutations in intron	YPGly	Protein expression
pAG24	A	single	Y44 → F	TAT → TTT	N13 (AAT → AAC)	none	G → A (7 nt) T → C (58 nt)	-	NT
pAG34	A	single	R11 → S	AGA → AGT	I31 (ATT → ATC)	A → G (-6 nt)	A → C (17 nt) A → G (85 nt)	-	-
pAG40	A	single	K2 → E	AAA → GAA	none	none	T → C (57 nt)	-	NT
pAG53	A	single	K2 → E	AAA → GAA	none	none	none	-	NT
pAG68	A	single	K2 → E	AAA → GAA	none	none	A → G (53 nt)	-	NT
pAG48	A	double	S28 → G K35 → E	AGT → GGT AAG → GAG	K42 (AAA → AAG)	none	A → G (54 nt)	-	-
pAG50	A	double	K2 → E H50 → R	AAA → GAA CAT → CGT	D30 (GAT → GAC)	T → A (-83 nt)	T → A (27 nt)	-	NT
pAG58	A	double	R41 → G I47 → N	AGA → GGA ATT → AAT	none	T → C (-153 nt) T → C (-75 nt)	none	-	NT
pAG8	A	single	F32 → I	TTC → ATC	none	A → T (-180 nt) T → C (-140 nt)	none	+/-	+
pAG70	A	single	K35 → E	AAG → GAG	none	none	none	+/-	+
pAG37	A	double	N17 → H L43 → S	AAT → CAT TTA → TCA	none	A → G (-180 nt) A → X (-177 nt)	T → X (39 nt)	+/-	+
pAG49	A	double	N17 → H L43 → S	AAT → CAT TTA → TCA	none	A → G (-180 nt) T → X (-177 nt)	T → X (37 nt) T → X (38 nt)	+/-	+
pAG66	A	double	F32 → V T33 → A	TTC → GTC ACA → GCA	Y44 (TAT → TAC)	T → C (-142 nt)	A → G (53 nt)	+/-	NT
pAG27	A	triple	I25 → T S28 → G R41 → S	ATC → ACC AGT → GGT AGA → AGT	S39 (TCA → TCG)	none	T → C (37 nt)	+/-	+
pAG61	A linker	double	K2 → E N117 → I	AAA → GAA AAT → ATT	none	none	none	-	+
pAG23	A linker	triple	F32 → S I54 → T N142 → D	TTC → TCC ATT → ACT AAT → GAT	none	none	none	-	+

Continued:

Plasmid	Mutated region	No. missense mutations	Amino acid substitution	Change in codon	Silent mutations	Mutations in promoter region	Mutations in intron	YPGly	Protein expression
pAG67	A linker	triple	E10 → G S39 → P L149 → F	GAG → GGG TCA → CCA TTA → TTT	none	none	none	+/-	+
pAG59	linker	single	Y84 → C	TAT → TGT	none	none	T → C (52 nt)	-	NT
pAG72	linker	single	S131 → P	TCT → CCT	none	T → C (-15 nt)	A → G (50 nt) A → G (85 nt)	-	-
pAG29	start codon	double	M1 → K K97 → R	ATG → AAG AAG → AGG	Q144 (CAA → CAG)	none	none	-	-
pAG35	start codon	single	M1 → T	ATG → ACG	none	T → C (-98 nt) A → G (-30 nt)	A → G (53 nt)	-	NT
pAG56	start codon	single	M1 → V	ATG → GTG	none	none	none	-	-
pAG69	start codon	multiple	M1 → V K2 → E L16 → H N113 → S N115 → S N120 → I	ATG → GTG AAA → GAA CTC → CAC AAC → AGC AAT → AGT AAT → ATT	R11 (AGA → AGG) R89 (AGA → AGG)	none	none	-	-
pAG9	start codon	single	K2 → X	AAA → AA-	S77 (TCA → TCG)	none	none	-	-
pAG64	intron	intron	none	none	none	none	A → T (54 nt)	-	NT

Table 1B. Description of plasmids carrying *maf1* allele conveying no defected growth on medium containing glycerol (YPGly) at 37ºC. Table represents plasmids encoding Maf1 mutated in the A domain, the A domain and linker between the A and BC domains, linker or intron. Plasmids organized according to the region mutagenized, and quantity of mutations that occur.

Plasmid	Mutated region	No. missense mutations	Amino acid substitution	Change in codon	Silent mutations	Mutations in promoter region	Mutations in intron	YPGly
pAG5	A	single	F32 → S	TTC → TCC	F93 (TTT → TTC)	none	none	WT
pAG11	A	single	D40 → G	GAT → GGT	none	none	none	WT
pAG47	A	single	F3 → S	TTT → TCT	none	none	none	WT
pAG51	A	single	K2 → R	AAA → AGA	none	none	none	WT
pAG62	A	single	L43 → F	TTA → TTT	K2 (AAA → AAG)	none	A → G (24 nt) A → T (45 nt)	WT
pAG21	A	double	D30 → G Y44 → C	GAT → GGT TAT → TGT	I31 (ATT → ATC)	none	none	WT
pAG33	A	double	Q14 → R H50 → Q	CAA → CGA CAT → CAA	P132 (CCA → CCG)	A → X (-198 nt) A → G (-183 nt)	none	WT
pAG17	A	triple	N13 → S S39 → L D48 → V	AAT → AGT TCA → TTA GAT → GTT	none	none	none	WT
pAG10	A linker	double	D30 → V N58 → D	GAT → GTT AAT → GAT	none	none	none	WT
pAG19	A linker	triple	F32 → L N62 → D N106 → D	TTC → CTC AAT → GAT AAT → GAT	F135 (TTT → TTC)	A → T (-2 nt)	none	WT
pAG25	linker	single	C79 → S	TGC → AGC	T15 (ACT → ACC) A38 (GCA → GCG)	T → C (-185 nt) T → C (-141 nt)	none	WT
pAG74	linker	triple	N112 → S N122 → S K137 → R	AAC → AGC AAT → AGT AAA → AGA	N128 (AAT → AAC)	none	none	WT
pAG16	linker	single	Y84 → H	TAT → CAT	none	A → G (-162 nt)	none	WT+
pAG22	intron	intron	none	none	none	none	A → G (23 nt)	WT
pAG30	intron	intron	none	none	none	A → G (-30 nt)	T → C (57 nt)	WT

maf1 mutant retain additional mutations in the intron sequence (Table 1A), which impaires Maf1 maturation and is responsible for the observed growth defect. Such observation supports the importance of intron splicing in *MAF1*, which could play a part in the cellular regulation of Maf1 expression and mediate the regulation of Pol III by Maf1.

- **Analysis of potential regions exhibiting increased mutagenesis frequency localized within the A domain of mutated Maf1.**

The obtained *maf1* mutants were subsequently analyzed to determine the specific region of the Maf1 protein important for disruption of its activity. Comparison of mutated amino acid residues and temperature sensitivity on glycerol-containing medium at 37°C did not allow to specify the region of Maf1 responsible for manifestation of the temperature-sensitive growth (Fig. 17).

Nevertheless, analysis of *maf1* mutants with amino acid substitutions leading to the appearance of premature STOP codons has shown that the A domain with the linker region seems not sufficient for Maf1 activity. This observation is supported by the N120S-S166STOP (pAG6) *maf1* mutant, in which, *maf1* translation is expected to be stopped after aa 166 residue. Although the full-length Maf1 A domain is hypothetically expressed (aa 1-49) with the concomitant linker region (aa 50 – 166), the N120S-S166STOP (pAG6) *maf1* mutant exhibits temperature-sensitive growth on glycerol-containing medium (similar to *maf1Δ* strain), which indicates inactive form of Maf1. This observation suggest that the presence of the BC domain (that is absent in the N120S-S166STOP (pAG6) *maf1* mutant) is necessary for Maf1 activity.

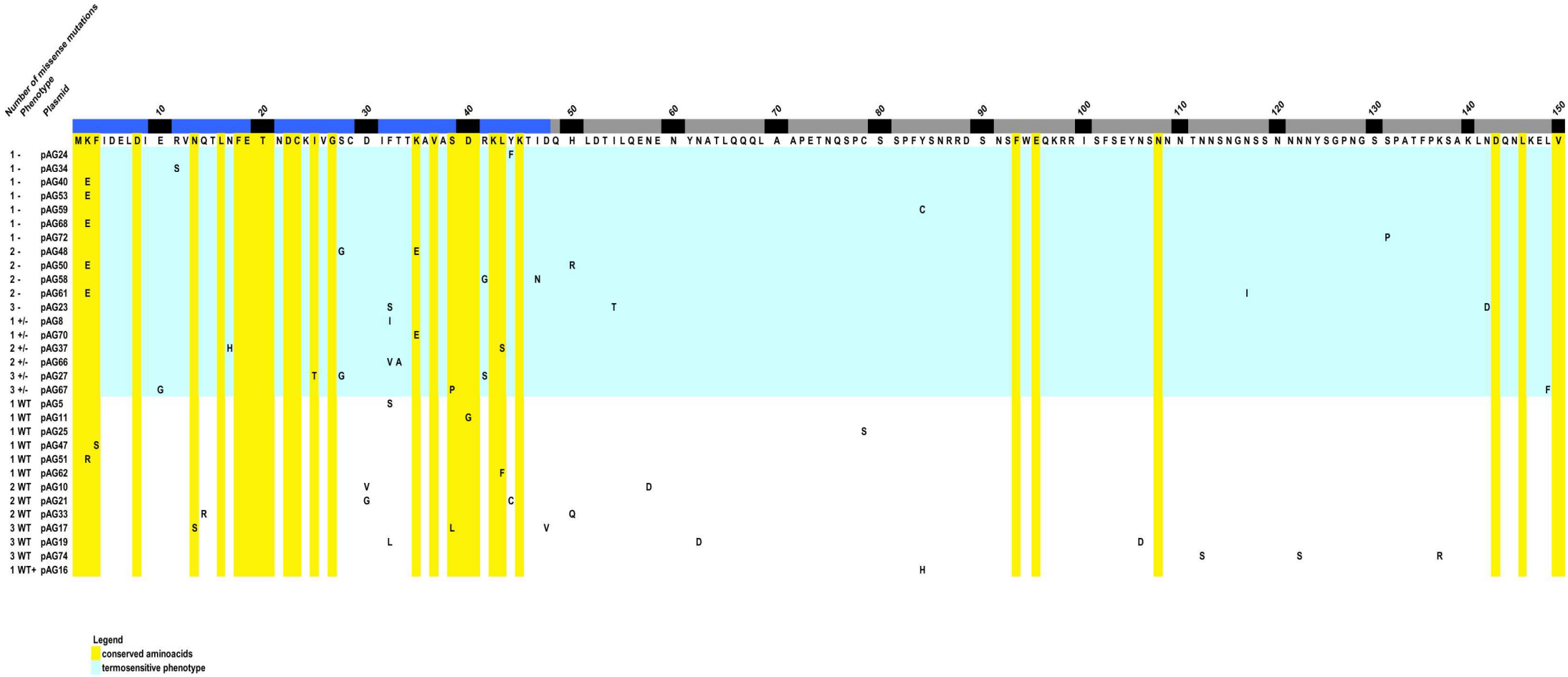

Figure 17. Schematic representation of Maf1 A domain and the linker amino acid sequence with marked regions of mutation incidence that occurred during global mutagenesis of the *MAF1* gene. The A domain encompass region 1 – 49 aa (blue) while the linker region ranges from 50 – 150 aa (grey). In yellow highly conserved amino acid residues have been highlighted. Temperature-sensitive phenotype on glycerol-containing medium at 37°C (YPGly), both: lack of growth (-) and moderate growth defect (+/-) caused by the identified mutations in *maf1* are highlighted with light blue colour. Mutations in *maf1* causing no growth defect in restricted conditions (WT) are also included.

1.2. Maf1 mutations in the BC domain.

To obtain library of Maf1 mutated in the BC domain, a "Gap repair" strategy similar to that used to construct the A domain *maf1* mutants has been applied (Muhlrad *et al.,* 1992). Sequence encoding the BC domain (174-375 aa) was amplified by low-fidelity PCR and co-transformed to the YPH500 *maf1Δ* strain together with *MAF1*-harboring plasmid gapped within the BC region (Fig. 18). Resulting transformants have been screened for a temperature-sensitive growth phenotype on medium supplemented with glycerol. After retransformation of constructs to *maf1Δ* the *S. cerevisiae* strain (YPH500 *maf1Δ*), 61 *maf1* mutants were further analyzed. Sequencing revealed the type of mutation of the *maf1* gene in each of the analyzed plasmids (Table 2). Selected mutants have been tested for Maf1 expression by Western blotting with polyclonal anti-Maf1 antibodies.

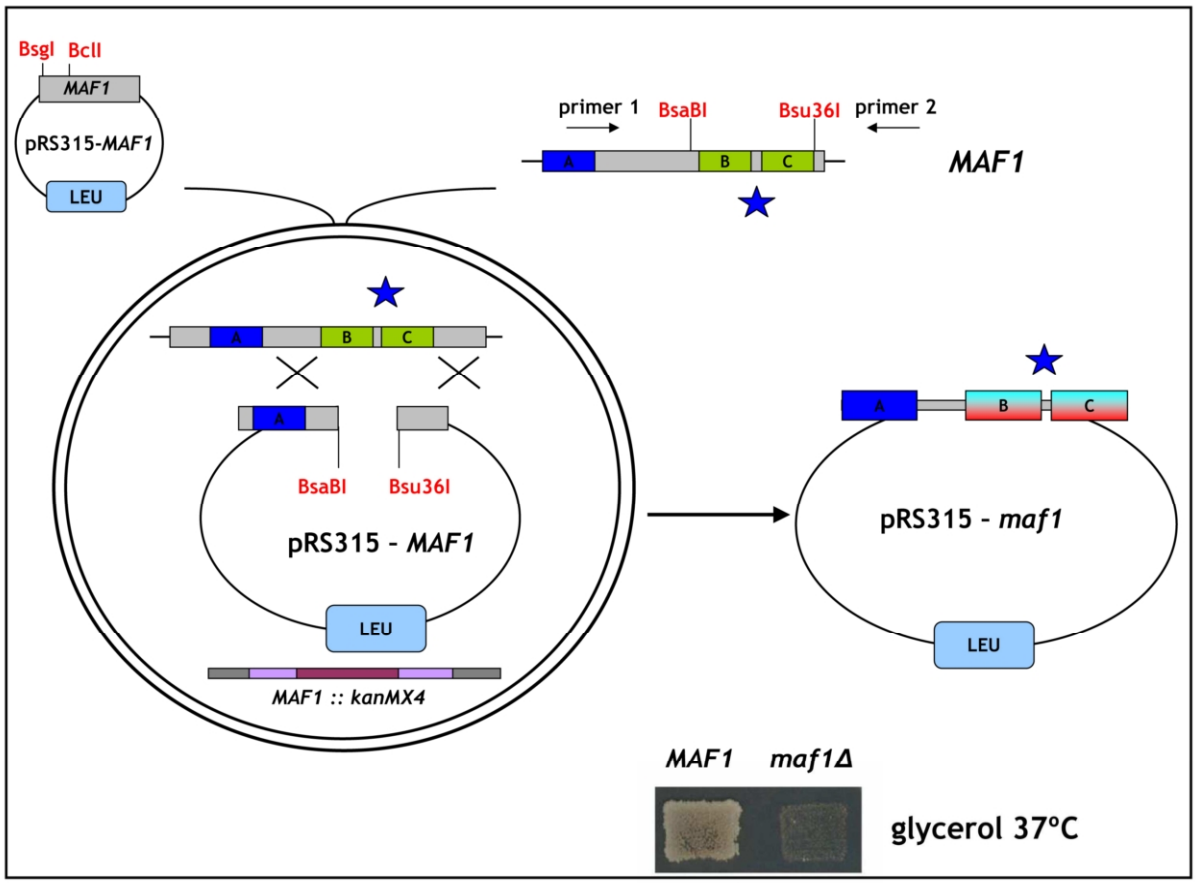

Figure 18. Schematic representation of the experimental strategy applied to construct Maf1 mutated in the BC domain. The Maf1 BC domain is indicated with green color. The "gap-repair" technique based on homologous recombination *in vivo* has been presented. Sequence, mutated by low-fidelity PCR, encoding the BC domain is designated with a blue star. Resulting plasmid carrying *maf1* mutated in the sequence encoding the BC domain is shown on the right.

Among the 61 analyzed *maf1* mutants: 3 represented single amino acid substitutions, 10 - double amino acid substitutions and 5 - triple amino acid substitutions (Tab. 2). Higher mutagenesis level was observed for the BC domain in comparison to the construction of A domain *maf1* mutants. The remaining *maf1* mutants represented: multiple mutations (20), premature STOP codons (9) and frameshift mutations (14) (Data shown in supplementary material, Tables S3-5). Similarly to *maf1* mutants in the A domain, the growth phenotype on a nonfermentable carbon source (glycerol medium - 37°C) observed for the BC domain *maf1* mutants ranged from: lack of growth (-) similar to the *maf1Δ* strain, moderate growth defect (+/-) up to no growth defect (WT). The description of mutations and correlated growth phenotypes are included in Table 2. Plasmids carrying the mutated *maf1* allele that convey WT growth are listed in supplementary Table S3.

- **Analysis of potential regions exhibiting increased mutagenesis frequency localized within the BC domain of mutated Maf1.**

The obtained *maf1* mutants were classified according to their growth phenotype. An attempt has been made to identify the specific region of the BC domain responsible for the disruption of Maf1activity resulting in temperature-sensitive growth on medium containing glycerol. Like in the case of mutations in the A domain, identification of mutations leading to the apparent growth defect of yeast cells did not allow to specify any particular region of the BC domain responsible for the impairment of Maf1 activity. High mutagenesis level within the BC domain (most mutants carried multiple mutations) was a problem in assigning a particular mutation to a specific phenotype. Nevertheless, the analyzed mutations having impact on yeast growth were determined to be predominantly localized in highly conserved amino acid residues of Maf1: L238, I239, L242, N243, S252, E272, M294, C299, F302, S305, E314 and in residues close to the nuclear localization signal (328-332 aa, RKRKR-NLS2) L325, Y326, N227, K329, R332 (Fig. 19).

Table 2. Plasmids carrying *maf1* allele mutated in sequence encoding the BC domain. Growth phenotype on glycerol-containing medium at 37°C (YPGly) signed as a: lack of growth (-) or moderate growth defect (+/-). Protein expression was confirmed by Western blotting with polyclonal anti-Maf1 antibodies. Plasmids organized according to the growth phenotype resulting from mutated Maf1 and number of missense mutations that occur.

Plasmid	No. missense mutations	Amino acid substitution	Change in codon	Silent mutations	YPGly
pAG107	single	M294 → R	ATG → AGG	none	-
pML6	double	I241 → F R332 → G	ATC → TTC AGA → GGA	K356 (AAA → AAG) K357 (AAA → AAG) G360 (GGA → GGG)	-
pAG110	double	S252 → T R332 → G	TCA → ACA AGA → GGA	none	-
pAG132	double	L242 → P K329 → I	CTC → CCC AAA → ATA	A334 (GCT → GCA) G348 (GGC → GGT)	-
pAG136	double	M294 → R L354 → S	ATG → AGG TTG → TCG	S252 (TCA → TCT) D366 (GAT → GAC)	-
pAG147	double	L242 → P H249 → Q	CTC → CCC CAT → CAA	none	-
pAG171	double	I239 → F D258 → V	ATT → TTC GAT → GTT	S252 (TCA → TCG) P315 (CCT → CCC)	-
pMM2	triple	E272 → L C299 → R Q359 → L	GAA → AAA TGC → CGC CAG → CTG	L301 (CTT → CTC) A355 (GCA→ GCT)	-
pAG113	triple	I239 → V Y317 → F S341 → P	ATT → GTT TAT → TTT TCG → CCG	F310 (TTT → TTC) A334 (GCT → GCC)	-
pAG148	triple	S305 → P N327 → D N344 → D	TCA → CCA AAC → GAC AAT → GAT	I339 (ATT → ATA) D352 (GAT → GAC)	-
pMM4	double	F302 → S L311 → W	TTT → TCT TTG → TGG	A355 (GCA → GCT)	+/-
pAG139	double	I241 → N N243 → T	ATC → AAC AAC → ACC	none	+/-
pAG167	double	N243 → S F267 → S	AAC → AGC TTT → TCT	Q303 (CAA → CAG) P306 (CCT → CCC)	+/-
pAG116	triple	L238 → P E314 → G K329 → I	CTG → CCG GAG → GGG AAA → ATA	G224 (GGT → GGA) I290 (ATT → ATA)	+/-
pAG127	triple	N327 → Y I339 → T S341 → P	AAC → TAC ATT → ACT TCG → CCG	S309 (TCT → TCC)	+/-
pMM1	multiple (5)	L242 → S L325 → P Y326 → F L354 → S L362 → Q	TTG → TCG CTT → CCT TAC → TTC TTG → TCG CTT → CAG	none	+/-

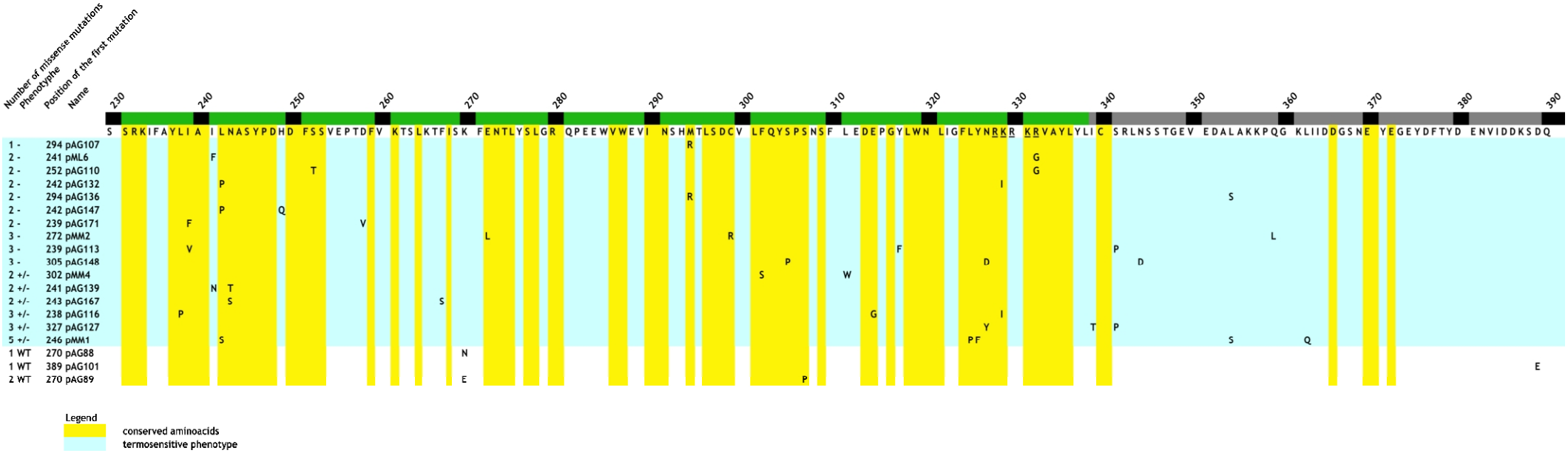

Figure 19. Schematic representation of the Maf1 BC domain amino acid sequence with marked regions of mutation incidence that occurred during global mutagenesis of the *MAF1* gene. The BC domain covers region 231 – 338 aa (green). Region outside the BC domain, including the acidic tail, ranges from 339 – 390 aa (grey). In yellow highly conserved amino acid residues have been highlighted. Temperature-sensitive phenotypes on glycerol-containing medium at 37°C (YPGly), both: lack of growth (-) and moderate growth defect (+/-) caused by the identified *maf1* mutations are highlighted with light blue color. Mutations in *maf1* causing no growth defect in restricted conditions (WT) are also included.

Table 3. Classification of plasmids carrying *maf1* allele. Table presents organization of plasmids according to the mutagenized region of Maf1 and growth phenotype on glycerol-containing medium at 37°C (YPGly). Plasmids subjected to further analysis are bolded. Mutations are indicated below name of bolded plasmids.

Region mutagenized	**A**		**A + linker**		**linker**	**BC**	
YPGly phenotype	**-**	**+/-**	**-**	**+/-**	**-**	**-**	**+/-**
	pAG24	**pAG8** F32I-*maf1*	-	-	pAG59	pAG107	-
	pAG34	**pAG70** K35E-*maf1*	-	-	pAG72	-	-
	pAG40	-	-	-	-	-	-
	pAG53	-	-	-	-	-	-
	pAG68	-	-	-	-	-	-
	pAG48	pAG37	**pAG61** K2E-N117I-*maf1*	-	-	**pML6** I241F-R332G-*maf1*	**pMM4** F302S-L311W-*maf1*
	pAG50	pAG49	-	-	-	pAG110	**pAG139** I241N-N243T-*maf1*
	pAG58	pAG66	-	-	-	**pAG132** L242P-K329I-*maf1*	**pAG167** N243S-F267S-*maf1*
	-	-	-	-	-	**pAG136** M294R-L354S-*maf1*	-
	-	-	-	-	-	**pAG147** L242P-H249Q-*maf1*	-
	-	-	-	-	-	**pAG171** I239F-D258V-*maf1*	-
	-	pAG27	**pAG23** F32S-I54T-N142D-*maf1*	**pAG67** E10G-S39P-L149F-*maf1*	-	**pMM2** E272L-C299R-Q359L-*maf1*	**pAG116** L238P-E314G-K329I-*maf1*
	-	-	-	-	-	pAG113	**pAG127** N327Y-I339T-S341P-*maf1*
	-	-	-	-	-	**pAG148** S305P-N327D-N344D-*maf1*	-
multiple	-	-	-	-	-	-	**pMM1** L242S-L325P-Y326F-L354S-L363Q-*maf1*

1.3. Preliminary characterisation of Maf1 mutants.

By applying low-fidelity PCR and "Gap-repair" *in vivo* system a library of Maf1 mutated in evolutionarily conserved regions - A and BC domains has been created. Obtained *maf1* mutants exhibit thermosensitive growth phenotype on medium containing glycerol, a nonfermentable carbon source, which forces a change in the cellular metabolism from fermentation to respiratory growth – a phenotype typical for *maf1Δ S. cerevisiae* cells (Boguta *et al.,* 1997). The presence of a thermosensitive growth phenotype is conncted either with the absence of Maf1 or a nonfunctional Maf1 unable to repress Pol III. Impairment of Maf1 function may correspond to defects in several steps of Maf1 activity: expression, phosphorylation state, transport from cytoplasm to nucleus or interaction with the Pol III apparatus.

Several *maf1* mutants carrying mutations in different regions of Maf1 and exhibiting different growth phenotype, were subjected to further investigation (Table 3). More attention has been drawn to Maf1 mutated in the BC domain, which, due to its the higher evolutionary conservation in comparison to the A domain, seems more be crucial for Maf1 activity.

1.3.1 Does mutations in the BC domain of Maf1 trigger destabilization of the protein?

In first attempt, the expression profiles of mutated Maf1s have been studied in standard growth conditions (YPD, exponential phase). Investigated plasmids harbouring the *maf1* allele were introduced to the YPH500 *maf1Δ* strain and the respective Maf1 mutant proteins have been examined by Western blotting with polyclonal anti-Maf1 antibodies. The analysis verified the lack of Maf1 expression for *maf1* alleles mutated in the START codon sequence (Table 1A) harbored by pAG29, pAG56, pAG69 and pAG9 plasmids that conveyed previously observed growth defect of yeast cells on glycerol-containing medium at 37°C (Fig. 20B).

Differences in protein expression between Maf1 mutated in A domain and the linker (K2E-N117I (pAG61), F32S-I54T-N142D (pAG23), F32I (pAG8) and E10G-S39P-L149F (pAG67) *maf1* mutants) and the wild-type Maf1 (WT) were insignificant (Fig. 20A). Contrary to the effect of mutations localized in the A domain, several *maf1* alleles mutated in the sequence encoding BC domain exhibited major disproportion in the Maf1 expression profile (Fig. 20A)

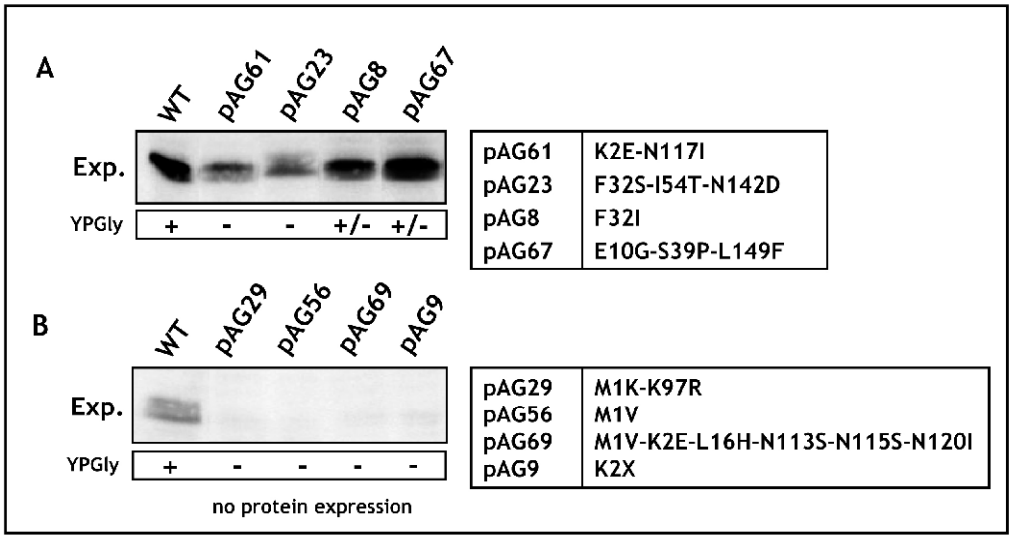

Figure 20. Analysis of the protein expression profile among Maf1 mutated in A domain and the linker region between the A and BC domains. The YPH500 *maf1Δ* strain harboring plasmids carrying mutated *maf1* allele was grown to exponential phase (Exp.) in rich glucose medium. Cells were harvested and crude cell extracts prepared by trichloroacetic acid precipitation (TCA) were analysed using SDS-PAGE followed by immunoblotting with polyclonal anti-Maf1 antibodies. Growth phenotypes on glycerol-containing medium at 37°C (YPGly) resulting from the analyzed mutated *maf1* allele are indicated below; (-) thermosensitivity, (+/-) moderate thermosensitivity. B. Plasmids carrying *maf1* mutated in start codon.

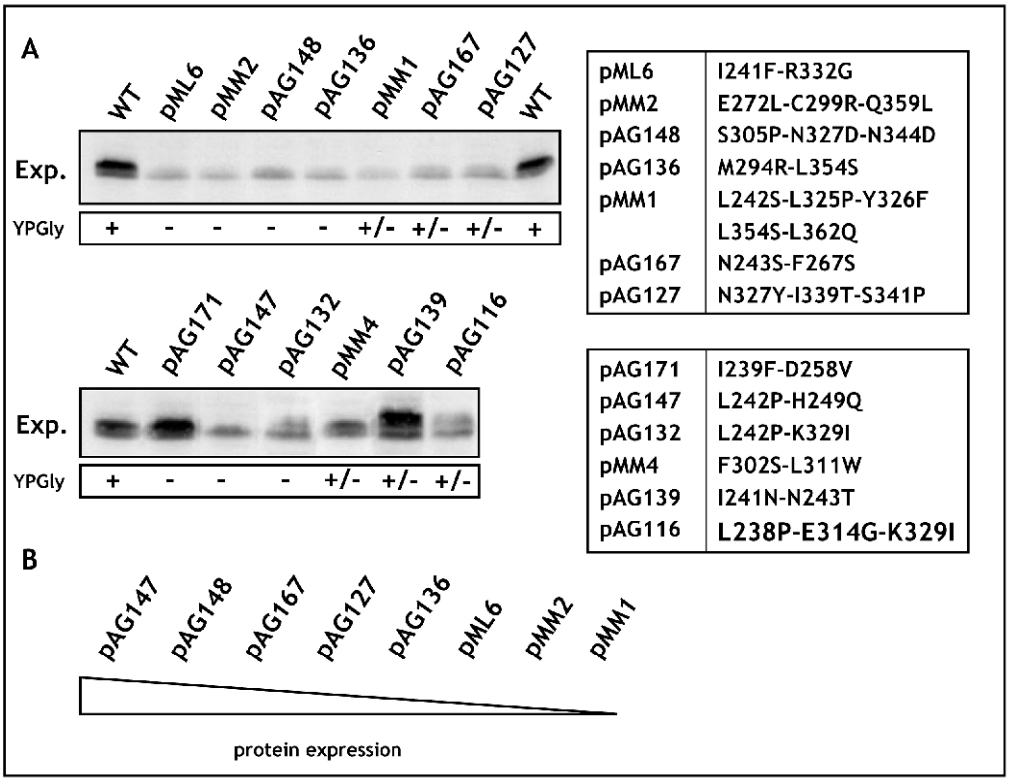

Figure 21. Maf1 is expressed to a different extent depending on localization of identified mutations. The YPH500 *maf1Δ* strain harboring plasmids carrying *maf1* allele mutated in the sequence encoding BC domain was grown to exponential phase (Exp.), cells were harvested and subsequently analyzed by Western blotting with polyclonal anti-Maf1 antibodies as described in the legend to Fig. 20. Growth phenotype on glycerol-containing medium at 37°C (YPGly) resulting from the analyzed mutated *maf1* allele indicated below; (-) thermosensitivity, (+/-) moderate thermosensitivity. B. Decreasing expression of Maf1 in identified *maf1* allele mutated in the sequence coding BC domain is symbolized.

Furthermore L242P-H249Q (pAG147), S305P-N327D-N344D (pAG148), N243S-F267S (pAG167), N327Y-I339T-S341P (pAG127), M294R-L354S (pAG136), I241F-R332G (pML6), E272L-C299R-Q359L (pMM2) and L242S-L325P-Y326F-L354S-L363Q (pMM1) *maf1* mutants demonstrated reduced Maf1 expression compared to nonmutated Maf1 (WT) and other Maf1s mutated in the BC domain. The decreased level of Maf1 among the analyzed *maf1* allele is depicted on Fig. 21B. The disproportion of Maf1 expression did not correlate to the growth phenotype of relevant yeast cells (see Fig. 21A) suggesting that the observed growth phenotype does not reflect the amount of cellular Maf1 but rather its ability to inhibit Pol III. One might also suspect that other factors, like protein stability or degradation, might be responsible for noticeable differences in Maf1 expression profile.

We might hypothesize that amino acid substitutions impose some conformational changes to the protein structure that do not affect its ability to interact with the Pol III apparatus and repress transcription, but physically destabilize the protein leading to its shortened life-time. On the other hand, it might be also possible also that amino acid substitutions cause conformational changes in a way that it makes the protein susceptible for accidental interactions with some other unspecific

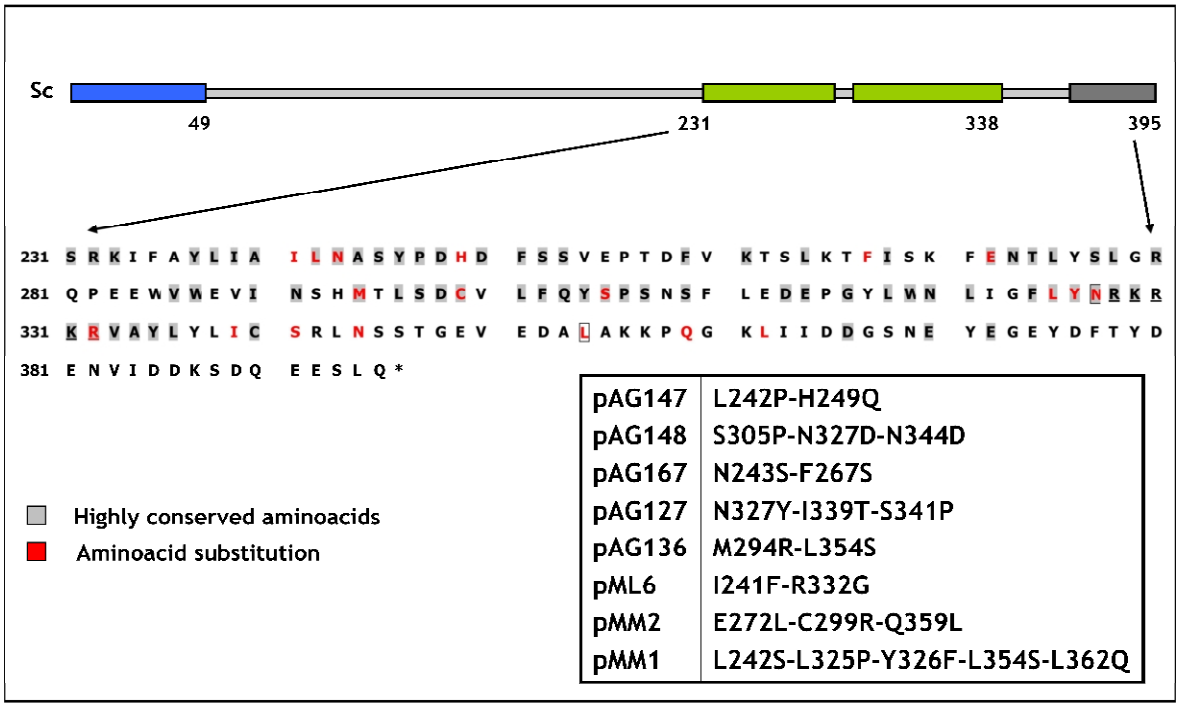

Figure 22. Identified mutations leading to decreased Maf1 cellular expression localize in the BC domain. The image is a schematic representation of Maf1 organization. The A domain is coloured with blue while the BC domain with green. The amino acid sequence of the Maf1 BC domain is presented in details. Evolutionarily conserved residues are marked with grey colour. Amino acid substitutions identified in *S. cerevisiae* cells expressing lower levels of Maf1 are indicated with a red type. Amino acid substitutions that occurred repeatedly are marked with grey squares. Studied plasmids harboring *maf1* alleles with identified mutations are indicated on the bottom right.

environmental factors that ultimately direct it to degradation pathway.

Localization of the identified mutations in *maf1* alleles exhibiting decreased Maf1 expression indicated the BC domain of Maf1 to be important for protein stability (Fig. 22).

1.3.2 Dephosphorylation of mutated Maf1 in terms of starvation induced by rapamycin.

The rapamycin is a convenient drug agent that by inhibiting the TOR signalling pathway, induces a response in *S. cerevisiae* yeast cells similar to conditions of starvation. In terms of nutrient deprivation wild-type (WT) Maf1 is activated - undergoes dephosphorylation and is transported to nucleus leading to repression of Pol III transcription. The described *maf1* mutants, previously analyzed for the Maf1 expression profile in standard growth conditions were subsequently examined for their dephosphorylation ability under rapamycin treatment.

To this aim, cells were grown in rich medium containing glucose until they reached the exponential growth phase, then treated by adding rapamycin to the medium at a final concentration of 0,2 μg/ml and incubated for 60 min. at 30ºC. Crude cell extracts isolated from the YPH500 *maf1Δ S. cerevisiae* strain expressing mutated *maf1* alleles were subjected to electrophoresis in denaturating conditions (SDS-PAGE) with modified acrylamide:bisacrylamide ratio (Oficjalska-Pham *et al.,* 2006) that enabled discrimination between phosphorylated and dephosphorylated Maf1 forms. SDS-PAGE electrophoresis was followed by immunoblotting with polyclonal anti-Maf1 antibodies.

During the exponential growth phase wild-type Maf1 (WT) migrates as several bands: a dephosphorylated corresponding to faster migrating band and slower migrating diffuse bands corresponding to phosphorylated Maf1 forms that disappear under rapamycin treatment (Fig. 23). Deviations from this rule will be called in further parts of this work “affected dephosphorylation”.

Presented analysis demonstrated that there is no correlation between region of Maf1 mutagenized and its capability to undergo dephosphorylation under rapamycin induction. Indeed, among *maf1* alleles mutated in sequence encoding the A domain or the linker we observed either dephosphorylation comparable to wild-type Maf1 (WT) – K2E-N117I (pAG61), F32I (pAG8) and E10G-S39P-L149F (pAG67) *maf1* mutants or affected dephosphorylation observed in F32S-I54T-N142D (pAG23) *maf1* mutant (Fig. 23). Moreover, we can not conclude from the phenotype

of analyzed *maf1* mutants on ability of mutated Maf1 to undergo dephosphorylation for the reason that respective yeast cells presented both: growth defect and moderate growth defect on glycerol-containing medium.

Similarly, in case of *maf1* alleles mutated in sequence encoding the BC domain we observed Maf1 dephosphorylation either comparable to nonmutated Maf1 (WT) e.g. I239F-D258V (pAG171) *maf1* mutant exhibiting growth defect on glycerol-containing medium (Fig. 24) and F302S-L311W (pMM4), I241N-N243T (pAG139) *maf1* mutants exhibiting moderate growth defect (Fig. 25) or affected dephosphorylation of Maf1 in mutants exhibiting both: thermosensitive phenotype – I241F-R332G (pML6), E272L-C299R-Q359L (pMM2), M294R-L354S (pAG136), L242P-H249Q (pAG147), L242P-K329I (pAG132) and S305P-N327D-N344D (pAG148) *maf1* mutants (Fig. 24) and moderate thermosensitive phenotype – N243S-F267S (pAG167), N327Y-I339T-S341P (pAG127), L242S-L325P-Y326F-L354S-L363Q (pMM1) and L238P-E314G-K329I (pAG116) *maf1* mutants (Fig. 25).

Nevertheless, there is an evident link between the Maf1 expression profile and its capability to undergo dephosphorylation in terms of rapamycin induced cellular starvation. Each of mutated *maf1* allele that formerly were reported to convey diminished expression level now demonstrated disordered phosphorylated form in exponential growth phase and then affected dephosphorylation under examined conditions. Compare Fig. 24 with Fig. 21 (both panels) - I241F-R332G (pML6), L242P-K329I (pAG132), M294R-L354S (pAG136), L242P-H249Q (pAG147), E272L-C299R-Q359L (pMM2), S305P-N327D-N344D (pAG148) and compare Fig. 25 with Fig. 21 (both panels) - N243S-F267S (pAG167), (L238P-E314G-K329I) pAG116, N327Y-I339T-S341P (pAG127), L242S-L325P-Y326F-L354S-L363Q (pMM1). This apparent correlation might support the hypothesis that the improperly folded Maf1 mutant forms are unstable and possibly degraded. Perturbations of phosphorylation and dephosphorylation phenomena of Maf1 mutant forms might reflect this inappropriate protein folding preventing from regular phosphorylation.

However, one of the isolated *maf1* mutants, demonstrated no alterations in the Maf1 expression profile (thereby no expected destabilization or degradation) but was shown to be affected in phosphorylation and dephosphorylation process (F32S-I54T-N142D (pAG23) *maf1* mutant). This indicates that the observed disorder in Maf1 phospho-forms is a direct consequence of mutations within the Maf1 encoding sequence.

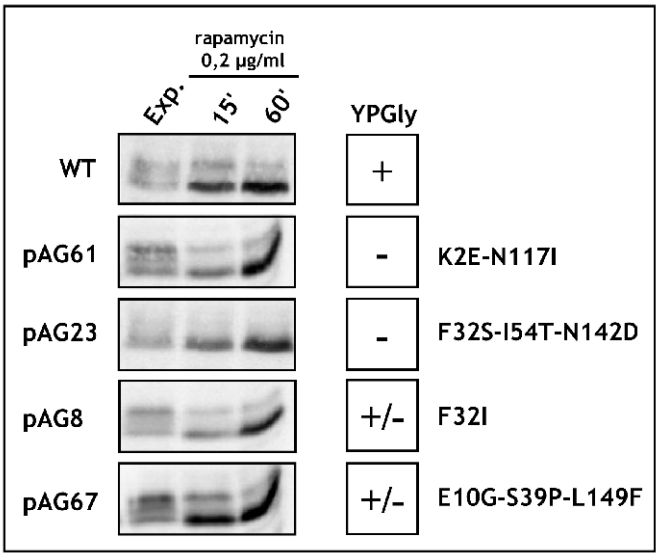

Figure 23. Analysis of dephosphorylation of Maf1 mutated in the A domain and the linker region upon conditions of starvation induced by rapamycin. The YPH500 *maf1Δ* strain harboring plasmids carrying mutated *maf1* allele was grown to exponential phase (Exp.) in rich glucose medium, exposed to rapamycin at a final concentration of 0,2 µg/ml in the medium and further incubated at 30°C. Cells were harvested as described in the legend to Fig. 20 and subsequently analyzed by SDS-PAGE with a modified acrylamide:bisacrylamide ratio followed by immunoblotting with polyclonal anti-Maf1 antibodies. The slower migrating diffuse bands correspond to phosphorylated forms of Maf1. Growth phenotypes on glycerol-containing medium at 37°C (YPGly) resulting from analyzed mutated *maf1* allele and the identified mutations are indicated on the right; (-) thermosensitivity, (+/-) moderate thermosensitivity.

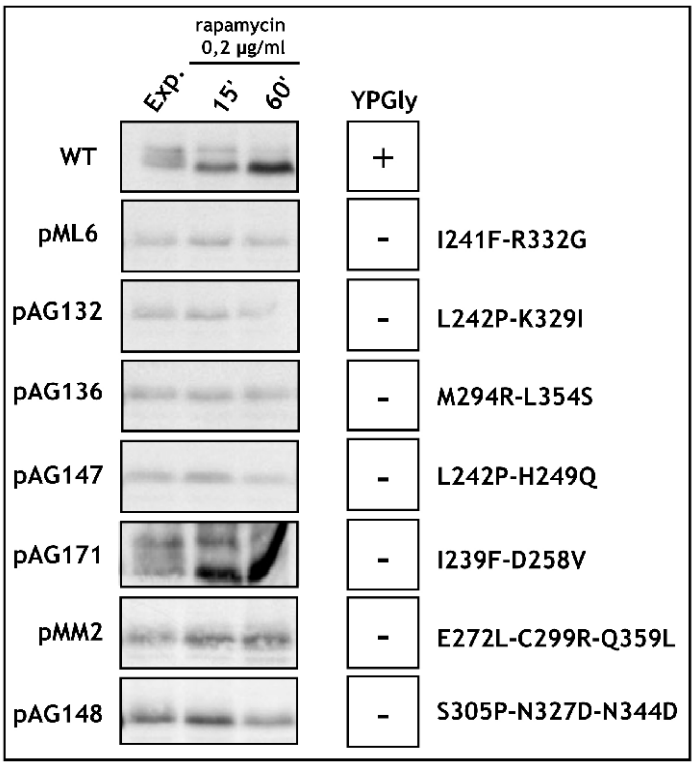

Figure 24. Analysis of dephosphorylation of Maf1 mutated in the BC domain in terms of starvation induced by rapamycin. Figure presents the YPH500 *maf1Δ* strain harboring plasmids carrying mutated *maf1* allele that influence thermosensitive growth on medium containing glycerol at 37°C (YPGly) (-). Identified mutations indicated on the right. Analysis performed as described in the legend to Fig. 23.

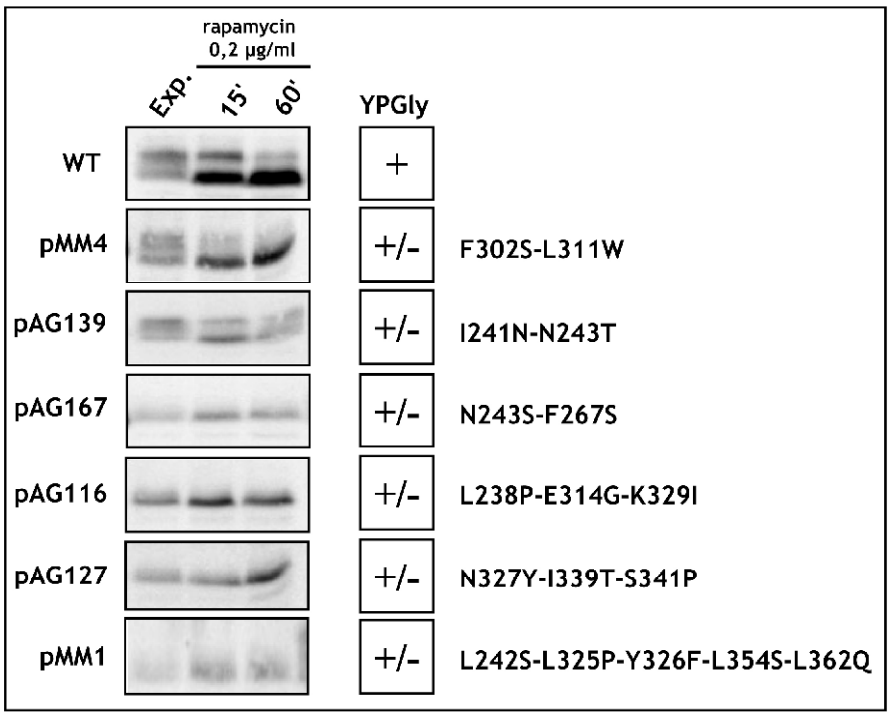

Figure 25. Analysis of dephosphorylation of Maf1 mutated in the BC domain in terms of starvation induced by rapamycin. Figure presents the YPH500 *maf1Δ* strain harboring plasmids carrying mutated *maf1* allele that influence moderate thermosensitive growth on medium containing glycerol (+/-). The identified mutations are indicated on the right. Analysis performed as described in the legend to Fig. 23.

Moreover, an interesting issue occurred under rapamycin treatment that is visible in all *maf1* mutants independently from its phosphorylation and capability to undergo dephosphorylation in nonpermissive conditions. The repeatedly appearance of the increased quantity of Maf1 in *S. cerevisiae* cells while rapamycin treatment, independently of strain tested, which indicated, that observed effect is due to increased expression of Maf1 under starvation stress conditions (compare lane 15' and 60' after rapamycin treatment on Fig. 23-25). Similar increased level of Maf1 synthesis upon stress conditions was visible on Western blotting analyses presented in Oficjalska-Pham *et al.,* 2006 (for rapamycin) and Roberts *et al.,* 2006 (for chlorpromazine, CPZ).

One might suspect that apart from the phosphorylation state of Maf1 the level of Maf1 expression is an additional mode of Maf1 activity regulation. Thus it might be possible that in more harsh stress conditions, when rapid inhibition of Pol III transcription is required, an increased synthesis of Maf1 occurs, which leads to more efficient Pol III repression. This hypothesis is supported by the bioinformatic analysis of *MAF1* promoter sequence (Graczyk, 2006 – master thesis, data unpublished). Comparative analysis of the *MAF1*promoter sequence of such yeast species as: *S. cerevisiae, S. paradoxus, S. kudriavzev, S. mikatae, S. bayanus* and

S. pombe revealed the presence of conserved consensus sequence for following transcription factors: Pho 4 (gnktgcac(-)), Abf1 (rTCAyTnnnnAc) and Msn4 (mAGGGG). The used abbreviation correspond to: N – nonspecific nucleotide, R – purine, Y – pirymidine, M – adenine or cytosine, K – guanidine or tymidine, with the lower-case letters are signed for nucleotides of a minor impact on transcription factor binding.

The increased quantity of Maf1 under rapamycin treatment might be due to the up-regulation by Msn4 transcription factor, which possibly binds to the *MAF1* promoter sequence. Msn4 is the transcription factor that regulate the general stress response of *S. cerevisiae* (Martinez-Pastor *et al.,* 1996). Msn4 regulates the expression of ~200 genes in response to several stresses, including heat shock, osmotic shock, oxidative stress, low pH, glucose starvation, sorbic acid and high ethanol concentrations, by binding to the STRE element (stress response element), mAGGGG, located in the promoters of these genes (Gasch *et al.,* 2000; Causton *et al.,* 2001).

Perturbations in phosphorylation and dephosphorylation phenomena observed among the selected *maf1* mutants (Table 4) was cautiously analyzed by bioinformatic approach revealing detailed impact of identified amino acid substitutions on preservation of potential phosphorylation sites in mutated Maf1 forms or possible manifestation of novel phosphorylation sites that appear due to introduction of amino acid substitutions into Maf1 sequence. To predict both: changed and novel phosphorylation sites in *maf1* protein, NetPhos v 2.0 software has been applied (http://www.cbs.dtu.dk/services/NetPhos/) (Bloom *et al.,* 1999). Potentially phosphorylated serine, threonine and tyrosine residues have been depicted in Table 5. Concomitant kinases targeting the indicated phosphorylation sites were allocated by NetPhosK v 1.0 software, a kinase-specific eukaryotic protein phosphorylation sites prediction tool (http://www.cbs.dtu.dk/services/NetPhosK/). (Bloom *et al.,* 2004). Currently, NetPhosK covers the following kinases: PKA, PKC, PKG, CKII, Cdc2, CaM-II, ATM, DNA PK, Cdk5, p38 MAPK, GSK3, CKI, PKB, RSK, INSR, EGFR and Src.

Indeed, performed analyses revealed major discrepancies between the already existing in Maf1 potential phosphorylation sites and both modification and emerging novel phosphorylation sites in *maf1* proteins presenting disturbance in phosphorylation and dephosphorylation phenomena. (Table 5). Furthermore modifications of phosphorylation sites implied also alteration of set of kinases targeting indicated phosphorylation sites. E. g in many *maf1* alleles substitution

S245 was detected. This serine was depicted as a potential phosphorylation site, a target for kinases: DNAPK and cdc2. Alteration in sequence of context caused by adjacent mutations led to the abolition of cdc2 kinase activity in advantage of the DNAPK kinase (L242P-K329I (pAG132), L242P-H249Q (pAG147), L242S-L325P-Y326F-L354S-L363Q (pMM1) *maf1* mutants) or the contrary - abolition of the DNAPK kinase activity in advantage of cdc2 (N243S-F267S (pAG167) *maf1* mutant) or abolition of other kinases like PKA - also in (N243S-F267S (pAG167) *maf1* mutant).

However, crucial alterations significantly affecting phosphorylation and dephosphorylation phenomena may be the effect of elimination of potential phosphorylation sites in *maf1* proteins (in. pAG23, pAG136, pMM2, pAG148, pAG127 plasmids) or a manifestation of novel phosphorylation sites (in pAG23, pAG132, pAG136, pAG147, pAG167 and pMM1 plasmids).

	WT dephosphorylation		**Affected dephosphorylation**	
A	**-**	**+/-**	**-**	**+/-**
	pAG61 (K2E-N117I-*maf1*)	**pAG8** (F32I-*maf1*)	**pAG23** (F32S-I54T-N142D-*maf1*)	-
	-	**pAG67** (E10G-S39P-L149F-*maf1*)	-	-
BC	**pAG171** (I239F-D258V-*maf1*)	**pMM4** (F302S-L311W-*maf1*)	**pML6** (I241F-R332G-*maf1*)	**pAG167** (N243S-F267S-*maf1*)
	-	**pAG139** (I241N-N243T-*maf1*)	**pAG132** (L242P-K329I-*maf1*)	**pAG116** (L238P-E314G-K329I-*maf1*)
	-	-	**pAG136** (M294R-L354S-*maf1*)	**pAG127** (N327Y-I339T-S341P-*maf1*)
	-	-	**pAG147** (L242P-H249Q-*maf1*)	**pMM1** (L242S-L325P-Y326F-L354S-L363Q- *maf1*)
	-	-	**pMM2** (E272L-C299R-Q359L-*maf1*)	-
	-	-	**pAG148** (S305P-N327D-N344D-*maf1*)	-

Table 4. Classification of analyzed plasmids carrying *maf1* allele according to observed ability of mutated Maf1 to undergo dephosphorylation under conditions of starvation induced by rapamycin. Growth phenotype on glycerol-containing medium at 37°C (YPGly) resulting from analyzed mutated *maf1* allele is indicated above lanes: (-) thermosensitivity; (+/-) moderate thermosensitivity.

Table 5. Analysis of potential phosphorylation sites in Maf1 mutants, which disruption by concomitant mutations in sequence of context, may cause defect in phosphorylation and following dephosphorylation of mutated Maf1 under rapamycin treatment. Prediction of potentially phosphorylated serine, threonine and tyrosine residues performed by NetPhos v 2.0 software(http://www.cbs.dtu.dk/services/NetPhos/). Prediction of kinases involved in phosphorylation of indicated residues by NetPhosK v 1.0 software. (http://www.cbs.dtu.dk/services/NetPhosK/). Output score is a value in the range [0.000-1.000]. Only scores above the threshold of 0.500 are taken into account. Table presents both: changed or disrupted phosphorylation sites already existing in Maf1 sequence and novel phosphorylation sites appeared in according to amino acid substitutions identified in mutated Maf1 forms.

Plasmid	Amino acid substitution	Predicted phosphorylation sites	Context sequence	Score (≥0.5)	Predicted kinases	Score (≥0.5)	Novel phosphorylation sites
pAG23	F32S I54T N142D	T34 - lost S138 - changed	DI**S**T**T**KAVA TFPK**S**AKL**D**	0.658 0.983	PKC not detected	0.57 -	yes
		S32 – new T33 – new	SCDI**S**TTKA CDIS**T**TKAV	0.684 0.574	cdc2 PKC	0.54 0.81	
pML6	I241F R332G	S245 - changed	**F**LNA**S**YPDH	0.962	DNAPK / cdc2	0.51 / 0.51	none
pAG132	L242P K329I	S245 - changed	I**P**NA**S**YPDH	0.989	DNAPK / cdc2 - lost	0.51 / -	yes
		Y246 - new	**P**NAS**Y**PDHD	0.866	not detected	-	
pAG136	M294R L354S	T295 - lost	NSH**MR**LSDC	0.523	not detected	-	yes
		S297 – new S354 - new	HRTL**S**DCVL VEDA**S**AKKP	0.919 0.947	RSK / PKA PKC	0.54 / 0.76 0.69	
pAG147	L242P H249Q	S245 - changed	I**P**NA**S**YPD**Q**	0.991	DNAPK / cdc2 - lost	0.51	yes
		Y246 – new S252 – new S253 - new	PNAS**Y**PDQD D**Q**DF**S**SVEP **Q**DFS**S**VEPT	0.640 0.937 0.994	not detected CKII not detected	- 0.58 -	
pMM2	E272L C299R Q359L	S277 - lost T274 - lost Y276 - lost T295 - changed	**L**NTLY**S**LGRQ KF**L**N**T**LYSL **L**NTL**Y**SLGR NSHM**T**LSD**R**	0.685 0.786 0.586 0.658	CKI / PKC DNAPK not detected not detected	0.61 / 0.67 0.50 - -	none
pAG148	S305P N327D N344D	S305 - lost S309 - changed S345 - changed S346 - changed	LFQY**PP**SNS **P**PSN**S**FLED SRL**DS**STGE RL**D**S**S**TGEV	0.819 0.663 0.949 0.989	GSK3 CKII RSK / PKA CKII	0.50 0.59 0.53 / 0.61 0.57	none
pAG167	N243S F267S	S245 - changed S263 - changed T262 - changed	IL**S**A**S**YPDH FVKT**S**LKT**S** DFVK**T**SLKT**S**	0.992 0.895 0.753	DNAPK - lost / cdc2 CKI / PKC / PKA - lost PKC	- / 0.55 0.57 / 0.59 / - 0.65	yes
		S267 – new S269 - new	SLKT**S**ISKF KT**S**I**S**KFEN	0.980 0.842	not detected not detected	- -	

Continued:

Plasmid	Amino acid substitution	Predicted phosphorylation sites	Context sequence	Score (≥0.5)	Predicted kinases	Score (≥0.5)	Novel phosphorylation sites
pAG116	L238P E314G K329I	S309 - changed Y317 - changed	SPSN**S**FLEDG D**G**PG**Y**LWNL	0.651 0.848	CKII not detected	0.55 -	none
pAG127	N327Y I339T S341P	S345 - lost S346 - changed	**P**RLN**S**STGE **P**RLNS**S**TGE	0.824 0.959	RSK / PKA CKII	0.52 / 0.67 0.53	none
pMM1	L242S L325P Y326F L354S L362Q	S245 - changed Y246 – new S354 - new	I**S**NA**S**YPDH **S**NAS**Y**PDHD VEDA**S**AKKP	0.994 0.950 0.947	DNAPK / cdc2 - lost not detected PKC	0.51 / - - 0.69	yes

The described bioinformatic analysis could explain the detected disturbance in the ability of Maf1 mutant forms to undergo proper phosphorylation followed by dephosphorylation under rapamycin treatment. Nevertheless, an additional experiments are required to validate these bioinformatic models.

1.3.3 Analysis of phosphorylation patterns of Maf1 mutatnt proteins.

Since preceding survey highlighted the problem of defect in mutated Maf1 phosphorylation forms an attempt to better discriminate between different alterations has been made. Using Odyssey™ Infrared Imaging System, I could more clearly analyze the phosphorylation pattern of wild-type Maf1 and its mutated derivatives. Odyssey™ Infrared Imaging System bases on Western blotting analysis but instead of HRP-conjugated secondary antibodies employs secondary antibodies labeled with IRDye™ infrared dyes. This system provides higher sensitivity and enables to obtain sharper, more detailed bands and visualize subtle mobility shifts caused by protein modifications such as phosphorylation. Since then served as a valuable tool to study phosphorylation pattern among analyzed *maf1* alleles.

To this aim, cells were grown in rich medium containing glucose to exponential growth phase. Crude cell extracts isolated from YPH500 *maf1Δ S. cerevisiae* strain expressing mutated *maf1* allele were subjected to SDS-PAGE with modified acrylamide:bisacrylamide ratio as described previously (Oficjalska-Pham *et al.,* 2006) and subjected to immunoblotting with polyclonal anti-Maf1 antibodies followed by incubation with secondary antibodies labeled with IRDye™ infrared dyes in accord with protocol provided by LI-COR™ Biosciences.

Preliminary study of Maf1 mutated forms shows diverse phosphorylation pattern among examined *maf1* alleles.

Studied *maf1* alleles were partitioned into two groups: exhibiting not affected dephosphorylation under rapamycin induced conditions of starvation and that of observed affected dephosphorylation (Table 4). Comparative analysis of *maf1* alleles by Odyssey™ Infrared Detection System revealed that *maf1* alleles presenting in previous Western blotting analysis not affected dephosphorylation, similar to that observed in wild-type Maf1 (WT), have in exponential growth phase, as well, analogous phosphorylation pattern to that observed in WT Maf1 (Fig.26).

The second group of *maf1* alleles presented in previous Western blotting analysis affected phosphorylation and dephosphorylation under rapamycin

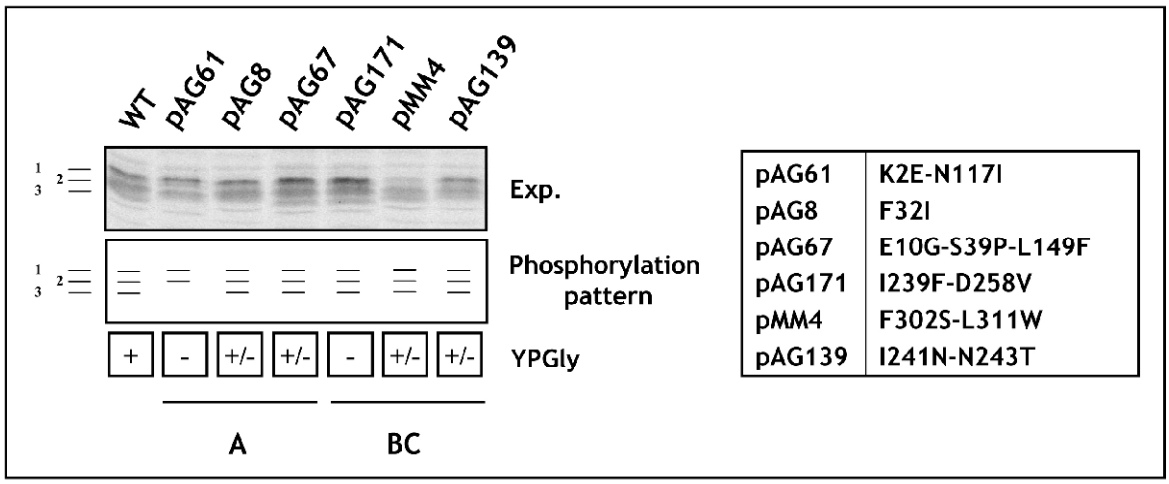

Figure 26. Phosphorylation patter of mutated Maf1s comparable to nonmutated Maf1. Mutated Maf1 that are regularly dephosphorylated under rapamycin treatment (see Table 4) exhibit, in exponential growth phase (Exp.), phosphorylation pattern comparable to nonmutated (WT) Maf1 unspecific to region mutagenized and growth phenotype observed among examined yeast cells. The YPH500 *maf1Δ* strain harboring plasmids carrying mutated *maf1* allele was grown to exponential phase (Exp.) in rich glucose medium. Cells were harvested as described in legend to Fig. 20 and subsequently analyzed by SDS-PAGE with a modified acrylamide:bisacrylamide ratio followed by immunoblotting with polyclonal anti-Maf1 antibodies. For visualization of Maf1 phospho forms Odyssey™ infrared fluorescence detection system involving secondary polyclonal antibodies labelled with IRDye™ infrared dyes was used. Growth phenotype on glycerol-containing medium at 37°C (YPGly) resulting from analyzed mutated *maf1* allele indicated below; (-) thermosensitivity, (+/-) moderate thermosensitivity.

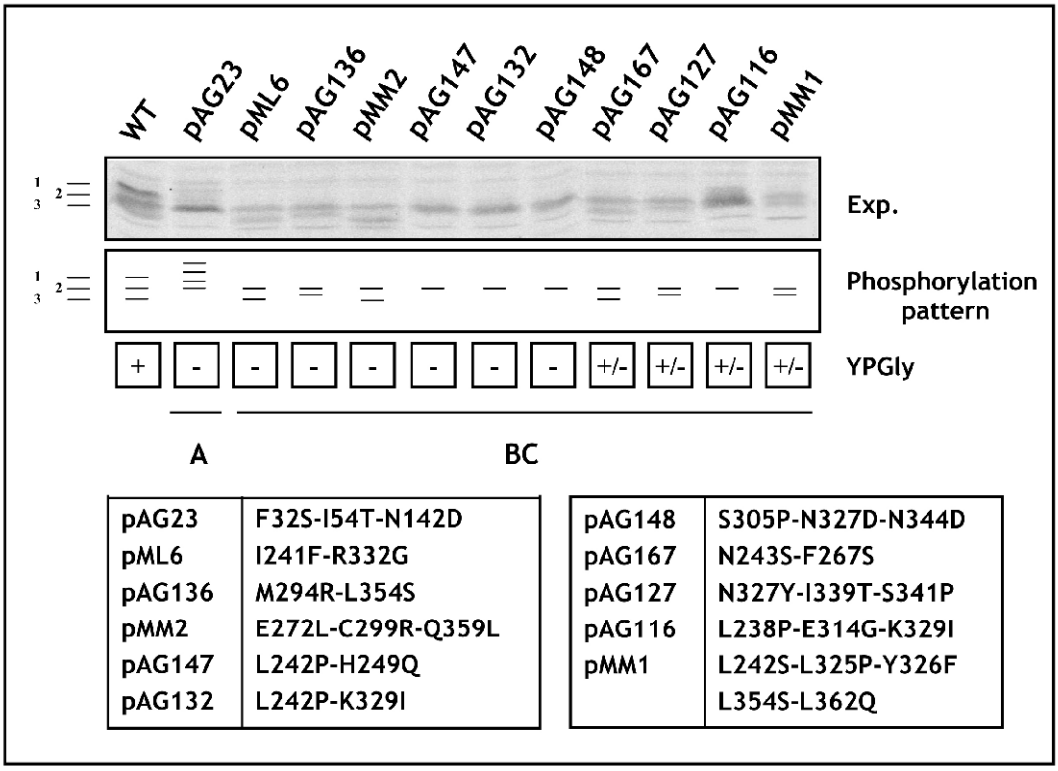

Figure 27. Changed phosphorylation pattern of mutated Maf1. Mutated Maf1s that exhibit defect in dephosphorylation under rapamycin treatment (see Table 4) exhibit miscellaneous phosphorylation pattern even in exponential growth phase (Exp.), unspecific to region mutagenized and growth phenotype observed among examined yeast cells. Analysis performed as described in legend to Fig. 26.

treatment in comparison with WT. Even in absence of rapamycin, in exponential growth phase, this group presented diverse phosphorylation pattern (Fig. 27).

Detected phosphorylation patterns did not correlate neither to the growth phenotype on glycerol-containing medium of relevant yeast cells nor to the region of Maf1 mutagenized (A domain or BC domain). However, investigated *maf1* alleles visibly portrayed several "classes" of phosphorylation patterns indicating some universal changes in mutated Maf1 folding reflected by a different type of phosphorylation. Also this "classes" of phosphorylation patterns could not be simply elucidated by detailed analysis of potential phosphorylation sites that were altered or created *de novo* in Maf1 amino acid sequence (Table 5).

Unfortunately, analyses of *maf1* alleles by Odyssey™ Infrared Detection System in presence of rapamycin were not performed due to a lack of time.

The appearance of particular "classes" of phosphorylation patterns (Fig. 27) (i- F32S-I54T-N142D (pAG23); ii – I241F-R332G (pML6), N243S-F267S (pAG167); iii – M294R-L354S (pAG136), N327Y-I339T-S341P (pAG127), L242S-L325P-Y326F-L354S-L362Q (pMM1) and iv – L242P-H249Q (pAG147), L242P-K329I (pAG132), S305P-N327D-N344D (pAG148), L238P-E314G-K329I (pAG116) *maf1* mutants) implies some typical for each "class" alteration of mutated Maf1 activity. Thus capability of these mutated Maf1 forms to approach nucleus was subsequently studied as a next phenomena characterizing Maf1.

1.3.4 Cellular localization of Maf1 mutated proteins.

To investigate cellular localization of mutated Maf1 forms particular representatives of *maf1* allele were chosen from each of studied groups:

maf1 mutants undergoing nonaffected dephosphorylation under rapamycin treatment mutated in A domain K2E-N117I (pAG61) and mutated in the BC domain (I239F-D258V (pAG171), F302S-L311W (pMM4)).

maf1 mutants undergoing affected dephosphorylation under rapamycin treatment belonging to several "classes" of phosphorylation patterns described previously - mutated in A domain (i - F32S-I54T-N142D (pAG23) *maf1* mutant) and mutated in the BC domain (ii – I241F-R332G (pML6), N243S-F267S (pAG167); iii - N327Y-I339T-S341P (pAG127), L242S-L325P-Y326F-L354S-L362Q (pMM1) and iv – L238P-E314G-K329I (pAG116) *maf1* mutants).

To this aim cells were grown in rich medium containing glucose to exponential growth phase, treated with rapamycin (final concentration 0,2 μg/ml) and

incubated for 60 min. at 30°C. Localization of mutated Maf1s was analyzed by immunofluorescence microscopy using polyclonal anti-Maf1 antibodies. Nuclei were stained with 4',6-diamidino-2-phenylindole (DAPI).

The fluorescence signal of wild-type Maf1 (WT), during exponential phase of growth in glucose containing medium is dispersed through whole cell. After rapamycin treatment the concentration of Maf1 specific signal is observed in nucleus in accordance with published results (Oficjalska-Pham *et al.,* 2006) (Fig. 28).

Analysis of cellular localization of mutated Maf1 with preserved dephosphorylation capability showed that under rapamycin induction Maf1 might be present both: through all cell (K2E-N117I (pAG61) *maf1* mutant) as well as concentrated in nucleus as for wild-type Maf1 (I239F-D258V (pAG171) and F302S-L311W (pMM4) *maf1* mutants). Both cellular localizations of these *maf1* mutants indicate that the migration of mutated Maf1s from cytoplasm to nucleus is influenced by amino acid substitutions identified in these *maf1* alleles and that migration is not connected to dephosphorylation of these Maf1s.

Cellular localization of mutated Maf1 with disrupted dephosphorylation capability showed also diverse localization of mutated Maf1 forms (Fig. 28):

i - F32S-I54T-N142D (pAG23) *maf1* mutant is constantly present in cytoplasm.

ii – I241F-R332G (pML6) *maf1* mutant is constantly present in cytoplasm, which is not surprising since this *maf1* allele harbors mutation in nuclear localization signal sequence (NLS2) – R332G that disrupts transport to nucleus. Belonging to the same "class" of phosphorylation pattern, N243S-F267S (pAG167) *maf1* mutant presents nuclear localization under rapamycin induction.

iii – N327Y-I339T-S341P (pAG127) *maf1* mutant is constantly present in cytoplasm, while L242S-L325P-Y326F-L354S-L362Q (pMM1) *maf1* mutant exhibits nuclear localization under rapamycin treatment. That implies that we cannot deduce the cellular localization of Maf1 from the phosphorylation pattern. However, noteworthy is fact that N327Y-I339T-S341P (pAG127) *maf1* mutant harbors mutation N327Y, which is very close to NLS2 (328 – 332 aa) that raises possibility that cytoplasmatic localization is a result of disturbed NLS2 sequence.

iv – L238P-E314G-K329I (pAG116) *maf1* mutant is also constantly cytoplasmatic but as in case of I241F-R332G (pML6) *maf1* mutant this *maf1* allele harbors mutation in NLS2 sequence – K329I.

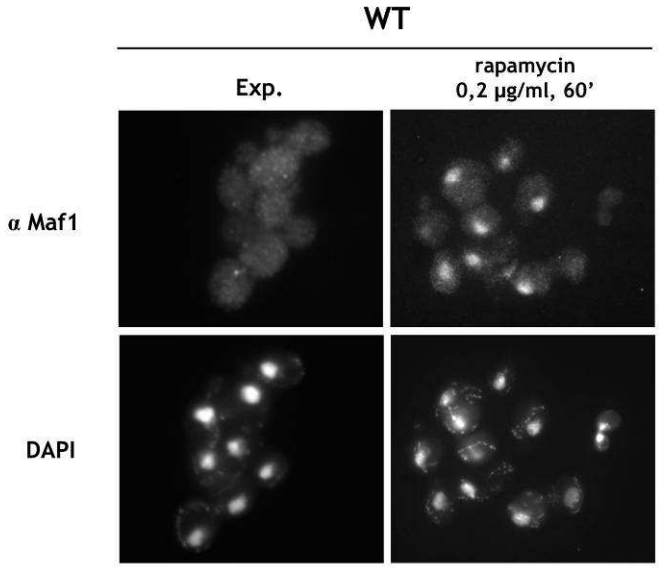

Exp. → rapamycin
cytoplasm → nucleus

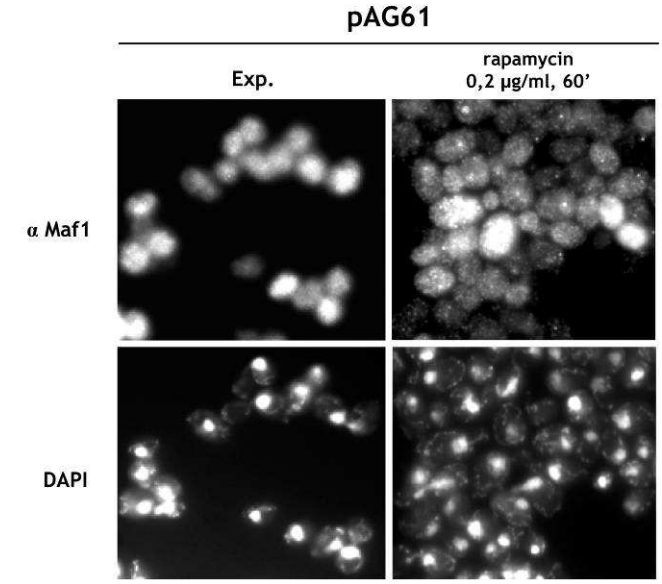

Exp. → rapamycin
cytoplasm → cytoplasm

pAG61 – K2E-N117I

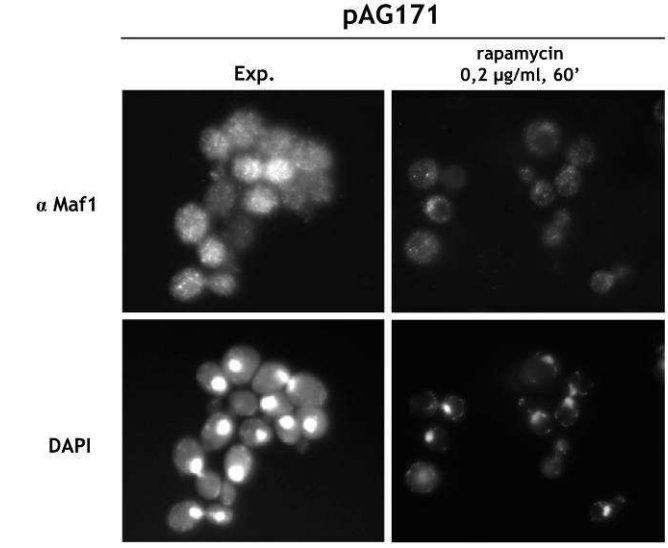

Exp. → rapamycin
cytoplasm → nucleus

pAG171 – I239F-D258V

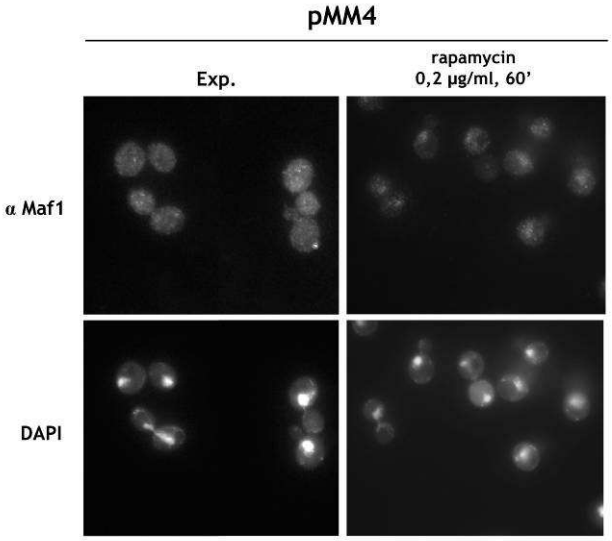

Exp. → rapamycin
cytoplasm → nucleus

pMM4 – F302S-L311W

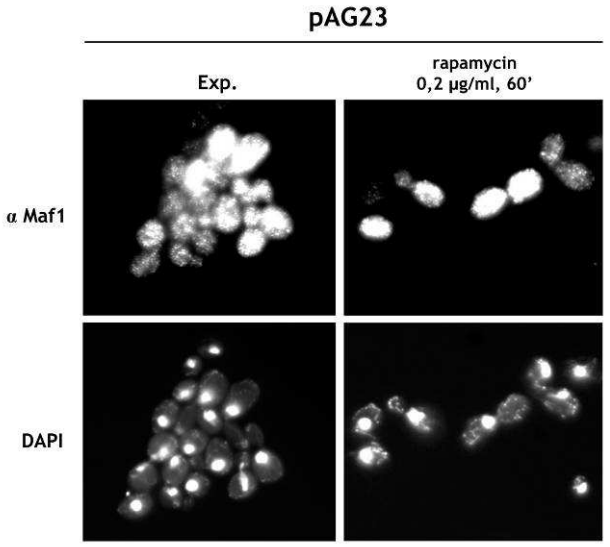

Exp. → rapamycin
cytoplasm → cytoplasm

pAG23 – F32S-I54T-N142D

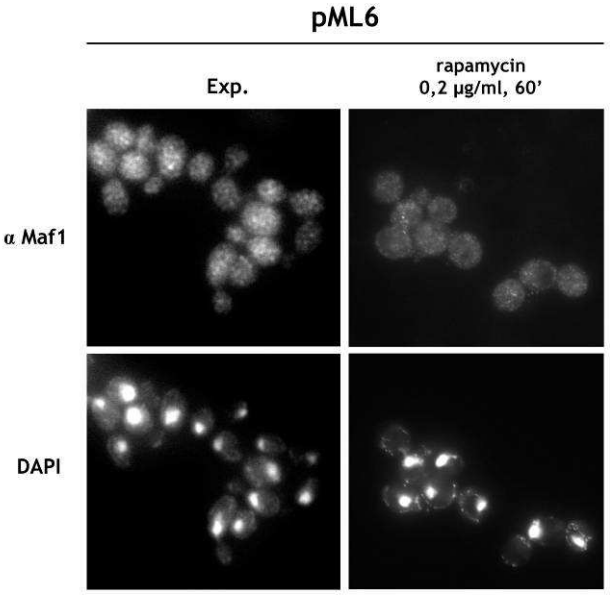

Exp. → rapamycin
cytoplasm → cytoplasm

pML6 – I241F-R332G

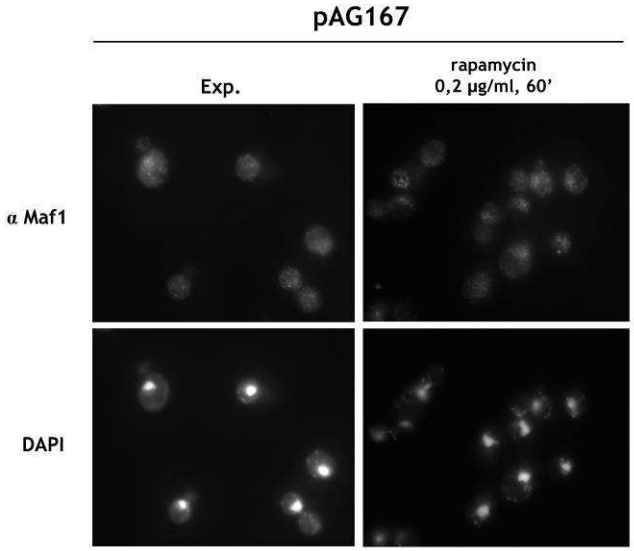

Exp. → rapamycin
cytoplasm → nucleus

pAG167 – N243S-F267S

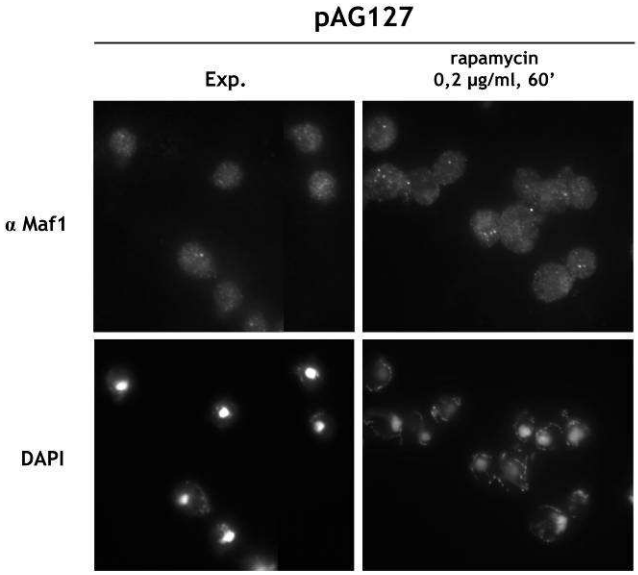

Exp. → rapamycin
cytoplasm → cytoplasm

pAG127 – N327Y-I339T-S341P

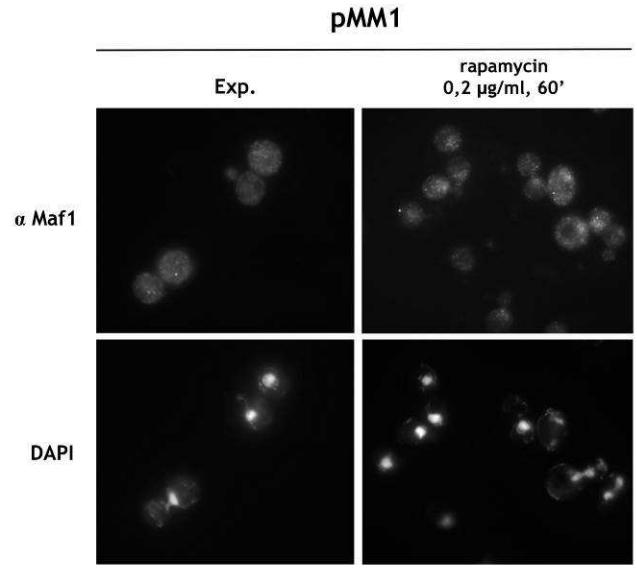

Exp. → rapamycin
cytoplasm → nucleus

pMM1 – L242S-L325P-Y326F-L354S-L362Q

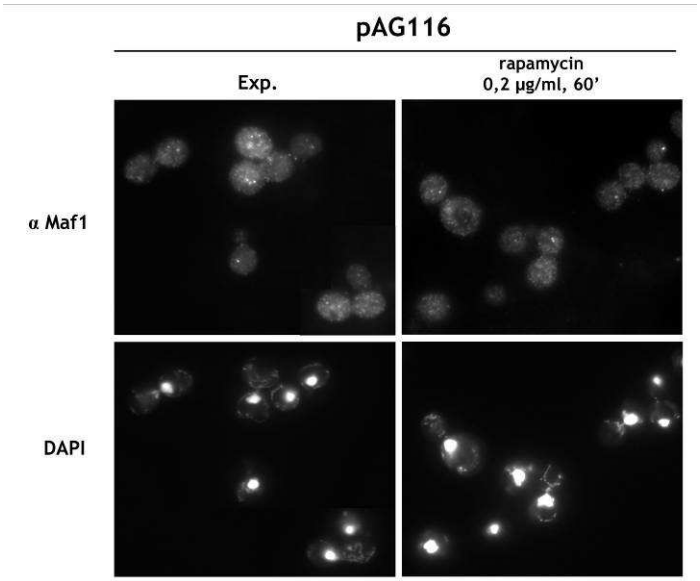

Exp. → rapamycin
cytoplasm → cytoplasm

pAG116 – L238P-E314G-K329I

Figure 28. Cellular localization of mutated Maf1 is independent from its ability to dephosphorylate under rapamycin treatment and observed initial phosphorylation pattern. The YPH500 *maf1Δ* strain harboring plasmids carrying mutated *maf1* allele was grown to exponential phase (Exp.) in rich glucose medium, exposed to rapamycin in final concentration of 0,2 µg/ml in medium and incubated further at 30°C for 60' (minutes). Cells were harvested as indicated. Maf1 localization was analysed by immunofluorescence microscopy using polyclonal anti-Maf1 antibodies. Nuclei were stained with 4',6-diamidino-2-phenylindole (DAPI); WT, wild-type.

Taken together there is not enough data to state about correlation between cellular localization and phosphorylation pattern of mutated Maf1 forms. However, supported on the fact, that N243S-F267S (pAG167) and L242S-L325P-Y326F-L354S-L362Q (pMM1) *maf1* mutants are transported to nucleus although exhibit affected phosphorylation and dephosphorylation phenomena while K2E-N117I (pAG61) *maf1* mutant is constantly cytoplasmatic although undergoes regular dephosphorylation under rapamycin treatment, one might deduce, that there is no correlation between capability of Maf1 to undergo dephosphorylation in terms of rapamycin treatment and its translocation to nucleus.

1.4. Summary

Dedicated study presented here, devoted to analysis of mutated Maf1 forms, revealed several important issues that are a promising field for further researches. Position analysis of identified among library of *maf1* alleles mutations could not uncover the region of Maf1 responsible for abolition of Maf1 activity as a Pol III repressor – as deduced from thermosensitive phenotype of relevant yeast cells on glycerol-containing medium. The BC domain seems to be more significant for Maf1 activity because with a higher evolutionarily conservation in comparison to A

domain. Moreover, mutations in the BC domain might lead to decreased synthesis of Maf1 or its degradation as assumed from diminishing expression profile of L242P-H249Q (pAG147), S305P-N327D-N344D (pAG148), N243S-F267S (pAG167), N327Y-I339T-S341P (pAG127), M294R-L354S (pAG136), I241F-R332G (pML6), E272L-C299R-Q359L (pMM2) and L242S-L325P-Y326F-L354S-L363Q (pMM1) *maf1* mutants. Furthermore these *maf1* mutants presented multiple differences in phosphorylation pattern and potential ability to undergo dephosphorylation. However, cautious examination of *maf1* mutants with altered phospho-forms showed that the disturbance in both: phosphorylation/dephosphorylation of Maf1 is region independent since either Maf1 mutated in the A domain or Maf1 mutated in the BC domain may present nonaffected phosphorylation/ dephosphorylation as well as affected. This observation appointed involvement of identified in *maf1* alleles amino acid substitutions in modification of potential phosphorylation sites present in Maf1. In addition detailed study over the *maf1* alleles presenting defect in phosphorylation/dephosphorylation phenomena revealed that it is possible to discriminate between several "classes" of defective phosphorylation patterns in SDS-PAGE. That insight suggests some universal changes in folding of mutated Maf1 reflected by a different type of phosphorylation. The appearance of particular "classes" of phosphorylation patterns implies some common characteristic for the different Maf1 functions. Furthermore, no correlation between capability of Maf1 to undergo dephosphorylation and its translocation to nucleus could be detected since either *maf1* alleles with preserved phosphorylation/dephosphorylation phenomena or affected dephosphorylation present both cellular localizations (nuclear or dispersed through all cell) under rapamycin treatment. The other functions of Maf1 (interaction with the Pol III enzyme, inhibition of Pol III transcription, exit from the nucleus after removal of rapamycin, etc.) should be studied in the future to decipher if there are some relationship between a class of phosphorylation pattern and a modification of a function of Maf1.

2. Full repression of RNA polymerase III transcription requires interaction between two domains of its negative regulator Maf1.

The results obtained by Christoph Műller's group upon *H. sapiens* Maf1 indicating interactions between the A and BC domains of Maf1 encouraged me to undertake a study upon the relation between evolutionarily conserved regions of Maf1 – A and BC domains. To investigate if the interaction between domains of Maf1 is conserved through evolution, the proposed hypothesis was analyzed in another organism, *S. cerevisiae* yeast, that is also more amenable to study structure-function relationships of Maf1. As a first raised problem, the potential genetic interaction between Maf1 domains has been studied and further predicted physical interaction between them.

2.1. Genetic interaction between evolutionarily conserved regions – A and BC domains of *S. cerevisiae* Maf1.

2.1.1 Screening for mutations localized in BC domain that suppress single point mutations identified in A domain.

One approach to study the genetic interaction between protein domains is to identify second-site mutations that compensate for the initially observed defects. I looked therefore for second site suppressor mutations within the BC-encoding region of *MAF1* that allowed thermosensitive *S. cerevisiae* cells harboring mutated A-encoding region of *MAF1* to grow on glycerol-containing medium at 37°C.

To this aim, among the library of Maf1 mutated in A domain, K35E-*maf1* (pAG70) mutant was chosen as an initial *maf1* allele. K35E-*maf1* mutant carries single amino acid substitution in highly conserved through evolution residue. This mutation results in moderate growth defect of relevant yeast cells on glycerol-containing medium at 37°C. The phenotype observed indicates partial disruption of Maf1 activity as previously described (see also Fig. 16). To obtain suppressor mutants a rapid method for localized mutagenesis ("Gap-repair") was applied as for library of Maf1 mutants construction (Muhlrad *et al.,* 1992). Using low-fidelity PCR, the sequence encoding BC domain (174-375 aa) of K35E-*maf1* allele was mutagenized and co-transformed to YPH500 *maf1*Δ *S. cerevisiae* strain with linearized plasmid carrying K35E mutation in *MAF1* sequence encoding A domain and gap in the sequence encoding BC domain. *In vivo* homologous recombination allowed for repair of gapped plasmid with the mutated sequence encoding BC domain of Maf1. As a result the library of *maf1* alleles mutated in the sequences

encoding both: A and BC domains was achieved (Fig. 29). Obtained library of mutated Maf1s was screened for recovery of growth ability on glycerol-containing medium at 37 °C (WT growth phenotype). Almost 1 000 potential suppressors were analyzed (Malgorzata Legowiak, master thesis). Selected transformants exhibiting WT growth phenotype were used to isolate plasmids carrying *maf1* allele and subsequently retransform to YPH500 *maf1*Δ *S. cerevisiae* strain to confirm that the phenotype observed results from mutations in *maf1* allele. Among investigated *maf1* alleles 6 represented WT growth on glycerol-containing medium (Table 6). However, sequencing revealed that only 2 *maf1* alleles carried mutations localized in either A domain or the BC domain that resulted in recovery of WT growth. Remaining could possibly demonstrate spontaneous mutations outside *MAF1* gene (3 plasmids pML13-15, Table 6) and 1 showed reversion of initial mutation K35E to nonmutated *MAF1* sequence (plasmid pML16, Table 6). The suppositious, spontaneous revertants outside *MAF1* gene were not subjected to further analysis.

Identified suppressor mutants in plasmids pML11 and pML12 harbored *maf1* carrying initial K35E mutation in sequence encoding A domain and respectively suppressor mutations in the sequence encoding BC domain with single D250E and double V260D-N344I amino acid substitutions (positions of the mutations are shown on Fig. 29).

Phenotypic analysis of identified suppressor mutants K35E-D250E-*maf1* and K35E-V260D-N344I-*maf1* revealed indeed WT growth on glycerol-containing medium at 37°C contrary to parental K35E-*maf1* mutant in sequence encoding A domain. This phenotypic suppression indicates genetic interaction between the Maf1 A and BC domains (Fig. 29).

Plasmid	Amino acid substitutions	Changes in codon	YPGly
pAG70	K35 → E	AAG → GAG	+/-
pML11	K35 → E D250→E	AAG → GAG GAT → GAG	WT
pML12	K35 → E V260 → D N344 → I	AAG → GAG GTC → GAC AAT → ATT	WT
pML13	K35 → E	AAG → GAG	WT
pML14	K35 → E	AAG → GAG	WT
pML15	K35 → E	AAG → GAG	WT
pML16	K35 → E → K	AAG → GAG → AAG	WT

Table 6. Plasmids carrying *maf1* mutated allele obtained in screen for suppressors of K35E A domain mutated Maf1 K35E-*maf1* (pAG70). Growth phenotype on glycerol-containing medium at 37°C (YPGly) tested by replica plating. (+/-) moderate growth defect, WT, wild-type - no growth defect.

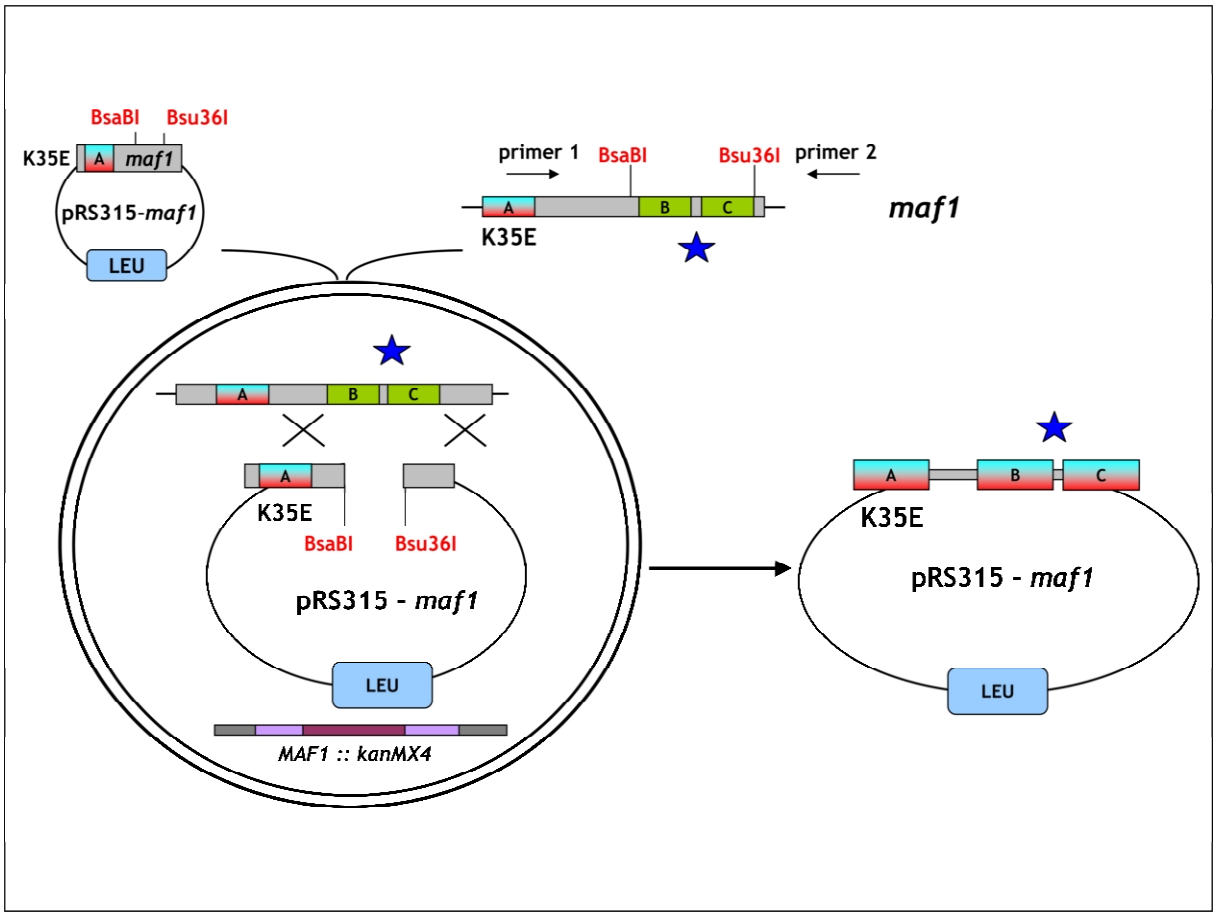

Figure 29. Schematic representation of experimental strategy applied for screening suppressor mutations localized in the BC domain of Maf1 that compensate the effect of single point mutation identified in the Maf1 A domain. Mutated A domain indicated with blue-red colour with signed identified amino acid substitution K35E. Maf1 BC domain indicated with green colour, "Gap-repair" system based on homological recombination *in vivo* has been presented. Mutated by low-fidelity PCR sequence encoding BC domain is designated with blue star. Resulting plasmid harbouring *maf1* mutated in the sequence encoding both: A and BC domains of Maf1 is shown on the right.

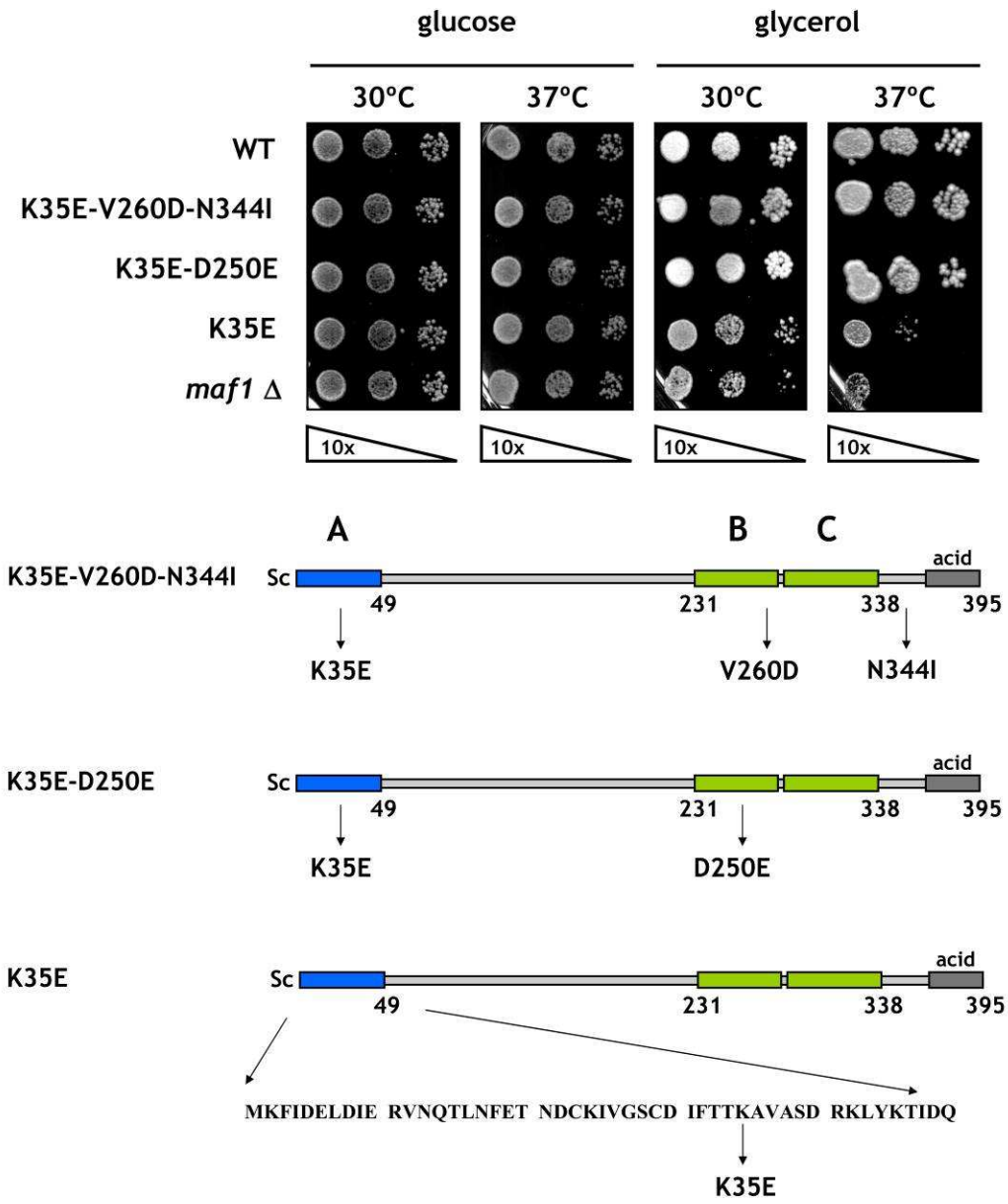

Figure 30. Phenotypic characterization of the two suppressor strains shows that they compensate for the defect of growth on glycerol-containing medium at 37°C (YPGly) of the primary K35E mutation. Tenfold serial dilutions of cells were plated on medium containing glucose (YPD) or glycerol (YPGly) and incubated at indicated temperatures. The control WT is YPH500 *maf1Δ* strain transformed with pRS315-*MAF1* plasmid. Suppressor strains are YPH500 *maf1Δ* strain transformed with plasmids harboring: K35E-V260D-N344I (pML12) and K35E-D250E (pML11) *maf1* alleles as well as initial K35E-*maf1* allele (pAG70). Location of the respective mutations in Maf1 amino acid sequence is presented below.

- **Separation of identified suppressor mutations.**

Identified suppressor mutations were subsequently separated from initial K35E mutation to distinguish the effect of second-site mutations from the cooperative effect. To introduce D250E, N344I, V260D and V260D-N344I mutations to pRS315-*MAF1* plasmid the QuickChange Site-Directed Mutagenesis Kit (Stratagene) was used. Growth phenotype on glycerol medium was tested. Separated mutations:

D250E, V260D and N344I did not influence growth of relevant yeast cells indicating no disturbance in Maf1 activity (Fig. 31). Contrary the double V260D-N344I mutant caused moderate growth defect. That accentuate the collective effect of joint: K35E and V260D-N344I mutations as a support for genetic interaction between the A and BC domains of Maf1 in yeast cells presenting recover of growth on glycerol-containing medium. Meaning, that the presence of V260D-N344I mutation, which separately causes disturbance in Maf1 activity, in joint with K35E mutation, which separately also causes disturbance in Maf1 activity, all together abolish their negative effect as deduced by recovery of the growth phenotype on glycerol-containing medium.

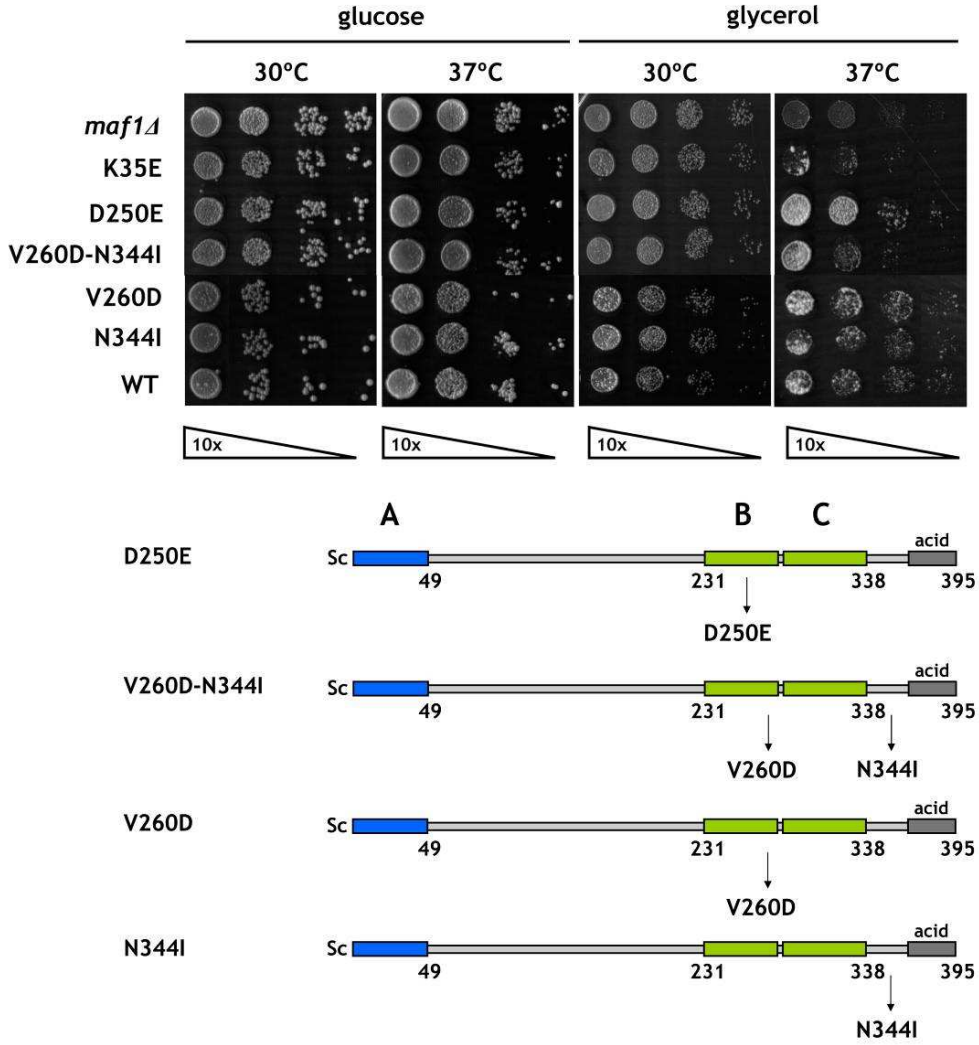

Figure 31. Phenotypic characterization of the strains harboring *maf1* allele with separated mutations that were originally found in suppressors of the K35E *maf1* allele. Tenfold serial dilutions of cells were plated on medium containing glucose (YPD) or glycerol (YPGly) and incubated at indicated temperatures. As described in legend to Fig. 30, all presented *maf1* alleles (harbored on the plasmid) were tested in YPH500 *maf1Δ* background strain. Location of the respective mutations in Maf1 amino acid sequence is presented below.

2.1.2 Suppressor mutations in BC domain recover the function of Maf1 mutated in A domain.

- **Suppressor mutations recover the capacity of Maf1 mutated in A domain to repress Pol III in correlation to growth phenotype on glycerol-containing medium.**

To inspect the effect of K35E mutation in Maf1 on Pol III activity, RNA isolated from cells grown in the presence of glucose and transferred to glycerol medium at 37°C was analyzed by Northern blotting using probes for pre-tRNA^{Leu} and tRNA^{Phe} (Figure 32A). Following transfer to the medium with the nonfermentable carbon source, pre-tRNA levels (that indicate the level of transcription) were decreased in the wild type but not in *maf1Δ* cells (Figure 32A, compare lanes 1, 5 and 6, 10). Similarly to *maf1Δ*, the K35E mutant was defective in its ability to repress pre-tRNA synthesis upon transfer to glycerol medium (Figure 32A, lanes 2 and 7). Thus, the single missense mutation within the Maf1 A domain precluded Pol III repression in K35E-*maf1* strain.

Phenotypic characterization of the two suppressor strains showed that they compensate for the defect of growth on glycerol medium at 37°C of the primary K35E mutation (Figure 32B). The increased growth capacity of the suppressors on glycerol medium was due to a compensation of the defect in Pol III regulation observed for the K35E mutation. As determined by Northern blotting, the suppressor mutations restored the ability to repress pre-tRNA synthesis upon transfer from glucose to glycerol medium (Figure 32A, compare lanes 3, 4 and 8, 9).

These results indicate that the detected genetic interaction between the two Maf1 domains is a functional one.

Moreover, the separated mutations D250E, V260D and N344I neither influenced growth capacity of relevant yeast cells on glycerol-containing medium (Fig. 33B and 18D) nor affected repression of Pol III in analogous conditions (Fig. 33A, compare lanes 2 and 6; Fig. 33C, compare lanes 1, 2 and 4, 5). Contrary, the double V260D-N344I mutant that showed a temperature-sensitive growth in glycerol-containing medium, was also defected in regulation of tRNA synthesis (Fig. 33A, compare lanes 3, 7 and 18B).

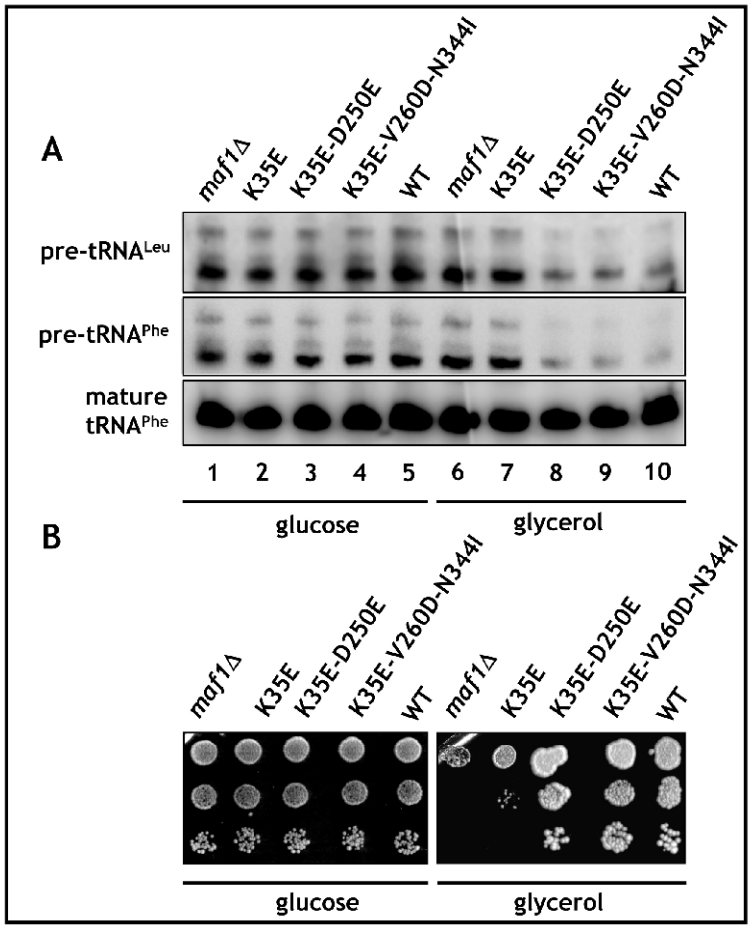

Figure 32. Regulation of Pol III transcription and growth is impaired by the K35E mutation in region encoding A domain and restored by second-site suppressor mutations in the BC domain of *MAF1*. *maf1Δ*, K35E-*maf1*, K35E-D250E-*maf1* and K35E-V260D-N344I-*maf1* mutants (harbored on a plasmid) and isogenic wild type strain YPH500 *maf1Δ* strain transformed with pRS315-*MAF1* plasmid (WT) were used. A. Cells were grown to exponential phase in glucose medium (YPD) at 30°C, then transferred to glycerol medium (YPGly) and incubated at 37°C for 1.5 h. Total RNA isolated from cells was tested by Northern blotting with pre-tRNA^{Leu} and tRNA^{Phe} probes. B. Ten-fold serial dilutions of cells grown to exponential phase in glucose medium were plated on glucose medium (YPD) and incubated at 30°C or on glycerol medium (YPGly) and incubated at 37°C for 2-3 days.

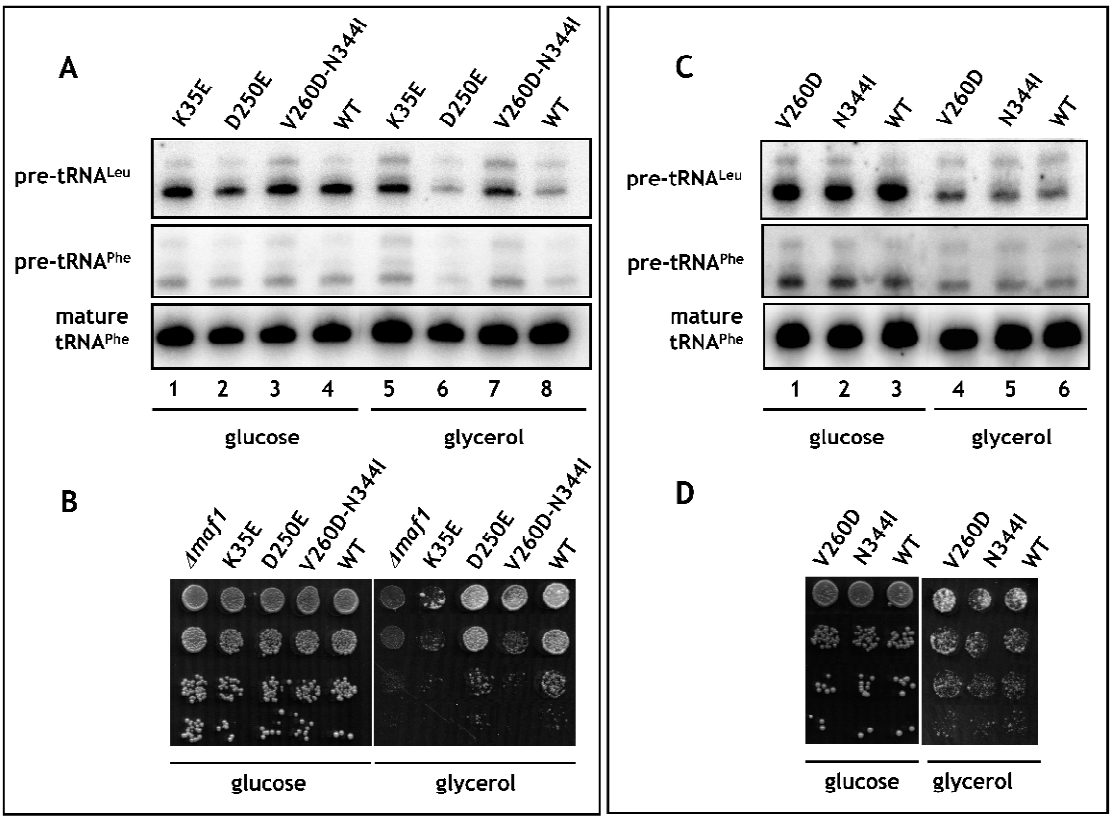

Figure 33. Regulation of Pol III transcription is correlated with growth of mutants originating from suppressor strains. Mutations were generated in the BC domain of Maf1 in the context of the wild type A domain. Double mutations V260D-N344I impaired regulation of tRNA synthesis and growth of yeast on glycerol-containing medium, whereas single mutation D250E (A) V260D and N344I (C) showed no effect. Cells were grown to exponential phase in YPD glucose medium at 30°C (Exp), then transferred to glycerol YPGly medium and incubated at 37°C for 1.5 h. Total RNA isolated from cells was tested by Northern blotting with pre-tRNA^{Leu} and tRNA^{Phe} probes. (B,D) Ten-fold serial dilutions of cells grown to exponential phase in glucose medium were plated on glucose medium (YPD) and incubated at 30°C or on glycerol medium (YPGly) and incubated at 37°C for 2-3 days.

- **Suppressor mutations overcome the defect in dephosphorylation of Maf1 mutated in A domain.**

As shown before, phosphorylation of Maf1 precluded Pol III repression when *S. cerevisiae* cells were grown on glucose medium (Towpik *et al.,* 2008). Transfer of yeast cells to a nonfermentable carbon source resulted in Maf1 dephosphorylation, import of Maf1 into the nucleus and inhibition of tRNA synthesis (Ciesla *et al.,* 2007).

As the phosphorylation and subsequent dephosphorylation of Maf1 is linked to the regulation of Maf1 activity , I have studied this phenomena in Maf1 mutated in A domain (K35E-*maf1*), identified suppressor mutants (K35E-D250E-*maf1* and K35E-V260D-N344I-*maf1*) and Maf1 mutated in the BC domain with D250E, V260D, N344I and V260D-N344I mutations separated from initial mutation K35E. Differentially phosphorylated forms of Maf1 were resolved by SDS-PAGE and

identified by immunoblotting at various times after culture transfer from glucose to glycerol medium (Fig. 34).

As reported previously, wild type Maf1 was quickly dephosphorylated upon this transition. Remarkably, the K35E mutation in A domain appeared to preclude the dephosphorylation of Maf1. Significantly suppressor mutations, restoring the capability of Maf1 to repress Pol III, K35E-D250E (pLM11) and K35E-V260D-N344I (pLM12) re-established rapid dephosphorylation of Maf1 following transfer from glucose to a nonfermentable carbon source (Fig. 34A). Maf1 dephosphorylation in the suppressor mutants was only a little slower than in the wild type strain. The relative ratio between phosphorylated and nonphosphorylated form of Maf1 normalized to that observed in exponential growth phase for each strain supplied underneath the pictures shows approximate speed of Maf1 dephosphorylation in mutants strains (quantification is shown in supplementary material - Table S6).

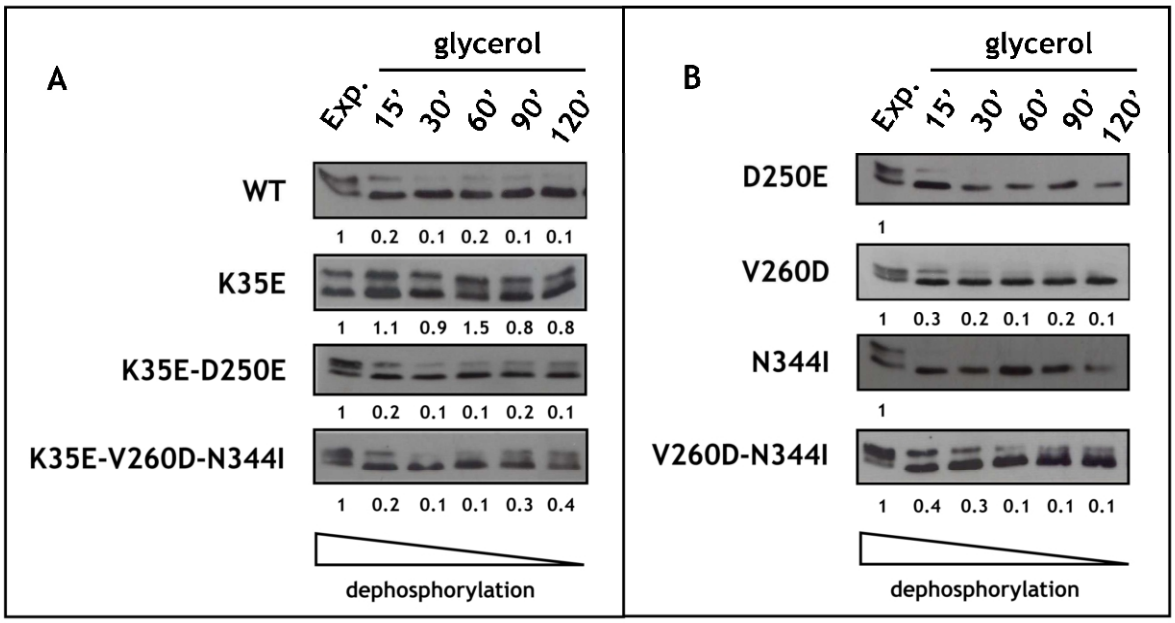

Figure 34. Mutations altering Maf1 dependent Pol III repression affect kinetics of Maf1 dephosphorylation upon transfer of *S. cerevisiae* cells from glucose to medium containing glycerol. A. K35E-*maf1*, K35E-D250E-*maf1* and K35E-V260D-N344I-*maf1* mutant strains and isogenic YPH500 *maf1Δ* strain transformed with pRS315-*MAF1* plasmid (WT) were grown to exponential phase in YPD glucose medium (Exp), then transferred to glycerol YPGly medium, incubated at 37ºC and harvested as indicated. Cell crude extracts were subsequently analyzed by SDS-PAGE with a modified acrylamide:bisacrylamide ratio followed by immunoblotting with polyclonal anti-Maf1 antibodies. The slower migrating diffuse bands correspond to phosphorylated forms of Maf1. B. D250E-*maf1*, V260D-*maf1*, N344I-*maf1* mutants originating from identified suppressor mutants were constructed in the BC domain of Maf1 in the context of the wild type A domain. Yeast cells were subjected to analogous analysis as described above. Double V260D-N344I mutations precluded dephosphorylation of Maf1 upon transfer of yeast to glycerol medium, whereas single D250E, V260D and N344I mutations showed no effect. Values below each lane indicate the relative ratio between phosphorylated and nonphosphorylated Maf1 form normalized to Exp. Quantification is supplied in Table S6-S7.

Interestingly, double V260D-N344I mutation in context of wild type A domain visibly delayed Maf1 dephosphorylation upon transfer of *S. cerevisiae* to glycerol medium (Fig. 34B, quantification is shown in supplementary Table S7) in correlation to observed previously defect in growth on glycerol medium and inability to repress Pol III after transition to nonfermentable carbon source. In opposite separated mutations D250E, V260D and N344I showed dephosphorylation as rapid and efficient as WT strain that corresponds to the WT growth phenotype and nondefected repression of Pol III.

- **Suppressor mutations recover defected cellular transport of Maf1 mutated in A domain.**

Immunofluorescence microscopy indicates that the wild type Maf1 is visible through all cell during exponential phase of growth in glucose medium. Subsequent transfer to glycerol medium causes accumulation of fluorescence signal in nucleus in correlation with Maf1 nuclear activity towards RNA Pol III repression (Fig. 35A).

In single point A domain mutant (K35E-*maf1*) Maf1 is distributed in exponential phase through all cell. Transfer of yeast cells to glycerol-containing medium causes translocation of K35E-*maf1* to nucleus but its transport is visibly impaired comparing to the wild type Maf1. After 2 hours of incubation in medium with glycerol there is almost 3 times less cells with K35E-*maf1* located in nucleus (29%) in comparison to wild type cells (84%) (Fig. 35B). It might be related to the observation of impaired dephosphorylation of K35E-*maf1* mutant. The fluorescence signal of Maf1 in suppressor mutants (K35E-D250E-*maf1* and K35E-V260D-N344I-*maf1*) follows Maf1 localization in wild type cells (Fig. 35A) but the percentage amount of cells with nuclear Maf1 in suppressors is slightly lower than in wild type strain (67% and 61% respectively) comparing to wild type cells (84%) (Fig. 35B). Observed dissimilarity could be related to the slight delay in Maf1 dephosphorylation in suppressor mutants in comparison to wild type Maf1.

Detailed quantification of cells with nuclear and cytoplasmatic localization of mutated Maf1 (K35E-*maf1,* K35E-D250E-*maf1* and K35E-V260D-N344I-*maf1*) in exponential growth phase and after transition to glycerol-containing medium is presented in supplementary Table S8.

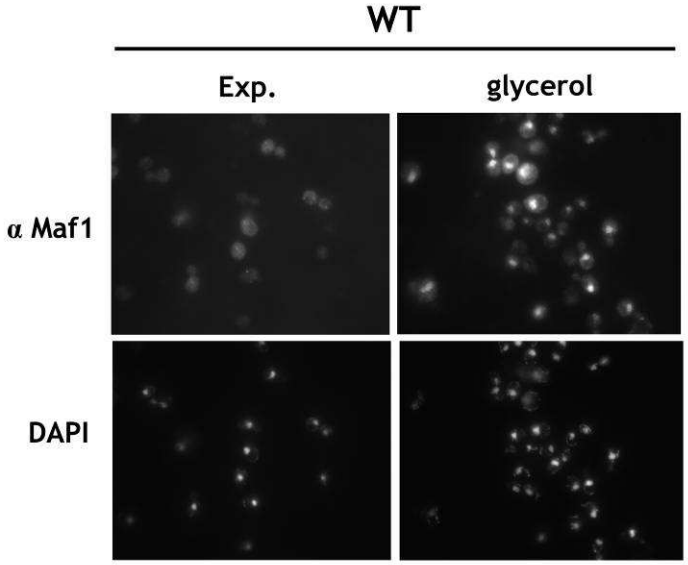

Exp. → YPGly
cytoplasm → nucleus

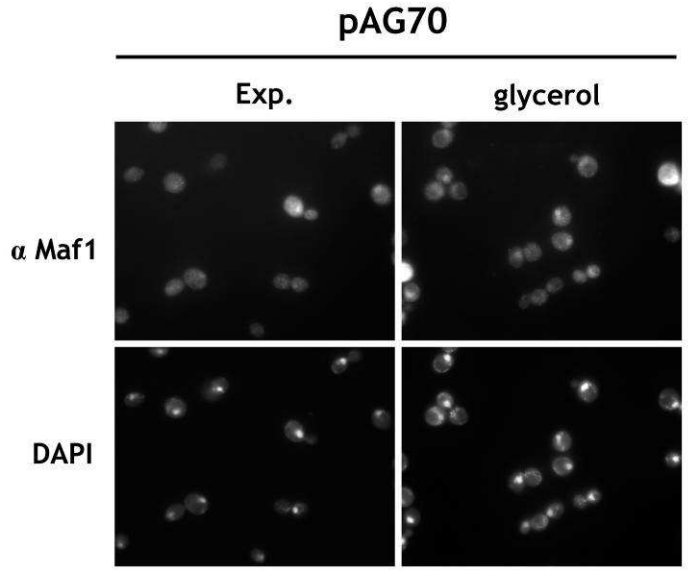

Exp. → YPGly
cytoplasm → nucleus

pAG70 – K35E

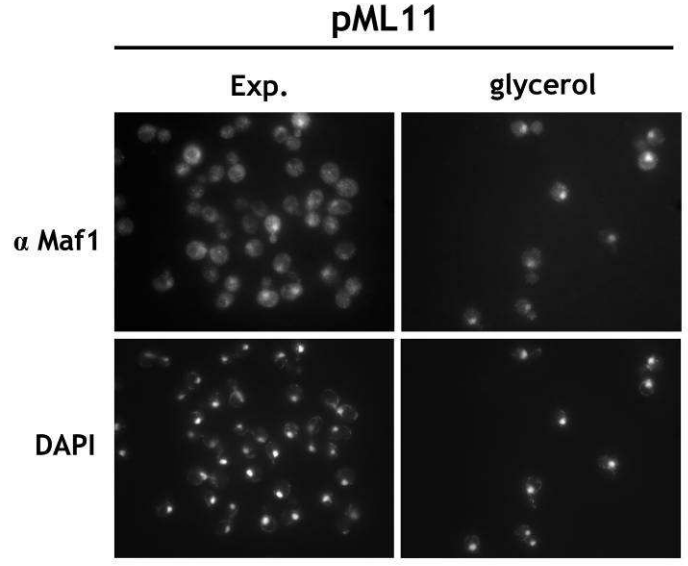

Exp. → YPGly
cytoplasm → nucleus

pML11 – K35E-D250E

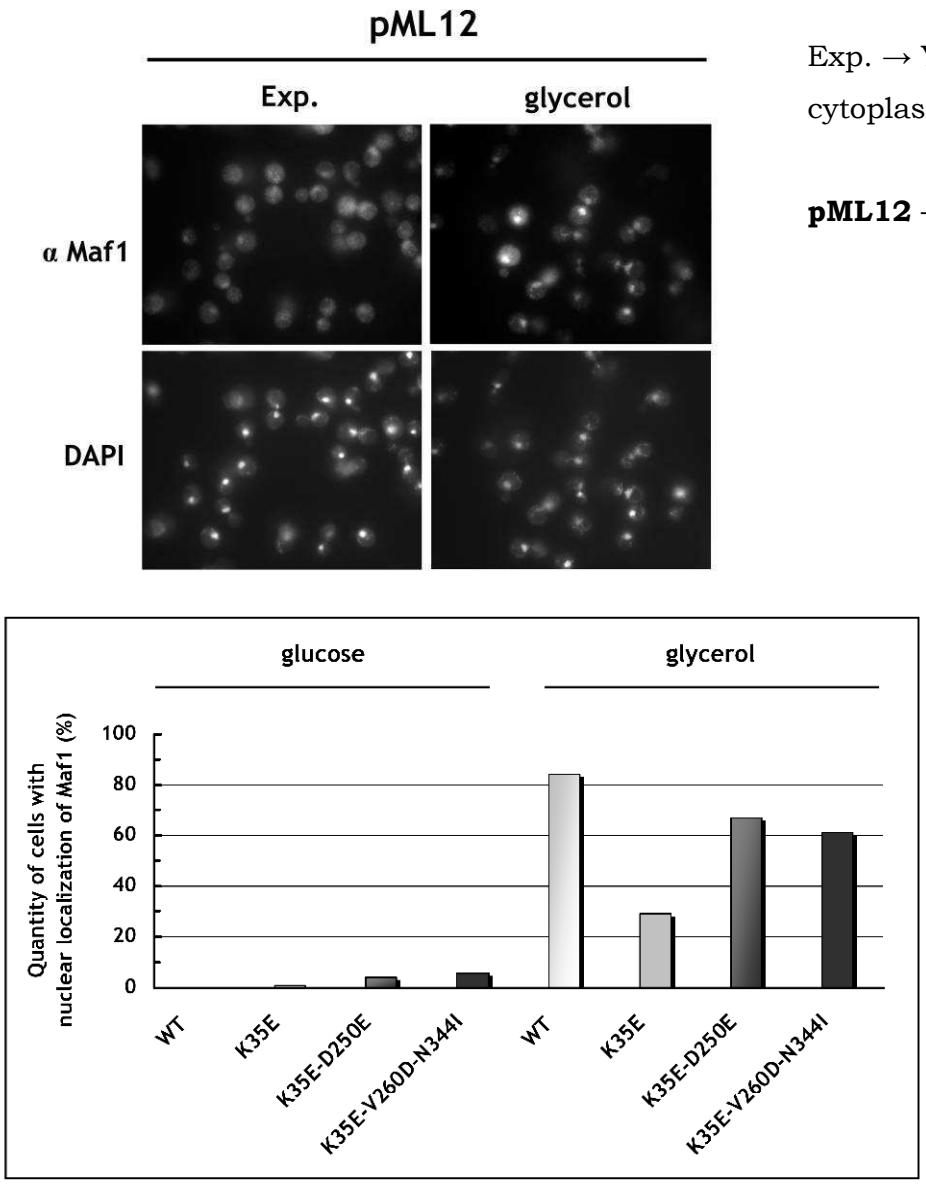

Exp. → YPGly

cytoplasm → nucleus

pML12 – K35E-V260D-N344I

Figure 35. Defect in cellular transport of Maf1 mutated in A domain is abolished by suppressor mutations in the BC domain. A. K35E-*maf1*, K35E-D250E-*maf1* and K35E-V260D-N344I-*maf1* mutants and isogenic WT (YPH500 *maf1Δ* strain transformed with pRS315-*MAF1* plasmid) were grown to exponential phase in YPD glucose medium (Exp), then transferred to glycerol YPGly medium, incubated at 37°C for 2 hours. Cells were harvested as indicated. Maf1 localization was analyzed by immunofluorescence microscopy using polyclonal anti-Maf1 antibodies. Nuclei were stained with 4',6-diamidino-2-phenylindole (DAPI). B. Graph presents average quantity of cells with nuclear localization of Maf1 in cells incubated in glucose containing medium and subsequently transferred to glycerol medium (Quantity estimated in two independent experiments). In WT strain upon transfer to glycerol medium Maf1 is enriched in nucleus (84%). K35E-*maf1* strain presents defect in nuclear transport of Maf1 (29%), K35E-D250E-*maf1* and K35E-V260D-N344I-*maf1* mutant suppressor strains present recovery of Maf1 nuclear transport (67%, 61% respectively). Detailed quantification is presented in Table S8.

2.1.3 Summary

The mutations localized in the BC domain of Maf1, that compensate defect caused by K35E mutation in A domain, were identified. Obtained suppressor mutants K35E-D250E-*maf1* and K35E-V260D-N344I-*maf1* were characterized due to cellular functionality. In opposite to initial K35E-*maf1* mutant, these suppressors are able to repress Pol III transcription during transition from glucose to glycerol-containing medium in correlation to suppression of the thermosensitive growth phenotype. Observed suppression is correlated with Western blotting analysis revealing recovery of WT dephosphorylation of Maf1 in suppressor mutants contrary to constantly phosphorylated Maf1 in K35E-*maf1* mutant. Moreover, presence of suppressor mutations in the BC domain recovers defect of transport from cytoplasm to nucleus of K35E mutated Maf1 as established by immunofluorescence microscopy. Taken together, these results indicate that Maf1 mutated in A domain is defected in its activity unless additional mutations in the BC domain occur. That clearly shows the genetic interaction between Maf1 domains.

2.2. Physical interaction between evolutionarily conserved regions – A and BC domains of *S. cerevisiae* Maf1.

To investigate further if the genetic interaction between domains of *S. cerevisiae* Maf1 appears as a physical contact of two domains, resembling *H. sapiens* Maf1 domains interaction, an analysis based on yeast-two-hybrid system (Y2H) has been performed. As the boundaries of the A and BC domains of *S. cerevisiae* Maf1 are not defined, I have performed a secondary sequence analysis to identify structures that could be involved in supposititious interaction of Maf1 domains

The Hydrophobic Cluster Analysis (HCA) (http://smi.snv.jussieu.fr/hca/hca-form.html) is a tool to investigate protein folding that uses two-dimensional (2D) helical representation of protein sequences in order to identify possible hydrophobic cores formed by several residues (Callebaut *et al,* 1997). The HCA analysis revealed the presence of two regions rich in hydrophobic cores corresponding to the A and BC domains of *S. cerevisiae* Maf1 (Fig. 11, “Introduction”). Between them a region poor in hydrophobic residues was found which, according to the alignment of Maf1 eukaryotic sequences, corresponds to the linker region between the A and BC domains. Similar analysis in human Maf1 revealed the same organization of two clusters of hydrophobic cores separated by a short region free of hydrophobic clusters. These domains of Maf1 correspond to the two fragments resistant to mild proteolysis and that interact together as shown by pull-down and size-exclusion

chromatography (Fig. 15, “Introduction”, results obtained by Christoph Müller’s group in EMBL Heidelberg, Appendix 1).

Supported on potential tertiary structures predictions by HCA, 8 different constructs encoding A domain (aa: 1-42, 1-57, 1-59, 1-77, 1-79, 1-91, 1-111, 1-172) and 4 encoding the BC domain (aa: 165-349, 165-367, 196-349, 196-367) of Maf1 have been designed (Fig. 36). A two series of plasmids for Y2H carrying fusions of sequence encoding several parts of the Maf1 A and BC domains with sequence encoding respectively Gal4 binding domain (pAS2-Maf1-A, pAS2-Maf1-BC) and Gal4 activating domain (pACT2-Maf1-A, pACT2-Maf1-BC) have been created (Fig. 36). These constructs were co-expressed in the yeast reporter strain Y190. Interactions between fusion proteins should result in activation of the β-galactosidase and histidine (HIS3) auxotrophy reporter genes. Using this approach, I have found a physical interaction between the BC domain of Maf1 encoded by all tested plasmids pAS2-Maf1-BC and fragments of A domain of Maf1 encoded by all plasmids pACT2-Maf1-A. Reciprocal interactions were impossible to study because the presence of pAS-Maf1-A activates reporter genes in the absence of a pACT2 fusion.

Figure 36 presents results of β-galactosidase overlay plate assay for pACT2-Maf1A(1-42) and pAS2-Maf1BC(196-349) evaluating the interaction observed in all tested combinations. The β-galactosidase activity for presented pair of the Maf1 A (1-42 aa) and the BC domain (196-349 aa) fragments generated in presence of Gal4 activating domain and Gal4 binding domain respectively (pACT2-Maf1A(1-42) and pAS2-Maf1BC(196-349)) with respective pairs of negative controls (pACT2-Maf1-A(1-42) with empty pAS2 and pAS2-Maf1-BC(196-349) with empty pACT2) and positive control (plasmids encoding τ95/τ55, two TFIIIC subunits – pair of known interactors) (Manaud *et al.,* 1998) has been measured in β-galactosidase activity liquid assay. Both negative controls showed no detectable β-galactosidase activity (Fig. 36). In contrast β-galactosidase activity, in case of plasmids expressing fragments of Maf1 domains the interaction observed was almost 5 times higher than this observed in positive control - τ95/τ55, two TFIIIC subunits, which indicates a strong and direct interaction between the A and BC domains of Maf1 (Fig. 36).

Apart from β-galactosidase activity overlay plate assay, presented interaction was confirmed by test of auxotrophy for histidine. Y190 strain co-expressing pACT2-Maf1-A(1-42) and pAS2-Maf1-BC(196-349) and both negative and positive

controls were replica plated on selective medium containing no histidine (-His) supplied with 10 mM 3 aminotriazole (3-amino-1,2,4-triazole).

3 aminotriazole is a competitive inhibitor of *HIS3* gene product blocking histidine synthesis pathway. In presence of 3 aminotriazole, only high affinity binding between two tested proteins activates enough transcription of *HIS3* gene to a level that impaires the competitive inhibition and enables *S. cerevisiae* cells to grow. In this conditions only Y190 yeast cells expressing pair of pACT2-Maf1-A(1-42) and pAS2-Maf1-BC(196-349) and τ95/τ55 TFIIIC subunits grown efficiently (Fig. 36).

Furthermore, no interaction of pAS2 full-length Maf1 with both the pACT2-Maf1-full-length and pACT2-Maf1-A was observed.

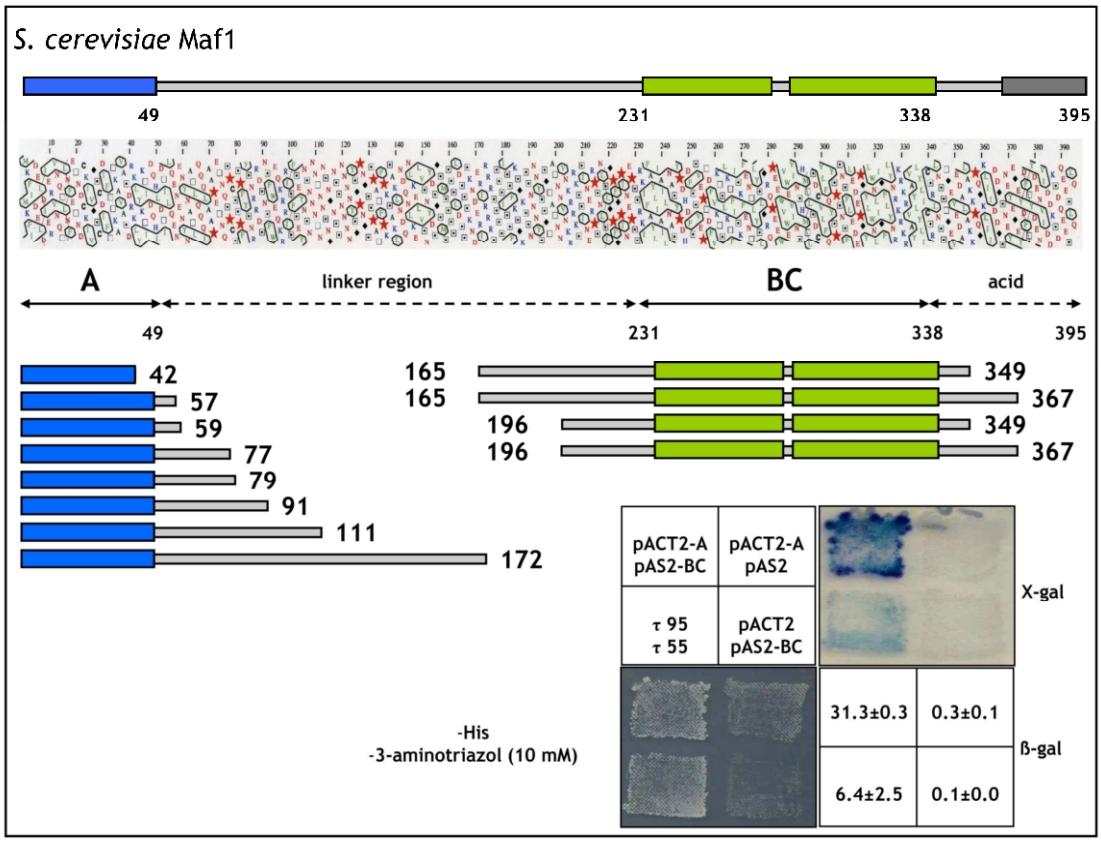

Figure 36. The A and BC domains of Maf1 physically interact. Yeast-two-hybrid system (Y2H) reveals interaction of all tested fragments of A domain of Maf1 encoded by: pACT2-Maf1-A(1-42), pACT2-Maf1-A(1-57), pACT2-Maf1-A(1-59), pACT2-Maf1-A(1-77), pACT2-Maf1-A(1-79), pACT2-Maf1-A(1-91), pACT2-Maf1-A(1-111) and pACT2-Maf1-A(1-172) with all tested fragments of the BC domain of Maf1 encoded by pAS2-Maf1-BC(165-349), pAS2-Maf1-BC(165-367), pAS2-Maf1-BC(196-349) and pAS2-Maf1-BC(196-367). Plasmids were transformed individually together with pAS2 (control plasmid for pACT2-Maf1-A) or pACT2 (control plasmid for pAS2-Maf1-BC) and reciprocally in all combinations into yeast reporter strain Y190. Transformants were assayed for β-galactosidase expression using overlay plate assay. As an example presented interaction between pACT2-Maf1-A(1-42) and pAS2-Maf1-BC(196-349) and respective negative controls with empty plasmid pACT2 and pAS2 and positive control of known interactors (τ95/τ55, two TFIIIC subunits) (Manaud *et al.,* 1998). Interaction confirmed by test for histidine (His) auxotrophy with 10 mM 3-aminotriazol (3-amino-1,2,4-triazole), an inhibitor of His3. β-galactosidase activity units with standard deviation, obtained in β-galactosidase liquid assay for presented interactions are indicated.

Importantly pAS2-Maf1-BC was also negative tested with pACT2-Maf1-BC (data not shown). These results demonstrate the specificity of the two-hybrid interaction between Maf1 domains.

Taken together, results as described above suggest a strong, direct interaction of the A and BC domains of *S. cerevisiae* Maf1.

2.2.1 Minimal fragment of A domain of Maf1 involved in interaction with BC domain.

Since all tested fragments of A domain exhibited strong interaction with tested fragments of the BC domain of Maf1, an effort to minimize the region of A domain involved in observed interaction has been made. Bioinformatic analysis of the A domain with the usage of a protein structure prediction software (PSIPRED v 2.6) (http://bioinf4.cs.ucl.ac.uk:3000/psipred/) (Bryson *et al.,* 2005) identified two α-helices (aa: 7-16 and 40-56) separated by two adjacent β-strands (aa: 24-27 and 29-35) (Fig. 37). The minimal part of A Maf1 domain involved in observed interaction was 1-42 aa in the previously described interaction. According to PSIPRED analysis the shorter fragments of A domain with broken β-strand structure (aa: 1-39, 1-34, 1-23 and 1-16) and first α-helice structure (1-12 aa) have been designated (Fig. 37).

The putative BC domain of *S. cerevisiae* Maf1 (196-349 aa) fused to the DNA-binding domain of Gal4 was co-expressed with every single shortened version of A domain fused to the Gal4 activation domain in the yeast reporter strain Y190. Using this approach, I have observed a physical interaction between the BC domain of Maf1 encoded by plasmid pAS2-Maf1-BC(196-349) and fragments of A domain of Maf1 encoded by plasmids pACT2-Maf1-A(1-42), pACT2-Maf1-A(1-39) and pACT2-Maf1-A(1-34) (Figure 38). The BC domain failed to interact with shorter fragments of A domain encoded by pACT2-Maf1-A(1-12), pACT2-Maf1-A(1-16) or pACT2-Maf1-A(1-23). Cells containing the pair pAS2-Maf1-BC and empty pACT2 had no detectable β-galactosidase activity (0.1 +/- 0 units). Either the pair pACT2-Maf1-A and empty pAS2 did not activated reporter gene (0.3 +/- 0.1 units). (data not shown in the figure).

A Western blotting analysis was used with anti-HA antibodies to determine the relative expression levels of the short versions of A domain cloned in pACT2-Maf1-A that are HA-tagged. All fusions were expressed (Fig. 39) indicating that observed fail in interaction of aa: 1-23, 1-16 and 1-12 fragments of A domain is not abolished due to lack of their expression. The levels of aa: 1-42 and 1-23 fusions were little higher then others, but this difference was not significant for interaction

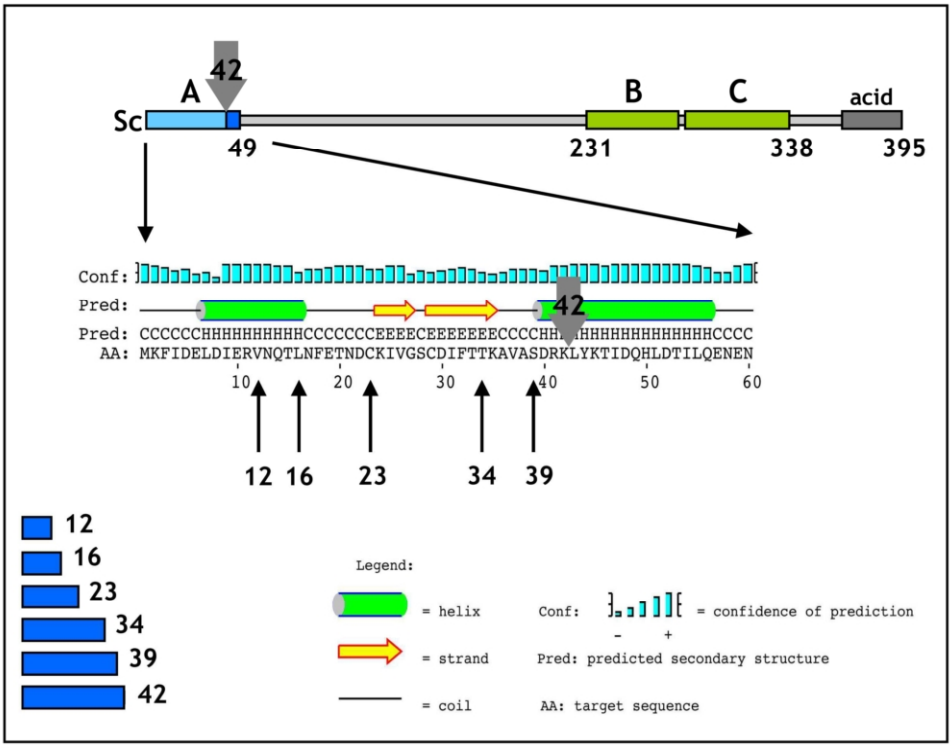

Figure 37. Secondary structure prediction of Maf1 protein. PSIPRED v 2.6 protein structure prediction software was used to identify secondary structure of *S. cerevisiae* Maf1 protein. Only A domains is presented. Green tube (or H letter), yellow arrow (or E letter) or black line (or C letter) represent alpha helix, beta strand or coil, respectively.

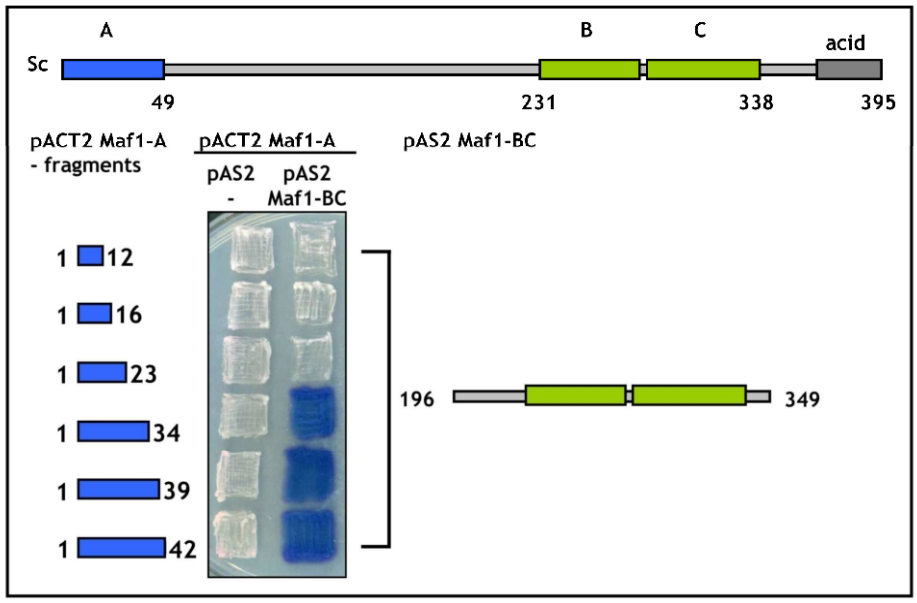

Figure 38. Determination of the minimal fragment of the A domain responsible for interaction with the BC domain. pACT2-Maf1-A(1-12), pACT2-Maf1-A(1-16), pACT2-Maf1-A(1-23), pACT2-Maf1-A(1-34), pACT2-Maf1-A(1-39) and pACT2-Maf1-A(1-42) plasmids were transformed individually together with pAS2 (control plasmid) or pAS2-Maf1- BC(196-349) plasmids into yeast strain Y190. Transformants were assayed for β-galactosidase expression using overlay plate assay. The relative levels of β-galactosidase activity measured in liquid assay were respectively: 170 +/- 6, 322 +/- 61, 161 +/- 37 units for interacting with the BC domain fragments of the A domain (aa: 1-42, 1-39 and 1-34) and respectively: 0, 11, 4 units for not interacting with the BC domain fragments of the A domain (aa: 1-23, 1-16 and 1-12).

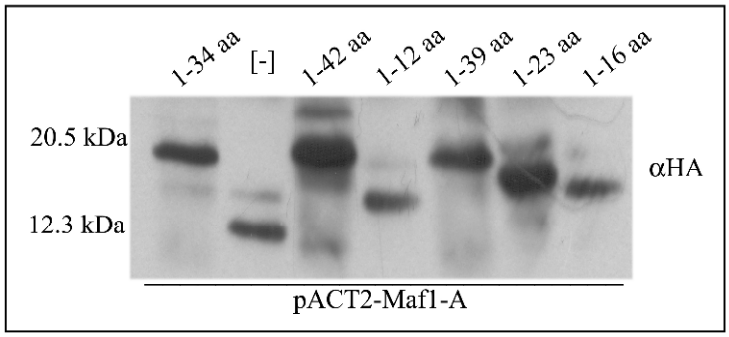

Figure 39. Expression of the truncated versions of Maf1 A domain fused to Gal4 Activating domain determined by Western blotting with HA-specific antibodies. (-) – empty pACT2 plasmid.

with the BC domain (there are no relationship between expression level and β-galactosidase activity as compared to results presented in Figure 38).

The attempt to minimize the Maf1 A domain identified 1-34 aa as the smallest fragment still enabling interaction with the domains. Thus let hypothesize that the interaction between the A and BC domains requires the first α-helix and two adjacent β-strands of the A domain.

2.2.2 The physical interaction between Maf1 domains is required for Pol III repression.

- **Mutations identified in mutant and suppressor strains affects the interaction between A and BC domains.**

As the Pol III regulation is defective in the presence of Maf1 mutated in the A domain (K35E) and recovered by the presence of additional suppressor mutations in the BC domain (D250E, V260D-N344I), an attempt to check possible influence of identified mutations on the physical interaction between the Maf1 A and BC domains was studied. The effects of K35E, D250E, V260D, N344I and double V260D-N344I mutations identified in the mutant and suppressor strains were studied by using the Y2H approach.

The respective mutations were generated (see Materials and Methods) in the Maf1 A domain fragment fused to the Gal4 activation domain in the pACT2-Maf1-A(1-42) plasmid and the Maf1-BC domain fused to the DNA-binding domain of Gal4 in pAS2-Maf1-BC(196-349) (Fig. 40). Various combinations of plasmids, one encoding a wild type Maf1 domain and the other with a mutated domain, both fused to the respective Gal domains, were co-expressed in the yeast reporter strain Y190 followed by determination of β-galactosidase activity liquid assay (Fig. 41).

The K35E mutation of A domain reduced the two-hybrid interaction with the wild type BC domain by ca. 40 % (Fig. 41, compare lanes 2 and 1). Similarly, both

the single D250E and the double V260D-N344I mutations in the BC domain decreased the interaction with wild type A domain by 22 and 62 %, respectively (Fig. 41, comparelanes 7 and 8 with lane 1). Confirming the genetic suppressor results, a combination of mutated Maf1 domains K35E-D250E and K35E-V260D-N344I restored their interaction (Fig. 41, compare lanes 3 and 4 with lane 1). Rather unexpectedly, the strongest level of two-hybrid interaction, 80% over the wild type one, was observed for the combination of the K35E A domain and the BC domain with a single V260D mutation (Fig. 41, compare lane 5, with lane 1). Furthermore its interaction with the wild type A domain was decreased by almost 60% (Fig. 41, compare lanes 1 and 9). This indicated that in the double suppressor mutations V260D-N344I, identified in genetic screen, the former one is in fact sufficient to restore the interaction with K35E A domain while N344I seemed to have a minor effect (Fig. 41, lanes 6 and 10).

Detailed results of β-galactosidase activity liquid assay and values of enzyme activity are presented in Table S9.

Presented Y2H results shows that K35E mutation in A domain disrupts the intramolecular interaction between Maf1 domains. Combination of mutated Maf1 domains restores their interaction and clearly shows that the interaction between Maf1 domains is necessary for its activity as a Pol III repressor.

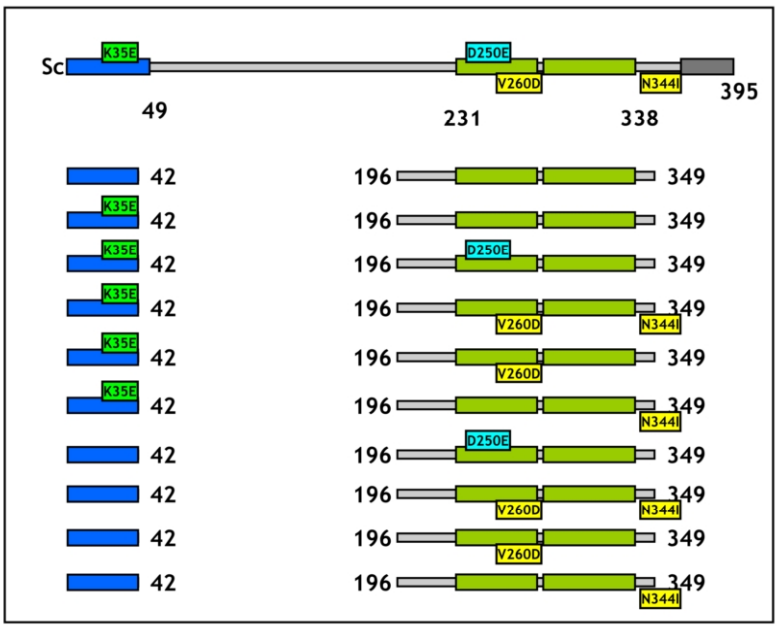

Figure 40. Combinations of plasmids co-expressed in yeast reporter strain Y190 to verify the effect of identified in mutant (K35E) and suppressor strains (D250E, V260D, N344I and V260D-N344I) mutations on the interaction between the A and BC domains of Maf1.

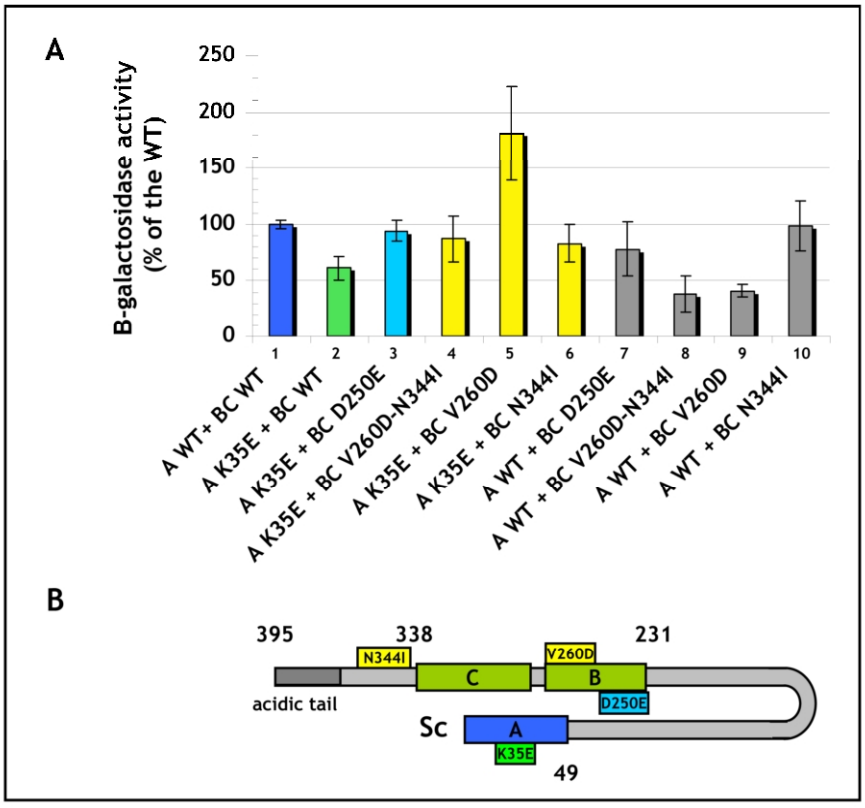

Figure 41. Two-hybrid interaction of Maf1 domains is impaired by primary mutations in these domains and restored by second-site suppressor mutations. A. pACT2-Maf1-A(1-42) plasmid and its mutated version were transformed individually with pAS2-Maf1- BC(196-349) plasmid or its mutated versions in yeast strain Y190. Transformants were assayed for β-galactosidase expression. Presented profile compares following two-hybrid interactions: wild type A and BC domains of Maf1 (1), mutated A domain K35E with wild type BC domain (2); mutated A domain K35E with four versions of mutated BC domain: D250E (3), V260D-N344I (4), V260D (5), N344I (6), and wild type A domain with mutated BC domain containing single D250E, V260D or N344I and double N344I-V260D mutations (7-10). B. Scheme of Maf1 domain interaction. Detailed values of β-galactosidase activity presented in Table S9.

3. Analysis of protein interactions involving evolutionarily conserved regions – A and BC domains of *S. cerevisiae* Maf1.

S. cerevisiae Maf1 was found to interact with the largest subunit of Pol III enzyme (C160). Observed interaction has an either genetic or physical form. Primarily it was shown that N-terminal part of C160 (1-235 aa) encoded on multicopy plasmid suppress thermosensitive phenotype of *maf1-1* mutant on glycerol-containing medium (Boguta *et al.*, 1997). Furthermore mutations in *RPC160* gene encoding C160 were identified as spontaneous suppressors of *maf1-1* and *maf1Δ* (Pluta *et al.*, 2001).

Finally, the physical interaction between N-terminal part of C160 and Maf1 was revealed by „pull-down" assay (Oficjalska-Pham *et al.*, 2006).

In human cells, similarly to yeast cells, an analogous interaction between Maf1 and the largest subunit of Pol III (C160) and Brf1 (subunit of transcription factor TFIIIB required to tRNA synthesis) was identified. Moreover, it was shown that Rpc1, the largest Pol III subunit (*S. cerevisiae* C160 ortholog) and Brf1 interact with different regions of Maf1. It was postulated that the A domain of *H. sapiens* Maf1 is responsible for interaction with Rpc1 Pol III subunit while the BC domain is necessary for interaction with Brf1 (Reina *et al.*, 2006).

According to this data, an effort to establish an interaction between *S. cerevisiae* Maf1 and C160 Pol III with the yeast-two-hybrid system (Y2H), has been made in the laboratory of Magdalena Boguta several years ago. These attempts have ended with no success.

The novel data presented in this study upon the importance of the A and BC domains interaction aroused a hypothesis, that the negative result of preceding investigations, was a consequence of improper protein conformation precluding revealing of the interaction. Supported on data obtained upon *H. sapiens* Maf1 (Reina *et al.*, 2006) several parts of the *S. cerevisiae* Maf1 A and BC domains have been tested in Y2H for possible interaction with full-length C160 and N-terminal part (1-235 aa) of C160.

In spite of such a strong data referring to Maf1 interaction with C160 Pol III subunit, an attempt to reveal region of *S. cerevisiae* Maf1 responsible for this interaction failed in all tested combinations.

The possible interaction of *S. cerevisiae* Maf1 (either complete protein or fragments of the Maf1 A and BC domains) with Pol III apparatus has been

subsequently tested by Y2H either. Performed study also failed to reveal interaction between tested parts of *S. cerevisiae* Maf1 and Pol III holoenzyme subunits.

Tested combinations of plasmids encoding fusions of Gal4 activating domain or Gal4 binding domain with relevant sequences encoding either Maf1 domains or components of Pol III apparatus shown in Table 7 and Table 8 were tested by β-galactosidase overlay plate assay.

Table 7. Plasmids negatively tested in yeast-two-hybrid system in attempt to detect interaction between Maf1 and Pol III apparatus subunits or other proteins. Presented plasmids harbor fusions of sequence encoding Gal4 activating domain (AD) with sequences encoding Pol III apparatus components and partner plasmids harboring fusions of sequence encoding Gal4 binding domain (BD) with sequence encoding different parts of the Maf1 BC domain. All combinations of Gal4 AD fusion protein and Gal4 BD fusion protein were tested.

Gal4 AD **Pol III apparatus**	**Gal4 BD** **Maf1 fragments**
pACT-TFIIIA	pAS2-Maf1-BC(165-349)
pACT-TFIIIB70	pAS2-Maf1-BC(165-367)
pACT-TFIIIB90	pAS2-Maf1-BC(196-349)
pGA-TBP	pAS2-Maf1-BC(196-367)
pACT-Tau138	
pACT-Tau131	
pACT-Tau95	
pACT-Tau91	
pACT-Tau60	
pACT-Tau55	
pGA-C128	
pACT-C82	
pGA-C53	
pGA-AC40	
pGA-C34	
pACT-C31	
pGA-ABC27	
pACT-C25	
pACT-ABC23	
pGA-AC19	
pACT-C17	
pGA-ABC14,5	
pACT-C11	
pACT-ABC10α	
pGA-ABC10β	
pGAD424-C160	
pGAD424-NTF-C160	
pGA-C160	
Other proteins	
pACT-Sub1	
pACT-Maf1	

Table 8. Plasmids negatively tested in yeast-two-hybrid system in attempt to detect interaction between Maf1 and Pol III apparatus subunits or other proteins. Presented plasmids harbour fusions of sequence encoding Gal4 binding domain (BD) with sequence encoding Pol III apparatus components and partner plasmids harbouring fusions of sequence encoding Gal4 activating domain (AD) with sequence encoding different parts of the Maf1 A and BC domains. All combinations of Gal4 AD fusion protein and Gal4 BD fusion protein were tested.

Gal4 BD **Pol III apparatus**	**Gal4 AD** **Maf1 fragments**
pAS-TFIIIA	pACT2-Maf1-A(1-42)
pAS-TFIIIB70	pACT2-Maf1-A(1-57)
pAS-TFIIIB90	pACT2-Maf1-A(1-59)
pAS-TBP	pACT2-Maf1-A(1-77)
pAS-Tau138	pACT2-Maf1-A(1-79)
pAS-Tau131	pACT2-Maf1-A(1-91)
pAS-Tau95	pACT2-Maf1-A(1-111)
pAS-Tau91	pACT2-Maf1-A(1-172)
pAS-Tau60	pACT2-Maf1-BC(165-349)
pAS-Tau55	pACT2-Maf1-BC(165-367)
pAS-C128	pACT2-Maf1-BC(196-349)
pAS-C82	pACT2-Maf1-BC(196-367)
pAS-C53	
pAS-AC40	
pAS-C37	
pAS-C31	
pAS-ABC27	
pAS-C25	
pAS-AC19	
pAS-C17	
pAS-ABC14,5	
pAS-C11	
pAS-ABC10α	
pMA-ABC10β	
pGBT9-C160	
pGBT9-NTF-C160	
pAS-C160	
Other proteins	
pAS-Sub1	
pAS-Maf1	

IV. DISCUSSION

1. Interaction between A and BC domains is important for the function of Maf1.

The family of all eukaryotic Maf1 share highly conserved amino acid sequence with easily recognizable two regions called the A and BC domains. This study is the first report relating Maf1 structure to RNA polymerase III (Pol III) transcription inhibition in *S. cerevisiae.* Importantly, the interaction between two Maf1 domains is required for its activity as a repressor of Pol III transcription.

The results of limited proteolysis of *H. sapiens* Maf1 performed in the laboratory of Christoph Műller (supplementary data; Appendix 1) resulted in two stable fragments (aa: 1-45 and 75-234) corresponding to the evolutionarily conserved A and BC domains. Size-exclusion chromatography of these proteolytic fragments corresponding to the two domains, showed their co-elution. Similar fragments were co-expressed in bacteria, and have been shown to co-purify and co-migrate during size-exclusion chromatography as soluble complex. In contrast, an additional construct - 82-236 aa fragment, which included the C-terminal acidic tail eluted as soluble aggregate when expressed in the absence of the N-terminal fragment - 1-45 aa (Gajda *et al.,* 2010). These results suggested that *H. sapiens* Maf1 A and BC domains form modules that do not fold independently but rather need to be co-expressed to form a stable and soluble entity. On the other side, the connecting linker (46-74 aa) and the C-terminal acidic tail (235-256 aa) appear to be solvent-exposed and unstructured.

Considering the high conservation of Maf1 in eukaryotes, the domain interaction and their functional role was probed in a model organism - yeast *Saccharomyces cerevisiae.*

Using the yeast-two-hybrid system, I have confirmed the physical interaction between the A and BC domains of Maf1 in *S. cerevisiae* and identified the first 34 residues as the shortest fragment of the A domain sufficient for interaction with the BC domain. Lack of interaction between further truncated fragments of the A domain (aa: 1-12, 1-16 or 1-23) with the BC domain shows the specificity of the method used and emphasizes the importance of structural features of the A domain for its interaction with the BC domain.

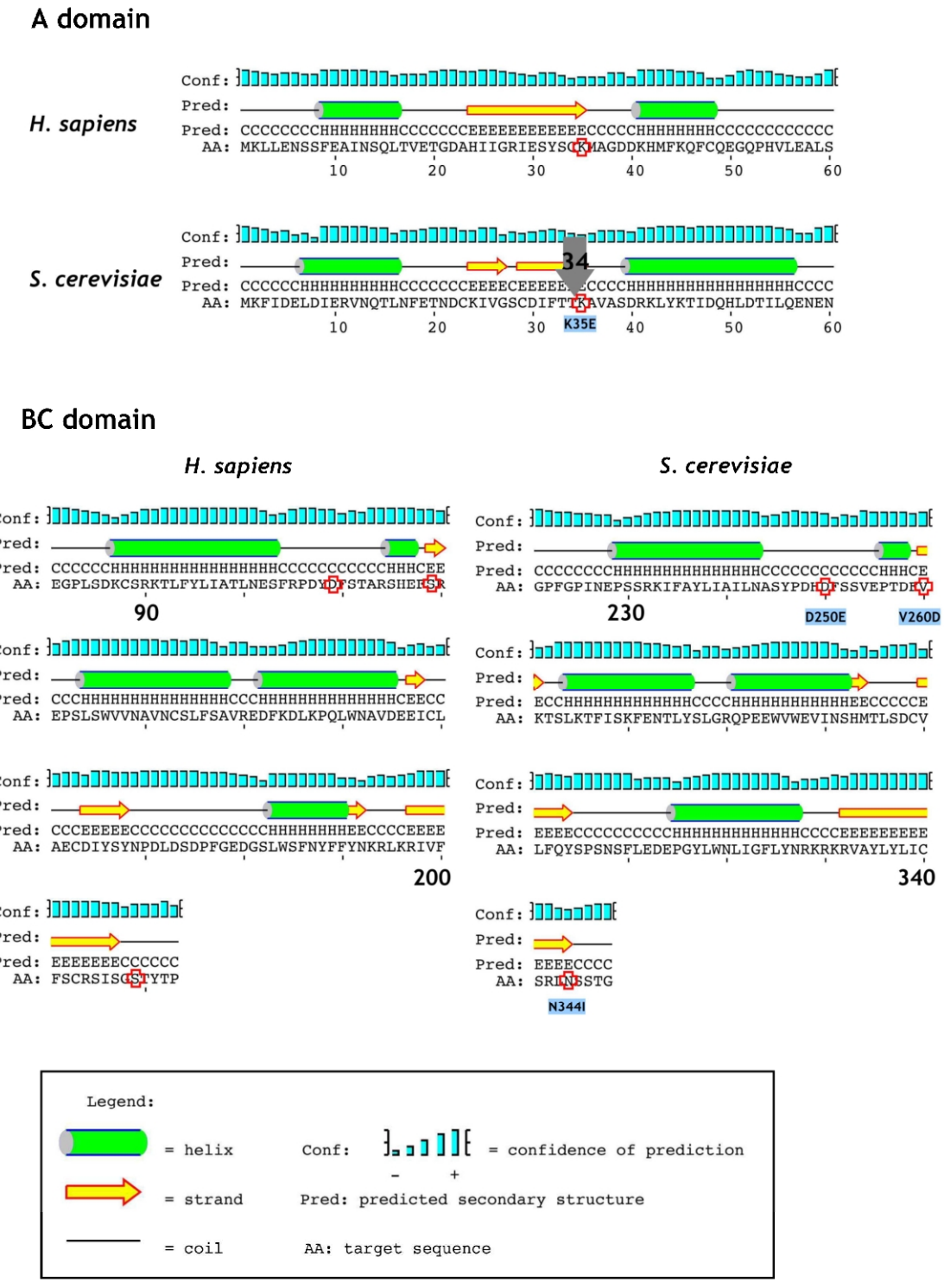

Figure 42. Secondary structure prediction of Maf1 protein. PSIPRED v 2.6 protein structure prediction server was used to identify secondary structure of *S. cerevisiae* Maf1 protein and *H. sapiens* Maf1. Only A and BC domains are presented. Green tube (or H letter), yellow arrow (or E letter) or black line (or C letter) represent alpha helix, beta strand or coil, respectively. Positions of K35E, D250E, V260D and N344I mutations in *S. cerevisiae* Maf1 amino acid sequence are indicated by a red cross. Relevant mutations in *H. sapiens* Maf1 indicated either.

Bioinformatic analysis using the protein structure prediction server (PSIPRED v 2.6) (Jones, 1999; Bryson *et al.,* 2005) provided further support for the study of Maf1 domains.

In A domain, two α-helices (aa: 7-16 and 40-56 – in *S. cerevisiae*) separated by two adjacent β-strands (aa: 24-27 and 29-35 – in *S. cerevisiae*) are predicted, while for the BC domain five α-helices and concomitant four β-strands are predicted (Fig. 42). No secondary structure elements are predicted for the linker region.

The identified 1-34 aa part of the Maf1 A domain, the smallest fragment still enabling interaction with the BC domain lead to hypothesis that the interaction between domains A and BC requires the first α-helix and two adjacent β-strands (Fig. 42).

The results of yeast-two-hybrid system show that the A and BC domains of *S. cerevisiae* Maf1 together form a stable complex.

The identified mutant in A domain - K35E-*maf1* as described in this study was defective in its ability to repress pre-tRNA synthesis upon transfer to glycerol medium. Thus the single missense mutation within the Maf1 A domain precluded Pol III repression in K35E-*maf1* strain in accordance to growth defect observed on glycerol-containing medium at 37°C. Notably, the K35E mutation that precluded Pol III repression is located at the end of the second β-strand of the A domain (Fig. 42) and just after the smallest fragment (1-34 aa) still enabling interaction with the BC domain.

One approach to confirm that the K35E mutation negatively affects the interaction with the BC domain of Maf1 was to identify second-site mutations that compensate for the observed defects. Therefore a screen for second-site suppressor mutations within the BC-encoding region of *MAF1* that allowed K35E-*maf1 S. cerevisiae* cells to grow on glycerol medium at 37°C has been performed. The BC domain of ScMaf1 is located between aa: 231 and 338 (size: 108 aa). The mutagenesis encompassed a region of 202 aa located between aa: 174 and 375 as indicated in the “Results” part so noticeably larger than the BC domain. The identification of suppressor mutations in the BC domain by PCR Random Mutagenesis was thus not sure. The localization of single D250E and combined V260D-N344I mutations, isolated suppressors of K35E mutation in A domain, in the BC domain strongly supports the interaction between these domains (Fig. 42).

The increased growth capacity of the suppressors on glycerol medium was due to a compensation of the defect in Pol III regulation observed for the K35E mutation. As determined by Northern blotting, the suppressor mutations restored

the ability to repress pre-tRNA synthesis upon transfer from glucose to glycerol medium. These results indicate that the detected genetic interaction between the two Maf1 domains is a functional one.

Moreover, K35E mutation in A domain appeared to preclude the dephosphorylation of Maf1 following transfer from glucose to a nonfermentable carbon source. Significantly, the suppressor mutations D250E and V260D-N344I re-established rapid dephosphorylation of Maf1 following transfer from glucose to a nonfermentable carbon source. The similar effect was observed for cellular localization of Maf1 in mutant strains. K35E mutation visibly impaired transport of Maf1 to nucleus upon transition to nonfermentable carbon source while presence of suppressor mutations recovered transport of mutated Maf1 to nucleus.

Moreover, as shown by the two-hybrid system, the K35E mutation reduced the interaction between the A and BC Maf1 domains by 40%. In support of structural and/or functional interactions between the Maf1 domains, isolated second-site suppressor mutations within the BC domain that compensated for the defect caused by the K35E mutation in A domain also reconstituted the physical interaction between the A and BC domains of Maf1. All these results indicated that the genetic interaction identified between Maf1 domains corresponds to a physical interaction indispensable for the Maf1 function.

The significance of reconstitution of Maf1 function by suppressor mutations support the results of analogous investigation upon separated mutations D250E, V260D and N344I originally found in suppressor mutants that have been generated in absence of K35E mutation.

The double V260D-N344I-*maf1* mutant was temperature-sensitive as K35E-*maf1* and growth of D250E-*maf1*, V260D-*maf1* or N344I-*maf1* strains was comparable to wild type. In accordance with growth phenotypes, Northern analysis have shown a defect in regulation of tRNA synthesis in V260D-N344I-*maf1* mutant transferred to glycerol medium whereas repression in D250E-*maf1*, V260D-*maf1* or N344I-*maf1* mutants was comparable to that observed in wild type.

Concomitant Western analysis have shown Maf1 dephosphorylation in D250E-*maf1*, V260D-*maf1* or N344I mutants occurring as in wild type cells transferred to glycerol medium contrary to V260D-N344I-*maf1* double mutant exhibiting severe defect in dephosphorylation of Maf1. Interestingly, double V260D-N344I mutation in absence of K35E mutation in A domain precluded interaction between domains with the surprising major impact of V260D mutation. Residue 260 in the BC domain seemed to be crucial for the interaction with A domain. While the V260D

BC domain mutant interacted with the K35E A domain mutants (Fig. 42 and 41) over 80% stronger in two-hybrid experiment as did the wild type BC domain, its interaction with the wild type A domain was decreased by almost 60% (Fig. 41, lanes 5 and 9). In opposite D250E and N344I mutations did not have a great impact on observed interaction in accordance to no growth and no Pol III repression defect.

Taken together mutations: D250E, V260D or N344I separately are silent for Maf1 function but the junction of both V260D-N344I mutations causes disturbance in Maf1 activity.

Altogether this analysis clearly shows that the observed reconstitution of Maf1 activity in suppressor mutants is a result of the both mutated Maf1 A and BC domains not the separate effect of mutations identified in the BC domain.

Thus the interaction of A and BC domains greatly facilitates the activity of Maf1 as a Pol III repressor.

2. Insights into the Maf1 protein structure.

The Hydrophobic Cluster Analysis (HCA), a tool to investigate protein stability and folding, that uses two-dimensional (2D) helical representation of protein sequences, to identify possible hydrophobic cores formed by several residues (Callebaut *et al.,* 1997) presented in "Introduction" part for both: *H. sapiens* and *S. cerevisiae* Maf1 similarly revealed the presence of two regions rich in hydrophobic cores corresponding to the A and BC domains of Maf1.(Fig. 11). Between them an unstructured region deprived of hydrophobic residues was found which, according to the alignment of Maf1 eukaryotic sequences (Fig. 11), corresponds to the linker region between the A and BC domains, that is consistent with limited proteolysis results of Christoph Műller's group.

While this study has been being written, the first crystallographic data on the structure of *H. sapiens* Maf1 were reported on the 7th International Biennial Conference on RNA Polymerases I and III "OddPols" in June 2010 (Rieke Ringel of the Patrick Cramer laboratory, Gene Center Munich). These data are in accordance with the results of Christoph Műller's group devoted to limited proteolysis and to obtained bioinformatic data: HCA (Hydrophobic Cluster Analysis) and PSIPRED (prediction of secondary structures present in Maf1) that together firmly revealed two highly structured regions in Maf1 separated by unstructured linker, independently of the organism studied.

As in the Christoph Műller's group, in Patric Cramer's laboratory human Maf1 was subjected to a mild-proteolysis analysis that revealed the presence of two structured regions, corresponding to the A and BC domains, linker and an acidic C-terminal tail (published very recently on 1st October 2010 by Vannini *et al.*). Human Maf1 has been overproduced without the acidic tail and without the linker between the A and BC domains (all the amino acids of the linker and even some amino acids of the C-terminus of the A domain). Maf1 crystals have been obtained after 2.5 years of effort (a lot of different construction checked) and allowed to define a structure at 1.5 Ångström.

H. sapiens Maf1 is a globular protein with a hydrophobic core of five-stranded antiparallel beta-sheet surrounded by one alpha-helix on one side and three helices on the other (Vannini *et al.,* 2010). This new structure has no structural homolog so it is not possible to predict a function of Maf1 due to this absence of structural homolog. A domain is composed of a beta-sheet (in the middle of the structure) and an alpha-helix (outside of the structure) (Fig. 43 kindly provided for the purpose of this study by Rieke Ringel). The structure of the A domain seems very similar to that predict by PSIPRED (compare Fig 43 and 42).

Since Maf1 domains are highly conserved between *H. sapiens* and *S. cerevisiae* (with the exclusion of unstructured linker between domains that is absent in presented *H. sapiens* Maf1 structure) it is plausible to transfer the positions of mutations identified in *S. cerevisiae* Maf1 onto the model of *H. sapiens* Maf1 to visualize their predicted influence on Maf1 domains interaction.

The position of K35E, D250E, V260D and N344I mutations in *S. cerevisiae* Maf1 respond to position of K35, D109, S119 and S209 residues in *H. sapiens* Maf1 respectively (Fig. 43 and 42). The position of N344I mutation in *S. cerevisiae* Maf1 responding to S209 in *H. sapiens* Maf1 is not indicated since S209 residue belongs to the acidic tail region of *H. sapiens* Maf1, which was excluded to obtain crystals. In presented structure of the *H. sapiens* Maf1, S109 residue should be found in close proximity to C-terminal end – 205 aa.

Interestingly the mutations that were identified in either in A domain single point Maf1 mutant disabled in Pol III repression regulation (K35E-*maf1*) and two suppressor Maf1 mutants recovering Maf1 capability to regulate Pol III transcription (K35E-D250E-*maf1* and K35E-V260D-N344I-*maf1*) are localized in close proximity (but not in contact) supporting their impact on the interaction between Maf1 domains as evaluated by genetic approach and yeast-two-hybrid system presented in this study.

Intriguingly, the V260D mutation in *S. cerevisiae* Maf1 that was reported to have a major impact on Maf1 domains interaction, which corresponds to S119 residue in *H. sapiens* Maf1 is positioned closest to K35 residue supporting the results obtained in the yeast-two-hybrid system.

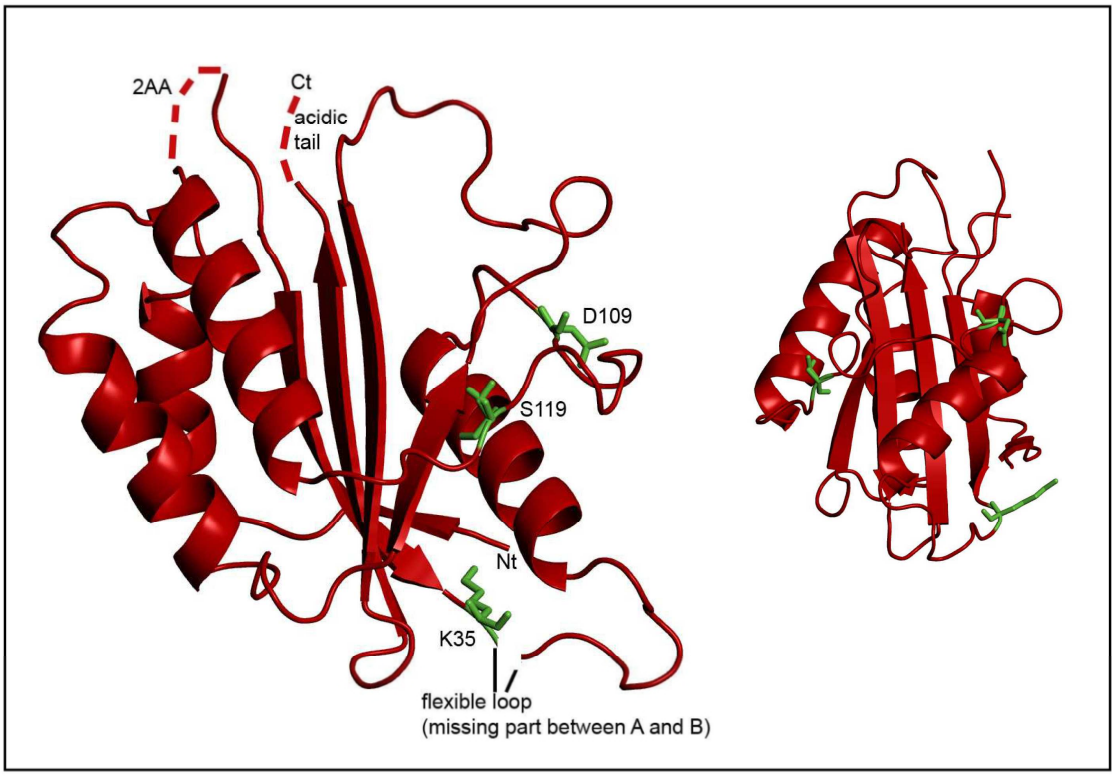

Figure 43. The crystal structure of *H. sapiens* Maf1. Structure presented in two views – The one on the right rotated by 90 degree. Structure defined at 1.5 Angstrom (Å). The position of amino acid residues identified in *S. cerevisiae maf1* mutants: K35E, D250E, and V260D indicated as a respective residues in *H. sapiens MAF1*: K35, D109 and S119 (in green). The N344I responding to S209 is absent since S209 belongs to acidic tail excluded while crystallization. Last C-terminal residue (Ct) is 205 aa (Prepared by Rieke Ringel for the purpose of this study, 2010).

3. Elucidation of Maf1 as a member of intrinsically disordered proteins family.

We used to consider proteins as a stable structures but there might be also proteins that although posses a higher structural organisation they also consist of large areas of unstructured regions. They play a crucial role in cell lifespan and are called intrinsically unstructured proteins (IUPs) (Garza *et al.,* 2009).

Structurally, intrinsically disordered proteins range from completely unstructured polypeptides through extended partially structured forms up to compact disordered ensembles containing substantial secondary structure. Intrinsically disordered regions are respectively common in nature. Approximately

~50% of eukaryotic proteins likely contain at least one disordered region that exaggerate 30 amino acids in length. Furthermore, many proteins are likely to be absolutely disordered (e.g. ~20% of eukaryotic proteins are expected to be mostly disordered) (Uversky and Dunker, 2008). In budding yeast *S. cerevisiae* Gsponer *et al.* (2008) assigned all proteins to one of three groups according to their predicted levels of intrinsic disorder: highly ordered proteins (0 to 10% predicted disorder), moderately disordered proteins (10 to 30% predicted disorder), and highly disordered proteins (30 to 100% predicted disorder). *S. cerevisiae* Maf1 according to this classification might be considered as highly disordered protein thus 182 aa part of a total sequence (395 aa) states for unstructured linker region between the A and BC domains, which is 46% of Maf1 sequence. Intrinsically disordered proteins (and regions) are generally enriched in most polar and charged residues and are depleted of hydrophobic residues (other than proline) (Uversky and Dunker, 2008). What is characteristic for unstructured proteins, is the presence of PEST motives (regions rich in proline, glutamic acid, serine and threonine) (Gsponer *et al.,* 2008), which is also the observable feature of the linker region of the *H. sapiens* and *S. cerevisiae* Maf1.

Proteins with unstructured regions predominantly play role in transducing intracellular signals, regulating processes including the cell division cycle, and recognizing various binding partners (e.g. ligands, other proteins and nucleic acids). Intrinsically unstructured proteins (IUPs) are often reused in multiple pathways to produce different physiological effects (Gsponer *et al.,* 2008). Similarly, *S. cerevisiae* Maf1 was demonstrated to play a central role in coupling different signal transduction pathways to Pol III transcriptional machinery. Secretory pathway defects, nutrient limitation, DNA damage, low nutrients availability, cell growth rate, oxidative stress, transition to respiratory metabolism and chemical treatment with different drugs influence repression of the Pol III transcription according to the Maf1 activity, the one and only Pol III regulator in *S. cerevisiae* cells known up to date.

Thus it may support the presence of the linker between the A and BC domains of Maf1 that although seems to be redundant for Maf1 activity as a Pol III repressor, though evolutionarily not conserved, might be part of cellular adaptation of single cell organism as yeast, to rapidly changing life conditions. The presence of other regulatory proteins of Pol III in higher eukaryota (e.g. tumour suppressors p53; RB, retinoblastoma protein and proto-oncogene, c-Myc in *H. sapiens*) and developed

other mechanisms of Pol III regulation in diverse conditions might be explanation for the diminished sequence encoding the linker and its possible marginal function.

Furthermore literature data state that altered abundance of IUPs can result in undesirable interactions (e.g. titration of unrelated proteins by inappropriate interaction through exposed peptide motives), thereby disturbing the balance of the signaling networks leading to dampened or inappropriate activities. It was shown that altered abundance of several intrinsically unstructured proteins (IUPs) has been associated with perturbed cellular signalling that may lead to uncontrolled proliferation of the cells typical for cancer (Gsponer *et al.,* 2008).

A general feature of transformed and tumour cells is abnormally high rates of Pol III transcription. This was initially discovered in mice with myelomas, where Pol III was found to be hyperactive (Schwartz *et al.,* 1974). Since then many type of tumour cell lines have also been found to overexpress the products of Pol III including ovarian and liver carcinomas (Marshall, 2008). *H. sapiens* Maf1 was shown to represses Pol III transcription *in vitro* and *in vivo* (Rollins *et al.,* 2007) and is required for maximal Pol III repression after exposure to alkylating agent and carcinogen - methyl methanesulfonate (MMS) (Reina *et al.,* 2006). Furthermore, Johnson *et al.,* (2007) have shown that changes in *H. sapiens* Maf1 expression affect Pol I- and Pol III-dependent transcription in human glioblastoma lines. The phenotypic consequences of reducing Maf1 expression included changes in cell morphology and the accumulation of actin stress fibers. Maf1 overexpression suppressed anchorage-independent growth. Together with the ability of Maf1 to reduce biosynthetic capacity, these findings supported the idea that Maf1 regulates the transformation state of cells.

Above findings support the idea that eukaryotic Maf1s might belong to the family of intrinsically unstructured proteins (IUPs).

What is more, computational studies with a usage of phosphorylation sites prediction methods revealed that unstructured regions are enriched in sites that may be posttranslationaly modified Gsponer *et al.* (2008) determined experimentally yeast kinase - substrate network, and showed that highly unstructured proteins are targeted by many kinases twice more as compared to structured proteins. What is more, 85% of the kinases for which, more than 50% of their substrates are highly unstructured, were either regulated in a cell cycle–dependent manner (e.g. Cdc28) or activated upon exposure to particular stimuli (e.g. Fus3) or stress (e.g. Atg1). This suggested that the posttranslational modification of intrinsically unstructured proteins (IUPs) through phosphorylation may be an important mechanism in

regulating their function and possibly their availability under different conditions (Gsponer *et al.,* 2008).

In correlation, Maf1 is a protein rich in serine residues. (15, 7% serines for *S. cerevisiae*). According to bioinformatic survey with SwissProt PROSITE, Maf1 posses almost 30 potential phosphorylation sites. The analysis of potential phosphorylation sites by NetPhos 2.0 server (Bloom *et al.,* 1999) in four Maf1 orthologs containing linkers of different lengths revealed that predicted phosphorylation sites were mostly found in the long unstructured linkers between the Maf1 A and BC domains of *S. cerevisiae* and *C. glabrata* relatively, while they were more uniformly distributed along Maf1 sequence of *C. elegans* and *H. sapiens*, although they were also present in their shorter linkers (Fig. 44). Human Maf1 was shown to be phosphorylated on at least 5 residues, of which, three S60, S68, S75 are the main sites. These sites are located between the conserved A and BC domains of human Maf1 (Michels *et al.,* 2010; Kantidakis *et al.,* 2010; Shor *et al.,* 2010). In *S. cerevisiae*, Maf1 is phosphorylated on at least 6 residues: S90, S101, S177, S178, S179, S209 and S210) (Huber *et al.,* 2009; Moir *et al.,* 2006; Willis and Moir, 2007). Yet in *S. cerevisiae* all identified phosphorylation sites lay between the A and BC domains. Thus the presence of phosphorylation sites in the region separating the A and BC domains has been conserved from yeast to man, even though the specific amino acid sequence has not been conserved.

Considering that Maf1 contains two conserved domains it could be proposed that the unstructured linker becomes phosphorylated and thus modulates the conformational state of Maf1. Accordingly, different forms of Maf1 observed on polyacrylamide gels, interpreted as phosphorylated and subsequently dephosphorylated form of Maf1, might represent different conformational states depending on the interaction between the A and BC domains. Note that, the S90A, S101A and S177A, S178A mutations in the linker were found by Lee *et al.,* 2009 to change the proportion between slow- and fast-migrating Maf1 forms in favor of the former, without strongly affecting the phosphorylation state of Maf1. This might indicate that residues in the linker could affect the Maf1 shape even in a denaturating electrophoresis.

The interaction between the A and BC domains presented in this study occurred not only to be necessary for the full repression of Pol III activity but also to facilitate Maf1 dephosphorylation. One might hypothesize that, in the same time, the

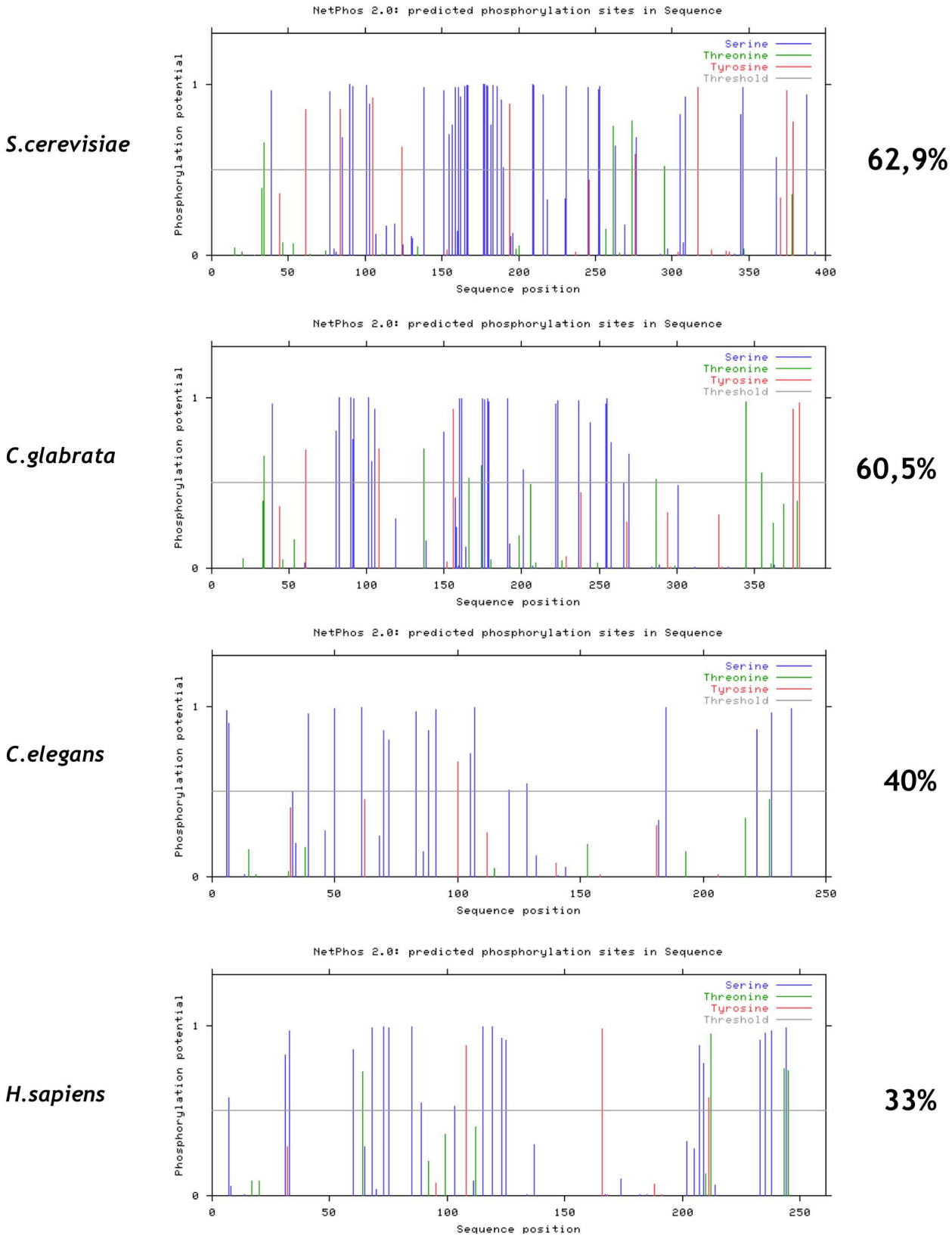

Figure 44. Predicted phosphorylation sites in Maf1 sequences. Protein sequences were analyzed with NetPhos 2.0 Server. Diagram presents probability of phosphorylation in the range [0.000-1.000]. The figure presents localization of serine (blue), threonine (green) and tyrosine (red) residues predicted to be phosphorylated. Comparison of predicted phosphorylation sites in eukaryotic orthologs of Maf1 with long (*S. cerevisiae* and *C. glabrata*) and short (*C. elegans* and *H. sapiens*) linker region between the A and BC domains. Percentage ratio of potential phosphorylation sites localized in the linker region is indicated.

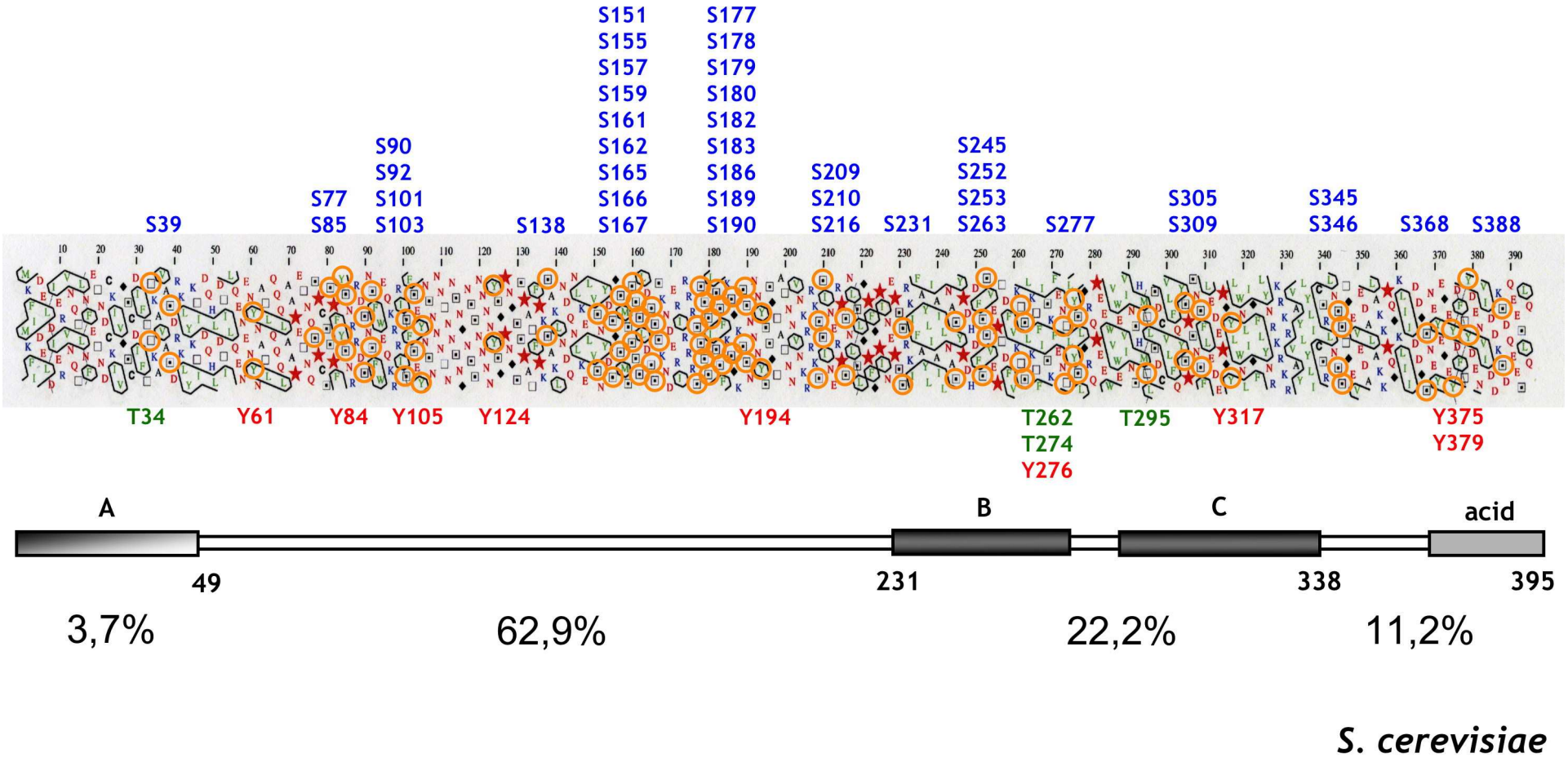

Figure 45. Localization of phosphorylated residues in *S. cerevisiae* Maf1 sequence. Figure presents localization of serine (blue), threonine (green) and tyrosine (red) residues predicted to be phosphorylated in *S. cerevisiae* Maf1 sequence. Potentially phosphorylated residues (highlighted with orange circles) are merged with Hydrophobic Cluster Analysis (Callebaut *et al.,* 1997). Below, schematic representation of Maf1 domains. Percentage ratio of phosphorylated residues localized in either A and BC domains or the linker region indicated.

interaction between domains of Maf1 is influenced by its phosphorylation state.

Therefore it is tempting to speculate that the phosphorylation and dephosphorylation of the exposed linker evokes a specific conformation of the protein that changes the distance between domains modulating their interaction and Pol III repression (Fig. 45). The interaction of the domains, mediated by dephosphorylation of the linker may affect both, the import of Maf1 into the nucleus and its interaction with Pol III. This conjecture is supported by data of (Moir *et al.,* 2006) showing that PKA-mediated phosphorylation of serine residues located in linker inhibited nuclear import of Maf1 and Pol III repression and further researches of Huber *et al.,* (2009) who have proposed that Maf1 phosphorylation by Sch9 at phosphorylation sites localized in linker, although not sufficient, contributes to prevent Maf1 nuclear localization.

Also current Maf1 crystalographic data presented by Vannini *et al.,* 2010 seem to support this hypothesis. The crystal structure of human Maf1 revealed that the two NLS sequences (in *S. cerevisiae* NLS1 aa: 205-208 and NLS2 aa: 328-332) are surface accesible. The N-terminal, NLS1 is part of the linker region and the C-terminal, NLS2 is positioned in close proximity to NLS1. Thus it was proposed that the phosphorylation of the linker causes structural rearangements of Maf1 that mask NLS sequences and prevent Maf1 nuclear localization.

Taken together we may hypothesize the conformational changes of Maf1 evoked by dephosphorylation of linker affects the interaction between the A and BC domains of Maf1 thus facilitating Maf1 activity as a Pol III repressor.

4. Current context of the presented data.

Recent crystallographic data obtained on human Maf1 (Vannini *et al.,* 2010) clarified the mechanism of Pol III regulation by Maf1.

Preceding data upon Maf1 indicated that nuclear pool of Maf1 either binds to Pol III preventing Pol III interaction with TFIIIB and promoters (Desai *et al.,* 2005; Moir *et al.,* 2006; Roberts *et al.,* 2006) (see Fig. 1 “Introduction”). Maf1-dependent repression of Pol III was correlated with decreased Brf1 (a subunit of TFIIIB) and Pol III occupancy at class III genes in *S. cerevisiae* (Oficjalska-Pham *et al.,* 2006; Roberts *et al.,* 2006). Similar results have been obtained for human Maf1.

The current data provided by Vannini *et al.,* 2010 revealed that, according to cryo-EM, human Maf1 while binding with Pol III is positioned on top of the Pol III “clamp domain” corresponding to published biochemical and genetic interactions of

S. cerevisiae and human Maf1 with the N-terminal region of C160, which forms most of the "clamp" (Boguta *et al.,* 1997; Oficjalska-Pham *et al.,* 2006; Reina *et al.,* 2006). Consistent with this location C160, C82 and C34 subunits of Pol III are Maf1 interacting partners in the yeast interactome (Gavin *et al.,* 2006). Moreover, the comparison of cryo-EM structures, revealed that human Maf1 bound to Pol III rearranges the C82/34/31 subunits of Pol III (see Fig. 2 and Fig. 1 in "Introduction") preventing Pol III interaction with Brf1 at class III genes promoters (Brf1-TBP-DNA complex) and initiation of transcription (Vannini *et al.,* 2010). Furthermore, human Maf1 bound to Pol III did not affect nucleic acid binding in the active center and RNA synthesis as was shown by *in vitro* assays (initiation factor-independent transcription assay and RNA extension assay) (Vannini *et al.,* 2010) thus the mechanism of Pol III repression bases on Maf1 dependent abolishment of the Pol III interaction with promoter and disabling previously reported reinitiation of multiple-round transcription by Pol III (Cabart *et al.,* 2008). In described model of Maf1-dependent repression of Pol III, both the A and BC domains of Maf1 seem to contribute equally with no individual function of particular domain. That is consistent with the data decribed in this study showing that cooperation between the A and BC domains of *S. cerevisiae* Maf1 (the physical interaction) is indispensable for Pol III repression.

The uncovering of Maf1 crystal structure and mechanism, by which, Maf1 repress Pol III broadens the possibilities of future researches conducted upon regulation of Pol III activity. Since deregulation of Pol III activity was shown to mediate oncogenic transformation (Marshall *et al.,* 2008a; Marshall *et al.,* 2008b) there might be a possibility to construct a terapeutic agents, resembling structurally Maf1, that could specifically repress hyperactivated Pol III in tumor cells.

On the other side, currently, there are prerequisites that Maf1 has a dual nuclear function and contributes to pre-tRNA proccessing (Karkusiewicz – data unpublished). As reported by Kwapisz *et al.,* 2002, inactivation of *MAF1* gene (*maf1*Δ) results in decreased tRNA nonsense suppressor efficiency. That observation seems to argue with the fact that in absence of active Maf1 there is an elevated quantity of cellular tRNA, which should lead to increase of tRNA-mediated nonsense suppression efficiency. The hypothesis explaining this phenomena assume that tRNA synthesized in *maf1*Δ cells are incorectly or incompletely processed or they fail to be appropriately delivered to ribosomes. Recent data of our group, (Karkusiewicz - data unpublished) indeed show that, in absence of Maf1, tRNA processing is

defected and both: initial tRNA transcript and partially processed, intron containing tRNA precursors accumulate. Moreover, that regulation of pre-tRNA proccesing is mediated by nuclear form of Maf1 since restriction of Maf1 to the nucleus in an *msn5*Δ *S. cerevisiae* strain correlates with accelerated tRNA proccessing. Since it is known that not all nuclear Maf1 is bound to Pol III and that Maf1 association is dynamic it is plausible that apart from interaction with Pol III complex, Maf1 interacts with other nuclear proteins involved in early steps of tRNA proccessing or tRNA export to cytoplasm (Karkusiewicz – data unpublished). This dual function of Maf1 in down-regulation of Pol III and positive regulation of processing could be separable functions of nuclear Maf1. Thus it would be interesting to test if these opposing functions of Maf1 equally involve both, the A and BC Maf1 domains or the function in tRNA processing is restricted to particular domain.

V. MATERIALS AND METHODS

- **Media**

The following media were used for growing yeast: rich media - YPD (2% glucose, 2% peptone, 1% yeast extract), YPGly (2% glycerol, 2% peptone, 1% yeast extract), minimal media - SC (2% glucose, 0.67% yeast nitrogen base without amino acids), SC-leu or SC-leu-trp, SC-his contained 20 µg/ml of the amino acids required for growth, except for leucine or leucine and tryptophan or histidine respectively (Sherman, 2002). As required, the YPD medium was supplemented with rapamycin (0,2 µg/ml). Solid media contained 2% agar. All reagents used for media were Difco products.

- **Yeast *S. cerevisiae* strains and genetic procedures**

The yeast strains used in this study are listed in Table 9a. For analysis of the phenotype, yeast strains grown on YPD were spotted or replica-plated on plates and incubated for 3 days at the desired temperatures.

Yeast cells were transformed with plasmid by using the lithium acetate method (Chen *et al.,* 1992) and were cultivated at 30°C in SC selective medium for 3 days. Plasmid DNA from yeast cells was isolated using the procedures described previously by Rose *et al.,* 1990. The growth rate in liquid cultures was monitored by OD_{600} measurements.

For long term preservation of yeast strains, 100 µl of fresh stationary phase cells were mixed with 1 ml of 15% glycerol in YPD, immediately frozen in liquid nitrogen and stored at -80°C.

Table 9a. The yeast strains used in this study.

Strain	Genotype	Reference or source
YPH500	*MAT*α, *ade2-101, his3-Δ200, leu2-Δ1, lys2-801, trp1-Δ63, ura3-52*	Sikorski and Hieter, 1989
YPH500 *maf1*Δ	*MAT*α, *ade2-101, his3-Δ200, leu2-Δ1, lys2-801, trp1-Δ63, ura3-52, maf1-Δ*	Oficjalska-Pham *et al.,* 2006
Y190	*MATa, gal4–542, gal80–538, his3, trp1–901, ade2–101, ura3–52, leu2–3, 112, URA3::GAL1-lacZ, LYS2::GAL1(UAS)::HIS3, cyh^R*	Harper *et al.,* 1993

- **Plasmids**

Yeast/*E. coli* vectors used in this study are listed in Table 3. Transformation and growth of *E. coli* strains containing plasmids were carried out as described (Sambrook and Russell, 2001). LB medium (1% bacto-tryptone, 0.5% yeast extract,

1% NaCl; pH 7.5) was used for growing *E. coli* strains. As required, the LB medium was supplemented with ampicillin (60 μg/ml). Solid medium contained 2% agar. All reagents used for the medium were Difco products. Standard DNA manipulations were performed using *E. coli* strains listed in Table 2b (Bullock *et al.,* 1987; Woodcock *et al.,* 1989).

Table 9b. The *E. coli* strains used in this study.

Strain	Genotype	Reference or source
XL1-blue	*recA1, endA1, gyrA96, thi-1, hsdR17, supE44, relA1, lac [F – proAB, lacIq ZΔM15 Tn10(tetR)]*	Stratagene
DH5α	F⁻,Φ80d*lacZ*ΔM15(*lacZ*YA-*arg*F)U169,*deoR recA1,endA1,hsdR17* (r_{K^-},m_{K^+}), *supE44, λ-, thi-1, gyrA96, relA1*	Stratagene

Table 10A. Yeast/*E. coli* vectors used in this study.

Name of plasmid	Yeast gene cloned	Parental vector	*E. coli*/Yeast Markers	Description	Reference or source
pRS315	-	-	*amp^R, lacZ / LEU2, CEN6*	-	Sikorski and Hieter
pRS315-MAF1	*MAF1*	pRS315	*amp^R, lacZ / LEU2, CEN6*	Graczyk 2010, PhD thesis	D.Graczyk
pAG5, 6, 7, 8, 9, 10, 11, 12, 13, 14, 15, 16, 17, 18, 19, 20, 21, 22, 23, 24, 25, 27, 28, 29, 30, 33, 34, 35, 37, 38, 40, 42, 43, 44, 46, 47, 48, 49, 50, 51, 52, 53, 54, 55, 56, 58, 59, 60, 61, 62, 63, 64, 65, 66, 67, 68, 69, 70, 72, 73, 74	*MAF1*	pRS315	*amp^R, lacZ / LEU2, CEN6*	*maf1* mutants, mutagenesis of *MAF1* encoding 1-180 aa, *	this study
pAG88, 89, 101, 107, 108, 110, 111, 113, 114, 115, 116, 117, 118, 119, 120, 121, 123, 124, 125, 126, 127, 128, 129, 130, 131, 132, 133, 134, 136, 138, 139, 141, 143, 144, 145, 146, 147, 148, 149, 151, 152, 156, 158, 161, 163, 165, 166, 167, 168, 169, 170, 171, 172, 173, 174, 175, 176,	*MAF1*	pRS315	*amp^R, lacZ / LEU2, CEN6*	*maf1* mutants, mutagenesis of *MAF1* encoding 174-375 aa, *	this study

Continued:

Name of plasmid	Yeast gene cloned	Parental vector	*E. coli*/Yeast Markers	Description	Reference or source
pML6	*MAF1*	pRS315	*amp*^{R}, *lacZ* / *LEU2, CEN6*	*maf1* mutant, mutagenesis of *MAF1* encoding 174-375 aa, *	M.Legowiak
pMM1, 2, 4	*MAF1*	pRS315	*amp*^{R}, *lacZ* / *LEU2, CEN6*	*maf1* mutants, mutagenesis of *MAF1* encoding 174-375 aa, *	M.Maciak
pML11, 12	*MAF1*	pRS315	*amp*^{R}, *lacZ* / *LEU2, CEN6*	*maf1* mutants, suppressor of *maf1*-K35E, *	M.Legowiak
pAG11-1	*MAF1*	pRS315	*amp*^{R}, *lacZ* / *LEU2, CEN6*	D250E-*maf1*, derivative of pML11	this study
pAG12-1	*MAF1*	pRS315	*amp*^{R}, *lacZ* / *LEU2, CEN6*	V260D-*maf1*, derivative of pML12	this study
pAG12-2	*MAF1*	pRS315	*amp*^{R}, *lacZ* / *LEU2, CEN6*	N344I-*maf1*, derivative of pML12	this study
pAG12-3	*MAF1*	pRS315	*amp*^{R}, *lacZ* / *LEU2, CEN6*	V260D-N344I-*maf1*, derivative of pML12	this study

* Precise DNA mutations and corresponding amino acid changes are described in Tables: 1A, 1B and 2 in "Results" part and Supplementary Tables S1-S5.

Table 10B. Yeast/*E. coli* vectors for yeast-two-hybrid system used in this study.

Name of plasmid	Yeast gene cloned	Parental vector	*E. coli*/Yeast Markers	Description	Reference or source
pACT2	-	-	*amp*^{R}/*LEU2*, 2μ	two-hybrid vector carrying Gal4 activating domain (AD)	Clonetech
pAS2	-	-	*amp*^{R}/*TRP1*, 2μ	two-hybrid vector carrying Gal4 binding domain (BD)	Clonetech
pACT2-Maf1-A (1-12)	*MAF1*	pACT2	*amp*^{R}/*LEU2*, 2μ	two-hybrid vector carrying sequence encoding truncated A domain (1-12 aa)	this study
pACT2-Maf1-A (1-16)	*MAF1*	pACT2	*amp*^{R}/*LEU2*, 2μ	two-hybrid vector carrying sequence encoding truncated A domain (1-16 aa)	this study
pACT2-Maf1-A (1-23)	*MAF1*	pACT2	*amp*^{R}/*LEU2*, 2μ	two-hybrid vector carrying sequence encoding truncated A domain (1-23 aa)	this study
pACT2-Maf1-A (1-34)	*MAF1*	pACT2	*amp*^{R}/*LEU2*, 2μ	two-hybrid vector carrying sequence encoding truncated A domain (1-34 aa)	this study
pACT2-Maf1-A (1-39)	*MAF1*	pACT2	*amp*^{R}/*LEU2*, 2μ	two-hybrid vector carrying sequence encoding truncated A domain (1-39 aa)	this study
pACT2-Maf1-A (1-42)	*MAF1*	pACT2	*amp*^{R}/*LEU2*, 2μ	two-hybrid vector carrying sequence encoding truncated A domain (1-42 aa)	this study
pACT2-Maf1-A (1-57)	*MAF1*	pACT2	*amp*^{R}/*LEU2*, 2μ	two-hybrid vector carrying sequence encoding truncated A domain (1-57 aa)	this study
pACT2-Maf1-A (1-59)	*MAF1*	pACT2	*amp*^{R}/*LEU2*, 2μ	two-hybrid vector carrying sequence encoding truncated A domain (1-59 aa)	this study
pACT2-Maf1-A (1-77)	*MAF1*	pACT2	*amp*^{R}/*LEU2*, 2μ	two-hybrid vector carrying sequence encoding truncated A domain (1-77 aa)	this study
pACT2-Maf1-A (1-79)	*MAF1*	pACT2	*amp*^{R}/*LEU2*, 2μ	two-hybrid vector carrying sequence encoding truncated A domain (1-79 aa)	this study

Continued:

Name of plasmid	Yeast gene cloned	Parental vector	*E. coli*/Yeast Markers	Description	Reference or source
pACT2-Maf1-A (1-91)	*MAF1*	pACT2	*amp*^{R}/*LEU2*, 2µ	two-hybrid vector carrying sequence encoding truncated A domain (1-91 aa)	this study
pACT2-Maf1-A (1-111)	*MAF1*	pACT2	*amp*^{R}/*LEU2*, 2µ	two-hybrid vector carrying sequence encoding truncated A domain (1-111 aa)	this study
pACT2-Maf1-A (1-172)	*MAF1*	pACT2	*amp*^{R}/*LEU2*, 2µ	two-hybrid vector carrying sequence encoding truncated A domain (1-172 aa)	this study
pAS2-Maf1-BC (165-349)	*MAF1*	pAS2	*amp*^{R}/*TRP1*, 2µ	two-hybrid vector carrying sequence encoding truncated BC domain (165-349 aa)	this study
pAS2-Maf1-BC (165-367)	*MAF1*	pAS2	*amp*^{R}/*TRP1*, 2µ	two-hybrid vector carrying sequence encoding truncated BC domain (165-367 aa)	this study
pAS2-Maf1-BC (196-349)	*MAF1*	pAS2	*amp*^{R}/*TRP1*, 2µ	two-hybrid vector carrying sequence encoding truncated BC domain (196-349 aa)	this study
pAS2-Maf1-BC (196-367)	*MAF1*	pAS2	*amp*^{R}/*TRP1*, 2µ	two-hybrid vector carrying sequence encoding truncated BC domain (196-367 aa)	this study
pACT2-Maf1-A K35E	*MAF1*	pACT2	*amp*^{R}/*LEU2*, 2µ	two-hybrid vector carrying *maf1*-K35E, derivative of pACT2-Maf1-A (1-42)	this study
pAS2-Maf1-BC D250E	*MAF1*	pAS2	*amp*^{R}/*TRP1*, 2µ	two-hybrid vector carrying *maf1*-D250E, derivative of pAS2-Maf1-BC (196-349)	this study
pAS2-Maf1-BC V260D	*MAF1*	pAS2	*amp*^{R}/*TRP1*, 2µ	two-hybrid vector carrying *maf1*-V260D, derivative of pAS2-Maf1-BC (196-349)	this study
pAS2-Maf1-BC N344I	*MAF1*	pAS2	*amp*^{R}/*TRP1*, 2µ	two-hybrid vector carrying *maf1*-N344I, derivative of pAS2-Maf1-BC (196-349)	this study
pAS2-Maf1-BC V260D-N344I	*MAF1*	pAS2	*amp*^{R}/*TRP1*, 2µ	two-hybrid vector carrying *maf1*-V260D-N344I, derivative of pAS2-Maf1-BC (196-349)	this study
pGAD424	-	-	*amp*^{R}/*LEU2*, 2µ	two-hybrid vector carrying Gal4 activating domain (AD)	Clontech
pGBT9	-	-	*amp*^{R}/*TRP1*, 2µ	two-hybrid vector carrying Gal4 binding domain (BD)	Clontech
pGAD424-NTF C160	*RPC160*	pGAD424	*amp*^{R}/*LEU2*, 2µ	two-hybrid vector carrying sequence encoding truncated C160 (1-235 aa)	K. Balicki
pGBT9-NTF C160	*RPC160*	pGBT9	*amp*^{R}/*TRP1*, 2µ	two-hybrid vector carrying sequence encoding truncated C160 (1-235 aa)	K. Balicki
pGAD424-C160	*RPC160*	pGAD424	*amp*^{R}/*LEU2*, 2µ	-	M.Boguta
pGAD2F-C160	*RPC160*	pGAD424	*amp*^{R}/*LEU2*, 2µ	-	SBIGeM*
pACT-TFIIIA	*PZF1*	pACT2	*amp*^{R}/*LEU2*, 2µ	-	SBIGeM*
pACT-TFIIIB70	*BRF1*	pACT2	*amp*^{R}/*LEU2*, 2µ	-	SBIGeM*
pACT-TFIIIB90	*BDP1*	pACT2	*amp*^{R}/*LEU2*, 2µ	-	SBIGeM*
pGA-TBP	*TBP1*	pGAD424	*amp*^{R}/*LEU2*, 2µ	-	SBIGeM*

Continued:

Name of plasmid	Yeast gene cloned	Parental vector	*E. coli*/Yeast Markers	Description	Reference or source
pACT-Tau138	*TFC3*	pACT2	*amp^R*/*LEU2*, 2μ	-	SBIGeM*
pACT-Tau131	*TFC4*	pACT2	*amp^R*/*LEU2*, 2μ	-	SBIGeM*
pACT-Tau95	*TFC1*	pACT2	*amp^R*/*LEU2*, 2μ	-	SBIGeM*
pACT-Tau91	*TFC6*	pACT2	*amp^R*/*LEU2*, 2μ	-	SBIGeM*
pACT-Tau60	*TFC8*	pACT2	*amp^R*/*LEU2*, 2μ	-	SBIGeM*
pACT-Tau55	*TFC7*	pACT2	*amp^R*/*LEU2*, 2μ	-	SBIGeM*
pGA-C128	*RET1*	pGAD424	*amp^R*/*LEU2*, 2μ	-	SBIGeM*
pACT-C82	*RPC82*	pACT2	*amp^R*/*LEU2*, 2μ	-	SBIGeM*
pGA-C53	*RPC53*	pGAD424	*amp^R*/*LEU2*, 2μ	-	SBIGeM*
pGA-AC40	*RPC40*	pGAD424	*amp^R*/*LEU2*, 2μ	-	SBIGeM*
pGA-C34	*RPC34*	pGAD424	*amp^R*/*LEU2*, 2μ	-	SBIGeM*
pACT-C31	*RPC31*	pACT2	*amp^R*/*LEU2*, 2μ	-	SBIGeM*
pGA-ABC27	*RPB5*	pGAD424	*amp^R*/*LEU2*, 2μ	-	SBIGeM*
pACT-C25	*RPC25*	pACT2	*amp^R*/*LEU2*, 2μ	-	SBIGeM*
pACT-ABC23	*RPO26*	pACT2	*amp^R*/*LEU2*, 2μ	-	SBIGeM*
pGA-AC19	*RPC19*	pGAD424	*amp^R*/*LEU2*, 2μ	-	SBIGeM*
pACT-C17	*RPC17*	pACT2	*amp^R*/*LEU2*, 2μ	-	SBIGeM*
pGA-ABC14,5	*RPB8*	pGAD424	*amp^R*/*LEU2*, 2μ	-	SBIGeM*
pACT-C11	*RPC11*	pACT2	*amp^R*/*LEU2*, 2μ	-	SBIGeM*
pACT-ABC10α	*RPC10*	pACT2	*amp^R*/*LEU2*, 2μ	-	SBIGeM*
pGA-ABC10β	*RPB10*	pGAD424	*amp^R*/*LEU2*, 2μ	-	SBIGeM*
pACT-Sub1	*SUB1*	pACT2	*amp^R*/*LEU2*, 2μ	-	SBIGeM*
pACT-Maf1	*MAF1*	pACT2	*amp^R*/*LEU2*, 2μ	-	SBIGeM*
pAS-TFIIIA	*PZF1*	pAS2	*amp^R*/*TRP1*, 2μ	-	SBIGeM*
pAS-TFIIIB70	*BRF1*	pAS2	*amp^R*/*TRP1*, 2μ	-	SBIGeM*
pAS-TFIIIB90	*BDP1*	pAS2	*amp^R*/*TRP1*, 2μ	-	SBIGeM*
pAS-TBP	*TBP1*	pAS2	*amp^R*/*TRP1*, 2μ	-	SBIGeM*
pAS-Tau138	*TFC3*	pAS2	*amp^R*/*TRP1*, 2μ	-	SBIGeM*

Continued:

Name of plasmid	Yeast gene cloned	Parental vector	*E. coli*/Yeast Markers	Description	Reference or source
pAS-Tau131	*TFC4*	pAS2	*amp*^{R}/*TRP1*, 2μ	-	SBIGeM*
pAS-Tau95	*TFC1*	pAS2	*amp*^{R}/*TRP1*, 2μ	-	SBIGeM*
pAS-Tau91	*TFC6*	pAS2	*amp*^{R}/*TRP1*, 2μ	-	SBIGeM*
pAS-Tau60	*TFC8*	pAS2	*amp*^{R}/*TRP1*, 2μ	-	SBIGeM*
pAS-Tau55	*TFC7*	pAS2	*amp*^{R}/*TRP1*, 2μ	-	SBIGeM*
pAS-C128	*RET1*	pAS2	*amp*^{R}/*TRP1*, 2μ	-	SBIGeM*
pAS-C82	*RPC82*	pAS2	*amp*^{R}/*TRP1*, 2μ	-	SBIGeM*
pAS-C53	*RPC53*	pAS2	*amp*^{R}/*TRP1*, 2μ	-	SBIGeM*
pAS-AC40	*RPC40*	pAS2	*amp*^{R}/*TRP1*, 2μ	-	SBIGeM*
pAS-C37	*RPC34*	pAS2	*amp*^{R}/*TRP1*, 2μ	-	SBIGeM*
pAS-C31	*RPC31*	pAS2	*amp*^{R}/*TRP1*, 2μ	-	SBIGeM*
pAS-ABC27	*RPB5*	pAS2	*amp*^{R}/*TRP1*, 2μ	-	SBIGeM*
pAS-C25	*RPC25*	pAS2	*amp*^{R}/*TRP1*, 2μ	-	SBIGeM*
pAS-AC19	*RPC19*	pAS2	*amp*^{R}/*TRP1*, 2μ	-	SBIGeM*
pAS-C17	*RPC17*	pAS2	*amp*^{R}/*TRP1*, 2μ	-	SBIGeM*
pAS-ABC14,5	*RPB8*	pAS2	*amp*^{R}/*TRP1*, 2μ	-	SBIGeM*
pAS-C11	*RPC11*	pAS2	*amp*^{R}/*TRP1*, 2μ	-	SBIGeM*
pAS-ABC10α	*RPC10*	pAS2	*amp*^{R}/*TRP1*, 2μ	-	SBIGeM*
pMA-ABC10β	*RPB10*	pGBT9	*amp*^{R}/*TRP1*, 2μ	-	SBIGeM*
pGBT9-C160	*RPC160*	pGBT9	*amp*^{R}/*TRP1*, 2μ	-	M.Boguta
pAS-C160	*RPC160*	pAS2	*amp*^{R}/*TRP1*, 2μ	-	SBIGeM*
pAS-Sub1	*SUB1*	pAS2	*amp*^{R}/*TRP1*, 2μ	-	SBIGeM*
pAS-Maf1	*MAF1*	pAS2	*amp*^{R}/*TRP1*, 2μ	-	SBIGeM*

* Service de Biologie Intégrative et Génétique Moléculaire, Institut de Biologie et de Technologies de Saclay (CEA/Saclay)

- **Standard DNA manipulation**

Routine DNA techniques: plasmid preparation, digestion, cloning and Tris-acetate-EDTA (TAE) agarose gel electrophoresis were carried out as described by Sambrook and Russell, 2001. Plasmid DNA was isolated with QIAprep Spin Miniprep Kit (Qiagen). Restriction and DNA-modifying enzymes and DNA ligase were

purchased from Invitrogen, Fermentas, Promega, New England Biolabs and Gibco BRL and used in accordance with the manufacturers' instructions. PCR reactions were catalyzed by *Taq* DNA polymerase (Promega or Finnzymes) or polymerase with proofreading activity (Expand High Fidelity PCR System, Roche), used according to the manufacturers' instructions. pGEM-T Easy Vector (Promega) was used to clone products of PCR. PCR products were purified on QIAquick PCR Purification Kit (Qiagen). DNA fragments were purified from TAE-agarose gel with QIAEX II Agarose Gel Extraction Kit (Qiagen) and NucleoSpin extraction kit (Macherey-Nagel) according to the manufacturer's instructions. Sequencing of plasmid DNA was performed with BigDye Terminator 3.1 Kit and by the Laboratory of DNA Sequencing and Oligonucleotide Synthesis, IBB PAN. DNA sequences were analyzed with FinchTV v 1.4 and Chromas Lite v 2.01 software.

- **Oligonucleotides**

All oligonucleotide primers were produced in the Laboratory of DNA Sequencing and Oligonucleotide Synthesis, IBB PAS except: MAF12F, MAF12R, MAF16F, MAF16R, MAF23F and MAF23R that were produced by Sigma-Genosys (Table 11).

- **Generation of yeast *S. cerevisiae* Maf1 mutants strains**

➢ **Maf1 mutated in the A domain.**

MAF1 gene was cut from pFL44-MAF1 (Boguta *et al.,* 1997) subcloned in pRS315 (LEU2, CEN) plasmid (Sikorski and Hieter, 1989) resulting in pRS315-*MAF1* (Graczyk, 2010 – PhD thesis). The plasmids harboring *maf1* were derived from pRS315-*MAF1* using a rapid method for localized mutagenesis (Muhlrad *et al.,* 1992). For this purpose *MAF1* fragment encoding 1-180 aa was PCR-amplified from pRS315-*MAF1* under mutagenic conditions (3, 5) using MAF1-1 and MAF1-2 primers and Diversify PCR Random Mutagenesis Kit (Clontech). The product of the low-fidelity PCR was transformed together with gapped linear plasmid pRS315-*MAF1* (digested with *Bcl*I and *Bsg*I, New England Biolabs) into the YPH500 *maf1*Δ strain (Muhlrad *et al.,* 1992). Transformants, selected on minimal medium lacking leucine (SC-leu), were subsequently tested for thermosensitivity by replica-plating on YPGly and incubation at 37°C for three days.

The potential *maf1* mutants were used to isolate plasmid DNA, which was subsequently tested by PCR with MAF1-1 and MAF1-2 primers to confirm the presence of the mutagenized region. Selected plasmids were amplified in *E. coli* and

Table 11. Oligonucleotide primers used in this study.

Primer	Sequence 5' – 3'	Description	Purpose	Reference or source
MAF1-1	CGAGTTGCTTGTCAATCAGG	forward primer for the A domain region, 276 bp upstream of *MAF1* translation start site	mutagenesis of the A domain	this study
MAF1-2	CTGCTACTGCTCCTTCTTCT	reverse primer for the A domain region, 619 bp downstream of *MAF1* translation start site	mutagenesis of the A domain	this study
MAF1-5	GTCCGTATTCGGTCCTCATT	forward primer for the region 502 bp upstream of *MAF1* translation start site	sequencing of DNA encoding Maf1 A domain	this study
MAF1-6	TTGCGGCTTGACGGTTCGTT	reverse primer for the region 1778 bp downstream of *MAF1* translation start site	sequencing of DNA encoding Maf1 A domain	this study
MAF1-8	TTGCCAAGGCATCTTCCACT	reverse primer for the region 1146 bp downstream of *MAF1* translation start site	sequencing of DNA encoding Maf1 A domain	this study
MAF1-3	AGAAGAAGGAGCAGTAGCAG	forward primer for the region 600 bp downstream of *MAF1* translation start site	mutagenesis of the BC domain	this study
MAF1-9	CGTATTCTCCTTCGTATTCA	reverse primer for the region 1206 bp downstream of *MAF1* translation start site	mutagenesis of the BC domain	this study
MAF1-4	CAGCCTGATTGAAGTTCCGT	reverse primer for the region 1528 bp downstream of *MAF1* translation start site	sequencing of DNA encoding Maf1 BC domain	this study
MAF1-7	TTGGAAGATGAGCCTGGCTA	forward primer for the region 1011 bp downstream of *MAF1* translation start site	sequencing of DNA encoding Maf1 BC domain	this study
MAF1-10	CTGGACCTAATGGTTCTTCT	forward primer for the region 454 bp upstream of *MAF1* translation start site	sequencing of DNA encoding Maf1 BC domain	this study
MAF12Fcut	GATCCGAATGAAATTTATTGATGAGC TAGATATAGAGAGAGTGC	synthetic (+) ssDNA encoding 1-12 aa of the A domain, sticky ends for *Xho*I, *Bam*HI clonning	two-hybrid system, generation of the truncated A domain	this study
MAF12Rcut	TCGAGCACTCTCTCTATATCTAGCTC ATCAATAAATTTCATTCG	synthetic (-) ssDNA encoding 1-12 aa of the A domain, sticky ends for *Xho*I, *Bam*HI clonning	two-hybrid system, generation of the truncated A domain	this study
MAF16Fcut	GATCCGAATGAAATTTATTGATGAGC TAGATATAGAGAGAGTGAATCAAACT CTCC	synthetic (+) ssDNA encoding 1-16 aa of the A domain, sticky ends for *Xho*I, *Bam*HI clonning	two-hybrid system, generation of the truncated A domain	this study
MAF16Rcut	TCGAGGAGAGTTTGATTCACTCTCTC TATATCTAGCTCATCAATAAATTTCAT TCG	synthetic (-) ssDNA encoding 1-16 aa of the A domain, sticky ends for *Xho*I, *Bam*HI clonning	two-hybrid system, generation of the truncated A domain	this study
MAF23Fcut	GATCCGAATGAAATTTATTGATGAGC TAGATATAGAGAGAGTGAATCAAACT CTCAATTTCGAGACAAATGACTGTC	synthetic (+) ssDNA encoding 1-23 aa of the A domain, sticky ends for *Xho*I, *Bam*HI clonning	two-hybrid system, generation of the truncated A domain	this study
MAF23Rcut	TCGAGACAGTCATTTGTCTCGAAATT GAGAGTTTGATTCACTCTCTCTATATC TAGCTCATCAATAAATTTCATTCG	synthetic (-) ssDNA encoding 1-23 aa of the A domain, sticky ends for *Xho*I, *Bam*HI clonning	two-hybrid system, generation of the truncated A domain	this study

MAF5A	TCATCGGGATCCGAATGAAATTTATT GATGAGCTAGATATAGAGAGAGTG	forward primer for the *MAF1* ORF, *Bam*HI restriction site at 5'	two-hybrid system, generation of the A domain	this study
MAF3A34	TCATCGCTCGAGTGTTGTGAAAATAT CGCAACTGCC	reverse primer for the region 182 bp downstream of *MAF1* translation start site, *Xho*I restriction site at 5'	two-hybrid system, generation of the truncated A domain	this study
MAF3A39	TCATCGCTCGAGTGATGCAACCGCC TTTGTTGTG	reverse primer for the region 197 bp downstream of *MAF1* translation start site, *Xho*I restriction site at 5'	two-hybrid system, generation of the truncated A domain	this study
MAF3A42	TCATCGCTCGAGTTTTCTATCTGATG CAACCGC	reverse primer for the region 206 bp downstream of *MAF1* ORF	two-hybrid system, generation of the A domain	this study
MAF3A57	TCATCGCTCGAGTTCCTGTAAAATAG TATCCAAATGCTG	reverse primer for the region 251 bp downstream of *MAF1* translation start site, *Xho*I restriction site at 5'	two-hybrid system, generation of the A domain	this study
MAF3A59	TCATCGCTCGAGCTCATTTTCCTGTA AAATAGTATCC	reverse primer for the region 257 bp down stream of *MAF1* translation start site, *Xho*I restriction site at 5'	two-hybrid system, generation of the A domain	this study
MAF3A77	TCATCGCTCGAGTGATTGGTTTGTTT CGGGAGC	reverse primer for the region 311 bp down stream of *MAF1* translation start site, *Xho*I restriction site at 5'	two-hybrid system, generation of the A domain	this study
MAF3A79	TCATCGCTCGAGGCAGGGTGATTGG TTTGTTTC	reverse primer for the region 317 bp downstream of *MAF1* translation start site, *Xho*I restriction site at 5'	two-hybrid system, generation of the A domain	this study
MAF3A91	TCATCGCTCGAGGTTGCTATCCCTCC TATTAG	reverse primer for the region 353 bp downstream of *MAF1* translation start site, *Xho*I restriction site at 5'	two-hybrid system, generation of the A domain	this study
MAF3A111	TCATCGCTCGAGAGTGTTATTATTGC TATTG	reverse primer for the region 413 bp downstream of *MAF1* translation start site, *Xho*I restriction site at 5'	two-hybrid system, generation of the A domain	this study
MAF3A172	TCATCGCTCGAGCCTCTCATCATTCT TAGAAGAAG	reverse primer for the region 596 bp downstream of *MAF1* translation start site, *Xho*I restriction site at 5'	two-hybrid system, generation of the A domain	this study
MAF5BC165	TCATCGGGATCCGATCTTCTTCTAAG AATGATGAGAGG	forward primer for the region 575 bp downstream of *MAF1* translation start site, *Bam*HI restriction site at 5'	two-hybrid system, generation of the BC domain	this study
MAF5BC196	TCATCGGGATCCGATCTGGTACAGC AACCAACAATG	forward primer for the region 668 bp downstream of *MAF1* translation start site, *Bam*HI restriction site at 5'	two-hybrid system, generation of the BC domain	this study
MAF3BC349	TCATCGCTCGAGTTCGCCTGTACTCG AATTTAG	reverse primer for the region 1127 bp downstream of *MAF1* translation start site, *Xho*I restriction site at 5'	two-hybrid system, generation of the BC domain	this study

MAF3BC367	TCATCGCTCGAGGCCATCATCTATTA TAAGCTTTCC	reverse primer for the region 1181 bp downstream of *MAF1* translation start site, *Xho*I restriction site at 5'	two-hybrid system, generation of the BC domain	this study
T7Prom	TAATACGACTCACTATAGGG	sequencing primer for pGEM-T plasmid	verification of pGEM-T plasmids harboring sequence encoding the A or BC domain	this study
Gal4BD	TCATCGGAAGAGAGTAG	forward primer complementary to region flanking polylinker in pAS2	verification of pAS2 plasmids harboring sequence encoding truncated A domain	this study
G203	CGGAATTAGCTTGGCTGC	reverse primer complementary to region flanking polylinker in pAS2	verification of pAS2 plasmids harboring sequence encoding truncated A domain	SBIGeM *
G242F	CTATTCGATGATGAAGATACC	forward primer complementary to region flanking polylinker in pACT2	verification of pACT2 plasmids harboring sequence encoding truncated A domain	SBIGeM*
G244R	CAGTTGAAGTGAACTTGCG	reverse primer complementary to region flanking polylinker in pACT2	verification of pACT2 plasmids harboring sequence encoding truncated A domain	SBIGeM*
Gal4AD	TACCACTACAATGGATG	sequencing primer for pACT2 plasmid and its derivatives	verification of pACT2 plasmids harboring sequence encoding *MAF1*	this study
N344I	TCATCGCTCGAGTTCGCCTGTACTCG AAATTAGACGCGAGC	derivative of MAF3BC349 primer modified to introduce N344I mutation	generation of N344I mutation in pAS2-Maf1-BC(196-349) plasmid	this study
D250E-f	CGCTTCTTATCCTGACCATGAGTTTT CATCGGTTGAGCCAACGG	forward primer for site directed mutagenesis modified to introduce mutation D250E	separation of suppressor mutations	this study
D250E-r	CCGTTGGCTCAACCGATGAAAACTCA TGGTCAGGATAAGAAGCG	reverse primer for site directed mutagenesis modified to introduce mutation D250E	separation of suppressor mutations	this study
V260D-f	GAGCCAACGGATTTTGACAAAACATC ATTG	forward primer for site directed mutagenesis modified to introduce mutation V260D	separation of suppressor mutations	this study
V260D-r	CAATGATGTTTTGACAAAATCCGTTG GCTC	reverse primer for site directed mutagenesis modified to introduce mutation V260D	separation of suppressor mutations	this study
N344I-f	GCTCGCGTCTAATCTCGAGTACAGG CGAAG	forward primer for site directed mutagenesis modified to introduce mutation N344I	separation of suppressor mutations	this study
N344I-r	CTTCGCCTGTACTCGAGATTAGACGC GAGC	reverse primer for site directed mutagenesis modified to introduce mutation N344I	separation of suppressor mutations	this study

analyzed with endonuclease *Eco*RI (Fermentas). Plasmids giving appropriate restriction pattern were retransformed to YPH500 *maf1Δ S. cerevisiae* strain due to confirmation of temperature-sensitive phenotype. Sequencing revealed type of mutation in each plasmid carrying *MAF1* mutated A domain. Mutated plasmids were sequenced using primers: MAF1-5 , MAF1-6, MAF1-8. Obtained plasmids were listed in Table 10A.

- **Maf1 mutated in the BC domain.**

pRS315-*MAF1* (constructed as previously described) was digested with *Bsa*BI and *Bsu*36I (New England Biolabs) and introduced into the YPH500 *maf1Δ* strain together with a *MAF1* fragment encoding the BC domain (174-375 aa) PCR-amplified under mutagenic conditions (1, 3) using primers: MAF1-3 , MAF1-9 and Diversify PCR Random Mutagenesis Kit (Clontech) (Muhlrad *et al.,* 1992). Transformants, selected on minimal medium lacking leucine (SC-leu), were subsequently tested for thermosensitivity by replica-plating on YPGly and incubation at 37°C for three days.

The obtained library of potential *maf1* mutants was screened for thermosensitivity on YPGly medium as described previously. Sequencing revealed type of mutation in each plasmid carrying *MAF1* the mutated BC domain. Mutated plasmids were sequenced using primers: MAF1-4 , MAF1-7, MAF1-10. Obtained plasmids were listed in Table 10A.

- **Maf1 mutated suppressor strains.**

Among 38 independent mutants, pAG70 (K35E-*maf1*) was selected from colonies that showed defective growth. To isolate pML11 (K35E-D250E-*maf1*) and pML12 (K35E-V260D-N344I-*maf1*) plasmids carrying suppressor mutations plasmid pAG70 (carrying the previously isolated *maf1* allele with the K35E mutation) was digested with *Bsa*BI and *Bsu*36I (New England Biolabs) and introduced into the YPH500 *maf1Δ* strain together with a *MAF1* fragment encoding the BC domain (174-375 aa) PCR-amplified under mutagenic conditions (1) using primers: MAF1-3, MAF1-9 and Diversify PCR Random Mutagenesis Kit (Clontech) (Muhlrad *et al.,* 1992). Transformants, selected on minimal medium lacking leucine (SC-leu). The obtained library of potential suppressor mutants was screened for overcoming the thermosensitivity on YPGly medium caused by the K35E mutation. Plasmids from selected mutants were retransformed to YPH500 *maf1Δ S. cerevisiae* strain due to confirmation of temperature WT phenotype. Sequencing revealed type of mutation

in each plasmid carrying mutated *MAF1*. Mutated plasmids were sequenced in regions encoding both, the A and BC Maf1 domains using primers: MAF1-4, MAF1-5, MAF1-6, MAF1-7, MAF1-8, MAF1-10.

D250E, N344I, V260D and V260D-N344I mutations were introduced to pRS315-*MAF1* plasmid with QuickChange Site-Directed Mutagenesis Kit (Stratagene) and following primers: D250E-f, D250E-r, V260D-f, V260D-r, N344I-f, N344I-r.

Obtained plasmids were listed in Table 10A.

- **Construction of plasmids to express fragments of *S. cerevisiae* Maf1 protein for two-hybrid study.**

DNA encoding fragments aa: 1-12, 1-16 and 1-23 of the A domain of *S. cerevisiae* Maf1 were synthesized *de novo* as oligonucleotides designed in a manner that enabled direct cloning to pACT2 and pAS2 two-hybrid vectors on *Bam*HI and *Xho*I restriction sites. Oligonucleotides were hybridized in pairs: MAF12F-MAF12R, MAF16F-MAF16R, MAF23F-MAF23R, kinased with a T4 polynucleotide kinase (New England Biolabs) and directly cloned to MATCHMAKER GAL4 Two-Hybrid Vectors (Clontech) – either the pACT2 plasmid (on *Bam*HI, *Xho*I restriction sites) carrying the activation domain of Gal4 or the pAS2 plasmid (on *Bam*HI, *Sal*I restriction sites) carrying the binding domain of Gal4 (Fig. 46). Presence of sequence encoding A domain was confirmed by the standard PCR reaction with primers complementary to region flanking cloned sequence: G242F and G244R for pACT2 derivatives and Gal4BD and G203 for pAS2 derivatives. Products of PCR were resolved by electrophoresis on 4% agarose gel. Selected plasmids harboring sequence encoding truncated Maf1 A domain were verified for nonspecific mutations by sequencing with primers Gal4AD for pACT2 derivatives, Gal4BD for pAS2 derivatives.

The larger DNA sequences, encoding aa: 1-34, 1-39, 1-42, 1-57, 1-59, 1-77, 1-79, 1-91, 1-111 and 1-172 fragments were amplified from pRS315-*MAF1* plasmid using forward primer MAF5A and respective reverse primers: MAF3A34, MAF3A39, MAF3A42, MAF3A57, MAF3A59, MAF3A77, MAF3A79, MAF3A91, MAF3A111, MAF3A172 with Expand High Fidelity ^{PLUS} PCR System (Roche). The intron sequence of the *MAF1* gene (localized between nt 7 and 87) was excluded.

DNA encoding fragments aa: 165-349, 165-367, 196-349 and 196-367 of the BC domain were amplified from pRS315-*MAF1* with respective forward primers:

MAF5BC165 and MAF5BC196 and respective reverse primers: MAF3BC349 and MAF3BC367 with with Expand High Fidelity PLUS PCR System (Roche).

All *MAF1* parts were amplified with *Bam*HI and *Xho*I termini fragments, cloned into pGEM-T Vector System (Promega) and verified by sequencing with primer T7Prom for nonspecific mutations. Selected plasmids were digested with *Bam*HI and *Xho*I restriction endonucleases (New England Biolabs) and inserted into MATCHMAKER GAL4 Two-Hybrid Vectors (Clontech) – either the pACT2 plasmid carrying the activation domain of Gal4 (on *Bam*HI, *Xho*I sites) or the pAS2 plasmid carrying the binding domain of Gal4 (on *Bam*HI, *Sal*I sites) (Fig. 46).

The resulting plasmids harboring sequence encoding A domain and plasmids harboring the sequence encoding BC domain listed in Table 10B. Expression of fusion proteins involving HA-tagged truncated versions of the A and BC domains was verified by Western blotting.

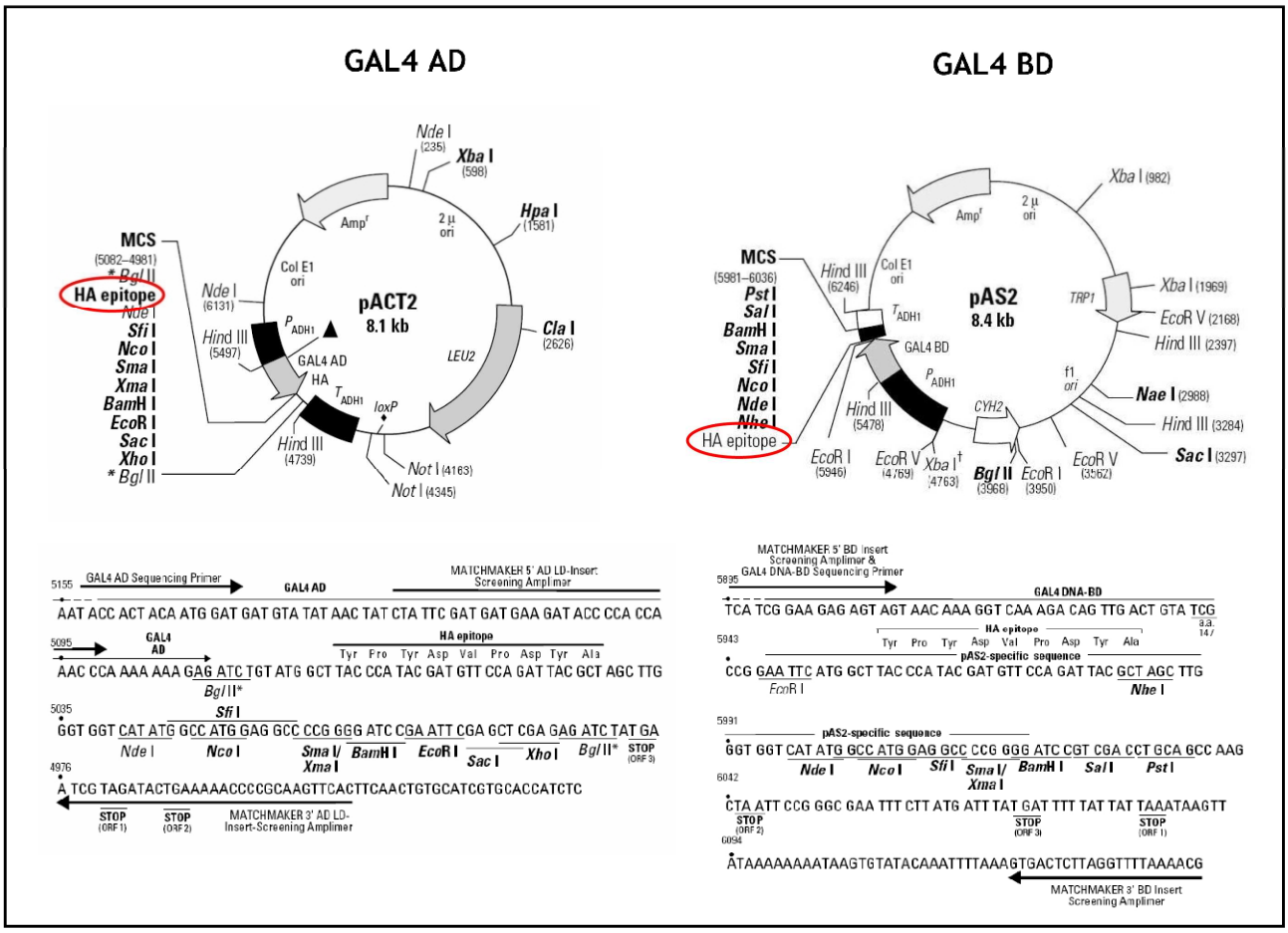

Figure 46. MATCHMAKER GAL4 Two-Hybrid Vectors (Clontech) – pACT2 plasmid carrying the activation domain of Gal4 (AD) and pAS2 plasmid carrying the binding domain of Gal4 (BD).

To generate mutations in the two-hybrid plasmids carrying fragments encoding Maf1 domains, the fragment encoding 1-42 aa of Maf1 was PCR-amplified from the pAG70 *maf1* allele K35E with forward primer MAF5A and reverse primer MAF3A42, digested with *Bam*HI *Xho*I restriction endonucleases (New England Biolabs) and cloned to pACT2 plasmid (*Bam*HI, *Xho*I restriction sites) (Fig. 46).

Similarly the mutations found in pML11 and pML12 were introduced into pAS2 plasmid by PCR amplification of the fragment encoding 196-349 aa of Maf1 from the pML11 and pML12 *maf1* alleles with forward primer MAF5BC196 and reverse primer MAF3BC349, subsequent digestion (*Bam*HI, *Xho*I) and cloning on *Bam*HI, *Sal*I restriction sites in pAS2 (Fig. 46). The N344I mutation found in the pML12 plasmid was introduced to pAS2 as described above but the fragment encoding 196-349 aa of Maf1 was PCR-amplified by using a modified reverse primer N344I-r with a mutation leading to the desired amino acid substitution. Resulting plasmids listed in Table 10B.

- **β - galactosidase activity assay**

Each of the derivatives of pACT2 and the single derivative of pAS2, were co-expressed pairwise in the two-hybrid reporter strain Y190. Cells containing these two plasmids were patched on SC medium lacking leucine and tryptophan. The patches were then examined for β-galactosidase activity using an overlay plate assay (Werner *et al.,* 1993). The intensity of the coloration was calibrated by comparison with a pair of known interactors (τ95/τ55, two TFIIIC subunits), for which, the β-galactosidase activity had been measured previously (Manaud *et al.,* 1998). For a β-galactosidase liquid assay cell lysates were prepared and the activity was measured colorimetrically as nmoles of ONPG (o-nitrophenyl- β-D-galactopiranoside) hydrolyzed per minute per mg of protein. Conversion 0.0045 x A_{420} = 1 nmole ONPG cleaved was used (Werner *et al.,* 1993). Protein content were determined by Bradford.

- **Northern analysis**

Cells (50 ml of liquid culture, OD_{600} of about 0.8) were harvested by centrifugation and resuspended in 50 mM Na acetate, pH 5.3, 10 mM EDTA. Total RNA was isolated by heating and freezing the cells in the presence of SDS and phenol as described previously (Schmitt et *al.*, 1990). RNA (5 µg per sample) was resolved by electrophoresis in 10% PAGE with 8 M urea, transferred to Hybond-N+ membrane (Amersham) by electroblotting in 0.5 x TBE (Tris-borate-EDTA) and

crosslinked by UV radiation (1200 mJ/cm^2). The membrane was prehybridized in 7% SDS; 0.5 M sodium phosphate pH 7.2; 1 mM EDTA pH 7.0; 1% BSA and hybridized at 37°C in the same solution with oligonucleotide probes labeled with [γ-^{32}P]-ATP and T4 polynucleotide kinase (New England Biolabs). The probes were: 5'TATTCCCACAGTTAACTGCGG3' for tRNA^{Leu}(CAA), 5'CCTCCAGATGACTTGACCG3' for tRNA^{Phe}(GAA) and 5'GGATTGCGGACCAAGCTAA3' for U3 snoRNA. After hybridization the blots were washed 2 x 10 min. with 1×SSC, 1% SDS and 3 x 10 min. with 0.5×SSC (Sodium chloride-Sodium citrate), 0.1% SDS at 37°C and exposed to an X-ray film or a phosphoimager screen (Molecular Dynamics). RNA was measured using the PhosphorImager STORM 820 (Molecular Dynamics).

- **Protein Extraction and Immunoblotting**

To avoid action of endogenous kinases or phosphatases during cell harvesting and protein extraction, yeast cells were rapidly harvested by centrifugation at 4°C, and 20% trichloroacetic acid (TCA) was added to the cell pellet as described earlier (Ciesla *et al.,* 2007; Oficjalska-Pham *et al.,* 2006). Cells were broken with acid-washed glass beads (15 min., 4°C), the supernatant was retained and TCA-precipitated proteins were pelleted by centrifugation (10 min., 4°C, 15000 rpm). The pellet was resuspended in sample buffer (pH 8.8) and boiled for 5 min. Protein extracts were separated on SDS-PAGE using a modified acrylamide: bisacrylamide ratio (33.5:0.3). One lane was loaded with protein from 1 OD of cell culture (10–20 µg). The membrane was blocked for 30 min. in TBST (10 mM Tris, 150 mM NaCl, 0.05% Tween 20) containing 5% fat-free dry milk and then incubated for 1 h with Maf1- specific antibody at 1:10 000 dilution (Ciesla *et al.,* 2007). After washing with TBST, the membrane was incubated with secondary anti-rabbit antibody coupled to horseradish peroxidase (DAKO) that, after washing with TBST, was then visualized by chemiluminescence using the ECL detection kit (Milipore).

Alternatively the membranes were incubated with secondary antibodies labelled with IRDye 800CW and IRDye 700DX infrared dyes and scanned by Odyssey™ Imager (LI-COR Biosciences) (Schutz-Geschwender *et al.,* 2004).

- **Immunofluorescence**

Cells were fixed in culture by adding formaldehyde to a final concentration of 3.7% for 1 h, spun down, washed and converted to spheroplasts, which were applied on microscopic slides covered with polylysine and subsequently treated as described previously (Oficjalska-Pham *et al.,* 2006). Maf1 antibody was added

(1: 500) followed by secondary CY3-conjugated anti-rabbit antibody (1: 1 000). Cells were viewed by Microphot-SA (Nikon). Images were collected using Photometrix CH350 camera.

VI. SUPPLEMMENTAL DATA

Table S1. Plasmids carrying truncated *maf1* allele. Plasmids organized according to the position of the STOP codon that occurs in *maf1*. Presented plasmids convey thermosensitive growth phenotype on glycerol-containing medium at 37°C (YPGly). Protein expression was not tested.

Plasmid	Amino acid substitution	Change in codon	Silent mutations	Mutations in promoter region	Mutations in intron	Position of the STOP codon	Mutations behind STOP codon
pAG28	none	none	none	A → G (-1 nt)	none	K2 → STOP (AAA → TAA)	none
pAG60	none	none	none	A → T (-108 nt)	none	K2 → STOP (AAA → TAA)	„E”57 → D (GAA → GAC)
pAG13	none	none	none	none	A → G (14 nt)	R11 → STOP (AGA → TGA)	none
pAG12	none	none	none	A → G (-56 nt)	none	K40 → STOP (AAG → TAG)	none
pAG14	none	none	none	none	A → G (23 nt)	Q56 → STOP (CAG → TAG)	„S”119 → R (AGT → AGA)
pAG18	D40 → V	GAT → GTT	none	T → C (-72 nt)	T → C (37 nt)	C79 → STOP (TGC → TGA)	none
pAG15	M1 → T Q68 → L	ATG → ACG CAG → CTG	none	T → C (-194 nt) T → C (-168 nt)	none	R98 → STOP (AGA → TGA)	none
pAG20	none	none	L55 (TTA → TTG)	none	none	R98 → STOP (AGA → TGA)	„S”101 → P (TCT → CCT)
pAG6	N120 → S	AAT → AGT	I31 (ATT → ATC)	none	none	S166 → STOP (TCT → TAG)	„S”167 → K (TCT → AAG)

Table S2. Plasmids carrying *maf1* mutated allele with frameshift mutations. Plasmids organized according to the order of identification. Presented plasmids convey thermosensitive growth phenotype on glycerol-containing medium at 37°C (YPGly). Protein expression was not tested.

Plasmid	Amino acid substitution	Change in codon	Silent mutations	Mutations in promoter region	Mutations in intron	Position of the frameshift	Mutations behind frameshift
pAG7	none	none	L65 (CTT → CTC)	T → C (- 74 nt) T → X (-20 nt)	none	W94 (TGG → GG)	none
pAG38	none	none	L65 (CTT → CTC)	A → G (- 156 nt) C → T (-33 nt)	none	N115 (AAT → AT)	none
pAG42	none	none	none	none	none	E95 (GAG → GGAG)	„N”117 (AAT → AGT)
pAG43	none	none	none	A → G (-180 nt)	T → C (21 nt)	V12 (GTG → GAGTG)	„E”104 (GAA → GAG)
pAG44	F18 → L L55 → S	TTC → CTC TTA → TCA	none	none	none	Q76 (CAA → CA)	none
pAG46	R11 → S	AGA → AGT	I31 (ATT → ATC)	A → G (-6 nt)	A → C (17 nt) A → G (85 nt)	L55 (TTA → TA)	none
pAG52	none	none	none	T → C (-66 nt)	none	G27 (GGC → GC)	none
pAG54	N60 → D	AAT → GAT	D89 (GAT → GAC)	none	none	N115 (AAA → AA)	none
pAG55	none	none	none	T → C (-134 nt) A → G (-47 nt)	none	N58 (AAT → AT)	„N”60 (AAT → AGT)
pAG63	none	none	none	none	none	W94 (TGG → TGGG)	„N”117 (AAT → AGT)
pAG65	L55 → S	TTA → TCA	none	none	none	N142 AAT → AT	none
pAG73	N58 → S	AAT → AGT	none	T → C (-132 nt)	none	N145 (AAT → AT)	none

Table S3. Plasmids carrying *maf1* allele mutated in the sequence encoding BC domain. Table presents plasmids harboring *maf1* alleles with multiple mutations or *maf1* alleles that convey no growth defect. Growth phenotype on glycerol-containing medium at 37°C (YPGly) signed as a: lack of growth (-); moderate growth defect (+/-) or no growth defect (WT, wild type). Plasmids organized according to the growth phenotype resulting from mutated Maf1 and number of mutations that occur. Protein expression was not tested.

Plasmid	Type of mutant	Amino acid substitution	Change in codon	Silent mutations	YPGly
pAG126	multiple (4)	R280 → G I290 → N E314 → G Y335 → C	AGA → GGA ATT → AAT GAG → GGG TAC → TGC	P215 (CCA → CCG) S230 (TCA → TCG)	-
pAG145	multiple (4)	T257 → A E288 → G S307 → P L321 → P	ACG → GCG GAG → GGC TCA → CCA CTT → CCT	none	-
pAG163	multiple (4)	F259 → S N273 → Y N308 → S L354 → S	TTT → TCT AAC → TAC AAC → AGC TTG → TCG	S305 (TCA → TCG) L336 (CTT → CTA) L338 (TTG → CTG)	-
pAG174	multiple (4)	T257 → S M294 → L R332 → G L343 → Q	ACG → TCG ATG → TTG AGA → GGA CTA → CAA	K356 (AAA → AAG)	-
pAG108	multiple (5)	I226 → M E228 → G L238 → P K265 → E Y317 → N	ATA → ATG GAA → GGA CTG → CCG AAA → GAA TAT → AAT	none	-
pAG133	multiple (5)	I241 → T S277 → P L301 → R L318 → H N320 → T	ATC → ACC TCT → CCT CTT → CGT CTT → CAC AAT → ACC	P256 (CCA → CCT) I268 (ATT → ATA)	-
pAG161	multiple (5)	E213 → A L238 → P S277 → P K329 → N T347 → S	GAA → GCA CTG → CCG TCT → CCT AAA → AAT ACA → TCA	T198 (ACA → ACC) S230 (TCA → TCG) L278 (CTT → CTC) S307 (TCA → TCC) G316 (GGC → GGT)	-
pAG111	multiple (6)	I181 → N S189 → L S209 → T L242 → H Y246 → N M294 → V	ATT → AAT TCA → TTA TCT → ACT CTC → CAC TAT → AAT ATG → GTG	A199 (GCA → GCT) L218 (TTA → CTA)	-
pAG170	multiple (6)	F235 → L F259 → L K270 → N W319 → R D352 → E K356 → R	TTT → CTT TTT → TTA AAA → AAT TGG → CGG GAT → GAA AAA → AGA	Q281 (CAA → CAG)	-
pAG173	multiple (6)	N192 → I S231 → G K261 → E F310 → L R328 → W S345 → P	AAT → ATT AGC → GGC AAA → GAA TTT → CTT AGG → TGG TCG → CCG	P247 (CCT → CCC) L264 (TTG → CTG)	-

Continued:

Plasmid	Type of mutant	Amino acid substitution	Change in codon	Silent mutations	YPGly
pAG123	multiple (7)	V203 → D S245 → T F251 → L F259 → L M294 → T L325 → H N344 → I	GTT → GAT TCT → ACT TTT → CTT TTT → CTT ATG → ACG CTT → CAT AAT → ATT	T198 (ACA → ACG) E228 (GAA → GAG) C299 (TGC → TGT)	-
pAG152	multiple (7)	K188 → E D248 → V H249 → Q Q281 → H W287 → G F324 → I K329 → N	AAA → GAA GAC → GTC CAT → CAA CAA → CAT TGG → GGG TTT → ATT AAA → AAT	I268 (ATT → ATC) L311 (TTG → CTG)	-
pAG156	multiple (7)	S209 → T S297 → P I322 → K K329 → I R332 → G Y337 → L	TCT → ACT TCT → CCT ATA → AAA AAA → ATA AGA → GGA TAC → CTC	L338 (TTG → CTG) T347 (ACA → ACT)	-
pAG172	multiple (7)	S180 → R N193 → S F223 → L I226 → A N291 → S F324 → I Y335 → F	AGT → AGA AAT → AGT TTT → TTA ATA → GCA AAT → AGT TTT → ATT TAC → TTC	P215 (CCA → CCG) P306 (CCT → CCA)	-
pAG149	multiple (8)	V254 → A K261 → I K265 → R S305 → P L321 → H I322 → L C340 → R E349 → G	GTT → GCT AAA → ATA AAA → AGA TCA → CCA CTT → CAT ATA → TTA TGC → CGC GAA → GGA	L264 (TTG → CTG) L311 (TTG → TTA)	-
pAG138	multiple (5)	E272 → G N291 → Y E314 → G N344 → D K356 → R	GAA → GGA AAT → TAT GAG → GGG AAT → GAT AAA → AGA	K331 (AAA → AAG)	+/-
pAG175	multiple (5)	N204 → D T257 → A F267 → L S269 → P L343 → P	AAC → GAC ACG → GCG TTT → CTT TCC → CCC CTA → CCA	N191 (AAC → AAT) S196 (TCT → TCA) A240 (GCT → GCA) S245 (TCT → TCC) P306 (CCT → CCC)	+/-
pAG118	multiple (6)	H249 → Q S253 → T V286 → A M294 → L D365 → G D366 → V	CAT → CAA TCG → ACG GTC → GCC ATG → TTG GAT → GGT GAT → GTT	none	+/-
pAG88	single	K270 → N	AAA → AAT	G323 (GGT → GGC) I364 (ATA → ATT)	WT
pAG101	single	D389 → E	GAT → GAA	none	WT
pAG89	double	K270 → E S307 → P	AAA → GAA TCA → CCA	S252 (TCA → TCT)	WT

Table S4. Plasmids carrying truncated *maf1* alleles Table represents plasmids encoding Maf1 mutated in the BC domain. Growth phenotype on glycerol-containing medium at 37°C (YPGly) signed as: (-) – growth defect, (+/-) – moderate growth defect. Plasmids organized according to the growth phenotype on YPGly and position of the STOP codon that occurs in mutated Maf1. Protein expression was not tested.

Plasmid	Amino acid substitution	Change in codon	Silent mutations	Position of the STOP codon	Mutations behind STOP codon	YPGly
pAG151	none	none	V254 (GTT → GAA) T295 (ACT → ACC) P306 (CCT → CCC) S309 (TCT → TCC)	K265 → STOP (AAA → TAA)	„L275**”** → F (TTA → TTC) „S307**”** → P (TCA → CCA) „R328**”** → K (AGG → AAG)	-
pAG146	K265 → E	AAA → GAA	F267 (TTT → TTC) S305 (TCA → TCT) L362 (CTT → CTG)	R280 → STOP (AGA → TGA)	„Q281**”** → H (CAA → CAT) „Y317” → H (TAT → CAT) „E351” → V (GAA → GTA) „D352” → G (GAT → GGT) „Q359” → L (CAG → CTG)	-
pAG166	F251 → S K265 → I	TTT → TCT AAA → ATA	V254 (GTT → GTC) K261 (AAA → AAG) L325 (CTT → CTA)	W285 → STOP (TGG → TAG)	„L338**”** → S (TTG → TCG)	-
pAG165	T257 → A T262 → S K270 → R	ACG → GCG ACA → TCA AAA → AGA	C299 (TGC → TGT) D366 (GAT → GAC)	Y304 → STOP (TAT → TAA) K331 → STOP (AAA → TAA)	„N327**”** → Y (AAC → TAC) „I339**”** → F (ATT → TTT)	-
pAG168	none	none	none	Y317 → STOP (TAT → TAG)	none	-
pAG117 pAG120	F251 → L T266 → A I290 → N	TTT → CTT ACT → GCT ATT → AAT	none	L338 → STOP (TTG → TAG)	none	-
pAG128	none	none	I239 (ATT → ATA)	S263 → STOP (TCA → TAA)	„R280” → I (AGA → ATA) „I322” → M (ATA → ATG)	+/-
pAG176	E288 → G H293 → L L336 → P	GAG → GGG CAC → CTC CTT → CCT	GAA → GAG (E349) CCT → CCC (P358)	L354 → STOP (TTG → TAG)	none	+/-

Table S5. Plasmids carrying *maf1* allele with frameshift mutations. Table represents plasmids encoding Maf1 mutated in the BC domain. All plasmids convey growth defect on glycerol-containing medium at 37°C (YPGly). Plasmids organized according to the order of identification. Protein expression not tested.

Plasmid	Amino acid substitution	Change in codon	Silent mutations	Position of the frameshift	Mutations behind frameshift
pAG114	N204 → S	AAC → AGC	none	S231 (AGC → GC)	„E255" (GAG → GGG) „F267" (TTT → TTA) „H293" (CAC → CGC)
pAG115	T200 → A	ACC → GCC	S183 (AGT → AGC) T198 (ACA → ACG) T295 (ACT → ACA) S297 (TCT → TCA)	L311 (TTG → G)	„C340" (TGC → GGC) „D352" (GAT → AAT)
pAG121	F251 → L F271 → S	TTT → CTT TTT → TCT	S245 (TCT → TCC) N320 (AAT → AAC) I339 (ATT → ATA)	H293 (CAC → C)	none
pAG124	H249 → L F271 → L	CAT → CTT TTT → CTT	none	P315 (CCT → CC)	„D352" (GAT → GGT)
pAG125	none	none	none	I268 (ATT → TATT)	„N344" (AAT → GAT) „L336" (CTT → CCT)
pAG129	R206 → S K233 → R	AGA → AGT AAA → AGA	L218 (TTA → CTA)	E288 (GAG → GA)	„L325" (CTT → CCT)
pAG130	none	none	K205 (AAA → AAG) I234 (ATA → ATT)	I239 (ATT → AT)	„K261" (AAA → ATA) „Y317" (TAT → CAT) „L354" (TTG → ATG)
pAG131	none	none	F310 (TTT → TTC)	P282 (CCA → CA)	„E314" (GAG → GGG)
pAG134	Y246 → D	TAT → GAT	GTA → GTT (V289)	S252 (TCA → CA)	„S297" (TCT → CCT) „W319" (TGG → CGG)
pAG141	none	none	G197 (GGT → GGC) Y237 (TAT → TAC) E272 (GAA → GAG)	K261 (AAA → A)	„D366" (GAT → GAA)
pAG143	K185 → E S186 → G	AAA → GAA AGT → GGT	I268 (ATT → ATC) P282 (CCA → CCT) D366 (GAT → GAC)	K188 (AAA → AA)	„N227" (AAC → ACC)
pAG144	S252 → T	TCA → ACA	none	Y276 (TAT → T)	none
pAG158	none	none	S252 (TCA → TCG) I339 (ATT → ATC)	V254 (GTT → GT)	„T266" (ACT → GCT) „F271" (TTT → TCT) „Y337" (TAC → AAC)
pAG169	L336 → P	CTT → CCT	S309 (TCT → TCC) L325 (CTT → CTC) K329 (AAA → AAG)	N344 (AAT → AT)	„S346" (AGT → GGT)

Table S6. Quantification of the relative amounts of the phosphorylated and nonphosphorylated Maf1 forms of K35E mutant and its suppressors (K35E-D250E and K35EV260D-N344I). Table presents relative ratio between phosphorylated and non-phosphorylated form of Maf1 for each time point after transfer to glycerol-containing medium (Fig. 19A). Bands intensities were quantified using Multi Gauge v 3.0 (Fujifilm) software. Ratio were normalized to that characteristic for exponentially growing cells (Exp). The relative ratio between phosphorylated and nonphosphorylated form of Maf1 normalized to that observed in exponential growth phase for each strain shows approximate speed of Maf1 dephosphorylation in mutants strains.

			glycerol				
	Maf1 phospho-form	**Exp.**	**15'**	**30'**	**60'**	**90'**	**120'**
WT	Phosphorylated	115 167	56 326	26 497	43 991	31 520	35 092
	Nonphosphorylated	87 569	185 210	234 162	173 818	198 230	249 981
Ratio		1.3	0.3	0.1	0.3	0.2	0.1
Normalization to Exp.		**1**	**0.2**	**0.1**	**0.2**	**0.1**	**0.1**
			glycerol				
	Maf1 phospho-form	**Exp.**	**15'**	**30'**	**60'**	**90'**	**120'**
K35E	Phosphorylated	90 102	148 252	109 899	154 009	98 210	96 377
	Nonphosphorylated	142 862	218 559	200 084	168 037	194 546	184 242
Ratio		0.6	0.7	0.5	0.9	0.5	0.5
Normalization to Exp.		**1**	**1.1**	**0.9**	**1.5**	**0.8**	**0.8**
			glycerol				
	Maf1 phospho-form	**Exp.**	**15'**	**30'**	**60'**	**90'**	**120'**
K35E-D250E	Phosphorylated	183 815	64 782	23 038	39 042	45 542	44 913
	Nonphosphorylated	96 533	138 514	130 264	165 668	144 117	160 710
Ratio		1.9	0.5	0.2	0.2	0.3	0.3
Normalization to Exp.		**1**	**0.2**	**0.1**	**0.1**	**0.2**	**0.1**
			glycerol				
	Maf1 phospho-form	**Exp.**	**15'**	**30'**	**60'**	**90'**	**120'**
K35E-V260D-N344I	Phosphorylated	106 601	54 230	15 050	25 410	51 437	60 560
	Nonphosphorylated	65 740	136 488	107 371	122 913	120 832	90 695
Ratio		1.6	0.4	0.1	0.2	0.4	0.7
Normalization to Exp.		**1**	**0.2**	**0.1**	**0.1**	**0.3**	**0.4**

Table S7. Quantification of the relative amounts of the phosphorylated and nonphosphorylated Maf1 forms of D250E, V260D, N344I and double V260D-N344I mutants originating from identified suppressors of K35E mutant. Table presents relative ratio between phosphorylated and non-phosphorylated form of Maf1 for each time point after transfer to glycerol-containing medium (Fig. 19B). Bands intensities were quantified as described in legend to Table S5. The relative ratio between phosphorylated and nonphosphorylated form of Maf1 normalized to that observed in exponential growth phase for each strain shows approximate speed of Maf1 dephosphorylation in mutants strains.

			glycerol				
	Maf1 phospho-form	**Exp.**	**15'**	**30'**	**60'**	**90'**	**120'**
D250E	Phosphorylated	104 832	11 061	3 584	679	1 282	373
	Nonphosphorylated	82 936	185 164	89 361	75 468	108 617	55 941
Ratio		1.3	0.1	-	-	-	-
Normalization to Exp.		**1**	**-**	**-**	**-**	**-**	**-**
			glycerol				
	Maf1 phospho-form	**Exp.**	**15'**	**30'**	**60'**	**90'**	**120'**
V260D	Phosphorylated	92 695	68 791	38 313	33 100	36 337	22 008
	Nonphosphorylated	93 034	227 208	228 189	228 991	222 350	206 794
Ratio		1.0	0.3	0.2	0.1	0.2	0.1
Normalization to Exp.		**1**	**0.3**	**0.2**	**0.1**	**0.2**	**0.1**
			glycerol				
	Maf1 phospho-form	**Exp.**	**15'**	**30'**	**60'**	**90'**	**120'**
N344I	Phosphorylated	57 604	2 762	2 433	675	44	468
	Nonphosphorylated	59 963	91 103	75 041	132 937	91 283	45 077
Ratio		1	-	-	-	-	-
Normalization to Exp.		**1**	**-**	**-**	**-**	**-**	**-**
			glycerol				
	Maf1 phospho-form	**Exp.**	**15'**	**30'**	**60'**	**90'**	**120'**
V260D-N344I	Phosphorylated	193 535	168 536	118 593	40 355	46 709	56 806
	Nonphosphorylated	76 941	184 554	180 032	204 832	206 615	232 277
Ratio		2.5	0.9	0.7	0.2	0.2	0.2
Normalization to Exp.		**1**	**0.4**	**0.3**	**0.1**	**0.1**	**0.1**

Table S8. Quantity of cells with nuclear localization of Maf1 during incubation in glucose medium and after transfer to glycerol-containing medium. K35E-*maf1*, K35E-D250E-*maf1* and K35E-V260D-N344I-*maf1* mutant strains and isogenic WT (YPH500 *maf1Δ* strain transformed with pRS315-*MAF1* plasmid) were grown to exponential phase in YPD glucose medium (Exp), then transferred to glycerol YPGly medium, incubated at 37°C for 2 hours. Cells were harvested as indicated. Maf1 localization was analysed by immunofluorescence microscopy using polyclonal anti-Maf1 antibodies. Nuclei were stained with 4',6-diamidino-2-phenylindole (DAPI). Quantified cells were partitioned into three groups of Maf1 localization: nuclear, cytoplasmatic and these of ambiguous localization in both compartments – cytoplasm and nucleus with a tendency to concentrate in nucleus (nuclear tendency). Quantification was performed from two independent experiments. Quantification was performed as a number of cells of particular kind per 100 cells evaluated (%).The average quantity is indicated below.

		glucose			glycerol		
		Nucleus (%°	**Nuclear tendency (%)**	**Cytoplasm (%)**	**Nucleus (%)**	**Nuclear tendency (%)**	**Cytoplasm (%)**
WT	**1**	0	16	84	91	8	1
	2	0	30	70	77	21	2
	average	**0**	**23**	**77**	**84**	**15**	**1**
		glucose			**glycerol**		
		Nucleus (%)	**Nuclear tendency (%)**	**Cytoplasm (%)**	**Nucleus (%)**	**Nuclear tendency (%)**	**Cytoplasm (%)**
K35E	**1**	0	25	75	33	48	19
	2	1	7	92	25	32	43
	average	**1**	**16**	**83**	**29**	**40**	**31**
		glucose			**glycerol**		
		Nucleus (%)	**Nuclear tendency (%)**	**Cytoplasm (%)**	**Nucleus (%)**	**Nuclear tendency (%)**	**Cytoplasm (%)**
K35E-D250E	**1**	6	31	63	89	3	8
	2	2	27	71	44	21	35
	average	**4**	**29**	**67**	**67**	**12**	**21**
		glucose			**glycerol**		
		Nucleus (%)	**Nuclear tendency (%)**	**Cytoplasm (%)**	**Nucleus (%)**	**Nuclear tendency (%)**	**Cytoplasm (%)**
K35E-V260D-N344I	**1**	2	26	72	76	2	22
	2	11	32	57	46	25	29
	average	**6**	**29**	**65**	**61**	**14**	**25**

Table S9. Evaluation of β-galactosidase activity for two-hybrid interaction of mutated Maf1 domains. Table presents values of β-galactosidase activity in units (u) and as a relative percentage activity. 100% is assumed for interaction of nonmutated A and BC domains of Maf1. Table represents data for interactions presented in Figure 27. A. pACT2-Maf1-A(1-42) plasmid and its mutated version were transformed individually with pAS2-Maf1- BC(196-349) plasmid or its mutated versions in yeast strain Y190. Transformants were assayed for β-galactosidase expression. Presented profile compares following two-hybrid interactions: wild type A and BC domains of Maf1 (1), mutated A domain K35E with wild type BC domain (2); mutated A domain K35E with four versions of mutated BC domain: D250E (3), V260D-N344I (4), V260D (5), N344I (6), and wild type A domain with mutated BC domain containing single D250E, V260D or N344I and double N344I-V260D mutations (7-10); SD, standard deviation; n, number of independent measures.

Tested interaction	ßgal activity (u)	SD of (u)	n	ßgal activity (%)	SD of (%)
A WT + BC WT	170	6	3	100%	4
A K35E + BC WT	103	18	4	61%	11
A K35E + BC D250E	159	16	4	94%	9
A K35E + BC V260D-N344I	148	35	5	87%	21
A K35E + BC V260D	307	72	3	181%	42
A K35E + BC N344I	141	29	3	83%	17
A WT + BC D250E	133	41	5	78%	24
A WT + BC V260D-N344I	65	28	5	38%	16
A WT + BC V260D	70	10	3	41%	6
A WT + BC N344I	169	38	3	99%	22

VII. APPENDIXES.

1. Publication in press : Gajda *et al.*, 2010

balt3/zbc-bc/zbc-bc/zbc04810/zbc3762-10z ZSUBMIT 17 xppws S=1 22/9/10 7:23 4/Color Figure(s) F2,3 ARTNO: M110.125286

THE JOURNAL OF BIOLOGICAL CHEMISTRY VOL. 285, NO. ??, pp. 1–xxx, ???? ??, 2010

Full Repression of RNA Polymerase III Transcription Requires Interaction between Two Domains of Its Negative Regulator Maf1*[S]

Received for publication, March 19, 2010, and in revised form, September 2, 2010 Published, JBC Papers in Press, September 3, 2010, DOI 10.1074/jbc.M110.125286

Anna Gajda[‡§], Joanna Towpik[‡], Ulrich Steuerwald[¶], Christoph W. Müller[¶], Olivier Lefebvre[§1], and Magdalena Boguta[‡‖2]

From the [‡]Institute of Biochemistry and Biophysics, Polish Academy of Sciences, Pawinskiego 5a, 02-106 Warsaw, Poland, the [§]Commissariat à l'Energie Atomique, iBiTecS, F-91191 Gif-sur-Yvette, France, the [¶]European Molecular Biology Laboratory, Meyerhofstrasse 1, 69117 Heidelberg, Germany and the [‖]Faculty of Chemistry, Warsaw University of Technology, Noakowskiego 3, 00-664 Warsaw, Poland

AQ:A,B

AQ: C **Maf1, first identified in yeast *Saccharomyces cerevisiae*, is a general negative regulator of RNA polymerase III (pol III). Transcription regulation by Maf1 is important under stress conditions and during the switch between fermentation and respiration. Maf1 is composed of two domains conserved during evolution. We report here that these two domains of human Maf1 are resistant to mild proteolysis and interact together as shown by pulldown and size exclusion chromatography and that the comparable domains of yeast Maf1 interact in a two-hybrid assay. Additionally, in yeast, a mutation in the N-terminal domain is compensated by mutations in the C-terminal domain. Integrity of both domains and their direct interaction are necessary for Maf1 dephosphorylation and subsequent inhibition of RNA pol III transcription on a nonfermentable carbon source. These data are the report relating Maf1 structure to RNA pol III transcription inhibition.**

Fn3 In eukaryotic cells, RNA polymerases (pol)[3] I and III are responsible for the synthesis of RNA species involved in ribosome biogenesis and the translation process. RNA synthesis by pol I and pol III represents >80% of all yeast nuclear transcription activity and is controlled in a coordinated way in response to various cellular and environmental conditions (1–3).

Pol III is responsible for the transcription of ~300 different genes in yeast (class III genes), mostly tRNA genes (4–6). Analyses of the pol III transcription system in yeast have revealed a series of protein-DNA and protein-protein interactions leading to the recruitment of pol III to its target tRNA genes: binding of the six-subunit TFIIIC factor to the intragenic promoter, TFIIIC-directed recruitment and assembly of the three components of TFIIIB (TBP, Brf1, and Bdp1), and subsequent recruitment of the 17-subunit pol III enzyme (7). Whereas the essential factors and the basal mechanisms of class III gene transcription are well defined, much less is known about the molecular mechanisms of pol III regulation.

The unique global negative regulator of pol III transcription in yeast is the Maf1 protein that mediates several signaling pathways, but is not essential (8, 9). In addition to the down-regulation that normally occurs in the stationary phase and in response to various drugs, also DNA damage, oxidative stress, secretory defects, and respiratory growth require Maf1 to achieve pol III repression (8, 10–12). The activity of Maf1 is regulated by its phosphorylation, which occurs in favorable conditions. Apart from decreasing direct Maf1 binding to pol III (13), this phosphorylation acts both to relocate the nuclear pool of Maf1 to the cytoplasm (14) and to prevent import of cytoplasmic Maf1 to the nucleus (15). Diverse unfavorable conditions lead to rapid Maf1 dephosphorylation and its nuclear accumulation, physical association of the dephosphorylated Maf1 with pol III, and genome-wide Maf1 targeting to pol III-transcribed genes (13, 16).

The pol III machinery is remarkably conserved between yeast and human. The most conserved components are those involved in transcription complex assembly: the τ131 subunit of TFIIIC and two components of TFIIIB (TBP, Brf1). The five pol III-specific subunits in yeast (C31, C34, C37, C53, and C82), all have structural and functional homologs in human cells (17). Also, Maf1 is conserved across eukaryotic organisms from yeast to man (9). This conservation is of particular interest considering that misregulation of pol III in human has been linked to malignant transformation. Excessive activation of pol III-directed transcription can lead to tumorgenesis (18–21), and, in line with this observation, two mammalian tumor suppressors, Rb and p53, have been shown to act as global repressors of pol III transcription (22). Recent results of several groups report Maf1-mediated repression of pol III transcription in human implicating HsMaf1 ortholog as a new class of mammalian pol III regulators (23–26). The involvement of HsMaf1 in the aberrant control of pol III transcription in cancer cells remains to be studied. In the light of the high evolutionary conservation of the pol III machinery including Maf1, insights into pol III (mis)-regulation by Maf1 gained by studying model organisms, such

* This work was supported by Ministry of Science and Higher Education, Poland, Grant N301 023 32/1117, French National Research Agency Grant ANR-07-BLAN-0039-01, and Association pour la Recherche contre le Cancer Grant 1078.

ZSI [S] The on-line version of this article (available at http://www.jbc.org) contains supplemental Figs. S1–S8 and Table S1.

[1] To whom correspondence may be addressed. Tel.: 33 1 69 08 59 57; Fax: 33 1 69 08 47 12; E-mail: Olivier.Lefebvre@Cea.Fr.

[2] To whom correspondence may be addressed: Institute of Biochemistry and Biophysics, Polish Academy of Sciences, Pawinskiego 5a, 02-106 Warsaw, Poland. Tel.: 4822 592 1312; Fax: 4822 592 2190; E-mail: magda@ibb.waw.pl.

AQ: Q [3] The abbreviations used are: pol, polymerase; aa, amino acids.

as yeast, should provide some insight into the role of HsMaf1 in cancer.

Our current interest concerns the relation between Maf1 structure and activity. All members of the Maf1 family have three fairly conserved segments (9) which, however, show no significant homology with protein domains of known function resulting in the striking lack of information on the functional significance of those regions. Point mutations have only highlighted the importance of several serine residues (mostly not phylogenetically conserved) and two nuclear localization sequences (15, 16, 27). We describe here identification of two conserved domains in HsMaf1 and show that the corresponding regions in yeast Maf1 interact. This interaction is crucial for the regulation of Maf1 activity by phosphorylation. Our data provide the first insight into the Maf1 structure in relation to pol III regulation.

EXPERIMENTAL PROCEDURES

Expression and Purification of HsMaf1 Protein—Human full-length Maf1 (HsMaf1) (aa 1–256) was expressed as a C-terminal His_6-tagged protein (HsMaf1-CHis) in insect cells. The protein was purified using cobalt affinity resin (Clontech). As a final purification step, the protein was applied to size exclusion chromatography equilibrated in buffer I (10 mM Tris, pH 7.4, 150 mM NaCl, 1 mM DTT).

HsMaf1 fragments consisting of aa 1–45, 1–59, 1–63, 1–74, and 85–210 were co-expressed for 15 h at 18 °C in *Escherichia coli* BL21 Gold (DE3) cells (Stratagene) using expression vector pETMCN-His (C. Romier, IGBMC) coding for tobacco etch virus-cleavable N-terminal His-tagged HsMaf1 aa 1–45, 1–59, 1–63, and 1–74 and expression vector pETMCN (as above) coding for nontagged Maf1 aa 85–210. The complex was purified by nickel affinity chromatography (nickel-nitrilotriacetic acid; Qiagen) followed by tobacco etch virus protease cleavage and a second nickel affinity chromatography to remove the His tag. The complex was further purified by anion-exchange chromatography (MonoQ 10/100; GE Healthcare) and size exclusion chromatography.

HsMaf1 fragment(82–236) was expressed from pETM11 (EMBL) as a potentially tobacco etch virus-cleavable, N-terminal His-tagged protein that was purified by nickel affinity chromatography (chelating Sepharose; GE Healthcare). However, the purified tagged protein HsMaf1(82–236) could not be cleaved by tobacco etch virus protease, most likely due to its aggregated state. The tagged protein was further purified by anion exchange chromatography (5-ml HiTrap Q-Sepharose HP; GE Healthcare) and size exclusion chromatography (S200 10/300; GE Healthcare).

Limited Proteolysis of HsMaf1 Protein— hMaf1-CHis protein at a concentration of 1 mg/ml was digested with trypsin for 30 min at 4 °C in buffer I using a protease:protein ratio of 1:150 (w/w). The reaction was stopped by adding PMSF to a final concentration of 1 mM. The proteolysis product was concentrated to 2 mg/ml using an Amicon MWCO 3000 concentrator (Millipore) and subsequently purified using two consecutive Superdex 200 10/300 columns (GE Healthcare) to improve resolution in buffer I. Purified HsMaf1 fragments were unambiguously identified using a combination of Edman degradation and mass spectrometry (quantitative time of flight).

Yeast Saccharomyces cerevisiae Strains and Media—The yeast strains used in this study included wild type YPH500 (*MATα*, *ade2-101*, *his3-Δ200*, *leu2-Δ1*, *lys2-801*, *trp1-Δ63*, *ura3-52*), *maf1-Δ*, a derivative of YPH500 (13), and the two-hybrid reporter strain Y190 (*MATa*, *gal4-542*, *gal80-538*, *his3*, *trp1-901*, *ade2-101*, *ura3-52*, *leu2-3*, *112*, *URA3::GAL1-lacZ*, *LYS2::GAL1(UAS):: HIS3*, cyh^R) (28). Rich media contained 1% yeast extract, 2% peptone, and 2% glucose (YPD) or 2% glycerol (YPGly). The minimal medium (SC) contained 2% glucose and 0.67% yeast nitrogen base without aa (29). Solid media contained 2% agar. All reagents were from Difco.

Construction of Plasmids to Express Fragments of Yeast Maf1 Protein for Two-hybrid Study—DNA encoding fragments(1–12), (1–16), and (1–23) of domain A of yeast Maf1 were synthesized as oligonucleotides. The larger DNA sequences, encoding aa 1–34, 1–39, and 1–42 were amplified using forward primer 5′-TCATCGGGATCCGAATGAAATTTATTGATGAGCTAGATATAGAGAGAGTG-3′ and reverse primers 5′-TCATCGCTCGAGTTTTCTATCTGATGCAACCGC-3′, 5′-TCATCGCTCGAGTGATGCAACCGCCTTTGTTGTG-3′, and 5′-TCATCGCTCGAGTGTTGTGAAAATATCGCAACTGCC-3′, respectively. The intron sequence of the *MAF1* gene (localized between bp 7 and 87) was excluded. DNA encoding the amino acid 196–349 fragment of BC domain was amplified with primers 5′-TCATCGGGATCCGATCTGGTACAGCAACCAACAATG-3′ and 5′-TCATCGCTCGAGTTCGCCTGTACTCGAATTTAG-3′. All *MAF1* parts were amplified with BamHI and XhoI termini fragments and inserted into MATCHMAKER GAL4 Two-hybrid Vectors (Clontech), either the pACT2 plasmid carrying the activation domain of Gal4 or the pAS2 plasmid carrying the binding domain of Gal4. The resulting plasmids were named pACT2-Maf1-A(1–12), pACT2-Maf1-A(1–16), pACT2-Maf1-A(1–23), pACT2-Maf1-A(1–34), pACT2-Maf1-A(1–39), pACT2-Maf1-A(1–42), and pAS2-Maf1-BC(196–349). Expression of fusion proteins involving HA-tagged truncated versions of A domain was verified by Western blotting. Each of the derivatives of pACT2 and the single derivative of pAS2 were co-expressed pairwise in the two-hybrid reporter strain Y190. Cells containing these two plasmids were patched on SC medium lacking leucine and tryptophan. The patches were then examined for β-galactosidase activity using an overlay plate assay (30). The intensity of the coloration was calibrated by comparison with a pair of known interactors (τ95/τ55, two TFIIIC subunits) for which the β-galactosidase activity had been measured previously (31). For a β-galactosidase liquid assay, cell lysates were prepared, and the activity was measured colorimetrically as nmol of *o*-nitrophenyl-β-D-galactopiranoside hydrolyzed per minute per mg of protein. Conversion $0.0045 \times A_{420} = 1$ nmol of *o*-nitrophenyl-β-D-galactopyranoside cleaved was used (30).

Generation of Yeast S. cerevisiae Maf1 Mutant Strains—*MAF1* gene was cut from pFL44-MAF1 (32) subcloned in pRS315 (LEU2, CEN) plasmid (33) resulting in pRS315-MAF1. The pAG70, pLM11 and pLM12 plasmids were derived from pRS315-MAF1 using a rapid method for localized mutagenesis (34). For this purpose, *MAF1* fragment(1–180) was PCR-ampli-

fied from pRS315-MAF1 under mutagenic conditions using 5′-CGAGTTGCTTGTCAATCAGG-3′ and 5′-CTGCTACTGCTCCTTCTTCT-3′ primers and a Diversify PCR Random Mutagenesis kit (Clontech). The product of the low fidelity PCR was transformed together with gapped linear plasmid pRS315-MAF1 (digested with BclI and BsgI) into the YPH500 *maf1*-Δ strain (13). Transformants, selected on minimal medium lacking leucine, were subsequently tested for Maf1 activity by replica-plating on YPGly and incubation at 37 °C for 3 days; among 38 independent mutants, pAG70 (*maf1*-K35E) was selected from colonies that showed defective growth. To isolate pML11 (*maf1*-K35E/D250E) and pML12 (*maf1*-K35E/V260D/N344I) plasmids carrying suppressor mutations, pRS315 plasmid pAG70 (carrying the previously isolated *maf1* allele with the K35E mutation) was digested with BsaBI and Bsu36I and introduced into the YPH500 *maf1*-Δ strain together with a *MAF1* fragment encoding BC domain (aa 174–375) PCR-amplified under mutagenic conditions using primers 5′-AGAAGAAGGAGCAGTAGCAG-3′ and 5′-CGTATTCTCCTTCGTATTCA-3′. The obtained library of potential suppressor mutants was screened for overcoming the thermosensitivity on YPGly medium caused by the K35E mutation. This screen resulted in identification of pLM11 and pLM12 suppressor mutations in the BC domain of Maf1.

To generate mutations in the two-hybrid plasmids carrying fragments encoding Maf1 domains, the BamHI-XhoI fragment encoding aa 1–42 of Maf1 in the pACT2-Maf1-A(1–42) plasmid was substituted with a PCR-amplified fragment of the *maf1* allele K35E from pAG70. Similarly, the mutations found in pML11 and pML12 were introduced in pAS2-Maf1-BC(196–349). The N344I mutation found in the pML12 plasmid was introduced to pAS2-Maf1-BC(196–349) by using a modified reverse primer 3′-TCATCGCTCGAGTTCGCCTGTACTCGAAATTAGACGCGAGC-5′ with a mutation leading to the desired amino acid substitution.

A QuikChange Site-directed Mutagenesis kit (Stratagene) was used to introduce D250E, N344I, V260D, and V260D/N344I to pRS315-MAF1. The sequences of primers used are available upon request.

Northern Blot Analysis—Cells (50 ml of liquid culture, A_{600} of approximately 0.8) were harvested by centrifugation and resuspended in 50 mM sodium acetate, pH 5.3, 10 mM EDTA. Total RNA was isolated by heating and freezing the cells in the presence of SDS and phenol as described previously (12, 35). RNA (5 μg/sample) was resolved by electrophoresis in 10% PAGE with 8 M urea, transferred to Hybond N+ membrane (Amersham Biosciences) by electroblotting in 0.5× TBE, and cross-linked by UV radiation (1200 mJ/cm^2). The membrane was prehybridized in 7% SDS, 0.5 M sodium phosphate, pH 7.2, 1 mM EDTA, pH 7.0, 1% BSA and hybridized at 37 °C in the same solution with oligonucleotide probes labeled with [γ-^{32}P]ATP and T4 polynucleotide kinase (New England Biolabs). The probes were 5′-TATTCCCACAGTTAACTGCGG-3′ for tRNA^{Leu}(CAA), 5′-CCTCCAGATGACTTGACCG-3′ for tRNA^{Phe}(GAA), and 5′-GGATTGCGGACCAAGCTAA-3′ for U3 snoRNA. After hybridization, the blots were washed 2 × 10 min with 1× SSC and 1% SDS and 3 × 10 min with 0.5× SSC and 0.1% SDS at 37 °C and exposed to an x-ray film or a PhosphorImager screen (Molecular Dynamics).

Protein Extraction and Immunoblotting—To avoid action of endogenous kinases or phosphatases during cell harvesting and protein extraction, yeast cells were rapidly harvested by centrifugation at 4 °C, and 20% trichloroacetic acid was added to the cell pellet as described earlier (12, 13). Cells were broken with acid-washed glass beads, the supernatant was retained, and trichloroacetic acid-precipitated proteins were pelleted by centrifugation. The pellet was resuspended in sample buffer, pH 8.8, and boiled for 5 min. Protein extracts were separated on SDS-PAGE using a modified acrylamide:bisacrylamide ratio (33.5:0.3). One lane was loaded with protein from 1 OD of cell culture (10–20 μg). The membrane was blocked for 30 min in TBST (10 mM Tris, 150 mM NaCl, 0.05% Tween 20) containing 5% fat-free dry milk and then incubated for 1 h with Maf1-specific antibody at 1:10,000 dilution (12). The membrane was incubated with secondary anti-rabbit antibody coupled to horseradish peroxidase (DAKO) which was then visualized by chemiluminescence using the ECL detection kit (Millipore).

RESULTS

Two Domains of Maf1 Do Interact—The yeast *MAF1* gene encodes a hydrophilic protein of 395 aa rich in serine and asparagine residues, with a predicted molecular mass of 44.7 kDa. Screening of multiple databases with the yeast Maf1 sequence revealed numerous orthologs in other eukaryotes: 1 in human, 50 in animals, 28 in plants, and 27 in lower eukaryotes, but none in prokaryotes. Maf1 proteins contain three phylogenetically conserved sequence regions, labeled A, B, and C (9). The similarity of the yeast and human Maf1 sequences is presented in Fig. 1, and more Maf1 proteins are aligned in supplemental Fig. S1. Because the distance between the B and C segments of ~10 aa is constant in evolution, with the exception of *Aspergillus nidulans* (insertion of 15 aa), we consider this region could be a single domain named here as BC. In contrast, the space between regions A and B largely varies between species. The A and BC domains are fused in *Encephalitozoon cuniculi* whereas in the yeast *S. cerevisiae* and *Candida glabrata* they are separated by a long linker of 182 and 174 aa, respectively. Within the BC domain signature sequences for the Maf1 protein family can be identified (PDYDFS and LWSFnYFFYNKklKR; supplemental Fig. S1) (9). These sequence "motifs" are not reported in the PROSITE database. Interestingly, in the majority of Maf1 orthologs, the second motif includes a nuclear targeting signal, which was proved to be functional in *S. cerevisiae* Maf1 (15).

To characterize the structure organization of human Maf1 (HsMaf1) experimentally, we carried out limited proteolysis experiments in combination with size exclusion chromatography as shown in Fig. 2. Proteolytically stable fragments are considered to be structurally well defined, whereas protease-sensitive sites often correlate with disordered regions of the proteins. Using limited proteolysis with trypsin, HsMaf1 protein (256 aa) was digested into two major stable fragments that were identified as HsMaf1(1–45) and Maf1(75–234) using a combination of N-terminal sequencing and mass spectrometry (quantitative time of flight). The HsMaf1 linker region between those fragments (aa 46–74) and the C-terminal acidic tail (aa 235–256)

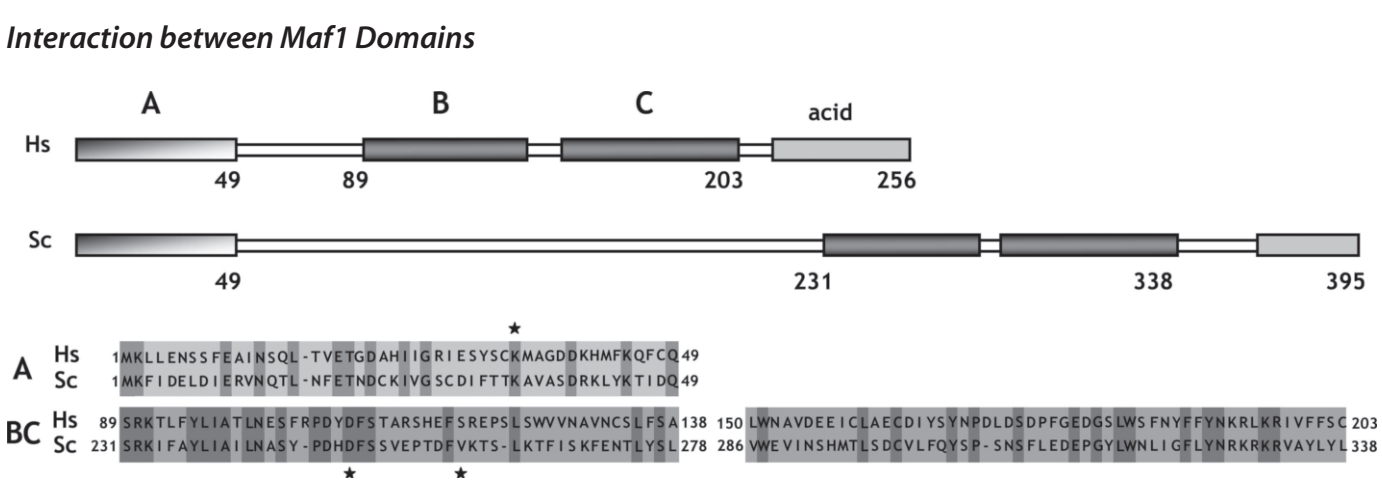

FIGURE 1. **Similarity of *S. cerevisiae* (*Sc*) and *H. sapiens* (*Hs*) Maf1 sequences.** Alignment of conserved A and BC domains is shown. A and BC domains are *boxed*, and conserved aa are *highlighted*. *Stars* indicate positions of K35E, D250E, and V260D mutations.

was degraded and thus presumably unstructured (Fig. 2*A*, *lane 2*). Both fragments were further analyzed by size exclusion chromatography. Surprisingly, the two HsMaf1 fragments, although of substantially different molecular masses, co-eluted in an apparent 1:1 stoichiometry, suggesting an intramolecular interaction between them (Fig. 2*B*, *red profile*).

Taking into account the limited proteolysis and secondary structure prediction results (data not shown), we designed N- and C-terminal constructs of HsMaf1 for co-expression in bacteria. The N-terminal construct aa 1–45 corresponds to the minimal domain defined by proteolysis whereas fragment encoding aa 85–210 was designed slightly shorter than the initial proteolytic fragment. During purification His tag-containing recombinant HsMaf1 fragment(1–45) but also slightly larger constructs (1–59), (1–63), and (1–74) co-precipitate the untagged C-terminal construct (85–210) in an apparent 1:1 stoichiometry, suggesting a direct interaction between the N- and C-terminal fragments (supplemental Fig. S2).

ZSI

Analysis by size exclusion chromatography supports the results obtained for the proteolytic fragments. Constructs(1–45) and (85–210) co-elute as a single peak at a volume corresponding to the expected molecular mass of ~20 kDa (Fig. 2*B*). These results provide further support for a direct interaction between A and BC domains of HsMaf1. Interestingly, the co-expressed complex is considerably more compact compared with the full-length protein, presumably because it is lacking the C-terminal acidic tail. In contrast, an additional construct of aa 82–236 that includes the C-terminal acidic tail eluted as soluble aggregate (Fig. 2*B*, *bottom panel*) when expressed in the absence of the N-terminal fragment of aa 1–45. We also tried to express the N-terminal fragment of aa 1–45 as GST fusion protein, but we only obtained minimal amounts presumably because the protein aggregates after tobacco etch virus cleavage (data not shown). Apparently, N- and C-terminal domains of HsMaf1 are both required for the soluble expression of HsMaf1 and co-elute during size exclusion chromatography, indicating a direct interaction between them.

To investigate whether the interaction between domains of Maf1 is conserved through evolution, we analyzed the proposed interaction in yeast, an organism more amenable to study structure-function relationships of Maf1 using the two-hybrid system. The putative BC domain of *S. cerevisiae* Maf1 (aa 196–349) was fused to the DNA-binding domain of Gal4 and co-expressed with various Maf1 A domain constructs fused to the Gal4 activation domain in the yeast reporter strain Y190. Interactions between fusion proteins should result in activation of the β-galactosidase reporter gene. Using this approach, we observed a physical interaction between the BC domain of Maf1 encoded by plasmid pAS2-Maf1-BC(196–349) and fragments of domain A of Maf1 encoded by plasmids pACT2-Maf1-A(1–42), pACT2-Maf1-A(1–39), and pACT2-Maf1-A(1–34) (Fig. 3). Domain BC failed to interact with shorter fragments of domain A encoded by pACT2-Maf1-A(1–12), pACT2-Maf1-A(1–16), or pACT2-Maf1-A(1–23). Cells containing the pair pAS2-Maf1-BC and empty pACT2 had no detectable β-galactosidase activity (data not shown in the figure). These results demonstrate the specificity of the two-hybrid interaction between Maf1 domains and define aa 1–34 as the smallest Maf1 A domain still able to bind the BC domain. Reciprocal interactions were impossible to study because the presence of pAS-Maf1-A activates the reporter gene in the absence of a pACT2 fusion. Importantly, pAS2-Maf1-BC was also negative tested with pACT2 encoding fusions of several genes unrelated to Maf1 and encoding components of pol III complex. Taken together, our results as described above suggest a strong, direct interaction of the A and BC domains of human and yeast Maf1.

F3

AQ: K

Interaction between A and BC Domains Is Important for the Function of Maf1—Limited proteolysis and two-hybrid results show that the A and BC domains of Maf1 together form a stable complex, possibly reflecting an active conformation of Maf1. To evaluate the physiological significance of the interaction between the Maf1 domains, we screened for mutants impaired in Maf1 function that were located in domain A and presumably compromised in domain BC binding. *MAF1* fragment(1–180) was PCR-amplified under mutagenic conditions and transformed into *maf1*-Δ cells together with a gapped single-copy plasmid encoding Maf1. Transformants were selected for poor growth at 37 °C on glycerol medium, suggesting a defect of Maf1 function in pol III repression (12). Sequencing of plasmid pAG70 encoding mutant Maf1 isolated in this manner revealed mutation K35E located in domain A.

To inspect the effect of the K35E mutation in Maf1 on pol III activity, RNA isolated from cells grown in the presence of glucose and transferred to glycerol medium at 37 °C was analyzed by Northern blotting using probes for pre-tRNA^{Leu} and

AQ: J

F4

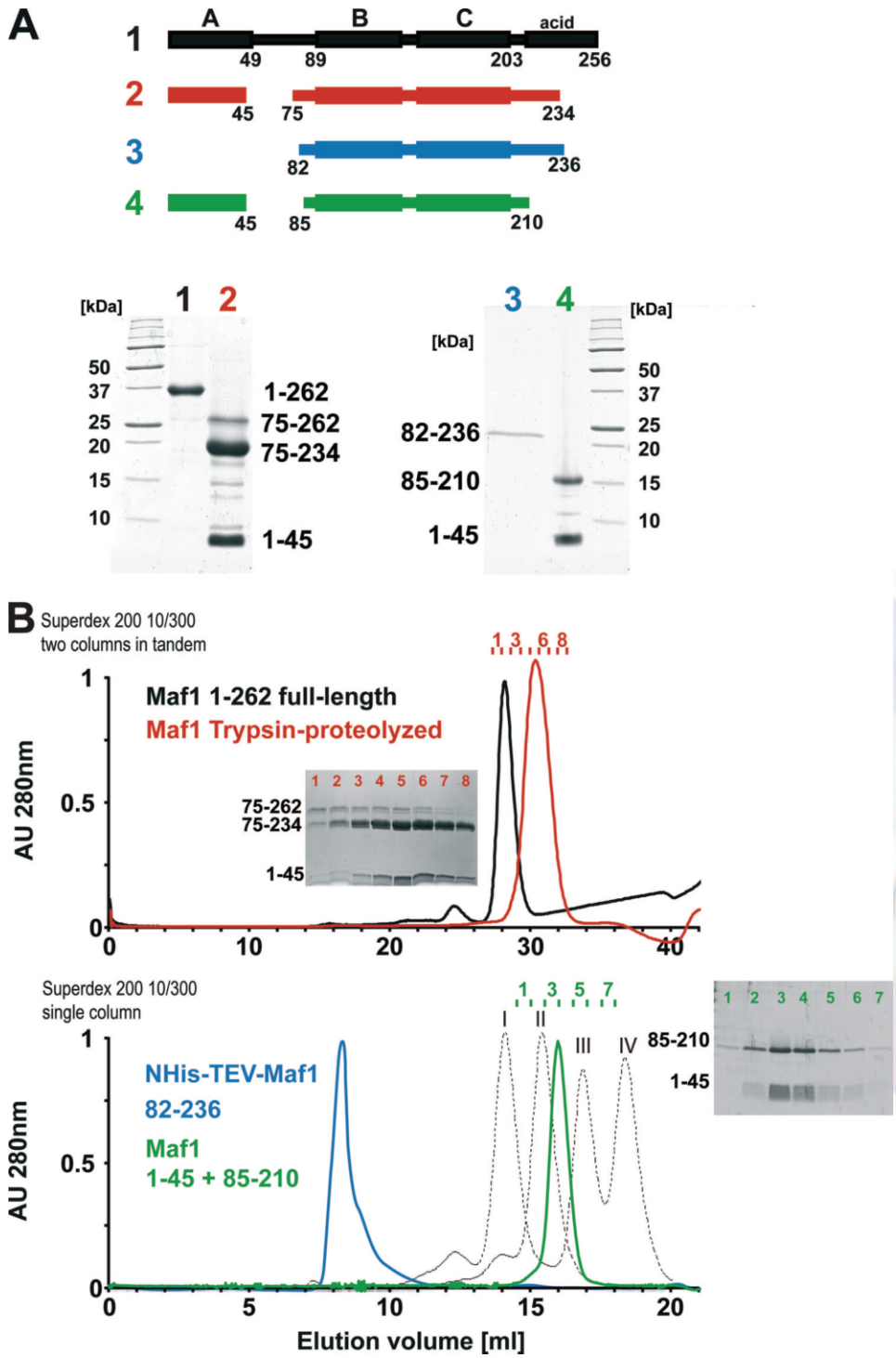

AQ: P

FIGURE 2. **Domain structure of human Maf1.** *A*, limited proteolysis and resulting proteolytic fragments of HsMaf1. PAGE of full-length human HsMaf1 protein (*1*, *black*) that is digested into two stable fragments(1–45) and (75–234) using trypsin are indicated as *2*, *red*. Bacterially co-expressed and co-purified HsMaf1 domains of aa 1–45 and 85–210 are shown as *4*, *green*. HsMaf1 aa 82–236 (*3*, *blue*) lacking the N-terminal 45 residues was expressed as a control. *B*, size exclusion chromatography profiles. Samples presented in *A* were separated on single or tandem Superdex 200 10/300 size exclusion columns (GE Healthcare). Only HsMaf1 construct 82–236 elutes in the void volume of the Superdex 200 size exclusion column, whereas all other samples are monodisperse and elute approximately at volumes corresponding to monomers. The elution profile of different molecular mass standards is shown as a *dashed line*. Peaks I, II, III, and IV correspond to ovalbumin (M_r = 44,000), carbonic anhydrase (M_r = 29,000), ribonuclease A (M_r = 13,700) and aprotinin (M_r = 6,500), respectively. Fractions corresponding to the *red* and *green* elution profiles were analyzed by denaturing gel electrophoresis and are shown as *insets*. Fragment(1–45) co-elutes with proteolytic fragments(75–234) and (75–262) (*red* profile) and with the recombinant fragment(85–210) (*green* profile).

tRNA^{Phe} (Fig. 4*A*). Following transfer to the medium with the nonfermentable carbon source, pre-tRNA levels were decreased in the wild type but not in *maf1*-Δ cells (Fig. 4*A*, compare *lanes 1*, *5* and *6*, *10*). Similarly to *maf1*-Δ, the K35E mutant was defective in its ability to repress pre-tRNA transcription upon transfer to glycerol medium (Fig. 4*A*, *lanes 2* and I7). Thus, the single missense mutation within the Maf1 A domain precluded pol III repression in *maf1*-K35E strain.

One approach to confirm that the K35E mutation negatively affects the interaction with the BC domain of Maf1 is to identify second-site mutations that compensate for the observed defects. We looked therefore for second-site suppressor mutations within the BC-encoding region of *MAF1* that allowed *maf1* K35E yeast cells to grow on glycerol medium at 37 °C. DNA encoding aa 174–375 of Maf1 was randomly mutagenized by PCR, and the mutant pool was co-transformed with the pAG70 plasmid containing the primary K35E mutation and gapped within the region of the BC domain. Sequencing of *in vivo* reconstituted *MAF1* from six transformants showing reversion of the original defect identified two plasmids with suppressor mutations: pLM11 (*maf1*-K35E/D250E) and pLM12 (*maf1*-K35E/V260D,N344I). The remaining transformants were either back-revertants of K35E mutation or contained suppressor mutations outside the *MAF1* gene. Both isolated suppressors of K35E mutation in A domain, single D250E, and combined V260D/N344I were located in the BC domain, thus supporting the interaction between these domains.

Phenotypic characterization of the two suppressor strains showed that they compensate for the defect of growth on glycerol medium at 37 °C of the primary K35E mutation (Fig. 4*B*). The increased growth capacity of the suppressors on glycerol medium was due to a compensation of the defect in pol III regulation observed for the K35E

COLOR

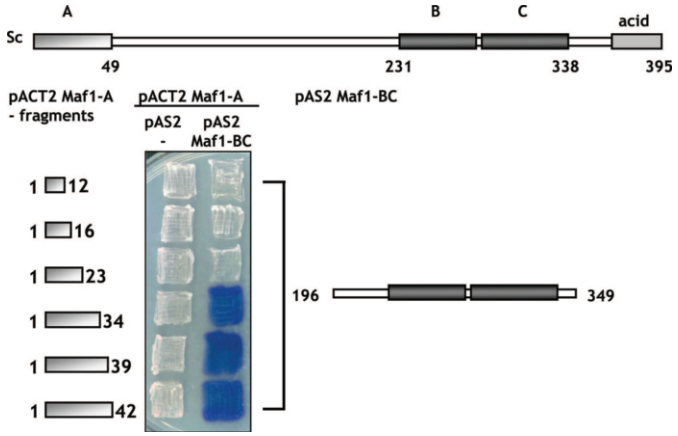

FIGURE 3. **Two-hybrid interaction of Maf1 domains.** pACT2-Maf1-A(1–12), pACT2-Maf1-A(1–16), pACT2-Maf1-A(1–23), pACT2-Maf1-A(1–34), pACT2-Maf1-A(1–39), and pACT2-Maf1-A(1–42) plasmids were transformed individually together with pAS2 (control plasmid) or pAS2-Maf1-BC(196–349) plasmids into yeast strain Y190. Transformants were assayed for β-galactosidase expression using an overlay plate assay.

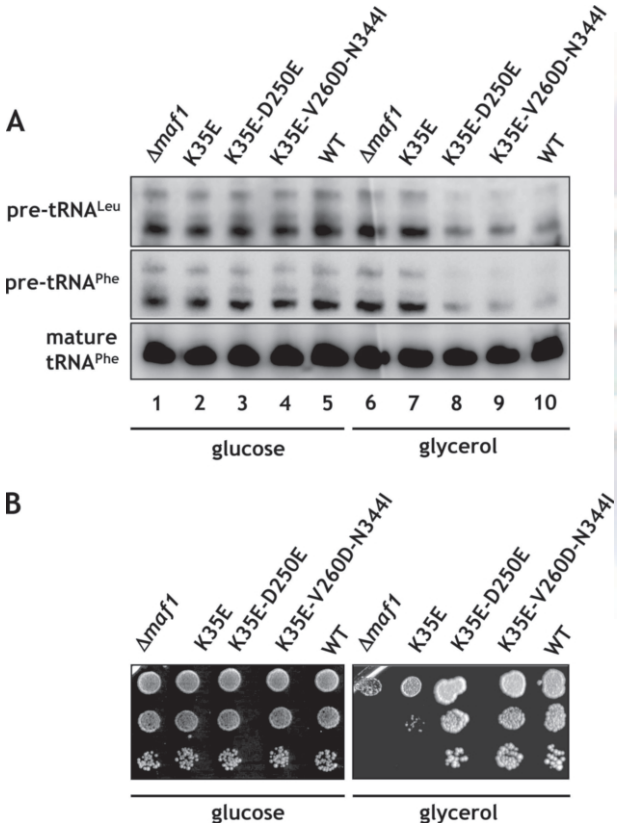

FIGURE 4. **Regulation of pol III transcription and growth is impaired by the K35E mutation in region encoding A domain and restored by second-site suppressor mutations in BC domain of *MAF1*.** *maf1*-Δ, *maf1*-K35E, *maf1*-K35E/D250E, and *maf1*-K35E/V260D/N344I mutants and isogenic wild type strain YPH500 (*WT*) were used. *A*, cells were grown to exponential phase in glucose medium (YPD) at 30 °C, then transferred to glycerol medium (YPGly) and incubated at 37 °C for 1.5 h. Total RNA isolated from cells was tested by Northern blotting with pre-tRNA^{Leu} and tRNA^{Phe} probes. *B*, 10-fold serial dilutions of cells grown to exponential phase in glucose medium were plated on glucose medium (YPD) and incubated at 30 °C or on glycerol medium (YPGly) and incubated at 37 °C for 2–3 days.

mutation. As determined by Northern blotting, the suppressor mutations restored the ability to repress pre-tRNA transcription upon transfer from glucose to glycerol medium (Fig. 4*A*,

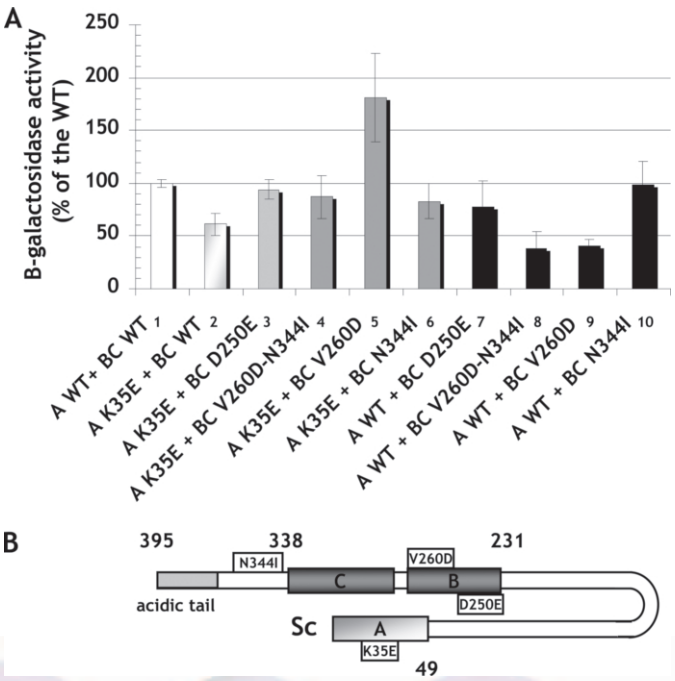

FIGURE 5. **Two-hybrid interaction of Maf1 domains is impaired by primary mutations in these domains and restored by second-site suppressor mutations.** *A*, pACT2-Maf1-A(1–42) plasmid and its mutated version were transformed individually with pAS2-Maf1-BC(196–349) plasmid or its mutated versions in yeast strain Y190. Transformants were assayed for β-galactosidase expression. Presented profile compares following two-hybrid interactions: wild type A and BC domains of Maf1 (*1*); mutated A domain K35E with wild type BC domain (*2*); mutated A domain K35E with four versions of mutated BC domain: D250E (*3*), V260D/N344I (*4*), V260D (*5*), N344I (*6*); and wild type A domain with mutated BC domain containing single D250E, V260D, or N344I and double N344I/V260D mutations (*7-10*). *B*, scheme of Maf1 domain interaction is shown.

lanes 3, *4*, *8*, and *9*). These results indicate that the detected genetic interaction between the two Maf1 domains is a functional one.

To characterize the association of A and BC domains further, we sought to verify the effects of K35E, D250E, V260D, and N344I mutations, identified in the mutant and suppressor strains, on the interaction of Maf1 domains in the two-hybrid system. The respective mutations were generated in the Maf1 A domain fragment fused to the Gal4 activation domain in the pACT2-Maf1-A(1–42) plasmid or the Maf1-BC domain fused to the DNA-binding domain of Gal4 in pAS2-Maf1-BC(196–349). Various combinations of plasmids, one encoding a wild type Maf1 domain and the other with a mutated domain, both fused to the respective Gal domains, were co-expressed in the yeast reporter strain followed by determination of β-galactosidase activity (Fig. 5). The K35E mutation of domain A reduced the two-hybrid interaction with wild type BC domain by approximately 40% (Fig. 5, compare *lanes 2* and *1*). Similarly, both the single D250E and the double V260D/N344I mutations in BC domain decreased the interaction with wild type A domain by 22 and 62%, respectively (Fig. 5, compare *lanes 7* and *8* with *lane 1*). Moreover, the double V260D/N344I mutant showed a defect in regulation of tRNA transcription and temperature-sensitive growth in glycerol medium (supplemental Fig. S3).

F5

ZSI

balt3/zbc-bc/zbc-bc/zbc04810/zbc3762-10z ZSUBMIT 17 xppws S=1 22/9/10 7:23 4/Color Figure(s) F2,3 ARTNO: M110.125286

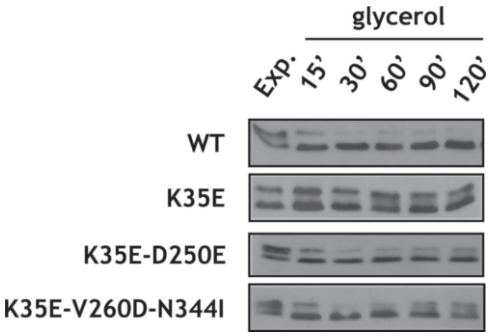

FIGURE 6. **Mutations altering interaction of Maf1 domains affect kinetics of Maf1 dephosphorylation upon transfer of yeast from glucose to medium with nonfermentable carbon source.** *maf1*-K35E, *maf1*-K35E/D250E, and *maf1*-K35E/V260D/N344I mutant strains and isogenic wild type strain YPH500 (*WT*) were grown to exponential phase in YPD glucose medium (*Exp*), then transferred to glycerol YPGly medium, incubated at 37 °C, and harvested as indicated. Protein extracts of lysed cells were analyzed by Western blotting with polyclonal anti-Maf1 antibodies.

Confirming the genetic suppressor results, a combination of mutated Maf1 domains restored their interaction (Fig. 5, compare *lanes 3* and *4* with *lane 1*). Rather unexpectedly, the strongest level of two-hybrid interaction, 80% over the wild type one, was observed for the combination of K35E domain A and domain BC with a single V260D mutation (Fig. 5, compare *lane 5* with *lane 1*). This indicated that in the double suppressor mutation V260D/N344I, identified in genetic screen, the former one is in fact sufficient to restore the interaction with K35E domain A.

Domain Interaction Supports Maf1 Dephosphorylation upon Transfer of Cells to a Nonfermentable Source—As shown before, phosphorylation of Maf1 precluded pol III repression when yeast cells were grown on glucose medium (14). Transfer of yeast cells to a nonfermentable carbon source resulted in Maf1 dephosphorylation, import of Maf1 into the nucleus, and inhibition of tRNA synthesis (12). Because we showed that the interaction between the Maf1 A and BC domains is crucial for its regulatory action on pol III, we now asked whether this interaction is also required for efficient regulation of Maf1 activity.

To investigate whether the altered domain interactions in the Maf1 mutant proteins were correlated with changes in the phosphorylation of Maf1, differentially phosphorylated forms of Maf1 were resolved by SDS-PAGE and identified by immunoblotting at various times after culture transfer from glucose to glycerol medium (Fig. 6). As reported previously, wild type Maf1 was quickly dephosphorylated upon this transition. Remarkably, the K35E mutation in domain A, preventing its interaction with the BC domain, appeared to preclude the dephosphorylation of Maf1. Significantly, restoring the domain interaction with D250E (pLM11) and V260D/N344I (pLM12) suppressor mutations reestablished rapid dephosphorylation of Maf1 following transfer from glucose to a nonfermentable carbon source. Maf1 dephosphorylation in the suppressor mutants was only a little slower than in the wild type strain (supplemental Table S1). Interestingly, double V260D/N344I mutation in the context of wild type A domain precluded interaction between domains (Fig. 5) and slowed the rate of dephosphorylation of Maf1 upon transfer of yeast to glycerol medium (supplemental Fig. S4). Altogether, these results suggest that the interaction of A and BC domain greatly facilitates the dephosphorylation of Maf1.

DISCUSSION

In this paper we describe the importance of the interaction between two Maf1 domains for its activity as a repressor of pol III transcription. Limited proteolysis of HsMaf1 resulted in two stable fragments(1–45) and (75–234) corresponding to the evolutionarily conserved A and BC domains. Size exclusion chromatography of the proteolytic fragments corresponding to the two domains showed their co-elution. Similar fragments were co-expressed in bacteria, where they co-purified and co-migrated during size exclusion chromatography as a soluble complex. In contrast, both fragments behaved poorly when individually expressed. Our results suggest that Maf1 A and BC domains form modules that do not fold independently but rather need to be co-expressed to form a stable and soluble entity. In contrast, the connecting linker (aa 46–74) and the C-terminal acidic tail (aa 235–256) appear solvent-exposed and unstructured as suggested by hydrophobic cluster analysis (supplemental Fig. S6).

Considering the high conservation of Maf1 in eukaryotes, the domain interaction and its functional role were probed in the model organism yeast *S. cerevisiae*. Using the yeast two-hybrid system we confirmed the physical interaction between A and BC domains of Maf1 in yeast and identified the first 34 residues as the shortest fragment of the A domain sufficient for interaction with the BC domain. Lack of interaction between further truncated fragments of the A domain (aa 1–12, 1–16 or 1–23) with the BC domain shows the specificity of the method used and emphasizes the importance of structural features of the A domain for its interaction with the BC domain.

To investigate further the role of domain A we isolated single-point mutant K35E (on plasmid pAG70). In accordance with its growth characteristics, this mutant failed to repress pol III activity. Moreover, as shown by the two-hybrid system, the K35E mutation reduced the interaction between the A and BC Maf1 domains by 40%. In support of structural and/or functional interactions between the Maf1 domains, we isolated second-site suppressor mutations within the BC domain that compensated for the defect caused by the K35E mutation in domain A. We found two such suppressors: D250E and V260D/N344I. Further phenotypic characterization of the suppressor strains revealed that these additional mutations in the BC domain restored not only the ability of the K35E-mutated Maf1 to grow on glycerol medium at 37 °C, but also its ability to repress pol III activity. Interestingly, residue 260 in domain BC seems to be crucial for the interaction with domain A. Although the V260D mutant BC domain interacted with K35E mutant domain A >80% stronger than did wild type domain BC, its interaction with the wild type domain A was decreased by almost 60% (Fig. 5, *fifth and ninth lanes*). All of these results indicated that the genetic interaction identified between Maf1 domains corresponds to a physical interaction indispensable for the Maf1 function.

Bioinformatic analysis using the protein structure prediction server (PSIPRED version 2.6) (36, 37) provides further support for our biochemical analysis. In the yeast and human Maf1 A

domain, two α-helices (aa 7–16 and 40–56) separated by two adjacent β-strands (aa 24–27 and 29–35) are predicted, whereas for the BC domain five α-helices and concomitant four β-strands are predicted (supplemental Fig. S5). No secondary structure elements are predicted for the linker region. Notably, the K35E mutation is located at the end of the second β-strand of the A domain. Our attempts to minimize the Maf1 A domain identified aa 1–34 as the smallest fragment still enabling interaction with the domains. We hypothesize that the interaction between domains A and BC requires the first α-helix and two adjacent β-strands. We also applied hydrophobic cluster analysis, a tool to investigate protein stability and folding that uses two-dimensional helical representation of protein sequences to identify possible hydrophobic cores formed by several residues (38). The hydrophobic cluster analysis revealed the presence of two regions rich in hydrophobic cores corresponding to the A and BC domains of *S. cerevisiae* Maf1 (supplemental Fig. S6). Between them a region poor in hydrophobic residues was found which, according to the alignment of Maf1 eukaryotic sequences, corresponds to the linker region between the A and BC domains. Similar analysis in human Maf1 revealed the same organization of two clusters of hydrophobic cores separated by a short region free of hydrophobic clusters consistent with our limited proteolysis results.

We found the interaction between the A and BC domains, facilitating Maf1 dephosphorylation, to be necessary for the full repression of pol III activity. One might hypothesize that in the same time the interaction between domains of Maf1 is influenced by its phosphorylation state. Accordingly, different forms of Maf1 observed on polyacrylamide gels, interpreted as phosphorylated and subsequently dephosphorylated form of Maf1, might represent different conformational states depending on the interaction between A and BC domains. Note that the S90A, S101A, and S177A/S178A mutations in the linker were found to change the proportion between slow and fast migrating Maf1 forms in favor of the former, without strongly affecting the phosphorylation status of Maf1, thus indicating that residues in the linker could strongly modify the Maf1 shape (39).

Considering that Maf1 contains two conserved domains, we propose the unstructured linker to become phosphorylated and thus modulating the conformational state of Maf1. To investigate this question further we used the NetPhos 2.0 server (40) to predict possible phosphorylation sites in four Maf1 orthologs containing linkers of different lengths. Predicted phosphorylation sites are frequently found in the long linkers between the Maf1 A and BC domains of *S. cerevisiae* and *C. glabrata* relatively, whereas they are more uniformly distributed along the Maf1 sequences of *Caenorhabditis elegans* and *Homo sapiens*, although they are also present in their shorter linkers (supplemental Fig. S7). We therefore speculate that phosphorylation and dephosphorylation of the exposed linker evoke a specific conformation of the protein that changes the distance between domains modulating their interaction and pol III repression (supplemental Fig. S8). The interaction of the domains, mediated by dephosphorylation of the linker may affect both the import of Maf1 into the nucleus and its interaction with pol III. This conjecture is supported by data of Ref. 15, showing that PKA-mediated phosphorylation of six residues located in linker inhibited nuclear import of Maf1 and pol III repression.

Acknowledgments—Mass spectrum analysis was carried out at the Proteomics Core Facility at EMBL Heidelberg. We are grateful to Andre Sentenac, Joël Acker, Christine Conesa, Danuta Oficjalska-Pham, Raphaël Guerois, and Isabelle Callebaut for stimulating discussions. We also thank Gudrun von Scheven for technical assistance.

REFERENCES

1. Willis, I. M., Desai, N., and Upadhya, R. (2004) *Prog. Nucleic Acids Res. Mol. Biol.* **77,** 323–353
2. Warner, J. R. (1999) *Trends Biochem. Sci.* **24,** 437–440
3. Warner, J. R., Vilardell, J., and Sohn, J. H. (2001) *Cold Spring Harbor Symp. Quant. Biol.* **66,** 567–574
4. Harismendy, O., Gendrel, C. G., Soularue, P., Gidrol, X., Sentenac, A., Werner, M., and Lefebvre, O. (2003) *EMBO J.* **22,** 4738–4747
5. Roberts, D. N., Stewart, A. J., Huff, J. T., and Cairns, B. R. (2003) *Proc. Natl. Acad. Sci. U.S.A.* **100,** 14695–14700
6. Moqtaderi, Z., and Struhl, K. (2004) *Mol. Cell. Biol.* **24,** 4118–4127
7. Geiduschek, E. P., and Kassavetis, G. A. (2001) *J. Mol. Biol.* **310,** 1–26
8. Upadhya, R., Lee, J., and Willis, I. M. (2002) *Mol. Cell* **10,** 1489–1494
9. Pluta, K., Lefebvre, O., Martin, N. C., Smagowicz, W. J., Stanford, D. R., Ellis, S. R., Hopper, A. K., Sentenac, A., and Boguta, M. (2001) *Mol. Cell. Biol.* **21,** 5031–5040
10. Boisnard, S., Lagniel, G., Garmendia-Torres, C., Molin, M., Boy-Marcotte, E., Jacquet, M., Toledano, M. B., Labarre, J., and Chédin, S. (2009) *Eukaryot. Cell* **8,** 1429–1438
11. Desai, N., Lee, J., Upadhya, R., Chu, Y., Moir, R. D., and Willis, I. M. (2005) *J. Biol. Chem.* **280,** 6455–6462
12. Cieœla, M., Towpik, J., Graczyk, D., Oficjalska-Pham, D., Harismendy, O., Suleau, A., Balicki, K., Conesa, C., Lefebvre, O., and Boguta, M. (2007) *Mol. Cell. Biol.* **27,** 7693–7702
13. Oficjalska-Pham, D., Harismendy, O., Smagowicz, W. J., Gonzalez de Peredo, A., Boguta, M., Sentenac, A., and Lefebvre, O. (2006) *Mol. Cell* **22,** 623–632
14. Towpik, J., Graczyk, D., Gajda, A., Lefebvre, O., and Boguta, M. (2008) *J. Biol. Chem.* **283,** 17168–17174
15. Moir, R. D., Lee, J., Haeusler, R. A., Desai, N., Engelke, D. R., and Willis, I. M. (2006) *Proc. Natl. Acad. Sci. U.S.A.* **103,** 15044–15049
16. Roberts, D. N., Wilson, B., Huff, J. T., Stewart, A. J., and Cairns, B. R. (2006) *Mol. Cell* **22,** 633–644
17. Schramm, L., and Hernandez, N. (2002) *Genes Dev.* **16,** 2593–2620
18. Marshall, L. (2008) *Cell Cycle* **7,** 3327–3329
19. Marshall, L., Kenneth, N. S., and White, R. J. (2008) *Cell* **133,** 78–89
20. Marshall, L., and White, R. J. (2008) *Nat. Rev. Cancer* **8,** 911–914
21. Johnson, S. A., Dubeau, L., and Johnson, D. L. (2008) *J. Biol. Chem.* **283,** 19184–19191
22. White, R. J. (2008) *Trends Genet.* **24,** 622–629
23. Goodfellow, S. J., Graham, E. L., Kantidakis, T., Marshall, L., Coppins, B. A., Oficjalska-Pham, D., Gérard, M., Lefebvre, O., and White, R. J. (2008) *J. Mol. Biol.* **378,** 481–491
24. Reina, J. H., Azzouz, T. N., and Hernandez, N. (2006) *PLoS ONE* **1,** e134
25. Johnson, S. S., Zhang, C., Fromm, J., Willis, I. M., and Johnson, D. L. (2007) *Mol. Cell* **26,** 367–379
26. Rollins, J., Veras, I., Cabarcas, S., Willis, I., and Schramm, L. (2007) *Int. J. Biol. Sci.* **3,** 292–302
27. Huber, A., Bodenmiller, B., Uotila, A., Stahl, M., Wanka, S., Gerrits, B., Aebersold, R., and Loewith, R. (2009) *Genes Dev.* **23,** 1929–1943
28. Harper, J. W., Adami, G. R., Wei, N., Keyomarsi, K., and Elledge, S. J. (1993) *Cell* **75,** 805–816
29. Sherman, F. (2002) *Methods Enzymol.* **350,** 3–41
30. Werner, M., Chaussivert, N., Willis, I. M., and Sentenac, A. (1993) *J. Biol. Chem.* **268,** 20721–20724
31. Manaud, N., Arrebola, R., Buffin-Meyer, B., Lefebvre, O., Voss, H., Riva,

balt3/zbc-bc/zbc-bc/zbc04810/zbc3762-10z ZSUBMIT 17 xppws S=1 22/9/10 7:23 **4/Color Figure(s) F2,3** ARTNO: M110.125286

M., Conesa, C., and Sentenac, A. (1998) *Mol. Cell. Biol.* **18,** 3191–3200
32. Boguta, M., Czerska, K., and Zoładek, T. (1997) *Gene* **185,** 291–296
33. Sikorski, R. S., and Hieter, P. (1989) *Genetics* **122,** 19–27
34. Muhlrad, D., Hunter, R., and Parker, R. (1992) *Yeast* **8,** 79–82
35. Schmitt, M. E., Brown, T. A., and Trumpower, B. L. (1990) *Nucleic Acids Res.* **18,** 3091–3092
36. Jones, D. T. (1999) *J. Mol. Biol.* **292,** 195–202
37. Bryson, K., McGuffin, L. J., Marsden, R. L., Ward, J. J., Sodhi, J. S., and Jones, D. T. (2005) *Nucleic Acids Res.* **33,** W36–W38
38. Callebaut, I., Labesse, G., Durand, P., Poupon, A., Canard, L., Chomilier, J., Henrissat, B., and Mornon, J. P. (1997) *Cell Mol. Life Sci.* **53,** 621–645
39. Lee, J., Moir, R. D., and Willis, I. M. (2009) *J. Biol. Chem.* **284,** 12604–12608
40. Blom, N., Gammeltoft, S., and Brunak, S. (1999) *J. Mol. Biol.* **294,** 1351–1362
41. Edgar, R. C. (2004) *Nucleic Acids Res.* **32,** 1792–1797

AQ: O

2. Résumé substantiel en Français.

- **INTRODUCTION**

Dans les cellules eucaryotes, les ARN polymérases (Pol) I et III sont responsables de la synthèse d'ARN impliqués dans la biogenèse des ribosomes et dans le processus de traduction. La synthèse d'ARN par la Pol I et la Pol III représente plus de 80% de l'activité de transcription nucléaire chez la levure *Saccharomyces cerevisiae* et est contrôlée de manière coordonnée en réponse à diverses conditions cellulaires et de l'environnement (Willis *et al.,* 2004; Warner, 1999; Warner *et al.,* 2001).

Chez la levure, la Pol III est responsable de la transcription d'environ 400 gènes (gènes de classe III), codant pour la plupart les ARNt et l'ARNr 5S (Harismendy *et al.,* 2003; Roberts *et al.,* 2003; Moqtaderi and Struhl, 2004). L'analyse du système de transcription de la Pol III chez la levure a révélé une série d'interactions protéine-ADN et protéine-protéine conduisant au recrutement de la Pol III sur les gènes cibles codant les ARNt. Dans un premier temps, le facteur de transcription TFIIIC (six sous-unités) se lie au promoteur intragénique puis dirige le recrutement et l'assemblage des trois composants de TFIIIB (TBP, Brf1 et Bdp1) et le recrutement ultérieur de l'enzyme Pol III constitué de dix-sept sous-unités (Geiduschek and Kassaventis, 2001). Bien que les facteurs essentiels et les mécanismes de base de la transcription des gènes de classe III soient maintenant bien définis, les mécanismes moléculaires permettant la régulation de la Pol III sont encore mal connus.

L'unique régulateur global négatif de la transcription par la Pol III chez la levure est la protéine Maf1 qui sert d'intermédiaire dans plusieurs voies de signalisation mais qui n'est pas indispensable à la survie cellulaire (Upadhya *et al.,* 2002; Pluta *et al.,* 2001). Maf1 est requis pour permettre l'inhibition de la transcription qui se produit normalement pendant la phase de croissance stationnaire mais aussi en réponse à diverses drogues induisant des dommages de l'ADN, un stress oxydatif, des défauts de la voie sécrétoire ou encore lors de la phase de croissance post-diauxique (Upadhya *et al.,* 2002; Boisnard *et al.,* 2009; Desai *et al.,* 2005; Ciesla *et al.,* 2007). L'activité de Maf1 est liée à sa phosphorylation lors de conditions favorables de croissance. Seule la forme déphosphorylée de Maf1 peut se lier à la Pol III (Oficjalska-Pham *et al.,* 2006). Cette phosphorylation est observée lorsque la protéine Maf1 est re-localisée du noyau vers le cytoplasme (Towpik *et al.,* 2008) et semble empêcher l'importation de Maf1 du cytoplasme vers le noyau (Moir *et al.,* 2006). Diverses conditions défavorables conduisent à la déphosphorylation rapide

de Maf1, à son accumulation dans le noyau ainsi qu'à l'association physique de la forme déphosphorylée de Maf1 avec la Pol III et à l'ensemble du génome transcrit par la PoI III (Oficjalska-Pham *et al.,* 2006; Roberts *et al.,* 2006).

La machinerie de la transcription par la Pol III est remarquablement conservée entre la levure et l'homme. Les composants les plus conservés sont ceux impliqués dans l'assemblage complexe de transcription: la sous-unité τ131 de TFIIIC et deux composantes de TFIIIB (TBP et Brf1). Les cinq sous-unités spécifiques de la Pol III chez la levure *S. cerevisiae* (C31, C34, C37, C53 et C82) ont tous des homologues structurels et fonctionnels dans les cellules humaines (Schramm and Hernandez, 2002). Maf1 est aussi conservée chez tous les organismes eucaryotes de la levure à l'homme (Pluta *et al.,* 2001). Cette conservation est très intéressante car la dérégulation de la transcription par la Pol III chez l'homme est liée à la transformation maligne. De plus, une activation excessive de la transcription par la Pol III peut générer des tumeurs (Marshall, 2008; Marshall *et al.,* 2008; Marshall and White, 2008; Johnson *et al.,* 2008). Enfin chez les mammifères, deux suppresseurs de tumeurs, Rb et p53, agissent comme des répresseurs globaux de la transcription par la Pol III (White, 2008). Des résultats récents de plusieurs groupes rapportent que Maf1 est aussi un régulateur de la transcription par la Pol III chez l'homme (Goodfellow *et al.,* 2008; Reina *et al.,* 2006; Johnson *et al.,* 2007; Rollins *et al.,* 2007). L'implication de la protéine Maf1 humaine dans le contrôle aberrant de la transcription par la Pol III dans les cellules cancéreuses reste à étudier. Néanmoins, la conservation de la machinerie de la Pol III (dont fait partie Maf1) lors de l'évolution indique que l'étude d'organisme modèle tel que la levure devrait donner des informations quant au rôle de la protéine Maf1 humaine dans le cancer

- **BUT DE CE TRAVAIL**

Mon travail de thèse consiste à étudier la relation entre la structure et la fonction de Maf1. Tous les membres de la famille Maf1 comportent trois domaines protéiques (nommées A, B et C) assez bien conservés au cours de l'évolution (Pluta *et al.,* 2001) et ne montrant cependant aucune homologie significative avec des domaines protéiques de fonction connue. Nous ne disposons pas actuellement d'information sur la fonction de ces régions. Des mutations ponctuelles ont seulement soulignées l'importance de plusieurs résidus sérine (qui ne sont pas phylogénétiquement conservés) et de deux séquences de localisation nucléaire (Moir *et al.,* 2006; Roberts *et al.,* 2006; Huber *et al.,* 2009). Au cours de mon travail de

thèse, j'ai pu identifier chez *S. cerevisiae* deux domaines de la protéine Maf1 qui sont conservés et qui interagissent entre eux. Cette interaction est cruciale pour la régulation de l'activité de Maf1 par phosphorylation. Les données présentées dans cette étude fournissent un premier aperçu de la structure Maf1 par rapport à la régulation de la Pol III.

- **RESULTATS**

1. Construction de mutations de la protéine Maf1 de *S. cerevisiae* au niveau des régions A et BC conservés au cours de l'évolution.

Une approche habituelle pour analyser la relation entre la séquence primaire d'une protéine et son activité est de construire plusieurs mutants dans le gène codant cette protéine et d'étudier son changement de comportement cellulaire en fonction de la mutation effectuée. Le gène *MAF1* a été muté pour isoler des mutants définis et localisés dans chaque domaine particulier afin d'acquérir une meilleure compréhension des fonctions de Maf1 dans la cellule de levure *S. cerevisiae*. Les mutants *maf1* qui ont été obtenus ont été caractérisés dans un premier temps pour définir les substitutions d'acides aminés et le phénotype de croissance. La méthode rapide de mutagenèse localisée du « Gap repair » a été utilisée pour obtenir une banque de protéines Maf1 mutées dans les domaines A, B et C qui sont conservés au cours de l'évolution (Muhlrad *et al.,* 1992). La stratégie de construction des mutants est basée sur une PCR basse fidélité. L'ADN codant le domaine A et un domaine non structuré (aa 1-180) ou le domaine B et C (aa 174-375) a été amplifié dans des conditions permettant d'obtenir 1 à 2 mutations dans ces régions. Les produits des PCR réalisées en condition de « faible fidélité » sont ensuite co-transformés dans une souche *maf1*-Δ avec un plasmide linéarisé ne contenant que les régions flanquantes du domaine A ou du domaine B et C. La recombinaison *in vivo* et la sélection sur un milieu permettant la croissance grâce au marqueur d'auxotrophie porté par le plasmide permet d'obtenir un gène *maf1* complet mais muté. Un phénotype de croissance thermosensible sur milieu contenant du glycérol (phénotype caractéristique des souches *maf1* mutées ; Boguta *et al.,* 1997) indique que la protéine Maf1 est soit absente soit non fonctionnelle et donc incapable de réprimer la transcription par la Pol III. L'identification de ces mutants a été confirmée par re-transformation des plasmides purifiés dans une souche dont le gène *maf1* été supprimé (YPH500 *maf1*-Δ). Le séquençage des plasmides a ensuite permis d'identifier les différentes mutations isolées. Des expériences de Western

blot utilisant des anticorps polyclonaux anti-Maf1 ont permis de tester l'expression de la protéine Maf1 dans les différentes souches mutantes.

La perturbation de cette répression peut correspondre à plusieurs déficiences de l'activité de Maf1 tels des problèmes d'expression, d'état de phosphorylation, de transport du cytoplasme vers le noyau ou d'interaction avec la Pol III.

L'analyse des positions des mutations parmi les allèles *maf1* n'a pas permis d'identifier une région de Maf1 plus particulièrement indispensable à l'activité de Maf1 en tant que répresseur de la transcription par la Pol III.

Plusieurs mutants *maf1*, représentatifs de mutations de différentes régions de Maf1 et de phénotypes de croissance différents, ont fait l'objet d'une étude plus approfondie. Une attention plus particulière a été portée sur des mutations du domaine BC car ce domaine est le plus conservé au cours de l'évolution en comparaison avec le domaine A et pourrait donc être plus crucial pour l'activité de Maf1. De plus les mutations dans le domaine BC semblent avoir plus particulièrement un effet sur le niveau de synthèse de la protéine Maf1 ou sur sa dégradation comme le montre le profile d'expression des mutants *maf1* L242P-H249Q (pAG147), S305P-N327D-N344D (pAG148), N243S-F267S (pAG167), N327Y-I339T-S341P (pAG127), M294R-L354S (pAG136), I241F-R332G (pML6), E272L-C299R-Q359L (pMM2) et L242S-L325P-Y326F-L354S-L363Q (pMM1) *maf1* mutants. De plus, ces mutants *maf1* présentent différents profils de phosphorylation tout en gardant la capacité de pouvoir être déphosphorylé sur milieu contenant du glycérol. Un examen plus minutieux de ces mutants a montré que des défauts dans la phosphorylation et la déphosphorylation ne sont pas liés plus particulièrement à certaines mutations du domaine BC. Les modifications des acides aminés suite aux mutations introduites changent vraisemblablement la spécificité des très nombreux sites de phosphorylation de Maf1 comme l'a montré une analyse informatique. Différents profils de phosphorylation définissant des classes ont pu être mis en évidence par électrophorèse en conditions dénaturantes. Ces classes pourraient correspondrent à certains changements de la structure de Maf1 en fonction du niveau de phosphorylation de cette protéine. Aucune corrélation n'a pu être mise en évidence entre la capacité de Maf1 d'être phosphorylée ou déphosphorylée (respectivement en absence ou en présence de rapamycine) et une localisation cellulaire plus particulière de cette protéine (nucléaire ou cytoplasmique). Les autres mécanismes moléculaires impliquant Maf1 (interaction avec la Pol III, inhibition de la transcription par la Pol III, la sortie du noyau après élimination de la rapamycine, etc) devront êtres étudiés dans le futur

pour essayer d'identifier s'il y a une relation entre un profil de phosphorylation et une fonction de Maf1.

2. La répression complète de la transcription par l'ARN polymérase III exige une interaction entre deux domaines de son régulateur négatif Maf1.

- **Deux domaines de Maf1 interagissent entre eux physiquement**

Le gène *MAF1* de la levure *S. cerevisiae* code une protéine de 395 acides aminés hydrophile et riche en résidus serine et asparagine. La masse moléculaire théorique est de 44,7 kDa. L'analyse des bases de données indique qu'il y a des orthologues chez tous les eucaryotes dont l'homme, les animaux (50), les plantes (28) et même les eucaryotes dit « inférieurs » mais pas chez les procaryotes (voir la Figure 2 pour quelques exemples). Les protéines Maf1 sont constituées de trois régions phylogénétiquement conservées et appelées A, B et C (Pluta *et al.*, 2001). Les similarités de séquence entre *S. cerevisiae* et l'homme sont présentées dans la Figure 1. La Figure 2 présente un alignement de plusieurs séquences de protéine Maf1 différentes.

Comme la distance de 10 acides aminés qui sépare les domaines B et C est est constante au cours de l'évolution, à l'exception d'*Aspergilus nidulans* (insertion of 15 acides aminés), nous considérons que cette région est un domaine unique que nous avons appelé BC. Par contre, la distance entre les régions A et B varie largement selon les espèces. Les domaines A et BC sont fusionnés chez *Encephalitozoon cuniculi* mais séparés de 182 et 174 acides aminés (séquence « linker ») respectivement chez *S. cerevisiae* et *Candida glabrata* (Figure 2).

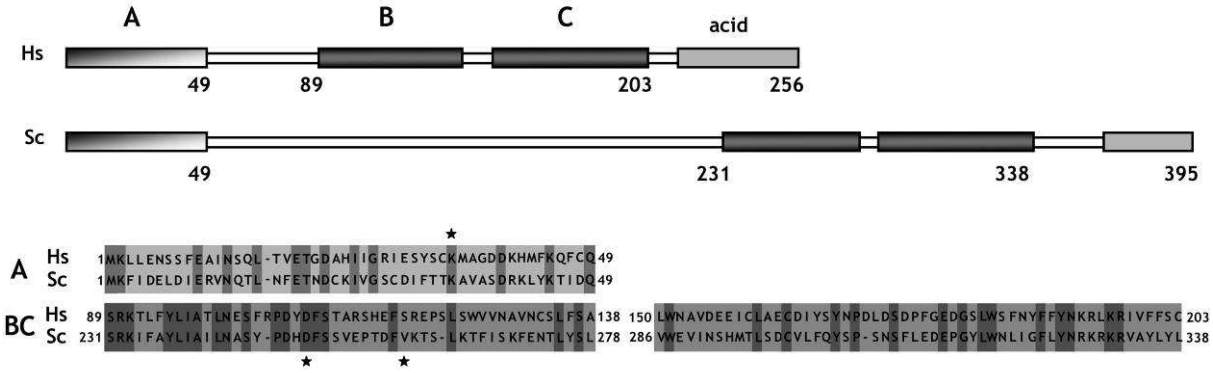

Figure 1. Similarité des séquences des protéines Maf1 de *H. sapiens* (Hs) et *S. cerevisiae* (Sc). Les domaines A et BC sont encadrés. Les séquences des domaines A et BC sont alignées et les acides aminés identiques sont mis en évidence par une couleur gris foncé. Les étoiles indiquent la position des mutations K35E, D250E et V260D.

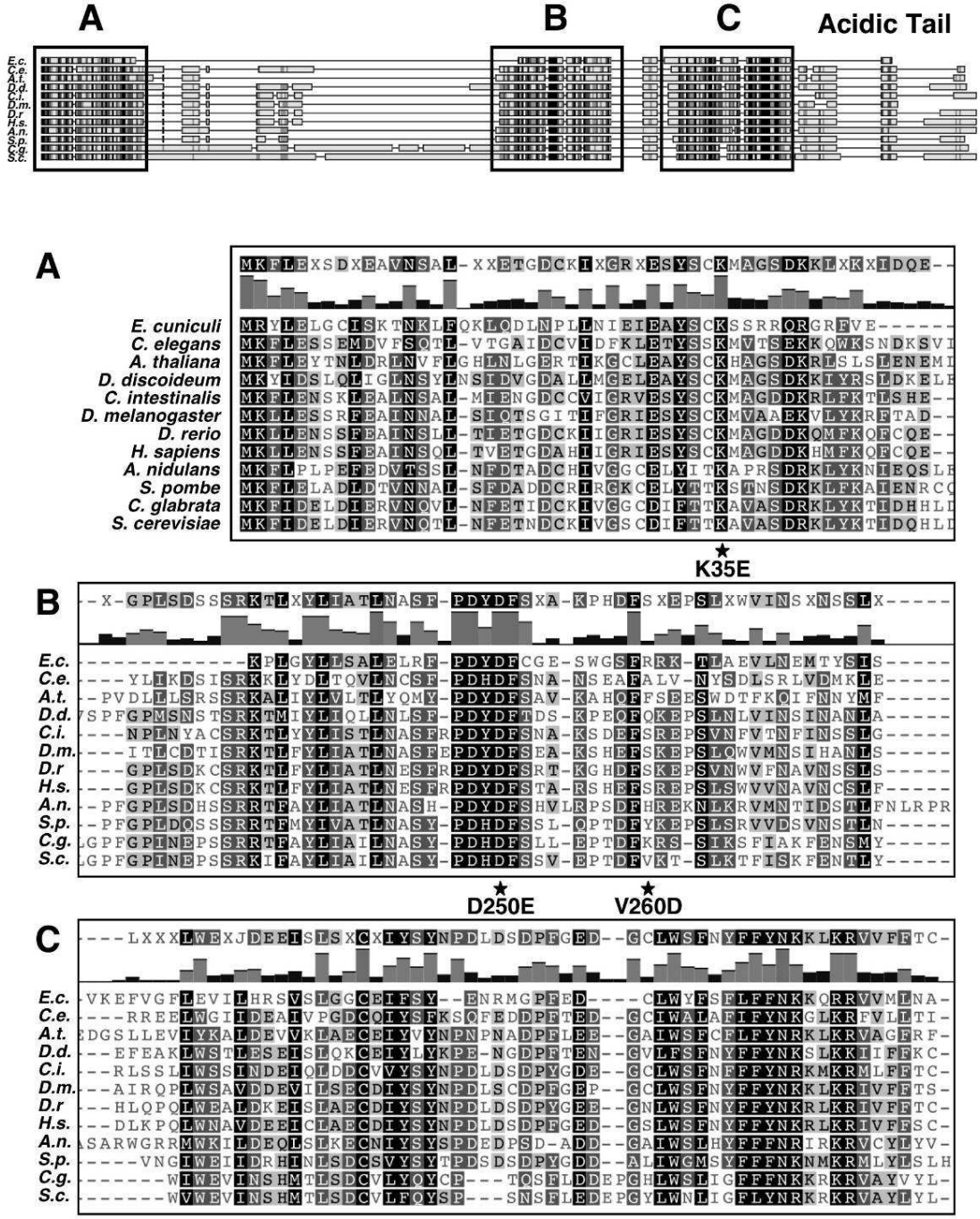

Figure 2. Alignement de séquences de protéines Maf1 de différents organismes. Les séquences des protéines ont été alignées avec le logiciel d'alignement multiple MUSCLE (41) et la figure a été créé avec le logiciel Geneious Pro 4.5.4. Représentation schématique de séquences de protéine Maf1 de différentes espèces : *Encephalitozoon cuniculi* (gi|19069247|, taille : 161 aa), *Caenorhabditis elegans* (gi|17506011|, taille : 245 aa), *Arabidopsis thaliana* (gi|22326767|, taille : 224 aa), *Dictyostelium discoideum* (gi|66816633|, taille : 278 aa), *Ciona intestinalis* gi|198415188|, taille : 233 aa), *Drosophila melanogaster* (gi|46409204|, taille : 226 aa), *Danio rerio* (gi|47087413|, taille : 247 aa), *Homo sapiens* (gi|49065352|, size : 256 aa), *Aspergillus nidulans* (gi|67901388|, taille : 314 aa), *Schizosaccharomyces pombe* (gi|254745531|, taille : 238 aa), *Candida glabrata* (gi|49529111|, taille : 391 aa) et *Saccharomyces cerevisiae* (gi|1170854|, taille : 395 aa). Les domaines conservés sont encadrés et nommés par des lettres : A, B et C dans la partie haute de la figure. Les alignements des séquences de chacun des domaines conservés (A, B et C) sont montrés dans la partie basse de la figure. Les histogrammes aux dessus des alignements indiquent le pourcentage d'identité entre les séquences. Les séquences consensus sont indiquées sous les alignements. Les positions des mutations K35E, D250E et V260D sont montrées par des étoiles sous les alignements (la mutation N344I est localisé 6 acides aminés après le domaine BC et n'est donc pas représentée).

Deux séquences « signatures » de la famille des protéines Maf1 sont localisées dans le domaine BC (les motifs PDYDFS et LWSFnYFFYNKklKR, Figure 2) (Pluta *et al.,* 2001). Ces séquences ne sont pas fonctionnellement caractérisées dans la base de donnée PROSITE. De manière intéressante, le second motif LWSFnYFFYNKklKR, présent dans la grande majorité des orthologues de Maf1, contient un signal de localisation nucléaire qui a été montré comme fonctionnel chez *S. cerevisiae* (Moir *et al.,* 2006).

Une étude détaillée de la protéine Maf1 humaine (*H. sapiens* Maf1 ou HsMaf1) a été réalisée dans le laboratoire de Christoph Müller (EMBL Heidelberg) en collaboration avec le laboratoire dirigé par Olivier Lefebvre (CEA/Saclay). Cette étude a permis de caractériser expérimentalement l'organisation structurelle de la protéine HsMaf1 après protéolyse ménagée (Appendix 1, Gajda *et al.,* 2010). En effet, des fragments protéolytiques stables sont considérés comme structurellement bien définis tandis que des sites sensibles à la protéase sont souvent corrélés à des régions désordonnées de la protéine. L'utilisation de trypsine pour effectuer une protéolyse ménagée a permis de digérer la protéine HsMaf1 (256 acides aminés) en deux fragments qui ont été identifiés aux acides aminés 1-45 et 75-234 par une combinaison de séquence N-terminale et d'analyse de spectrométrie de masse (Q-tof). Ces fragments correspondent aux domaines A et BC de la protéine HsMaf1. Le domaine « linker » entre ces fragments (aa 46-74) et l'extrémité C-terminale acide (aa 235-256) ont été dégradés et sont donc vraisemblablement non structurés. Les deux fragments ont ensuite été analysés par une chromatographie d'exclusion (tamisage moléculaire). De manière étonnante, les deux fragments de HsMaf1, bien que de masses moléculaires très différentes, éluent de manière concomitante avec une stœchiométrie apparente de 1 pour 1 ce qui suggère qu'ils interagissent physiquement. De plus, la co-expression de ces fragments N- et C-terminals de HsMaf1 dans des bactéries et leurs purifications indiquent que le fragment A étiqueté par une séquence de 6 histidines co-précipite le fragment BC non étiqueté avec une stœchiométrie apparente de 1 pour 1 suggérant, là aussi, une interaction directe. Ces protéines recombinantes éluent de manière concomitante lors d'une chromatographie d'exclusion ce qui renforce encore l'idée que les domaines A et BC interagissent directement.

Ces résultats obtenus dans l'équipe de Christoph Müller avec la protéine HSMaf1 ainsi que la très bonne conservation de séquence des domaines A et BC au cours de l'évolution nous ont permis d'étudier les relations entre les domaines A et

BC chez la levure *S. cerevisiae*, un organisme modèle très pratique pour étudier les relations entre la structure et la fonction d'une protéine.

Nous avons utilisé dans un premier temps la technique du double hybride afin de vérifier si une interaction entre les domaines A et BC existe chez cette levure. Le domaine putatif BC (aa 196-349) a été fusionné au domaine de liaison à l'ADN de Gal4 (plasmide pAS2) et co-exprimé avec diverses constructions du domaine A fusionné avec le domaine d'activation de la transcription de Gal4 (plasmide pACT2) dans la souche de levure Y190 dont l'activité β-galactosidase est mesurée. En effet, l'interaction entre les protéines de fusion devrait entraîner l'expression du gène exprimant la β-galactosidase. En utilisant cette approche, nous avons observé une interaction physique entre les domaines BC de Maf1 codé par le plasmide pAS2-Maf1-BC(196-349) et des fragments du domaines A de Maf1 codés par les plasmides pACT2-Maf1-A(1-42), pACT2-Maf1-A(1-39) et pACT2-Maf1-A(1-34) (Figure 3). Nous n'avons pas pu mettre en évidence d'interaction entre le domaine BC avec des fragments plus réduits du domaine A et codés par les plasmides pACT2-Maf1-A(1-12), pACT2-Maf1-A(1-16) ou pACT2-Maf1-A(1-23). Les cellules contenant les plasmides pAS2-Maf1-BC et pACT2 vide ne permettent pas de détecter d'activité β-galactosidase. Ces résultats démontrent la spécificité de l'interaction révélée par la technique du double-hybride et définissent les acides aminés 1-34 comme étant le plus petit fragment du domaine A de ScMaf1 encore capable de se lier au domaine BC. Les interactions réciproques n'ont pas pu être étudiées car la présence d'un plasmide pAS-Maf1-A même en absence d'un plasmide pACT2 active la transcription du gène testeur. Enfin, nous avons aussi vérifié que le plasmide pAS2-Maf1-BC en combinaison avec des plasmides pACT2 codant pour des fusions de la plupart des gènes de la machinerie de transcription de la Pol III donnent des résultats négatifs.

En conclusion, nos résultats suggèrent une forte interaction directe des domaines A et BC de Maf1 chez l'homme et chez la levure *S. cerevisiae*.

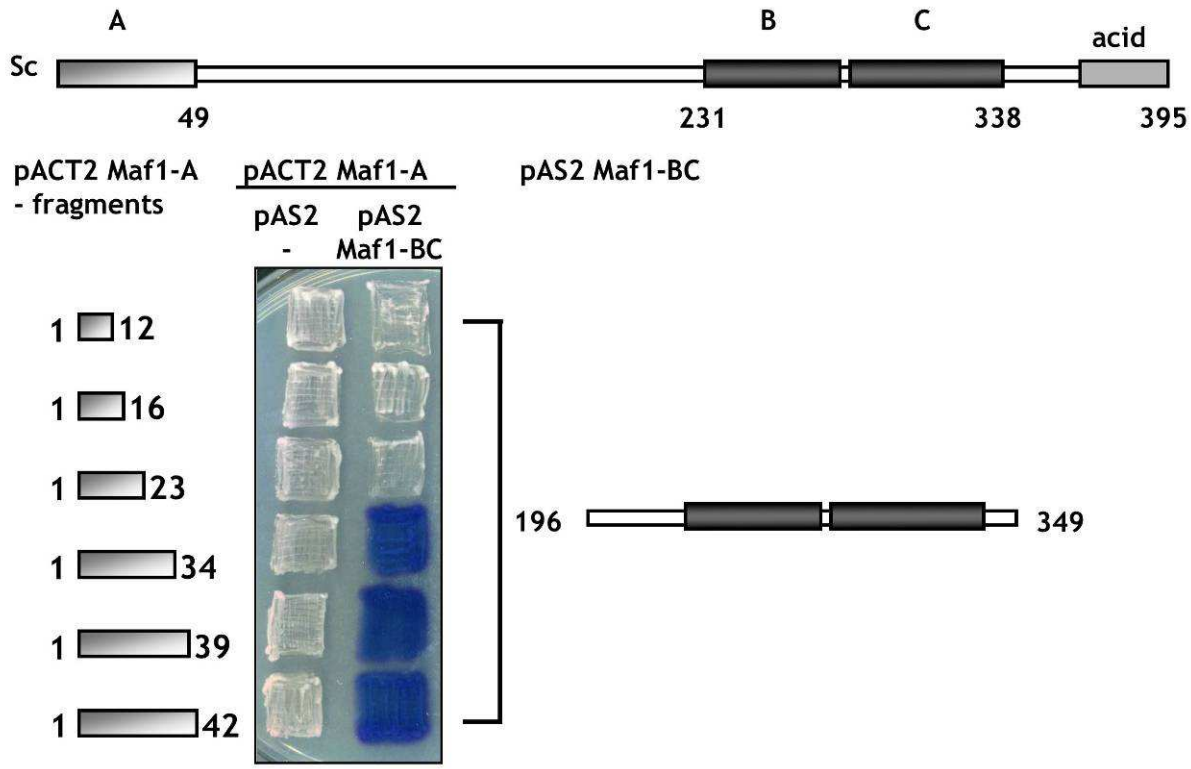

Figure 3. Interactions des domaines de Maf1 révélées par la technique du double-hybride. Les plasmides pACT2-Maf1-A(1-12), pACT2-Maf1-A(1-16), pACT2-Maf1-A(1-23), pACT2-Maf1-A(1-34), pACT2-Maf1-A(1-39) et pACT2-Maf1-A(1-42) ont été introduits par transformation individuellement ou avec les plasmides pAS2 (contrôle négatif) ou pAS2-Maf1- BC(196-349) dans la souche de levure *S. cerevisiae* Y190. Les transformants ont été testés pour l'expression de la β-galactosidase dans un test sur boîte de Petri.

- **L'interaction entre les domaines A and BC est importante pour la fonction de Maf1.**

Les expériences de protéolyse ménagée et de double-hybride montrent que les domaines A et BC forment un complexe stable qui pourrait être indispensable à la conformation correcte de la protéine Maf1. Pour évaluer le rôle physiologique de cette interaction, nous avons cherché des mutations localisées dans le domaine A qui affectent la fonction de Maf1 en altérant vraisemblablement la liaison au domaine BC. Des fragments d'ADN codant les acides aminés 1-180 ont été amplifiés dans des conditions de faible fidélité et introduits par transformation dans des cellules *maf1*-Δ avec un plasmide codant Maf1 et linéarisé dans la région codant le domaine A (technique du « Gap repair »). Les transformants ont été sélectionnés pour leur faible croissance à 37°C sur milieu contenant du glycérol ; phénotype qui est caractéristique d'un défaut de la fonction de Maf1 dans la répression de la transcription de la Pol III (Ciesla *et al.,* 2007). Le séquençage du plasmide pAG70 isolé par ce crible a permis d'identifier la mutation K35E localisée dans le domaine A.

Pour déterminer l'effet de la mutation K35E dans la protéine Maf1 sur l'activité de la Pol III, nous avons isolé les ARN de cellules ayant poussé en présence de glucose ou après transfert dans un milieu contenant du glycérol à 37°C. Ces ARN ont été analysés par Northern blot en utilisant des sondes codant pour les précurseurs des ARNt^{Leu} and ARNt^{Phe} (Figure 4A). Après transfert des cellules dans un milieu contenant une source de carbone non fermentable (glycérol), les niveaux des précurseurs des ARNt (qui sont un bon indicateur du niveau de transcription *in vivo* de la Pol III) sont diminués dans une souche sauvage mais pas dans des cellules *maf1*-Δ (Figure 4A, comparez les pistes 1 et 5 avec 6 et 10). De manière comparable à l'inactivation des cellules *maf1*-Δ, le mutant K35E est défectif dans sa capacité à réprimer la synthèse de précurseurs d'ARNt après transfert des cellules dans un milieu contenant du glycérol (Figure 4A, pistes 2 et 7). Ainsi, une simple mutation ponctuelle dans le domaine A de Maf1 prévient la répression de la transcription par la Pol III dans une souche *maf1*-K35E.

Une approche pour confirmer que la mutation K35E affecte négativement l'interaction avec le domaine BC de Maf1 est d'identifier des sites de mutations secondaires qui permettent de compenser l'effet observé. Nous avons donc recherché des mutations suppresseurs dans le domaine BC qui permettent aux cellules de croître sur milieu glycérol à 37°C. L'ADN codant pour les acides aminés 174-375 de Maf1 a été muté de manière aléatoire par PCR et introduit par transformation dans des cellules *maf1*-Δ avec un plasmide pAG70 linéarisé dans la région codant le domaine BC (technique du « Gap repair »). Le séquençage des gènes *maf1* reconstitués *in vivo* à partir des transformants a permis de montrer que les mutations codées dans les plasmides pLM11 (*maf1*-K35E-D250E) et pLM12 (*maf1*-K35E-V260D-N344I) permettent de restituer un phénotype sauvage sur milieu glycérol à 37°C (Figure 4B). La capacité de croissance restaurée sur milieu glycérol indique une compensation du défaut de la régulation de la transcription par la Pol III observée pour la mutation K35E. Les deux suppresseurs D250E ou V260D-N344I de la mutation du domaine A K35E sont localisés dans le domaine BC ce qui pourrait révéler une interaction physique entre ces domaines. Une analyse par Northern blot a permis de confirmer que les mutations suppresseurs restaure la capacité de Maf1 de réprimer la synthèse de précurseurs d'ARNt après transfert des cellules d'un milieu contenant du glucose à du glycérol (Figure 4A, comparez les pistes 3 et 4 avec 8 et 9). Ces résultats indiquent que l'interaction génétique entre les deux domaines de Maf1 est fonctionnelle.

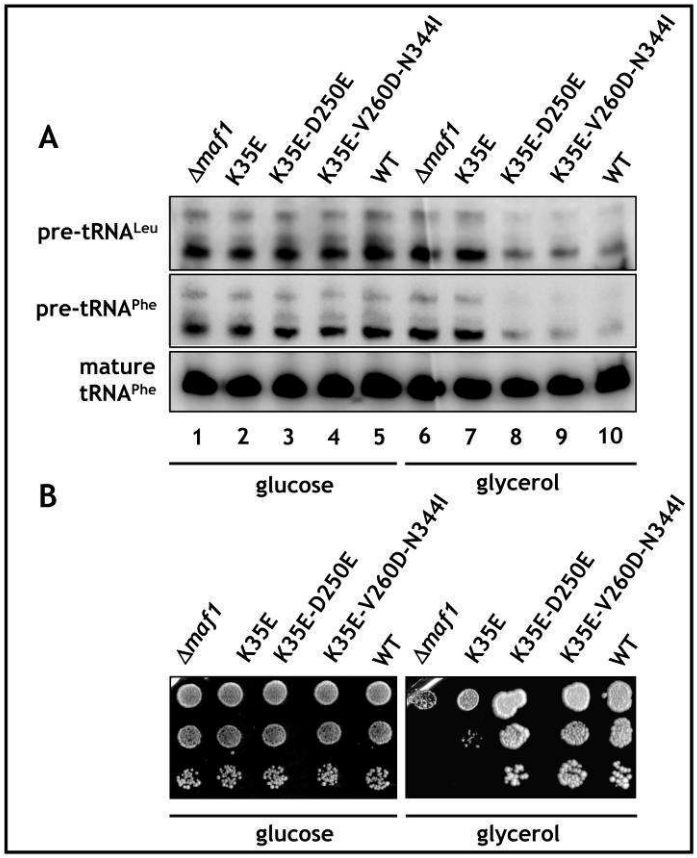

Figure 4. La régulation de la transcription par la Pol III et la croissance sur milieu glycérol sont affectées par la mutation K35E située dans la région codant le domaine A et restaurée par des mutations suppresseurs dans le domaine BC de *MAF1*. Les mutants *maf1*-Δ, *maf1*-K35E, *maf1*-K35E-D250E et *maf1*-K35E-V260D-N344I et la souche isogénique YPH500 (WT) ont été utilisés. **A.** Les cellules ont été récoltées en phase exponentielle de croissance après culture dans un milieu contenant du glucose (YPD) à 30°C puis transférées dans un milieu contenant du glycérol (YPGly) et incubées à 37°C pendant 1,5 h. L'ARN total isolé des cellules a été testé par Northern blot avec des sondes codant pour les précurseurs des ARNt^{Leu} and ARNt^{Phe}. **B.** Des dilutions sériées (par 10) de cellules récoltées en phase exponentielle de croissance ont été disposées sur des milieux gélifiés contenant du glucose (YPD) à 30°C ou du glycérol (YPGly) à 37°C et incubées pendant 2-3 jours.

Pour mieux caractériser l'association des domaines A et BC, nous avons vérifié les effets des mutations K35E, D250E, V260D et N344I par la technique du double hybride. Les mutations ont été introduites dans le domaine A fusionné au domaine d'activation de la transcription de Gal4 codé par le plasmide pACT2-Maf1-A(1-42) ou dans le domaine BC fusionné au domaine de liaison à l'ADN de Gal4 codé par le plasmide pAS2-Maf1-BC(196-349). Différentes combinaisons de plasmides ont été utilisées pour transformer la souche de levure Y190 et l'activité β-galactosidase a été déterminée (Figure 5). La mutation K35E réduit l'interaction dans la technique du double-hybride de 40% (Figure 5, comparez les pistes 2 et 1). De manière similaire, les mutations D250E et V260D-N344I du domaine BC diminuent l'interaction du domaine BC avec le domaine A sauvage de respectivement 22 % et 62 % (Figure 5, comparez les pistes 7 et 8 avec la piste 1). De plus, le mutant *maf1*-V260D-N344I présente un défaut de la régulation de la synthèse des ARNt et une

sensibilité de croissance sur un milieu contenant du glycérol (Figure 6A, comparez les pistes 3 et 7; Figure 6B).

Des combinaisons de domaines mutés de Maf1 permettent de restaurer une interaction similaire à celle observée chez le sauvage en accord avec les données de suppression génétique (Figure 5, comparez les pistes 3 et 4 avec la piste 1). De manière plutôt inattendue, un niveau d'interaction par la technique du double-hybride de 80% supérieur au niveau sauvage est observé pour la combinaison du domaine A portant la mutation K35E avec le domaine BC portant la mutation simple V260D (Figure 5, comparez la piste 5 avec la piste 1). Ceci pourrait indiquer que dans la mutation double suppresseur V260D-N344I identifiée dans le crible génétique, la mutation V260D pourrait permettre à elle seule de restaurer l'interaction avec le domaine A portant la mutation K35E.

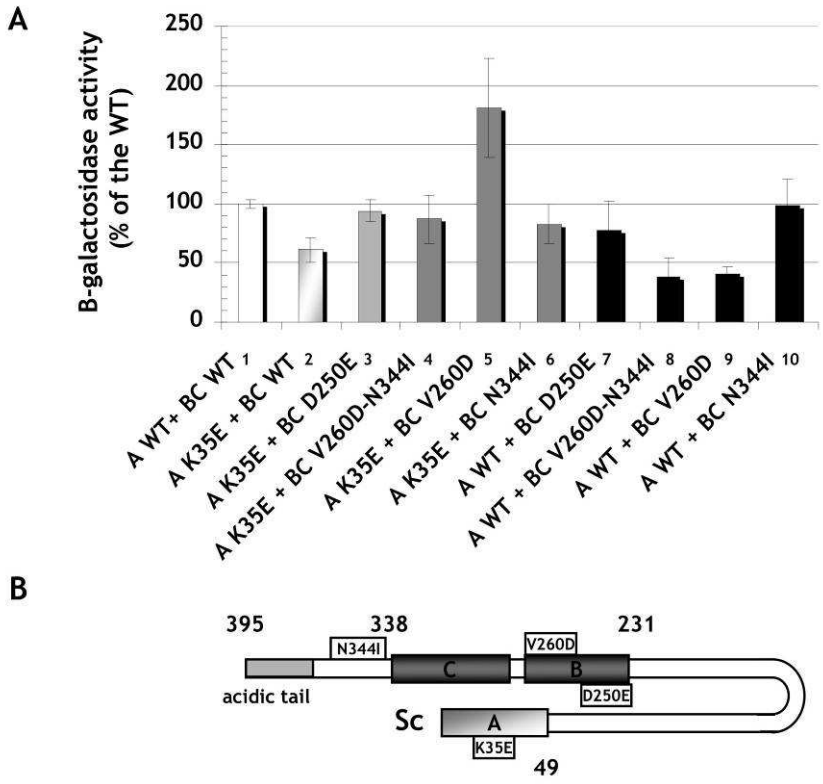

Figure 5. L'interaction des domaines de Maf1 dans la technique du double-hybride est réduite par des mutations primaires dans ces domaines et restaurée par des mutations secondaires suppresseurs. A. le plasmide pACT2-Maf1-A(1-42) ou ses versions mutées ont été introduites par transformation en combinaison avec le plasmide pAS2-Maf1- BC(196-349) ou ses versions mutées dans la souche de levure Y190. L'expression de la β-galactosidase a été testée dans les différents transformants. L'histogramme permet de comparer les interactions déterminées par la technique du double hybride pour différentes combinaisons : domaines A et BC sauvage (1), domaine A ayant la mutation K35E avec le domaine BC sauvage (2); domaine A ayant la mutation K35E avec quatre versions mutées du domaine BC: D250E (3), V260D-N344I (4), V260D (5), N344I (6), et domaine A sauvage avec des versions du domaine BC ayant les mutations : D250E, V260D or N344I et N344I-V260D (7-10). **B.** Schéma de l'interaction des domaines de Maf1. Les valeurs détaillées des activités β-galactosidase sont présentées dans la Table S9.

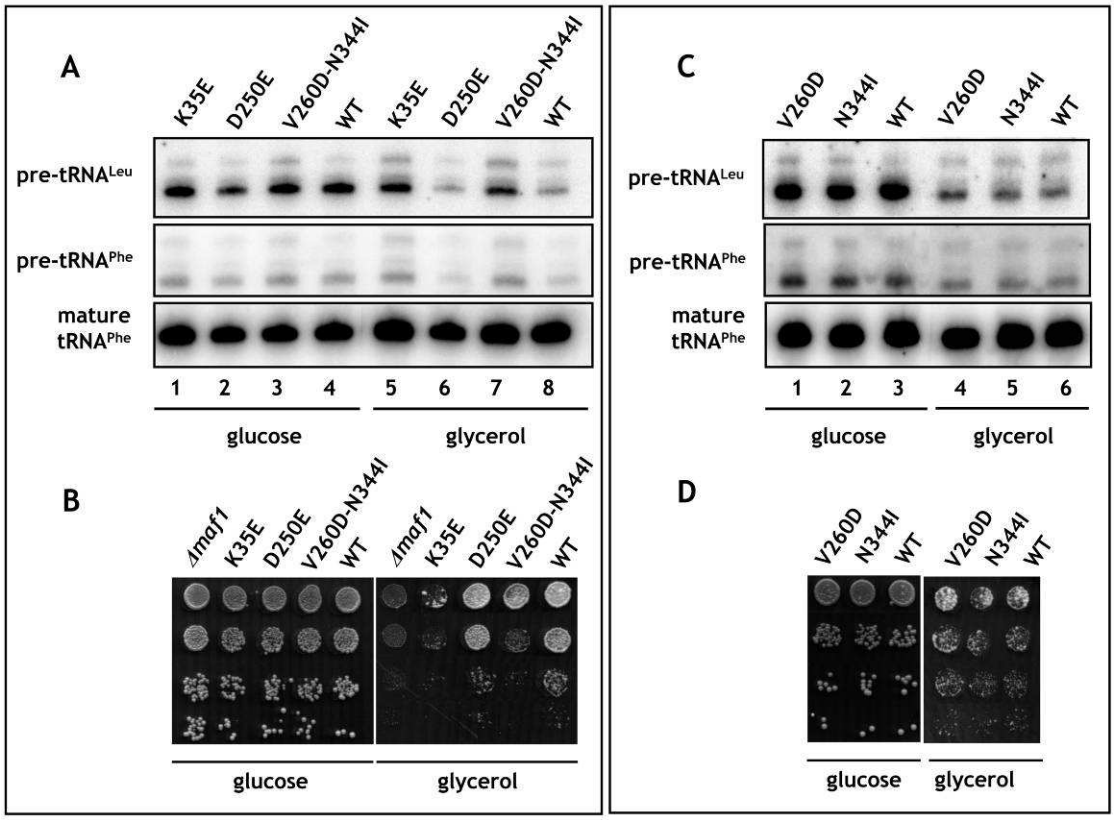

Figure 6. La régulation de la transcription par la Pol III est corrélée avec la croissance des souches mutantes sur un milieu contenant une source de carbone non fermentable. Les mutations du domaine BC en présence d'un domaine A sauvage ont été introduites par mutagenèse dirigée. **A. C.** Les cellules ont été récoltées en phase exponentielle de croissance après culture dans un milieu contenant du glucose (YPD) à 30°C puis transférées dans un milieu contenant du glycérol (YPGly) et incubées à 37°C pendant 1,5 h. L'ARN total isolé des cellules a été testé par Northern blot avec des sondes codant pour les précurseurs des ARNt^{Leu} and ARNt^{Phe}. **B. D.** Des dilutions sériées (par 10) de cellules récoltées en phase exponentielle de croissance ont été disposées sur des milieux gélifiés contenant du glucose (YPD) à 30°C ou du glycérol (YPGly) à 37°C et incubées pendant 2-3 jours. La double mutation V260D-N344I inhibe la régulation de la synthèse d'ARNt et la croissance sur un milieu contenant du glycérol. Au contraire, les mutations D250E (**A**) V260D and N344I (**C**) n'ont aucun effet.

- **L'interaction des domaines A et BC permet la déphosphorylation de Maf1 lors du transfert des cellules dans un milieu contenant une source de carbone non fermentable.**

La phosphorylation de Maf1 est observée lorsqu'il n'y a pas de répression de la transcription par la Pol III lorsque les cellules sont cultivées sur un milieu contenant du glucose (Towpik *et al.,* 2008). Le transfert des cellules dans un milieu contenant une source de carbone non fermentable induit une déphosphorylation de Maf1, son importation dans le noyau et l'inhibition de la synthèse d'ARNt (Ciesla *et al.,* 2007). Comme nous avons montré que l'interaction entre les domaines A et BC est cruciale pour la régulation de la Pol III, nous avons cherché à étudier les relations entre cette interaction et la régulation de Maf1 par la phosphorylation. Nous avons cherché à identifier si une altération de l'interaction des domaines de Maf1, dans les mutants précédemment identifiés, pourrait modifier la

phosphorylation de Maf1. Pour cela, les différentes formes phosphorylées de Maf1 ont été, résolues par électrophorèse en condition dénaturante (SDS-PAGE) et identifiées par immunodétection, ceci à différents temps après le transfert des cellules d'un milieu contenant du glucose dans un milieu contenant du glycérol (Figure 7A).

Comme il est décrit dans la littérature, la protéine Maf1 sauvage est rapidement déphosphorylée lors de ce changement de milieu. De manière remarquable la mutation K35E du domaine A, qui altère l'interaction avec le domaine BC, modifie aussi la déphosphorylation de Maf1. La restauration de l'interaction à un niveau sauvage grâce aux mutations secondaires suppresseurs D250E et V260D-N344I rétablit aussi la déphosphorylation rapide de Maf1 lors du transfert des cellules d'un milieu contenant du glucose vers un milieu contenant du glycérol. La déphosphorylation de Maf1 dans les mutants suppresseurs serait seulement un peu plus lente que dans une souche sauvage (Tables supplémentaires S6-7).

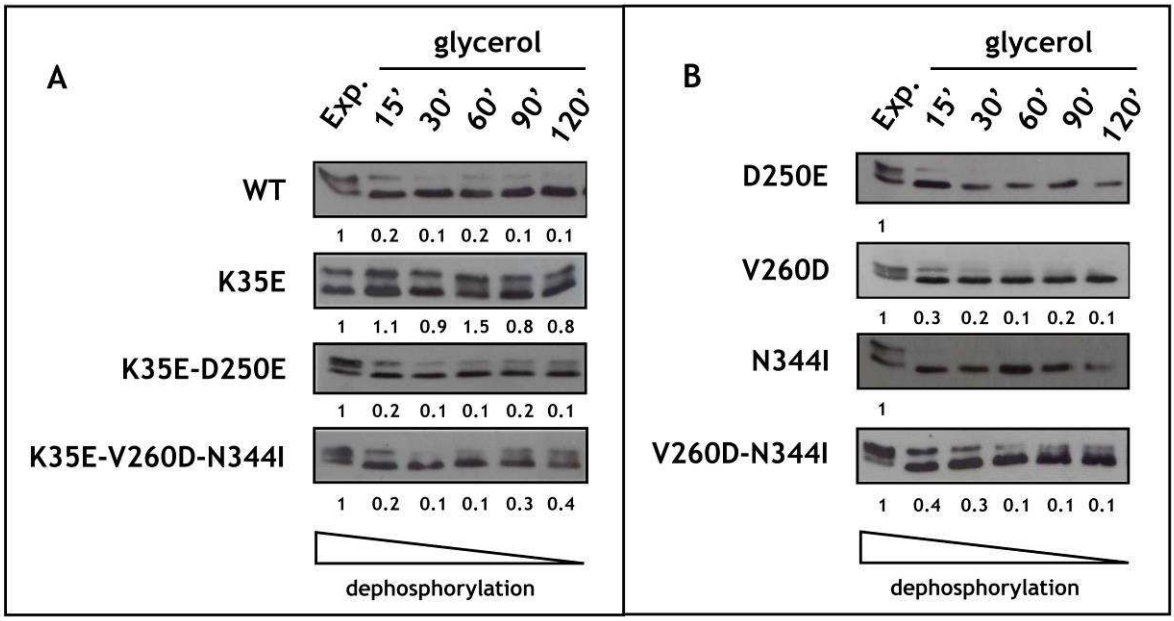

Figure 7. Les mutations de Maf1 affectant la répression de la transcription par la Pol III Mutations ont un effet sur la cinétique de déphosphorylation de Maf1 lors d'un transfert des cellules d'un milieu contenant du glucose dans un milieu contenant du glycérol. A. Les souches mutantes *maf1*-K35E, *maf1*-K35E-D250E et *maf1*-K35E-V260D-N344I et la souche isogénique YPH500 *maf1*-Δ transformée par le plasmide pRS315-*MAF1* (WT) ont été cultivées dans un milieu contenant du glucose jusqu'en phase de croissance exponentielle (Exp) puis transférées dans un milieu contenant du glycérol, incubées à 37°C et récoltées aux temps indiqués. Les extraits buts de levure ont été analysés par SDS-PAGE avec un ratio acrylamide:bisacrylamide modifié et révélé par immunodétection en utilisant des anticorps anti-Maf1. Les bandes ayant une migration ralentie correspondent aux formes phosphorylées de Maf1. **B.** Les mutants *maf1*-D250E, *maf1*-V260D et *maf1*-N344I ont été créés par mutagenèse dirigée. Les cellules de levure ont été soumises aux même analyses que précédemment. La double mutation V260D-N344I inhibe la déphosphorylation de Maf1 lors du transfert des cellules sur un milieu contenant du glycérol. Au contraire, les mutations D250E V260D and N344I n'ont aucun effet. Les valeurs sous chaque piste indiquent le ratio entre les formes phosphorylées et déphosphorylées de Maf1 normalisées pour la phase exponentielle (Exp). Les quantifications sont disponibles dans les Tables S6-S7.

De manière intéressante, la mutation double V260D-N344I du domaine BC en présence d'un domaine A sauvage empêche l'interaction de ces domaines (Figure 5) et altère la déphosphorylation de Maf1 (Figure. 7B).
En final, ces résultats suggèrent que l'interaction entre les domaines A et BC facilite grandement la déphosphorylation de Maf1.

• DISCUSSION

• L'interaction entre les domaines A et BC est importante pour la fonction de Maf1.

La famille des protéines Maf1 des Eucaryotes présente des caractéristiques de séquence en acides aminés qui sont conservées aux cours de l'évolution avec deux régions aisément reconnaissable : les domaines A et BC. Cette étude compare pour la première fois la structure de Maf1 à l'inhibition de la transcription par la Pol III chez *S. cerevisiae*. Nous montrons que l'interaction entre les deux domaines de Maf1 est requise pour son activité dans la répression de la transcription par la Pol III.

Une analyse bioinformatique utilisant un serveur de prédiction de structure de protéine (PSIPRED v 2.6 ; Jones, 1999 ; Bryson *et al.,* 2005) nous a permis de faire une analyse fine de nos résultats obtenus par la technique du double hybride. Chez l'homme et la levure *S. cerevisiae*, ce serveur prédit que le domaine A pourrait être constitué de deux hélices α (chez *S. cerevisiae*: aa 7-16 et aa 40-56) séparés par deux feuillets β (aa 24-27 et 29-35) tandis que le domaine BC serait constitué de cinq hélices α et de quatre feuillets β (Figure 8). Aucune structure secondaire n'est prédite entre les domaines A et BC.

La mutation K35E est localisée à la fin du second feuillet β du domaine A. Les acides aminés 1-34 du domaine A ont été identifiés, lors de ce travail, comme le domaine minimal encore capable de se lier au domaine BC. Nous faisons l'hypothèse que l'interaction entre le domaine A et BC requiert la première hélice α les deux feuillets β adjacents.

L'Analyse de Cluster Hydrophobe (HCA), un outil utilisant une représentation en hélice en deux dimensions de la séquence d'une protéine pour identifier des régions hydrophobes, permet d'identifier aussi des structures secondaires (Callebaut *et al.,* 1997). L'analyse HCA révèle la présence de deux régions riches en résidus hydrophobes qui correspondent aux domaines A et BC des protéines Maf1 de *H. sapiens* et *S. cerevisiae* (Figure 9). Une région pauvre en résidus hydrophobes se trouve entre ces domaines et correspond au « linker » qui peut être dégradé par

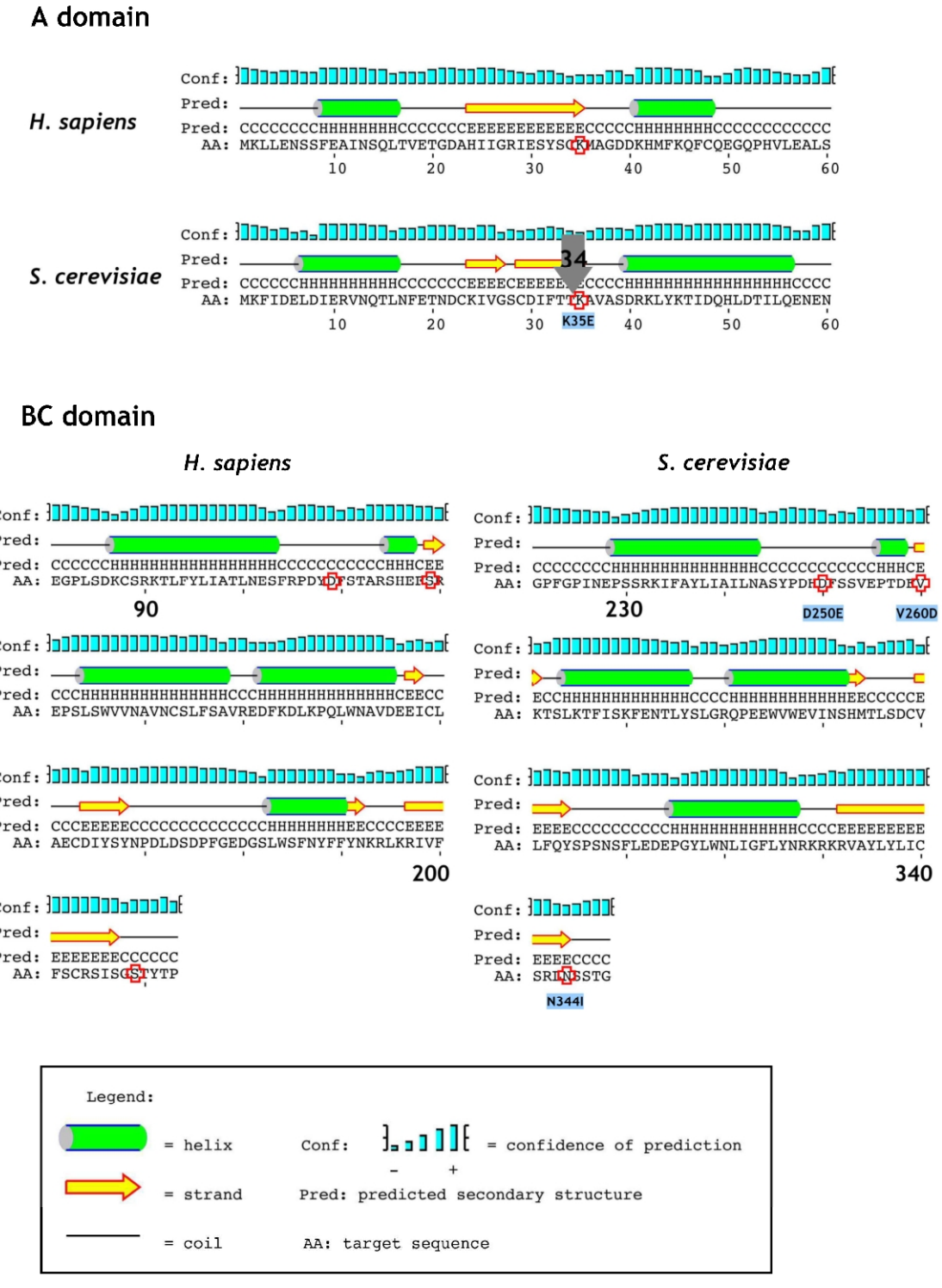

Figure 8. Prédiction de structure de la protéine Maf1. Le serveur de prédiction de structure de protéine PSIPRED v 2.6 a été utilisé pour identifier la structure secondaire des protéines Maf1 de *S. cerevisiae* et *H. sapiens*. Seuls les domaines A et BC sont présentés. Les tubes verts (ou lettre H), les flèches jaunes (ou lettre E) ou les lignes noires (ou lettre C) représentent respectivement les hélices α, les feuillets β et les boucles. Les positions des mutations K35E, D250E, V260D et N344I dans la protéine Maf1 de *S. cerevisiae* sont indiquées par des croix rouges. Les mutations correspondantes chez la protéine Maf1 de *H. sapiens* sont aussi indiquées.

protéolyse ménagée (voir plus haut, expérience réalisée dans le laboratoire de Christoph Müller).

Nous avons montré lors de ce travail que l'interaction entre les domaines A et BC facilite la déphosphorylation de Maf1 qui est nécessaire pour la répression de l'activité de la Pol III. Nous faisons aussi l'hypothèse que l'interaction entre ces domaines est influencée par l'état de phosphorylation de Maf1. Ainsi les différentes formes de Maf1 qui sont observées dans une électrophorèse en condition dénaturante et qui sont interprétées comme représentant différents niveaux de phosphorylation pourraient être dues, en fait, à différent états conformationnels dépendant de l'interaction entre les domaines A et BC. Il faut noter que les mutations S90A, S101A et S177A, S178A dans le « linker » changent profondément la proportion de formes lentes et rapides dans ce type d'électrophorèse sans changer notablement le niveau de phosphorylation de Maf1 (Lee *et al.*, 2009).

Nous proposons que le « linker » non structuré pourrait être phosphorylé et que son niveau de phosphorylation pourrait moduler l'état conformationnel de Maf1. Nous avons utilisé le serveur NetPhos 2.0 pour étudier cette question (Blom, 1999) et prédire les sites de phosphorylation chez quatre orthologues de Maf1 contenant des « linkers » de taille différente. Les sites de phosphorylation prédits sont plus fréquemment trouvés dans les longs « linkers » entre les domaines A et BC *S. cerevisiae* et *C. glabrata*. Ces sites sont plus uniformément distribués le long de la séquence de Maf1 chez *C. elegans* et *H. sapiens*, mais ils sont un peu plus présents dans leurs « linkers » (Figure 10). Nous faisons l'hypothèse que la phosphorylation et la déphosphorylation des résidus du « linker » modifie la conformation de la protéine, change la distance entre les domaines A et BC et donc module l'activité de répression par Maf1 de la transcription par la Pol III (Figure 11).

L'interaction des domaines A et BC, régulée par la phosphorylation, pourrait aussi affecter l'importation de Maf1 dans le noyau et l'interaction avec la Pol III. Cette supposition est soutenue par des données publiées qui montre que la phosphorylation de six résidus du « linker » par la kinase PKA inhibe l'import nucléaire de Maf1 et la répression de la transcription par la Pol III (Moir *et al.*, 2006).

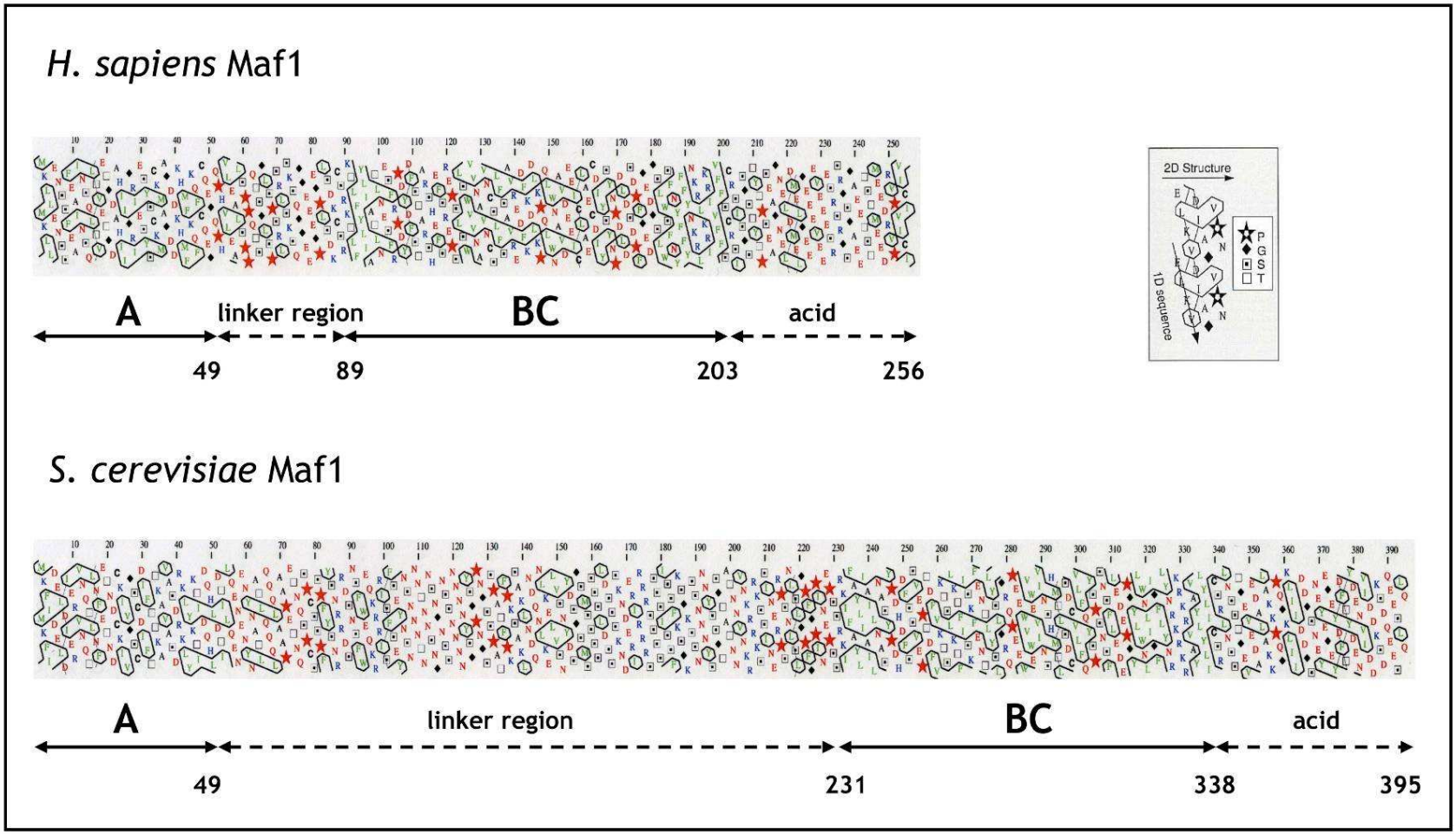

Figure 9. Analyse de cluster hydrophobe (HCA) dans la séquence de Maf1 de *H. sapiens* et *S. cerevisiae*. Représentation schématique de structure secondaire de Maf1 : une étoile rouge indique une proline, un losange une glycine, un carré avec ou sans point respectivement une serine et une thréonine. Les résidus acides (E, Q, N) sont en rouge, les résidus basiques (K, R) sont en bleu. Les clusters d'acides aminés hydrophobes sont en vert et entourés. Un cluster vertical correspond à un feuillet β tandis qu'un cluster horizontal est associé avec une structure en hélice α (Callebaut *et al.,* 1997). Les localisations des domaines A et BC sont indiquées par des flèches noires.

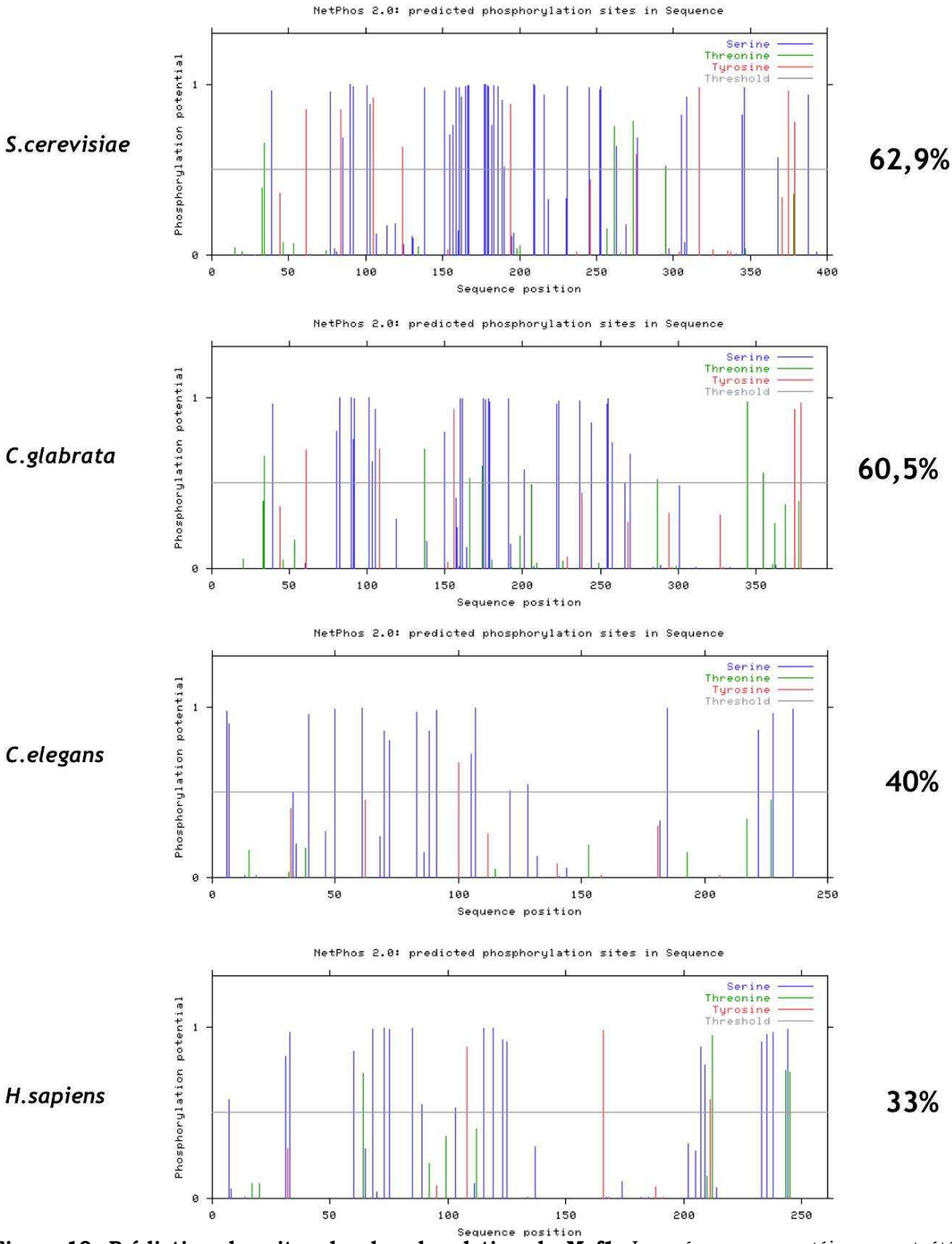

Figure 10. Prédiction des sites de phosphorylation de Maf1. Les séquences protéiques ont été analysées avec le serveur NetPhos 2.0. Les diagrammes représentent la probabilité de phosphoryaltion dans une échelle [0,000-1,000]. La figure présente les localisations des sérines (bleu), thréonine (vert) et tyrosine (rouge) prédites pour être phosphorylées. Les sites de phosphorylation sont comparés dans des séquences de Maf1 avec un long (*S. cerevisiae* et *C. glabrata*) et court (*C. elegans* and *H. sapiens*) « linker » entre les domaines A et BC. Les pourcentages des sites de phosphorylation localisés dans le « linker » sont indiqués sur le côté droit.

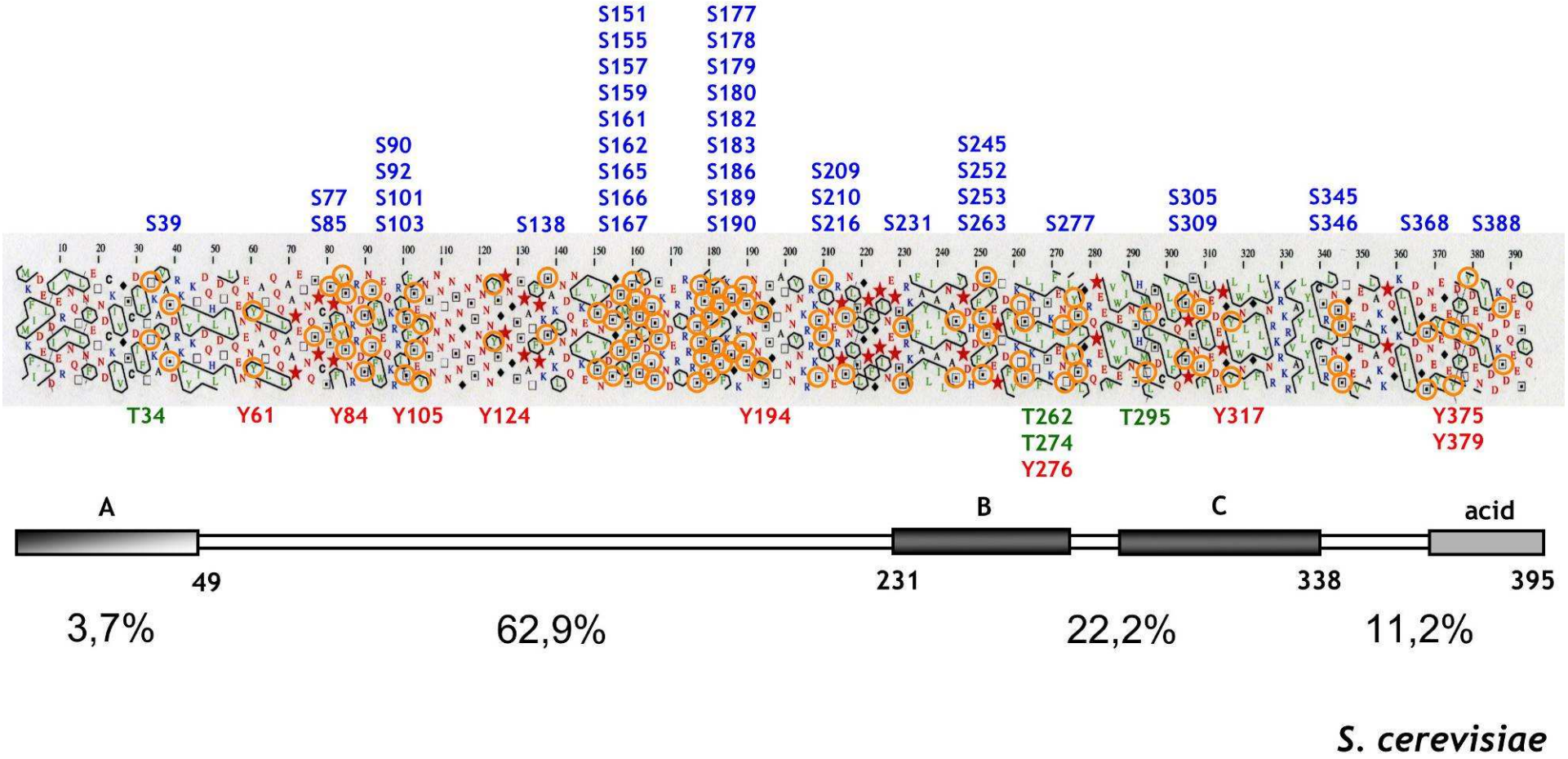

Figure 11. Localisation des résidus potentiellement phosphorylable dans la protéine Maf1 chez *S. cerevisiae*. La figure présente les localisations des sérines (bleu), thréonine (vert) et tyrosine (rouge) prédites pour être phosphorylées. Les résidus potentiellement phosphorylables (entourés par un cercle orange) sont représentés sur une représentation obtenue par analyse des clusters hydrophobes (HCA) (Callebaut *et al.*, 1997). Une représentation schématique des domaines de Maf1 est présentée en bas. Les pourcentages de résidus potentiellement phosphorylables dans chaque domaine A, « linker », BC et région acide sont indiqués.

- **Structure cristallographique de la protéine Maf1.**

Lors de la rédaction de ce rapport de thèse, les premières données cristallographiques sur la structure tridimensionnelle de Maf1 humaine ont été exposées lors du congrès scientifique biennal « The 7th International Biennial Conference on RNA Polymerases I & III. The Odd Pols '10 Meeting » en juin 2010 (Rieke Ringel du laboratoire de Patrick Cramer, Gene Center, Munich). Ces données coïncident sur bien des points avec nos données et celles qui ont été obtenues par le laboratoire de Christoph Müller et rapportent que la protéine Maf1 est composée de deux domaines structurés A et BC séparés par un « linker » non structuré.

Comme le laboratoire de Christoph Müller, Rieke Ringel a été en mesure de protéolyser de façon ménagée la protéine Maf1 humaine et d'isoler deux fragments correspondants aux domaines A et BC (données publiées très récemment le 1er octobre 2010 par Vannini *et al.*). La protéine humaine a été surproduite sans sa partie C-terminale acide et sans le « linker » entre les domaines A et BC. Tous les acides aminés du « linker » et même certains résidus de la partie C-terminale du domaine A ont été enlevés. La structure cristallographique de Maf1, définie avec une précision de 1,5 ångström, a été obtenue après deux ans et demi d'effort à temps plein et après de nombreuses tentatives.

Maf1 est une protéine globulaire constituée d'un coeur hydrophobe de feuillets β entourés par des hélices α (Figure 12 aimablement donnée avant publication par Rieke Ringel). Le domaine A est constitué principalement d'un feuillet β (localisé dans le milieu de la structure) et d'une hélice α (située à l'extérieur de la structure). Cette nouvelle structure n'a pas d'homologues structuraux dans les bases de données et il n'est donc pas possible de prédire de fonction à un domaine particulier de Maf1 (Vannini *et al.*, 2010).

Comme les domaines A et BC de Maf1 sont fortement conservés entre *H. sapiens* et *S. cerevisiae*, il est raisonnable de situer les mutations identifiés chez la levure, lors de mon travail de thèse, sur la structure de la protéine Maf1 humaine. Ce positionnement permet d'apprécier spatiallement l'effet des mutations de Maf1 sur l'interaction entre les domaines A et BC.

La position des mutations K35E, D250E, V260D et N344I chez la protéine Maf1 de *S. cerevisiae* correspond respectivement aux positions des résidus K35, D109, S119 et S209 chez *H. sapiens* (Figure 12). La position de la mutation N344I n'est pas indiquée chez l'homme car le résidu S209 correspondant appartient à l'extrémité C-terminale acide qui a été exclue pour obtenir le cristal de Maf1.

Néanmoins, le résidu S209 devrait être très proche de l'extrémité C-terminale du cristal (acide aminé 205)

Il est intéressant de noter que la mutation K35E dans le domaine A qui altère la régulation de la transcription par la Pol III et les mutations suppresseurs D250E (D109) et V260D (S119) du domaine BC qui permettent de restaurer cette activité sont localisées à proximité (mais pas en contact). Ces localisations proches sont en bon accord avec l'impact des mutations sur l'interaction des domaines A et BC comme nous avons pu le voir lors de cette thèse par notre approche génétique et notre étude par la technique du double-hybride.

Il faut, de plus, remarquer que la mutation V260D de la protéine Maf1 de *S. cerevisiae* (S119 chez l'homme) qui a un effet majeur sur l'interaction des domaines A et BC dans la technique du double-hybride est localisée le plus près du résidu K35.

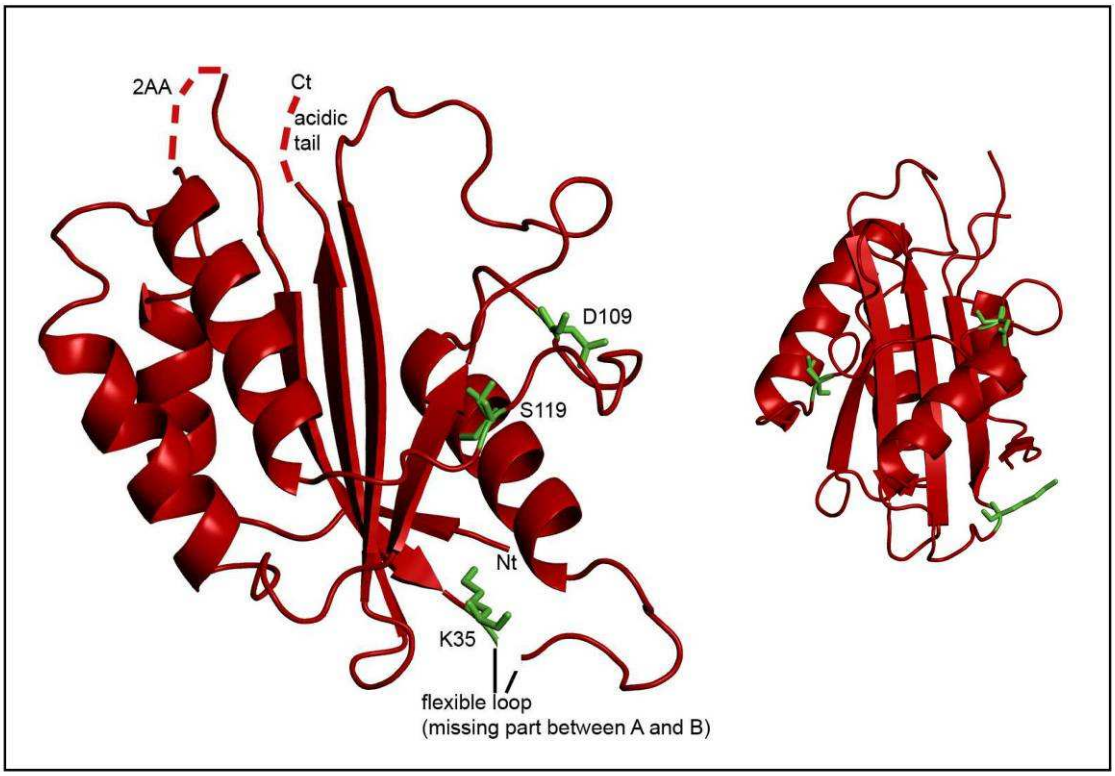

Figure 12. Structure tridimensionnelle de la protéine Maf1 de *H. sapiens* déterminée par cristallographie. La structure est présentée sous deux points de vue différents par une rotation de 90°. La structure est définie avec une précision de 1,5 ångström. La position des résidus K35, D109 et S119 correspondant respectivement aux mutations K35E, D250E, et V260D, identifiées chez *S. cerevisiae*, a été indiquée en vert. La position de la mutation N344I correspondant à S209 chez l'homme n'est pas montrée car ce résidu est localisé dans l'extrémité C-teminale acide qui n'a pas été cristallisée. Le dernier résidu C-terminal est l'acide aminé 205 (Figure aimablement donnée avant publication par Rieke Ringel).

Enfin, la structure cristallographique de la protéine Maf1 humaine révèle que les deux séquences de localisation nucléaire (NLS) sont accessibles car localisées en surface. Le premier NLS fait partie du « linker » et le deuxième est a proximité (Vannini *et al.*, 2010). Ainsi, les auteurs ont proposé que la phosphorylation du « linker » pourraient engendrer des changements structuraux de Maf1 qui masqueraient les séquences NLS et empêcheraient la localisation nucléaire de cette protéine.

Nous faisons l'hypothèse que ces changements de conformation pourraient aussi affecter l'interaction entre les domaines A et BC indispensable à l'activité de répresseur de Maf1.

- **PERSPECTIVES**

L'identification de la structure cristallographique de Maf1 et des mécanismes moléculaires qui conduisent à la répression de la transcription par la Pol III vont étendre les possibilités des futures recherches. Il a été montré qu'une dérégulation de l'activité de la Pol III était liée à la transformation maligne (Marshall et al., 2008a; Marshall et al., 2008b; Johnson et al., 2008). On peut donc imaginer que des agents thérapeutiques, structurellement similaires à Maf1, pourraient réprimer spécifiquement la transcription hyperactive de la Pol III dans les cellules tumorales et ainsi contrôler le développement anarchique de ces cellules.

Des résultats récents de notre laboratoire montrent que Maf1 pourraient avoir un rôle aussi dans la maturation des ARNt (Karkusiewicz – données non publiées). Il serait intéressant d'identifier si cette fonction requiert les deux domaines A et BC de Maf1 ou si un des domaines est plus particulièrement impliqué.

VIII. BIBLIOGRAPHY

Altschul S.F., Madden T.L., Schaffer A.A., Zhang J., Zhang Z., Miller W. and Lipman D.J. (1997) Gapped BLAST and PSI-BLAST: a new generation of protein database search programs. *Nucl. Acids Res.* vol.25: 3389-3402

Blom N., Gammeltoft S. and Brunak S. (1999) Sequence and structure-based prediction of eukaryotic protein phosphorylation sites. *J. Mol. Biol.* vol.294: 1351-1362

Blom N., Sicheritz-Ponten T., Gupta R., Gammeltoft S. and Brunak S. (2004) Prediction of post-translational glycosylation and phosphorylation of proteins from the amino acid sequence. *Proteomics* vol.4:1633-1649

Boguta M. (2009) Control of RNA polymerases I and III by the TOR signaling pathway. *Cell Cycle* vol.8: 4023-4024

Boguta M., Czerska K. and Zoladek T. (1997) Mutation in a new gene *MAF1* affects tRNA suppressor efficiency in *Saccharomyces cerevisiae*. *Gene* vol.185: 291-296

Boisnard S., Lagniel G., Garmendia-Torres C., Molin M., Boy-Marcotte E., Jacquet M., Toledano M.B., Labarre J. and Chedin S. (2009) *Eukaryot. Cell* vol.8: 1429-1438

Brun I., Sentenac A. and Werner M. (1997) Dual role of the C34 subunit of RNA polymerase III in transcription initiation. *EMBO J.* vol.16: 5730-5741

Bryson K., McGuffin L.J., Marsden R.L., Ward J.J., Sodhi J.S. and Jones D.T. (2005) Protein structure prediction servers at University College London. *Nucl. Acids Res.* vol.33: W36-W38

Bullock W.O., Fernandez J.M. and Short J.M.S. (1987) XL1-Blue: a highly efficient plasmid transforming *rec*A *Escherichia coli* strain with beta-galactosidase selection. *BioTechniques* vol.4: 376-378

Cabart P., Lee J. and Willis J.M. (2008) Facilitated recycling protects human RNA polymerase III from repression by Maf1 *in vitro*. *J. Biol. Chem.* vol.283: 36108-36117

Callebaut I., Labesse G., Durand P., Poupon A., Canard L., Chomilier J., Henrissat B. and Mornon J.P. (1997) Deciphering protein sequence information through hydrophobic cluster analysis (HCA) : current status and perspectives. *CMLS Cell. mol. life sci.* vol.53: 621-645

Canella D., Praz V., Reina J.H., Cousin P. and Hernandez N. (2010) Defining the RNA polymerase III transcriptome: Genome-wide localization of the RNA polymerase III transcription machinery in human cells. *Genome Res.* vol.20: 710-721

Carter R. and Drouin G. (2009) The evolutionarily rates of eukaryotic RNA polymerases and of their transcription factors are affected by the level of concerted evolution of the genes they transcribe. Mol. Biol. Evol. vol.26: 2515-2520

Causton H.C., Ren B., Koh S.S., Harbison C.T., Kanin E., Jennings E.G., Lee T.I., True H.L., Lander E.S. and Young R.A. (2001) Remodeling of yeast genome expression in response to environmental changes. *Mol. Biol. Cell* vol.12:323-337

Chen D.C., Yang B.C., and Kuo T.T. (1992) One-step transformation of yeast in stationary phase. *Curr. Genet.* vol21: 83-84

Ciesla M. and Boguta M. (2008) Regulation of RNA polymerase III transcription by Maf1 protein. *Acta Biochim. Polon.* vol.55: 215–225

Ciesla M., Towpik J., Graczyk D., Oficjalska-Pham D., Harismendy O., Suleau A., Balicki K., Conesa C., Lefebvre O. and Boguta M (2007) Maf1 is involved in coupling carbon metabolism to RNA polymerase III transcription. *Mol. Cell Biol.* vol.27: 7693–7702

Cramer P., Armache K.J., Baumli S., Benkert S., Brueckner F., Buchen C., Damsma G.E., Dengl S., Geiger S.R., Jasiak A.J., *et al.* (2008) Structure of eukaryotic RNA polymerases. *Annu. Rev. Biophys.* vol.37: 337-352

Desai N., Lee J., Upadhya R., Chu Y., Moir R.D. and Willis I.M. (2005) Two steps in Maf1-dependent repression of transcription by RNA polymerase III. *J. Biol. Chem.* vol.280: 6455–6462

Deshpande A.M. and Newlon C.S. (1996) DNA replication fork pause sites dependent on transcription. *Science* vol.272: 1030-1033

Estruch F. and Carlson M. (1993) Two homologous zinc finger genes identified by multicopy suppression in a SNF1 protein kinase mutant of Saccharomyces cerevisiae. *Mol. Cell Biol.* vol.13:3872-3881

Eudes R., Le Tuan K., Delettre J., Mornon J.P. and Callebaut I. (2007) A generalized analysis of hydrophobic and loop clusters within globular protein sequences. *BMC Struct. Biol.* vol.7:2

Flores A., Briand J.F., Gadal O., Andrau J.C., Rubbi L., Van Mullem V., Boschiero C., Goussot M., Marck C., Carles C., Thuriaux P., Sentenac A. and Werner M. (1999) A protein–protein interaction map of yeast RNA polymerase III. *Proc. Natl. Acad. Sci. USA* vol.96:7815–7820

Gaboriaud C., Bissery V., Benchetrit T. and Mornon J.P. (1987) Hydrophobic cluster analysis : an efficient new way to compare and analyse amino acid sequences. *FEB* vol.224: 149-155

Gajda A., Towpik J., Steuerwald U., Müller C.W., Lefebvre O. and Boguta M. (2010) Full repression of RNA polymerase III transcription requires interaction between two domains of its negative regulator Maf1. *J. Biol. Chem.* (in press)

Garza A.S., Ahmad N. and Kumar R. (2009) Role of intrinsically disordered protein regions/domains in transcriptional regulation. *Life Sciences* vol.84: 189-193

Gasch A.P., Spellman P.T., Kao C.M., Carmel-Harel O., Eisen M.B., Storz G., Botstein D. and Brown P.O. (2000) Genomic expression programs in the response of yeast cells to environmental changes. *Mol. Biol. Cell* vol.11: 4241-4257

Gavin A.C., Aloy P., Grandi P., Krause R., Boeshe M., Marzioch M., Rau C., Jensen L.J., Bastuck S. and Dumpelfeld B. (2006) Proteome survey reveals modularity of the yeast cell machinery. *Nature* vol.440: 631-636

Geiduschek E.P. and Kassavetis G.A. (2001) The RNA polymerase III transcription apparatus. *J. Mol. Biol.* vol.310: 1-26

Goodfellow S.J., Graham E.L., Kantidakis T., Marshall L., Coppins B.A., Oficjalska-Pham D., Gerard M., Lefebvre O. and White R.J. (2008) Regulation of RNA polymerase III transcription by Maf1 in mammalian cells. *J. Mol. Biol.* vol.378: 481–491

Gsponer J., Futschik M.E., Teichmann S.A. and Babu M.M. (2008) Tight Regulation of Unstructured Proteins: From Transcript Synthesis to Protein Degradation. *Science* vol.322: 1365-1368

Harismendy O., Gendrel C.G., Soularue P., Gidrol X., Sentenac A., Werner M. and Lefebvre O. (2003) Genome-wide location of yeast RNA polymerase III transcription machinery. *EMBO J.* vol.22: 4738–4747

Harper J.W., Adami G.R., Wei N., Keyomarsi K. and Elledge S.J. (1993) The p21 Cdk-interacting protein Cip1 is a potent inhibitor of G1 cyclin-dependent kinases.*Cell* vol.75: 805-816

Heitman J., Movva N.R. and Hall M.N. (1991) Targets for cell cycle arrest by the immunosuppressant rapamycin in yeast. *Science* vol.253: 905-909

Hofmann K., Bucher P., Falquet L. and Bairoch A. (1999) The PROSITE database, its status in 1999. *Nucl. Acids Res.* vol.27: 215-219

Huber A., Bodenmiller B., Uotila A., Stahl M., Wanka S., Gerrits B. Aebersold R. and Loewith R. (2009) Characterization of the rapamycin-sensitive phosphoproteome reveals that Sch9 is a central coordinator of protein synthesis. *Genes Dev.* vol.23: 1929-1943

http://bioinf4.cs.ucl.ac.uk:3000/psipred/ - Protein structure prediction server

http://smi.snv.jussieu.fr/hca/hca-form.html - Hydrophobic Cluster Analysis

http://www.cbs.dtu.dk/services/NetPhos/ - Phosphorylation sites predictions

http://www.cbs.dtu.dk/services/NetPhosK/ - Kinase specific eukaryotic protein phosphorylation sites prediction tool

http://bioinf.cs.ucl.ac.uk/disopred/ - The DISOPRED2 Prediction of Protein Disorder Server

http://bioinf.cs.ucl.ac.uk/dompred - DomPred Protein Domain Prediction Server

Johnson S.S., Zhang C., Fromm J., Willis I.M. and Johnson D.L. (2007) Mammalian Maf1 is a negative regulator of transcription by all three nuclear RNA polymerases. *Mol. Cell* vol.26: 367–379.

Johnson S.A., Dubeau L. and Johnson D.L. (2008) Enhanced RNA polymerase III-dependent transcription is required for oncogenic transformation *J. Biol. Chem.* vol.283: 19184-19191

Jones D.T. (1998) Do transmembrane protein superfolds exist? *FEBS Lett.* vol.423: 281-285

Jones D.T. (1999) GenTHREADER: an efficient and reliable protein fold recognition method for genomic sequences. *J. Mol. Biol.* vol.287: 797-815

Kantidakis T., Ramsbottom B.A., Birch J.L., Dowding S.N. and White R. (2010) mTOR associates with TFIIIC, is found at tRNA and 5S rRNA genes, and targets their repressor Maf1. *Proc. Natl. Acad. Sci. USA.* vol.107:11823-11828

Kassaventis G.A., Prakash P. and Shim E. (2010) The C53/C37 subcomplex of RNA polymerase III lies near the active site and participates in promoter opening. *J. Biol. Chem.* vol.285: 2695-2706

Kwapisz M., Smagowicz W.J., Oficjalska D., Hatin I., Rousset J.P., Zoladek T. and Boguta M (2002) Up-regulation of tRNA biosynthesis affects translational readthrough in maf1-delta mutant of Saccharomyces cerevisiae. *Curr. Genet.* vol.42:147-152

Landrieux E., Alic N., Ducrot C., Acker J., Riva M. and Carles C. (2006) A subcomplex of RNA polymerase III subunits involved in transcription termination and reinitiation. *EMBO J.* vol.25: 118-128

Lee J., Moir R.D. and Willis I.M. (2009) Regulation of RNA polymerase III transcription involves SCH9-dependent and SCH9-independent branches of the target of rapamycin (TOR) pathway. *J. Biol. Chem.* vol.284: 12604-12608

Lemesle-Varloot L., Henrissat B., Gaboriaud C., Bissery V., Morgat A. and Mornon J.P. (1990) Hydrophobic cluster analysis: procedures to derive structural and functional information from 2D representation of protein sequences. *Biochimie* vol.72: 555-574

Loewith R., Jacinto E., Wullschleger S., Lorberg A., Crespo J., Bonenfant D., Opplieger W., Jenoe P. and Hall M.N. (2002) Two TOR complexes, only one of which is rapamycin sensitive, have distinct roles in cell growth control. *Mol. Cell* vol.10: 457-468

Manaud N., Arrebola R., Buffin-Meyer B., Lefebvre O., Voss H., Riva M., Conesa C., and Sentenac A. (1998) A chimeric subunit of yeast transcription factor IIIC forms a subcomplex with tau95. *Mol. Cell Biol.* vol.18: 3191-3200

Marsden R.L., McGuffin L.J. and Jones D.T. (2002) Rapid protein A domainssignment from amino acid sequence using predicted secondary structure. *Protein Science* vol.11: 2814-2824

Marshall L. (2008) Elevated RNA polymerase III transcription drives proliferation and oncogenic transformation.*Cell Cycle* vol.7: 3327-3329

Marshall L., Kenneth N.S. and White R.J. (2008) Elevated tRNA(iMet) synthesis can drive cell proliferation and oncogenic transformation.*Cell* vol.133: 78-89

Marshall L. and White R.J. (2008) Non-coding RNA production by RNA polymerase III is implicated in cancer.*Nat. Rev. Cancer* vol.8: 911-914

Martinez-Pastor M.T., Marchler G., Schüller C., Marchler-Bauer A., Ruis H. and Estruch F**. (1996)** The Saccharomyces cerevisiae zinc finger proteins Msn2p and Msn4p are required for transcriptional induction through the stress response element (STRE). *EMBO J.* vol.15: 2227-2235

McGuffin L.J., Bryson K. and Jones D.T. (2000) The PSIPRED protein structure prediction server. *Bioinformatics* vol.16: 404-405

Michels A.A., Robitaille A.M., Buczynski-Ruchonnet D., Hodroj W., Reina J.H., Hall M.N. and Hernandez N. (2010) mTORC1 directly phosphorylates and regulates human MAF1. *Mol. Cell Biol.* vol.30:3749-3757

Moir R.D., Lee J., Haeusler R.A., Desai N., Engelke D.R., and Willis I.M. (2006) Protein kinase A regulates RNA polymerase III transcription through the nuclear localization of Maf1. *Proc. Natl. Acad. Sci. U S A* vol.103: 15044-15049

Moqtaderi Z. and Struhl K. (2004) Genome-wide occupancy profile of the RNA polymerase III machinery in *Saccharomyces cerevisiae* reveals loci with incomplete transcription complexes. *Mol. Cell Biol.* vol.24: 4118-4127

Moss T. ans Stefanovsky V.Y. (2002) At the center of eukaryotic life. *Cell* vol. 109: 545-548

Muhlrad D., Hunter R. and Parker R. (1992) *A rapid method for localized mutagenesis of yeast genes. Yeast* vol.8: 79-82

Murawski M., Szczesniak B., Zoladek T., Hopper A.K., Martin N.C. and Boguta M. (1994) maf1 mutation alters the subcellular localization of the Mod5 protein in yeast. *Acta Biochim. Polon.* vol.41: 441–448

Nguyen V.C., Clelland B.W., Hockman D.J., Kujat-Choy S.L., Mewhort H.E. and Schultz M.C (2010) Replication stress checkpoint signaling controls tRNA gene transcription. *Nat. Struct. Mol. Biol.* vol.17: 976-981

Oficjalska-Pham D., Harismendy O., Smagowicz W.J., Gonzalez de Peredo A., Boguta M., Sentenac A. and Lefebvre O. (2006) General repression of RNA polymerase III transcription is triggered by protein phosphatase type 2A-mediated dephosphorylation of Maf1. *Mol. Cell* vol.22: 623–632

Pluta K., Lefebvre O., Martin N.C., Smagowicz W.J., Stanford D.R., Ellis S.R., Hopper A.K., Sentenac A. and Boguta M. (2001) Maf1p, a Negative Effector of RNA Polymerase III in *Saccharomyces cerevisiae*. *Mol. Cell Biol.* vol.21: 5031-5040

Reina J.H., Azzouz T.N. and Hernandez N. (2006) Maf1, a new player in the regulation of human RNA polymerase III transcription. *PLoS ONE* vol.1: e134

Roberts D.N., Stewart A.J., Huff J.T. and Cairns B.R. (2003) The RNA polymerase III transcriptome revealed by genome-wide localization and activity-occupancy relationships. *Proc. Natl. Acad. Sci. USA* vol.100: 14695–14700

Roberts D.N., Wilson B., Huff J.T., Stewart A.J. and Cairns B.R. (2006) Dephosphorylation and genome-wide association of Maf1 with Pol III-transcribed genes during repression. *Mol. Cell* vol.22: 633–644

Rollins J., Veras I., Cabarcas S., Willis I. and Schramm L. (2007) Human Maf1 negatively regulates RNA polymerase III transcription *via* the TFIIB family members Brf1 and Brf2. *Int. J. Biol. Sci.* vol.3: 292–302

Rose M.D., Winson F. and Hieter P. (1990) Methods in yeast genetics. A Laboratory Course Manual. *Cold Spring Harbor Laboratory Press, New York, USA.*

Sambrook J. and Russell D.W. (2001) Molecular Cloning: A Laboratory Manual. *Cold Spring Harbor Laboratory Press, New York, USA*

Schmitt M.E., Brown T.A. and Trumpower B.L. (1990) A rapid and simple method for preparation of RNA from Saccharomyces cerevisiae. *Nucleic Acids Res.* vol.18: 3091-3092

Schutz-Geschwender A., Zhang Y., Holt T., McDermitt D. and Olive D.M. (2004) Quantitative, Two-Color Western Blot Detection With Infrared Fluorescence. *LI-COR Biosciences*

Sherman F. (2002) Getting Started with Yeast *Methods Enzymol.* vol.350: 3-41

Shor B., Wu J., Shakey Q., Toral-Barza L., Shi C., Follettie M. and Yu K. (2010) Requirement of the mTOR kinase for the regulation of Maf1 phosphorylation and control of RNA Polymerase III-dependent transcription in cancer cells. *J. Biol. Chem.* vol.285: 15380-15392

Schramm L. and Hernandez N. (2002) Recruitment of RNA polymerase III to its target promoters. *Genes Dev.* vol.16: 2593-2620

Sikorski, R. S., and Hieter, P. (1989) A system of shuttle vectors and yeast host strains designed for efficient manipulation of DNA in Saccharomyces cerevisiae.*Genetics* vol.122: 19-27

Schwartz L.B., Sklar V.E., Jaehning J.A., Weinmann R. and Roeder R.G.(1974) Isolation and partial characterization of the multiple forms of deoxyribonucleic acid-dependent ribonucleic acid polymerase in mouse myeloma MOPC 315. *J. Biol. Chem.* vol.249: 5889-5897

Thuillier V., Stettler S., Sentenac A., Thuriaux P. and Werner M. (1995) A mutation in the C31 subunit of Saccharomyces cerevisiae RNA polymerase III affects transcription initiation. *EMBO J.* vol.14: 351-359

Towpik J., Graczyk D., Gajda A., Lefebvre O. and Boguta M. (2008) Derepression of RNA polymerase III transcription by phosphorylation and nuclear export of its negative regulator, Maf1. *J. Biol. Chem.* vol.283: 17168–17174

Upadhya R., Lee J. and Willis I.M. (2002) Maf1 is an essential mediator of diverse signals that repress RNA polymerase III transcription. *Mol. Cell* vol.10: 1489–1494

Uversky V.N. and Dunker A.K. (2008) Controlled chaos. *Science* vol.322: 1340-1341

Varshavsky A. (1997) The N-end rule pathway of protein degradation. *Genes Cells* vol.2: 13-28

Vannini A., Ringel R., Kusser A.G., Berninghausen O., Kassaventis G. and Cramer P. (2010) Molecular Basis of RNA Polymerase III Transcription Repression by Maf1. *Cell* vol.143: 59-70

Ward J.J., McGuffin L.J., Bryson K., Buxton B.F. and Jones D.T. (2004) The DISOPRED server for the prediction of protein disorder. *Bioinformatics* vol.20: 2138-2139

Warner J.R. (1999) The economics of ribosome biosynthesis in yeast. *Trends Biochem. Sci.* vol.24: 437-440

Warner J.R., Vilardell J. and Sohn J.H. (2001) Economics of ribosome biosynthesis.*Cold Spring Harb. Symp. Quant. Biol.* vol.66: 567-574

Wei Y., Tsang C.K. and Zheng XF.S. (2009) Mechanisms of regulation of RNA polymerase III – dependent transcription by TORC1. *EMBO J.* vol.28: 2220-2230

Werner M., Chaussivert N., Willis I.M. and Sentenac A. (1993) Interaction between a complex of RNA polymerase III subunits and the 70-kDa component of transcription factor IIIB. *J. Biol. Chem.* vol.268: 20721-20724

White R.J. (2008) RNA polymerases I and III, non-coding RNAs and cancer. *Trends Genet.* vol.24: 622-629

Willis I.M., Desai N. and Upadhya R. (2004) Signaling repression of transcription by RNA polymerase III in yeast. *Prog. Nucleic Acid Res. Mol. Biol.* vol.77: 323–353

Willis I.M. and Moir R.D. (2007) Integration of nutritional and stress signaling pathways by Maf1. *Trends Biochem. Sci.* vol.32:51-53

Woodcock D.M., Crowther P.J., Doherty J., Jefferson S., DeCruz E., Noyer-Weidner M., Smith S.S., Michael M.Z. and Graham M.W. (1989) Quantitative evaluation of Escherichia coli host strains for tolerance to cytosine methylation in plasmid and phage recombinants. *Nucleic Acids Res.* vol.17: 3469-3478

Woodcock S., Mornon J.P. and Henrissat B. (1992) Detection of secondary structure elements in proteins by Hydrophobic cluster analysis. *Analysis. Prot. Eng.* vol.5: 629-635

Wullschleger S., Loewith R. and Hall M.N. (2006) TOR signaling in growth and metabolism. *Cell* vol.124: 471-484